

**DEVELOPMENT OF ANALYTICAL METHODOLOGY
FOR TRACE ELEMENTS IN
NUCLEAR/ENVIRONMENTAL SAMPLES USING
CHROMATOGRAPHY TECHNIQUES**

By
VIVEKCHANDRA GURUPRASAD MISHRA
(CHEM01201104010)

**Bhabha Atomic Research Centre,
Mumbai**

*A thesis submitted to the
Board of Studies in Chemical Sciences
In partial fulfillment of requirements
for the Degree of
DOCTOR OF PHILOSOPHY
of
HOMI BHABHA NATIONAL INSTITUTE*

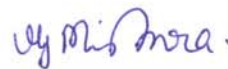


March, 2017

STATEMENT BY AUTHOR

This dissertation has been submitted in partial fulfillment of requirements for an advanced degree at Homi Bhabha National Institute (HBNI) and is deposited in the Library to be made available to borrowers under rules of the HBNI.

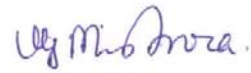
Brief quotations from this dissertation are allowable without special permission, provided that accurate acknowledgement of source is made. Requests for permission for extended quotation from or reproduction of this manuscript in whole or in part may be granted by the Competent Authority of HBNI when in his or her judgment the proposed use of the material is in the interests of scholarship. In all other instances, however, permission must be obtained from the author.



Vivekchandra G. Mishra

DECLARATION

I, hereby declare that the investigation presented in the thesis has been carried out by me. The work is original and has not been submitted earlier as a whole or in part for a degree / diploma at this or any other Institution / University.



Vivekchandra G. Mishra

List of Publications arising from the thesis

Journal

1. Direct extraction of molybdenum from solid uranium matrices employing pyrohydrolysis, a reagent free green separation method and its determination by Ion Chromatography.

Vivekchandra Guruprasad Mishra, Uday Kumar Thakur, Dipti Jayesh Shah, Neeraj Kumar Gupta, Subbiah Jeyakumar, Bhupendra Singh Tomar, Karanam Lakshminarayana Ramakumar

Anal. Chem. 87(2015)10728.

2. Simultaneous determination of borate, chloride and molybdate in pyrohydrolysis distillates of plant and soil samples by ion chromatography.

Vivekchandra Guruprasad Mishra, Mrinal Kanti Das, Dipti Jayesh Shah, Subbiah Jeyakumar, Bhupendra Singh Tomar, Karanam Lakshminarayana Ramakumar

J. Chromatogr. A 1532(2018)144-149.

3. Application of Ion chromatography for optimizing washing procedure for removal of Chloride and Nitrate from Li_2TiO_3 microspheres using LiOH solutions.

Vivekchandra G. Mishra, U. K. Thakur, T. V. Vittal Rao, Y. R. Bamankar, Dipti J. Shah, S. Jeyakumar, B. S. Tomar and K. L. Ramakumar

J. Res. Anal. 2(1)(2016)35.

4. Studies on U-Zr and U-Pu-Zr alloys for determination of Cl and F using pyrohydrolysis.

Vivekchandra Guruprasad Mishra, Sanjay Krishnarao Sali, Dipti Jayesh Shah, Uday Kumar Thakur, Ramesh Mahadeo Sawant, and Bhupendra Singh Tomar.

Radiochim. Acta 102(2014)895.

5. Development of ion chromatography and capillary electrophoresis methods for the determination of Li in Li-Al alloy.

V. G. Mishra, M. K. Das, V. V. Raut, S. Jeyakumar, R. M. Sawant, B. S. Tomar, and K. L. Ramakumar

J. Radioanal. Nucl. Chem. 300(2014)125.

6. Rapid Separation and Quantification of Iron in Uranium Nuclear Matrix by Capillary Zone Electrophoresis (CZE).

Vivekchandra Mishra, Mrinal Kanti Das, Subbiah Jeyakumar, Ramesh Mahadeo Sawant, Karanam Lakshminarayana Ramakumar.

Am. J. Anal. Chem., 2(2011)46.

Conferences

1. Extraction of Molybdenum from uranium matrix employing Pyrohydrolysis: A novel approach.

V.G. Mishra, U. K. Thakur, D. J. Shah, N. K. Gupta, S. Jeyakumar, B. S. Tomar and K. L. Ramakumar.

Proceedings of DAE -BRNS National Symposium on Nuclear and Radiochemistry 2015, 9-13 Feb, 2015, 409.

2. Feasibility study on the simultaneous separation and analysis of B, Cl, F, and Mo in the Pyrohydrolysis extract of Uranium samples employing ion chromatography.

V. G. Mishra, M.K. Das, D. J. Shah, S. Jeyakumar, B. S. Tomar and K. L. Ramakumar.

Proceedings of DAE-BRNS National Symposium on Nuclear and Radiochemistry 2015, 9-13 Feb, 2015, 415.

3. Determination of Chloride and Nitrate in LiOH solutions used for washing Li_2TiO_3 microspheres employing Ion Chromatography.

U. K. Thakur, **V. G. Mishra**, T. V. Vittal Rao, Y. R. Bamankar, D. J. Shah, S. Jeyakumar, B. S. Tomar

Proceedings of DAE-BRNS National Symposium on Nuclear and Radiochemistry 2015, 9-13 Feb, 2015, 413.

4. Determination of Lithium-Aluminium Alloy by Capillary Electrophoresis.

V.G. Mishra, M. K. Das, S. Jeyakumar, R. M. Sawant, B. S. Tomar, and K. L. Ramakumar

Proceedings of DAE-BRNS National Symposium on Nuclear and Radiochemistry 2013, 19-23 Feb, 2013, 445.

5. Separation and Quantification of Lithium in Aluminium Matrices using Ion Chromatography

V.G.Mishra, M.K.Das, B.K.Nagar, S.Jeyakumar, R.M.Sawant, B.S.Tomar and K.L.Ramakumar

Proceedings of DAE-BRNS Biennial Symposium on Emerging Trends in Separation Science and Technology 2012, 27 Feb-Mar 01, Mumbai, 159.

6. Study on pyrohydrolysis extraction and determination of Cl, F in U-Zr and U-Pu-Zr alloys.

D. J. Shah, **V. G. Mishra**, U. K. Thakur, R. M. Sawant, and B. S. Tomar

Proceedings of DAE-BRNS Biennial Symposium on Emerging Trends in Separation Science and Technology, Mumbai, February 25-28, 2014,104.

7. XRD study on pyrohydrolysed U-Zr and U-Pu-Zr alloys for halide extraction

U. K. Thakur, S. K. Sali, D. J. Shah, **V. G. Mishra**, R. M. Sawant, and B. S. Tomar

Proceedings of DAE-BRNS Biennial Symposium on Emerging Trends in Separation Science and Technology, Mumbai, February 25-28, 2014,106.

8. Separation and Determination of Iron from Uranium Matrix by Capillary Zone Electrophoresis (CZE).

V. G. Mishra, M. K. Das, S. Jeyakumar, R. M. Sawant, and K. L. Ramakumar.

Proceedings of DAE-BRNS Biennial Symposium on Emerging Trends in Separation Science and Technology 2010, IGCAR, Kalpakkam, March 1-4, 2010, 461.

Vivekchandra G. Mishra

Dedicated to.....

My Grandmother

Late Smt. Ramarati Mishra

&

My Parents

Smt. Kishori Devi Mishra

Shri Guru Prasad Mishra

Acknowledgment

I extend my sincere gratitude to all who put their efforts and spent time for me to get successful completion of the work, without whose support this would have been impossible.

It is my pleasure to thank my guide **Dr. K. L. Ramakumar**, for his continuous encouragement and motivation in mentoring me throughout the course of this thesis work. I would like to express the gratitude to my senior and technology advisor **Dr. S. Jeyakumar**, who has equally motivated and supported me during the entire period of work. I thank him for all the care, advice and encouragement he has given to me. Any words will not be sufficient to thank them for their support and contribution.

I also want to express my heartfelt thanks to my Head of Division and Chairman of Doctoral Committee, **Dr. B. S. Tomar**, for his cooperation and concern during the entire course of my PhD work. His guidance and suggestions helped in improving my work greatly. I also want to extend my thanks to all the other members of Doctoral Committee, **Dr. R. K. Verma, Dr. Sangita D. Kumar and Dr. G. G. Pandit** for their invaluable suggestions and insightful comments provided during the doctoral committee meetings. I am thankful to them for their strong support and cooperation throughout the course of my PhD program.

I sincerely thank all my lab mates, specially, **Smt Dipti J. Shah, Shri. Uday Kumar Thakur and Shri Mrinal Kanti Das**, who made me to carry the work in pleasant and effortless environment to keep me all the time comfortable in finishing the jobs. Without their kind support and keen contributions the work would have not been at its shape as it is now. I am grateful to all my friends for their emotional support, entertainment and being a great company all the time.

Last but always at the close to heart, I am fortunate to have blessings, love, support and encouragement from **my parents and family** who made me stable and studious at all odd and even happenings. I thank **Mayank, Mridula and Saket** who made all my time after office hours so joyful and cherishing and to come again as fresh as every time.

Above all I thank the almighty for enabling me to complete the task.

Vivekchandra G. Mishra

CONTENTS

<i>Synopsis</i>	I
<i>List of figures</i>	XIII
<i>List of tables</i>	XX
<i>Chapter-1- Introduction</i>	1-29
1.1 Basics of nuclear energy	1
1.2 Indian Nuclear Program	1
1.2.1 Nuclear fuel cycle	3
1.2.2 Types of nuclear fuels	4
1.2.3 Fusion Energy	9
1.2.4 Chemistry in nuclear fuel cycle	11
1.2.4.1 Determination of major elements	12
1.2.4.2 Isotopic composition analysis	17
1.2.4.3 Determination of Non-metallics	17
1.2.5 Scope of Present Investigations	20
1.3 References	23
<i>Chapter-2- Principles of Experimental Techniques</i>	30-60

2.1	Introduction	30
2.2	Chromatography	31
2.2.1	Types of Chromatography	31
2.2.2	Ion-Exchange Chromatography	34
2.2.2.1	Ion Exchange equilibria	34
2.2.2.2	Conductivity detection	36
2.2.3	Terms used in chromatography separations	37
2.2.4	Plate Height Equation	39
2.2.5	Instrumentation	42
2.3	Capillary Electrophoresis	44
2.3.1	Electrophoretic Mobility	45
2.3.2	Electro osmotic Flow	45
2.3.3	Instrumentation	46
2.3.4	Capillary Zone Electrophoresis (CZE)	47
2.4	X-ray powder diffraction analysis (XRD)	48
2.5	Thermogravimetric Analysis	50
2.6	Inductively Coupled Plasma Atomic Emission	51

Spectrometry	
2.7 Pyrohydrolysis	51
2.8 References	58
<i>Chapter-3- Direct Extraction of Molybdenum from Solid Uranium</i>	61-79
<i>Matrices Employing Pyrohydrolysis and Its Determination by Ion Chromatography</i>	
3.1 Introduction	61
3.2 Experimental Section	62
3.2.1 Reagents	62
3.2.2 Preparation of Standards Containing Mo	63
3.2.3 Instrumentation	63
3.2.4 IC Analysis of Mo	64
3.3 Results and Discussion	65
3.3.1 Thermogravimetric Analysis	65
3.3.2 Pyrohydrolysis of Mo Containing Standards	67
3.3.3 Kinetics of Mo Separation	70
3.3.4 Optimization of Pyrohydrolysis Conditions	73
3.3.5 Method Validation and Sample Analysis	75

3.4 Conclusion 76

3.5 References 77

Chapter-4-Studies On U-Zr And U-Pu-Zr Alloys For Determination of Cl And F Using Pyrohydrolysis 80-97

4.1 Introduction 80

4.2 Experimental Section 82

4.2.1 Pyrohydrolysis setup 82

4.2.2 Ionchromatography system 82

4.2.3 XRD instrument 83

4.2.4 Thermoanalyzer 83

4.2.5 Alloy fabrication and characterization 83

4.2.6 Pyrohydrolysis procedure 84

4.3 Results and discussion 84

4.4 Conclusions 94

4.5 References 95

Chapter-5-Development of Ion Chromatography and Capillary Electrophoresis Methods for the Determination of Li in Li-Al Alloy 98-109

5.1	Introduction	98
5.2	Experimental	99
5.2.1	Instrumentation	100
5.2.2	Reagents	100
5.2.3	Sample preparation	100
5.3	Results and discussion	100
5.3.1	Ion Chromatography Studies	100
5.3.2	Capillary electrophoresis studies	103
5.4	Conclusion	107
5.5	References	107
<i>Chapter-6-Rapid Separation and Quantification of Iron in Uranium Nuclear Matrix by Capillary Zone Electrophoresis (CZE)</i>		110-128
6.1	Introduction	110
6.2	Experimental	113
6.2.1	Instrumentation	113
6.2.2	Reagents and Solutions	113
6.2.3	Procedure for Conditioning Capillary and Sample Injection	114

6.3	Results and Discussion	114
6.3.1	Optimization of Background Electrolyte	116
6.3.2	Optimization of Applied Voltage	120
6.3.3	Matrix element tolerance	120
6.3.4	Validation of Method	121
6.4	Analysis of Certified Reference Materials	122
6.5	Real Sample Analysis	123
6.6	Advantages of the CZE Method	125
6.7	Conclusions	125
6.8	References	125
	<i>Chapter-7-Application of Ion chromatography for optimizing washing procedure for removal of Chloride and Nitrate from Li_2TiO_3 microspheres using LiOH solution.</i>	129-141
7.1	Introduction	129
7.2	Experimental	131
7.2.1	Materials and reagents	131
7.2.2	Instrumentation	131
7.3	Results and Discussion	132

7.3.1 Preparation and washing of Li_2TiO_3	132
7.3.2 Sample preparation for IC analysis	133
7.3.3 Ion chromatographic analysis	133
7.3.4 Reduction in volume and recycling of LiOH washing effluent	136
7.3.5 Determination of chlorine Li_2TiO_3 microspheres	138
7.4 Conclusions	140
7.5 References	140
<i>Chapter-8-Development of ion chromatographic method for the simultaneous separation and determination of B, Cl and Mo in plant and soil samples</i>	142-159
8.1 Introduction	142
8.2 Experimental	145
8.2.1 Reagents and materials	145
8.2.2 Apparatus and instrument	145
8.2.3 Samples	146
8.3 Result and Discussion	146
8.3.1 Separation studies	146

8.3.2 Explanation	151
8.3.3 Development of gradient elution procedure:	154
8.3.4 Sample Analysis	155
8.4 Conclusion	156
8.5 References	157

SYNOPSIS

Limited uranium resources and abundant thorium resources in the country prompted Dr. H.J. Bhabha, the initiator of Indian atomic energy program to envision a three stage nuclear energy program for sustained growth of nuclear power program. This obviously requires closed nuclear fuel cycle involving reprocessing of spent fuel from the first stage to fuel the second and third stages. The Department of Atomic Energy (DAE), India, is pursuing an indigenous power program linking the fuel cycle of Pressurized Heavy Water Reactor (PHWR), Liquid Metal Cooled Fast Breeder Reactors (LMFBR) and ^{232}Th - ^{233}U based advanced reactors [1-3]. Optimum utilization of fissile content in the nuclear fuels during reactor operation can result in increasing power production. Improving the fuel quality is one of the criteria to ensure longer residence time of fuel in the reactor. This in turn results in higher burn-up leading to enhanced power. Reactor physicists and fuel fabricators stipulate certain quality (specifications) to the nuclear fuel and other reactor materials for this purpose. In order to realize the smooth and efficient functioning of the reactor, the fuel should satisfy the specifications derived for it. The specification includes both physical and chemical qualities of the material. The chemical analyses pertaining to the Chemical Quality Control (CQC) process play a pivotal role in achieving the quality of the material fabricated. The CQC analyses mainly involve the analysis of feed (also known as starting materials) materials, intermediate and the finished products [4-7]. In addition to the nuclear fuels, strategically important nuclear materials like tritium generators [8] etc., are also require determination of percentage and trace level components for their optimum performance during reactor irradiation.

Nuclear energy is generated either by fission or fusion. Fusion energy is generated by fusing two light atoms, which are mostly the hydrogen isotopes. The waste generated during fusion will largely be either helium or water [8]. India is involved in the International Test Experimental Reactor (ITER) project (a fusion based reactor program) and DAE supports this program by fabricating tritium breeders (Li_2TiO_3) employing different methods [9]. This necessitates the development of analytical methods for the analysis of tritium breeders for their chemical characterization.

Several analytical techniques are employed for the chemical characterization or CQC analysis of nuclear materials [4]. Among them, elemental determinators, Inductively Coupled Plasma- Atomic Emission Spectroscopy (ICP-AES) [10], Inductively Coupled Plasma-Mass Spectrometry ICP-MS [11-12], Thermal Ionization Mass Spectrometry (TIMS) [13], alpha and gamma spectrometry[14,15], X-ray Diffraction (XRD) [16], electro analytical techniques, spectrophotometer etc are some of the important techniques routinely employed for chemical characterization analysis. In the recent past chromatographic techniques like High Pressure Liquid Chromatography (HPLC) and Ion Chromatography (IC) have been introduced into the CQC analyses of nuclear materials [17]. However, the CQC processes of various nuclear materials demand the development of new analytical methodologies. Improvement in the existing methodologies is also attempted with a view to improving accuracy and precision, low detection limit, high selectivity, simultaneous or multi-elemental analysis, minimum generation of analytical waste and minimum use of chemical reagents etc.

Chromatography is a physical method of separation wherein the analytes are separated due to their differential distribution between two immiscible phases. The major advantage of chromatographic techniques is that they offer simultaneous

separation and quantification. Ion chromatography is used for separating both cation and anion species wherein the separation occurs due to their different affinities toward the ion exchange process on the stationary phase [18] whereas, HPLC is mainly employed for the separation of organic as well as neutral molecules. Capillary Electrophoresis (CE) is a simple, rapid and high efficient separation method and is employed for separating ions as well as neutral molecules. Unlike HPLC and IC, separation in CE is achieved by applying an electric field which causes differential velocities of the ions or molecules due to their electrophoretic migration. The separation is carried out inside a thin capillary of 50 - 100 μm diameter and a length of 0.5 to 1 meter and the separation is complete within few minutes. CE is considered as a complementary technique to IC [19] and hence, both IC and CE are being used for separating several ions in a wide range of sample matrices.

Analytical methods which can analyze directly the dissolved sample solutions are preferred as they eliminate the cumbersome sample preparation procedures. Few applications of CE and IC, where direct analysis of the dissolved sample solution without employing matrix separation have been reported in literature [20,21]. Such direct analyses not only avoid the pre-separation of matrix or pre-concentration of analytes but also useful in the absence of reference materials. In the present study, efforts have been made to develop analytical methods for the direct analysis using IC and CE.

Pyrohydrolysis is a physical method of separation where the analyte is removed from the matrix by converting it into a volatile species. It is widely employed for separating halides from various nuclear materials. During pyrohydrolysis the sample

is heated at high temperature in presence of moist oxygen or a suitable carrier gas. Chlorine, fluorine and boron are separated in the form of hydrochloric, hydrofluoric and boric acids, respectively. Pyrohydrolysis separates halides and boron directly from a solid matrix and produces a clean sample solution, which is favorable in carrying out trace and ultra-trace level analysis [22,23]. Therefore, pyrohydrolysis finds many applications in the determination of halides at trace level concentrations in many complex matrices. Analysis of halides and boron in environmental and plant samples involves tedious sample preparation procedures due to the presence of organic compounds. The analytical methods that have been developed for the analyses of nuclear materials involving initial pyrohydrolysis separation followed by analytical determinations can be extended for the analyses of environmental samples. In this thesis, the analysis of environmental samples like soil and plants using pyrohydrolysis and ion chromatography have been reported.

In spite of the unique features of IC and CE, not many applications were reported for the analysis of nuclear materials. Therefore, efforts have been made to utilize these techniques for nuclear material analysis independently and validate the results. The present thesis is divided into eight chapters and the brief description of each chapter is given below.

CHAPTER ONE: This chapter discusses the need for high quality nuclear materials and the importance of their Chemical Quality Control (CQC) analysis. It also recounts the effect of the concentration of the specified elements (specification limits) on the performance of the nuclear material or fuel. It also discusses about the analytical techniques employed in the CQC analysis and emphasizes the need for developing new analytical methods with a view to achieving better accuracy and precision specially while determining the trace and ultra trace constituents (both

metallic and non-metallic impurities). It highlights the importance and advantages on the use of chromatographic methods like IC and CE in the CQC analysis of nuclear materials.

CHAPTER TWO: This chapter deals with the experimental part of the studies reported in the thesis. It describes the basic principles of the techniques employed. Special emphasis has been given to ion chromatography and capillary electrophoresis separations. Pyrohydrolysis is basically a non-instrumental separation technique which has been exploited employing an in-house designed equipment. Details of this technique have been discussed along with IC and CE. Other techniques like X-Ray Diffraction (XRD), Thermo Gravimetry (TG), Inductively Coupled Plasma -Atomic Emission Spectrometry (ICP-AES) were also used to obtain supportive information required for the investigation. The usefulness of these techniques in the present studies has been described in this chapter.

CHAPTER THREE: This chapter deals with the direct separation of molybdenum from solid uranium matrices employing pyrohydrolysis and its determination by ion chromatography. Pyrohydrolysis (PH) is a well-established technique for the direct extraction of non-metals like halides and boron from solid matrices without acid digestion and use of chemical reagents. However, PH extraction of metals or metal species has not been reported. This is for the first time the pyrohydrolysis separation of a metal, Mo in the form of MoO_4^{2-} was reported. Systematic studies were carried out to understand the high temperature chemistry of Mo and its oxides. It has been shown that MoO_3 volatilization is enhanced drastically in presence of moist atmosphere [24]. The volatilization behavior of MoO_3 in presence of moist Ar at 950°C was carried out with TG to explore the feasibility of PH extraction of Mo. To understand the mechanism and kinetics of the separation, the XRD patterns were

attained for the material after pyrohydrolysing at different time intervals. The study brings out the need for the suitable modification of the PH apparatus to improve the recovery of Mo. The Mo in the distillate was determined by IC. The developed method was extended to the analysis of Mo in ADU samples on routine basis.

CHAPTER FOUR: This chapter discusses the determination of chlorine and fluorine in U-Zr and U-Pu-Zr alloys using pyrohydrolysis separation followed by IC determination. U-Zr and U-Pu-Zr alloys are being considered as fuel for fast breeder reactors due to improved breeding possibilities associated with metallic fuel [25]. These newly developed materials have specification limits for Cl and F and hence, there is a need for developing an analytical method for the determination of chlorine and fluorine in U-Zr and U-Pu-Zr alloys. The study reports the pyrohydrolysis of the materials as well as the optimization of various pyrohydrolysis conditions required for the maximum recovery of Cl and F. The samples were pyrohydrolysed for different time intervals and their XRD patterns were recorded. The XRD data helped in understanding the mechanism of pyrohydrolysis and to optimize the time of pyrohydrolysis. This chapter also deals with the analysis of the real samples.

CHAPTER FIVE: This chapter discusses the development of ion chromatography (IC) and capillary electrophoresis (CE) methods for the determination of Li in Li-Al alloy. The Li-Al alloy is irradiated in reactor for the production of tritium (${}^6\text{Li}(n,\alpha)\text{T}$). The Li content in Li-Al alloy is about 4%. The common analytical methods employed for the determination of Li are ICP-AES and Atomic Absorption Spectroscopy (AAS). However, these techniques could not be utilized for certifying Li in Li-Al alloy because of certain inherent difficulties [26] (such as interferences are observed in AES and signal suppression is observed in AAS due to Al matrix). Hence, an IC method for the determination of Li in Li-Al alloy was developed.

Although IC is capable of separating the alkali and alkaline earth metals, presence of large amount of Al matrix may cause difficulty in separating Li. Since Al^{3+} ions will have strong retention on the ion exchange column than Li^+ , elution of Li^+ ahead of Al^{3+} ion is desirable for the determination of Li. A weak strength mobile phase to elute Li is the choice to realize this. otherwise it would get eluted along with un-retained components. Using the weak-strength eluent also helps in retaining Al^{3+} on the column. Therefore, IC separation was carried out on a high capacity cation exchange column with methane sulphonic acid (MSA) as eluent with a view to retaining Al on the column. While using MSA (20 mM MSA) as eluent, Li is eluted in reasonable time whereas Al^{3+} is retained on the column and it would not get eluted unless the mobile phase strength is increased five times. The developed procedure showed high tolerance for Al and provided a precision better than 0.2% (RSD). In the absence of a certified reference material to check the accuracy of the results, another method based on capillary electrophoresis was developed independently and the results obtained by this method were compared. Unlike IC the elution order in CE separation is Al followed by Li. This is because the tri-positive charged Al moves ahead of singly charged Li. However, for the purpose of analytical determination of Li such separation is not acceptable as the bulk Al peak significantly affects the recovery of Li. To reverse the elution order, imidazole was used as a co-ion, which forms complex with the metal cations also enables the indirect detection of cations. Imidazole forms complex with Al selectively and reduces its charge density, which resulted the appearance of Al peak after Li in the electrogram. Moreover the developed method showed high tolerance for Al matrix. The results obtained from both IC and CE were compared. IC provided better

sensitivity and precision, whereas CE has the advantages like fast analysis, low sample volume, and reduction in waste generation.

CHAPTER SIX: This chapter deals with the development of a Capillary Zone Electrophoresis (CZE) method for the determination of iron in uranium matrix without employing the pre-separation of uranium. Iron is a common contaminant picked up by the product material from various process equipments. In order to control the process to obtain the desired quality of the end product, it is necessary to check the Fe contents in both unfinished and finished products. This demands a rapid as well as reliable method for the determination of Fe. For this purpose, a CE method was developed as the dissolved sample solution can be injected directly into CE and the total analysis time is few minutes. However, while developing direct CE method for separating Fe from U matrices, the following conditions are to be considered (i) the Fe peak should appear before uranium, (ii) sufficient resolution between the Fe and U peak so that matrix is tolerated and (iii) the Fe peak should be interference-free from other transition metals. Hence, to realize the separation with the above conditions, CE separation was carried in the form of chloride complexes of Fe and U [27,28]. Uranium and iron form positively charged chloride complexes. The iron-chloride complex has higher positive charge density than uranium-chloride complex which is responsible for the separation as well as to provide the required elution order (iron peak is followed by uranium). Moreover, the chloride medium brings the advantage of interference free determination of Fe as the other transition metals form either anionic or neutral complexes [29]. The developed method was validated by analyzing ILCE (IV) and (V) reference materials and the results for Fe were within 5 % of certified value. Several other samples were also analyzed and reported.

CHAPTER SEVEN: This chapter discusses the application of ion chromatography for optimizing washing procedure to be used for removal of chloride and nitrate from Li_2TiO_3 microspheres using lithium hydroxide as wash solution. Li_2TiO_3 is proposed for Test Blanket Material (TBM) for International Thermonuclear Experimental Reactor (ITER). Li_2TiO_3 were produced through wet process where the microspheres are contaminated with chloride and nitrate. Subsequently chloride and nitrate were removed by washing with LiOH. Since the proposed Li_2TiO_3 contains 60% enriched ^6Li , washing is carried out with $^6\text{LiOH}$ to avoid depletion in the ^6Li content of Li_2TiO_3 . Therefore, the entire washing process is required to be completed with minimum volume of $^6\text{LiOH}$. The present work describes the ion chromatographic (IC) determination of Cl^- and NO_3^- in LiOH wash solutions at different washing stages. Based on the results, a procedure was for the repeated use of LiOH, which significantly reduces the volume of LiOH otherwise required. The final chlorine content of Li_2TiO_3 was determined by IC after its pyrohydrolysis extraction. The results obtained for the washing solutions helped in arriving at a washing procedure wherein maximum impurities could be extracted with minimum washing solution of LiOH.

CHAPTER EIGHT: This chapter reports an ion chromatographic method for the simultaneous separation and determination of borate, fluoride, chloride and molybdate ions, which is useful in the chemical characterization of nuclear fuels and environmental samples (plant and soil). Though the pyrohydrolysis separation of Mo from uranium matrix was discussed in chapter three, the present study deals with the simultaneous separation of Mo B, F and Cl as molybdate, borate, fluoride and chloride ions and their subsequent IC separation and determination. For the determination of boron by IC, use of mannitol in the eluent is necessary to convert

the weak H_3BO_3 into a strong anion complex form, which is amenable for the anion exchange separation [23]. During the IC separation, it was observed that MoO_4^{2-} peak area decreased with increasing mannitol concentration. In general, the decrease in peak area could be due to the effect of complexation, however, such effect should cause change in retention time of the analyte which was not observed in this case. Proper investigation was carried out to understand this behavior of mannitol and molybdate. The retention behaviors of these ions was studied on different anion exchange columns as well as with different mobile phase compositions. The study resulted in many interesting observations and based on results obtained, the unusual behavior was explained on the basis of complexation of Mo with mannitol at different pH and deprotonation of mannitol.

References:

1. http://www.barc.gov.in/about/anushakti_sne.html.
2. P. K. Vasudev, *Electrical India*, 54(2014)28.
3. G. Gopalkrishnan, *Annual Review of Energy and Environment*, 27(2002)369.
4. S. K. Patil, *Materials Science Forum*, 48(1989)371.
5. N. K. Rao, H. C. Shri, K. K. Katiyar, U. C. Sinha, et. al., *J. Nucl. Mater.*, 81(1979)171.
6. N. Kondal Rao, *J. Nucl. Mater.*, 106(1982)273.
7. B. Laxminarayanan, P. S. A. Narayanan, *Characterisation and Quality Control of Nuclear Fuels*, CQCNF-2002, Allied publication, pg. 578.
8. Y. Shimomura, W. Spears, *IEEE Transactions on Applied Superconductivity*, 14(2)(2004)1369.
9. T. V. Vittal Rao, Y. R. Bamankar, S. K. Mukerjee, *J Nucl Mater.*, 426(2012)102.

10. M. Krachler, R. Alvarez-Sarandes, S. V. Winckel, J. Radioanal. Nucl. Chem., 304(2015)1201.
11. I. G. Alonso, J.F. Babelot, J. P. Glatz, O. Cromboom, L. Koch, Radiochim. Acta., 62(1993) 71.
12. A. M. Meeks, J. M. Giaquinto, J. M. Keller, , J. Radioanal. Nucl. Chem., 234(1998)131.
13. D. Suzuki, F. Esaka, Y. Miyamoto, M. Magara, Appl. Radiat. Isot., 96(2015) 52.
14. Y.Y. Ebaid, Rom. Journ. Phys., 55(2010) 69.
15. A. M. Sanchez, F. V. Tome, J. D. Bejarano, M. J. Vargas, Nucl. Instrum. Methods Phys. Res. Sect. A, 313(1992)219.
16. G. C. Jain, K. B. Khan, S. Majumdar, H. S. Kamat, C. Ganguly, Characterisation and Quality Control of Nuclear Fuels, CQCNF-2002, Allied publication, pg. 376.
17. A. Kelkar, A. Prakash, M. Afzal, J. P. Panakkal, H. S. Kamath, J. Radioanal. Nucl. Chem., 284(2010)443.
18. P. R. Haddad and P. E. Jackson, Journal Of Chromatography Library - volume 46, Ion Chromatography Principles and Applications.
19. S. E. Y. Li, Journal Of Chromatography Library- volume 52, Capillary Electrophoresis Principles, practice and applications.
20. Determination of Aluminum in Complex Matrices Using Chelation Ion Chromatography, Dionex, Application note, AN 69, 1991.
21. A. Riaz, B. Kim, D. S. Chung, Electrophoresis, 24(2003)2788.
22. Ticiane Taflik, J. Braz. Chem. Soc., 23(2012)488.
23. S. Jeyakumar, V. V. Raut, K. L. Ramakumar, Talanta, 76(2008) 1246.

24. K. U. Rempel, A. A. Migdisov, A. E. Williams-Jones, *Geochim. Cosmochim. Acta.*, 70(2006) 687.
25. S. C. Chetal, P. Chellapandi, P. Puthiyavinayagam, S. Raghupathy, Balasubramanian, et. al. *Asian Nuclear Prospects*, 7(2011)64.
26. S.P. Mirjana, Z. P. Nebojsa, M. Momir, *J Anal At Spectrom.*, 4(1989)587.
27. C. Hennig, K. Servaes, P. Nockemann, et. al. *Inorganic Chemistry*, 47(2008)2987.
28. C. Hennig, J. Tutschku, A. Rossberg, G. Bernhard and A. C. Scheinost, *Inorganic Chemistry*, 44(2005) 6655.
29. J. Bjerrum, *Acta Chem. Scand. Series A*, 41(1987)328.

List of Figures

Fig. 1.1	Indian three stage nuclear program	3
Fig.1.2	Nuclear fuel cycle	4
Fig.1.3	Metallic fuels designed for FBR.	8
Fig.1.4	Fusion Reaction using deuterium and tritium	9
Fig. 2.1	Major types of Chromatography	32
Fig. 2.2	Schematic representation of Ion Exchange mechanism	35
Fig. 2.3	A typical Van Deemter plot	41
Fig. 2.4	Block diagram for an Ion Chromatography system	43
Fig. 2.5	Schematic representation of an Ion Chromatography system designed for radioactive samples	44
Fig. 2.6	Capillary Electrophoresis instrumentation	47
Fig. 2.7	Gibb's free energies of formation of various compounds	53
Fig. 2.8	Basic Pyrohydrolysis instrument	56
Fig. 2.9	The modified Pyrohydrolysis apparatus for Glove Box operation	57

- Fig. 3.1** Chromatogram of an anion mix standard containing F⁻ (0.5 ppm), Cl⁻ (1.0 ppm), NO₃⁻ (2.0 ppm), SO₄⁻² (2.0 ppm), and MoO₄²⁻ (10.0 ppm): column, IonPac AS-16; eluent, 15 mMNaOH; flow rate, 1 mL min⁻¹. 65
- Fig. 3.2** Isothermal thermograms of ~3 mg of MoO₃ at different temperatures and carrier gas conditions: (a) 1073K in dry Ar carrier gas; (b) 1073K in moist Ar carrier gas; (c) 1273K in moist Ar carrier gas; (d) 1473K in moist Ar carrier gas. 66
- Fig. 3.3** Recovery curve in moist O₂ carrier gas (a) for UO₂ + MoO₃ mixture standard containing 100 and 500 ppm Mo and (b) for UMo alloy standard containing 500 and 5000 ppm Mo. 68
- Fig. 3.4** XRD patterns of UO₂ and MoO₃ mixture recorded after (a) 1/2, (b) 1, (c) 1 1/2, and (d) 2 h of pyrohydrolysis. The downward arrow symbol indicates a few major peaks for MoO₃ 71
- Fig. 3.5** XRD patterns of (a) UMoO₆ powder and (b) U₃O₈ formed after pyrohydrolysis of UMoO₆ (all peaks are characteristic to U₃O₈): carrier gas, moist O₂; time, 2 1/2 h; temperature, 1273K. (c) The picture of UMoO₆ before and after pyrohydrolysis. 73

- Fig. 4.1** Pyrohydrolysis of U-6%Zr sample. (Conditions: 900⁰C moist Ar) 85
- Fig. 4.2** XRD patterns of pyrohydrolysed products of U-Zr alloy heated in moist Ar atmosphere at 900⁰C for (a) 10 min., (b) 30 min., (c) 50 min. and (d) 90 min. (o and * represent UO₂ and α -U₃O₈, respectively). 87
- Fig. 4.3** TG and DTA of U-Zr alloy in dry air with a heating rate of 10⁰C/min 90
- Fig. 4.4** XRD patterns of pyrohydrolysed product of (a) U-Zr and (b) U-Pu-Zr alloy heated in moist oxygen atmosphere at 900⁰C for 30 min. (* and # represent (α -U₃O₈)_{ss} and (PuO₂)_{ss}, respectively) 92
- Fig. 4.5** Chromatograms for different distillates analysed by IC. (a) standard solution, (b) blank run, (c) U₃O₈ standard (d) U-Zr sample and (e) U-Pu-Zr samples. 94
- Fig. 5.1** A standard sample chromatogram. Peaks 1–7 are (1) Li (2 mg/L), (2) Na (2 mg/L), (3) NH₄⁺, (4) K (5 mg/L), (5) Cs (5 mg/L), (6) Mg (3 mg/L) and (7) Ca (5 mg/L). Column: Ion Pac CS12; Eluent: 20 mM MSA; Flow rate 1 ml/min. 102

- Fig. 5.2** A typical sample chromatogram obtained for a sampleColumn: Ion Pac CS12; Eluent: 20 mM MSA. Flow rate 1mL/min. Detection Suppressed Conductivity. 103
- Fig. 5.3** Capillary 50 μm (i.d.) 9 60 cm (total length), BGE 20 mM Imidazole pH 2 Sample: (K, Na, Ca, Mg, Li) Li 1 mg/L others 0.5 mg/L. 105
- Fig. 5.4** Capillary 50 μm (i.d.) and 60 cm (total length), BGE 20 mM Imidazole pH 2, Sample: (real sample having 2.1 mg/L Li) 106
- Fig. 5.5** Calibration plot of peak area/peak time versus Li concentration. 106
- Fig. 6.1** Electropherograms obtained for a standard iron solution ($25 \text{ mg}\cdot\text{L}^{-1}$) with BGEs of different pH. 116
- Fig. 6.2** Effect of total chloride concentration on the peakarea of iron obtained with pH 2. (BGEs were of 10⁻² M HCl(fixed) and varying amounts of KCl). Capillary: 60 cm \times 50 μm , Applied voltage: 15 kV; Detection: direct UV at 214nm. 118
- Fig. 6.3** .Electropherograms obtained for a standard solution of Fe(III) and Uranium. (A) Fe(III) (5 $\mu\text{g}/\text{mL}$) + U(VI) (80,000 $\mu\text{g}/\text{mL}$) standard solution; (B) Fe(III) standard solution (1 $\mu\text{g}/\text{mL}$); (C) Fe(III) (0.08 $\mu\text{g}/\text{mL}$) standard 120

solution. BGE: 10 mM HCl in 65 mM KCl (pH 2),
Conditions: Capillary: 60 cm × 50 μm, Applied voltage:
15 kV. Detection: direct UV at 214 nm.

- Fig. 6.4** A typical electropherogram obtained for a sample solution. 124
- Fig.7.1** Effect of [NaOH] on the retention times of various anions. 134
(a) IonPac AS18 column and (b) IonPac AS16 column.
- Fig.7.2** Standard chromatograms obtained for standard with F⁻, Cl⁻, NO₃⁻ and SO₄²⁻(10.0 ppm each). (a) Column: AS16 column, Eluent: 15 mM NaOH. (b) Column: AS18 column, Eluent: 40 mM NaOH. 135
- Fig.7.3** The optimised reuse of LiOH washing solution. A, B, C, and D are different Li₂TiO₃ lots, the numbers 1, 2, 3 represent no. of washing. The washing solution containing lower impurity are reused for samples containing higher impurities 137
- Fig.7.4** Concentration of chloride and nitrate in wash solutions collected at different steps of optimised washing 137

method.

- Fig.7.5** Chromatograms obtained for the Li_2TiO_3 pyrohydrolysis distillates (a) before washing (initial product) (b) after washing. 138
- Fig.8.1** (a) Peak height of molybdatepeak(20ppm) (b) retention time of anions; Column: IC-Pak anion, Eluent: NaHCO_3 (0.01755M) and d-mannitol (concentration varied), flow rate 1 ml/min. 147
- Fig.8.2** (a) Peak height of molybdatepeak(20ppm) (b) retention time of anions; Column: Ion Pac AS16, Eluent: NaHCO_3 (0.01755M) and d-mannitol (concentration varied), flow rate 1 ml/min. 149
- Fig.8.3** Retention time of anions; Column: Ion Pac AS16, Eluent: NaOH (30mM) and d-mannitol (concentration varied), flow rate 1 ml/min. 150

Fig.8.4 (a) Peak height of molybdate peak (5ppm); No separation Column, Eluent: NaOH(30mM) and d-mannitol (concentration varied), flow rate:0.1ml/min. 151

Fig.8.5 Retention time of anions; Column: Ion Pac AS16, Eluent: NaOH(30mM) and boric acid(concentration varied), flow rate 1 ml/min. 153

List of Tables

Table.1.1	Different ceramic fuels and their composition used for Indian nuclear reactors.	6
Table.1.2	Breeding ratio and doubling time comparison of different nuclear fuels.	8
Table.1.3	Specification limits of metallics for thermal and fast reactor fuels.	14
Table.1.4	Specifications for non metallics.	20
Table.3.1	Minimum Time Required for Recovery of Mo Better than 95%, from Alloy and Oxide Standards.	69
Table.3.2	Comparison of results obtained for ADU Samples by the Developed Method, Solvent Extraction Followed by ICP-AES, and Pyrohydrolysis followed by ICP-AES Methods.	76
Table.4.1	Chemical analysis of U, Pu and Zr from U-Zr and U-Pu-Zr alloy.	84
Table.4.2	The summary of products identified by XRD on heat	88

	treatment of U-Zr alloy.	
Table.4.3	Pyrohydrolysis data for U-6wt%Zr alloys sample for varying time using moist oxygen as a carrier gas.	89
Table.4.4	Pyrohydrolysis data for U-19 wt% Pu-4.7 wt% Zr alloyssample for varying pyrohydrolysis time, with moist oxygen as carrier gas.	91
Table.4.5	The summary of products identified by XRD on heat treatment of U-Zr and U-Pu-Zr alloys.	92
Table.4.6	F and Cl content of some routine samples analysed by pyrohydrolysis using moist oxygen.	94
Table.5.1	Comparison of Li percentage determined by CE and IC in Li-Al alloy samples.	107
Table.6.1	Recoveries of spiked iron in uranium solutions of various concentrations.	121
Table.6.2	Comparison between iron determination via the developed method and certified method.	123
Table.6.3	Results obtained for the samples.	124

Table.7.1	chlorine obtained for real samples of Li_2TiO_3 finished products.	139
Table.8.1	The optimized gradient elution program for simultaneous separation and determination of B, Cl and Mo. Column: Ion Pac AS16, flow rate 1 ml/min.	155
Table.8.2	The concentration of B, Cl and Mo obtained in dried plant samples and Soil PH distillates by the developed IC method and their comparison with conventional methods.	156

Chapter: 1

Introduction

1.1 Basics of nuclear energy:

Nuclear energy is produced either by nuclear fission or nuclear fusion. In practice the nuclear energy or power is generated by carrying out nuclear fission in a nuclear reactor. The nuclear fuel materials have fissile isotopes such as ^{235}U , ^{233}U and ^{239}Pu . [1, 2]. Nuclear fuels contain both fissile and fertile isotopes, which on interaction with neutrons undergo fission. In every fission process two or three neutrons are produced and they help the self-sustaining chain reaction which releases energy with a controlled rate in a nuclear reactor. ^{235}U and ^{239}Pu are the commonly used fissile isotopes in nuclear reactors. Among the uranium isotopes ^{235}U is a naturally available fissile material whereas it's another fissile isotope, ^{233}U is not available in nature. ^{233}U is obtained by the neutron irradiation of thorium (Th) in a nuclear reactor. Thorium nuclei absorb neutrons and get converted into ^{233}U . Plutonium (^{239}Pu), another fissile material formed due to the irradiation of ^{238}U with neutrons. Thus ^{238}U and ^{232}Th are also valuable nuclear resources, and are called fertile materials, [3-6] as they can be converted into fissile material for fuelling nuclear reactors.

1.2 Indian Nuclear Program:

Nuclear Energy is an important and perhaps inevitable option for the country for its energy security in the long run. Nuclear energy is needed not only for producing electricity but also for meeting non-electricity energy needs. In comparison to other fossil fuels, nuclear power requires less quantities of fuel. No other source of energy

can produce such an amount of power from a very small quantity of material [7,8]. Moreover it is also a green source of energy. To utilise the large abundant of thorium in India, Dr. Homi J. Bhabha envisaged a three-stage Indian nuclear power program in 1954 [9-11].

Stage 1: In the first stage natural uranium is used in pressurized heavy water reactors (PHWR) to produce electricity and ^{239}Pu . PHWR uses natural uranium as fuel and heavy water as moderator and coolant. Plutonium produced is separated from the spent fuel in plutonium reprocessing plants.

Stage 2: The second stage deals with the fast reactor technology. In the second stage the plutonium obtained from the first stage is mixed with uranium (as a mixed-oxide (MOX) or as metallic fuel) and used in the Fast Breeder Reactors. The fast breeder reactors will fission plutonium for power and breed more plutonium from the ^{238}U . Thorium will also be used in the reactor to produce ^{233}U .

Stage 3: The third stage of Indian nuclear programme envisages utilisation of thorium in place of uranium for power generation. Advanced heavy water reactors (AHWR) will be used in this stage. Power will be generated from the ^{232}Th - ^{233}U fuel aided by plutonium. Currently this stage is still in the research stage [12]. Bhabha Atomic Research Centre is developing an advance heavy water reactor that will use both thorium ^{233}U and thorium-plutonium mixed oxide as fuel.

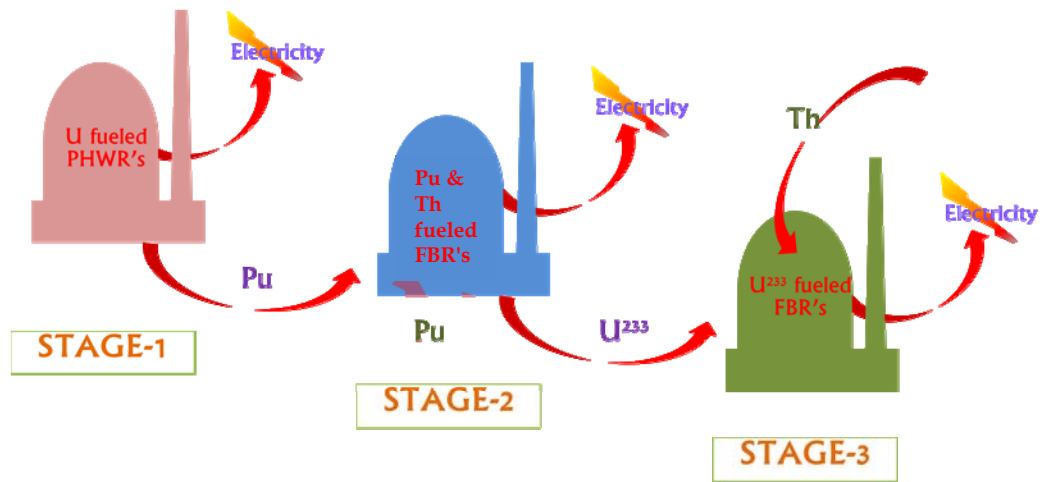


Figure 1.1: Indian three stage nuclear program

1.2.1 Nuclear fuel cycle:

The nuclear fuel cycle consists of mining, separation, refining, purifying, utilising as fuel and ultimately disposing of the nuclear waste generated. The nuclear fuel cycle, include a series of stages through which nuclear fuel progresses. The nuclear fuel cycle is divided into two parts namely front end and back end. The front end of the fuel cycle deals with all the processes (right from mining to fabrication) that are involved before the use of fuel in the reactor. The back end fuel cycle consists of reprocessing of the spent fuel and recovery procedures. If spent fuel is not reprocessed, the fuel cycle is referred to as an open fuel cycle (or a once-through fuel cycle); if the spent fuel is reprocessed, it is referred to as a closed fuel cycle [13, 14]. India is following close end fuel cycle [15] and following are the various processes. Figure 1.2 depicts the close end fuel cycle that India follows.

- (i) Uranium extraction from uranium ore, and conversion to yellowcake
- (ii) Conversion of yellow cake into uranium hexafluoride (UF₆)
- (iii) Enrichment to increase the concentration of U²³⁵ in UF₆

- (iv) Fuel fabrication to convert enriched UF_6 into fuel for nuclear reactors
- (v) Use of the fuel in reactors
- (vi) Interim storage of spent nuclear fuel
- (vii) Reprocessing (or recycling) of high-level waste
- (viii) Final disposal of high level waste.

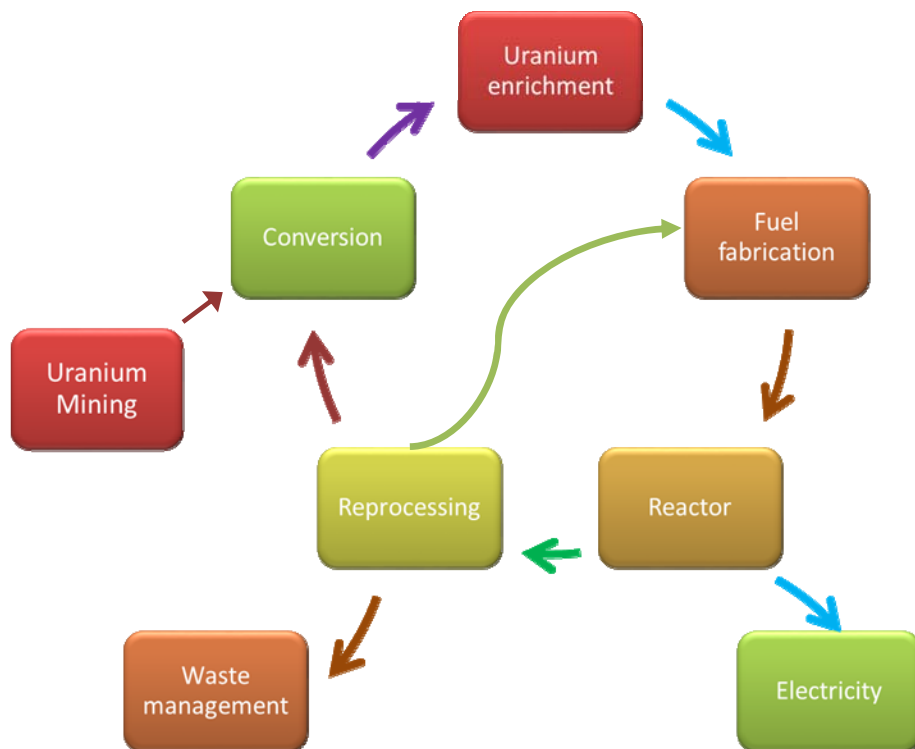


Figure 1.2: Nuclear fuel cycle

1.2.2 Types of nuclear fuels:

Typically, depending on the nature of nuclear reactor, different types of fuels are used. These are classified as, (i) ceramic fuels (ii) intermetallic fuels (iii) metallic fuels (iv) composite fuels and (v) advance fuels.

(i) Ceramic Fuels: The ceramic fuels are categorised into oxide and non-oxide ceramic fuels. The oxide fuels are oxides of U, Pu and mixed oxides of U and Pu (eg. UO_2 , and $(\text{U,Pu})\text{O}_2$) whereas the materials like $(\text{U,Pu})\text{C}$ and $(\text{U,Pu})\text{N}$ are known as non-oxide ceramic fuels.

Uranium oxide and mixed oxide fuels: Natural UO_2 is used as fuel in PHWR which uses heavy water as coolant and moderator. The boiling water reactor (BWR) and pressurised water reactor (PWR) use light water as coolant and moderator. As light water (H_2O) has somewhat higher absorption cross section for thermal neutrons, to compensate for their loss, UO_2 with some enrichment (up to 3% U-235 as against natural abundance of 0.72%) is employed. MOX fuels with 0.4% and 4% Pu are also being tested in combination with UO_2 in PHWR and BWR, respectively to realise higher energy output without significant changes in the reactor design.

The oxide fuels are chemically stable and compatible with water. They also show high temperature and high irradiation resistance. In addition to this, India has expertise on the fabrication of oxide fuel and complete knowledge on the oxide fuel performance in the reactor. Due to the above advantages of the oxide fuels and their compatibility with liquid Na, MOX fuels are the preferred choice for FBRs [16-18]. The proposed AHWR reactor designed for Th utilization will be using mixed oxide fuels of U, Pu and Th. Table 1.1 lists out the use of different ceramic fuels in various Indian nuclear reactors.

Table1.1: Different ceramic fuels and their composition used for Indian nuclear reactors.

Reactor	PHWR	BWR	PFBR	FBTR
Fuel composition	0.4%PuO ₂ (inside 7 pins)	UO ₂ of different enrichment,	(U _{0.79} Pu _{0.21})O ₂ (Inside)	(U _{0.3} Pu _{0.7})C (MKI)
	Nat.UO ₂ (outside 12 pins)	Low 0.9%	(U _{0.72} Pu _{0.28})O ₂ (outside)	(U _{0.45} Pu _{0.55})C (MKII)
		Med 1.55%		
		High 3.25%		

Non-oxide ceramic fuels (Carbide and Nitride): The non-oxide ceramic fuels have certain advantages such as better thermal conductivity, denser fissile content and better breeding ratio over the oxide fuels. The Fast breeder test reactor at Kalpakkam utilises the mixed carbides of U and Pu, (U,Pu)C, as fuel [19]. Since the FBTR core is smaller in size it requires fuel with high fissile content, mixed carbide fuel, it was considered for FBTR. However, due to their pyrophoric nature, their handling and fabrication call for enhanced safety requirements.

(ii) Intermetallic fuels: Uranium intermetallic fuels such as U–Al, U–Si, and U–Mo are mainly used in research and test reactors for neutron production [20, 21]. As compared to ceramic fuels intermetallic fuels can achieve higher densities thereby requiring lower fuel inventories. APSARA research reactor at Bhabha Atomic Research Centre was using U-Al based intermetallic fuel which is now modified to U-Si based intermetallic fuel to reduce the U enrichment requirements.

(iii) Composite fuels: Composite fuels consist of a fissile element phase dispersed in an inert matrix [22]. Composite fuels are of two types; cermet fuels and cer-cer fuels. Cermet fuels consist of ceramic fuel particles dispersed in a metallic matrix whereas the Cer-cer fuels consist of ceramic fuel particles dispersed in a ceramic matrix [23]. Cermet fuel cores are most often metallurgically bonded to the cladding material to improve heat transfer from the fuel core to the coolant. The composite fuels are generally considered for the research and test reactors, however, due to the higher fissile density, better thermal conductivity and possibility of improving breeding ratio these fuels are also being considered for fast breeder reactors. These fuels are also being considered for irradiation and power production from plutonium and minor actinides.

Metallic fuel: Metallic fuels have higher densities of fissile and fertile materials and high thermal conductivity. They are capable of providing high breeding ratio. Hence, they are considered to be suitable for fast reactors [24-27]. Table 1.2 gives a summary of some metallic fuels and their breeding ratio and doubling time. Metallic fuels are known to cause problems due to high swelling. Such problems were circumvented by reducing the fuel smear density to ~ 75% and by fission gas release before fuel-cladding contact. Mechanically bonded U-Pu binary fuels as well as sodium bonded U-Pu-Zr alloys (figure 1.3) are being considered as the most suitable metallic fuel compositions due to their solidus temperatures and compatibility with stainless steels. The spent metallic fuels can be reprocessed by pyro-process recycling method, which was economically more attractive than the PUREX method of reprocessing. Few metallic fuels were put into FBTR for test purposes and also to understand their behavior. It is expected that India would go for its fast reactor

program based on metallic fuels in future to achieve significant growth in nuclear power.

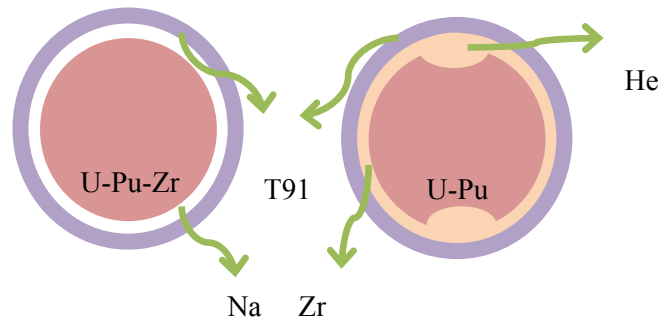


Figure 1.3: Metallic fuels designed for FBR.

Table 1.2: Breeding ratio and doubling time comparison of different nuclear fuels.

Fuel Material	U-Pu Oxide	U-Pu Carbide	U-Pu-10% Zr	U-Pu-6% Zr	U-Pu with 150 μ Zr liner
Breeding Ratio	1.09	1.19	1.36	1.47	1.56
Doubling time (y)	40	20	9.4	7.2	7

1.2.3 Fusion Energy:

Fusion can provide large amounts of energy and does not cause any adverse effects on the environment. One of the most prominent nuclear fusion reactions is that between deuterium and tritium. The former can be obtained from the seawater whereas the latter is obtained by the neutron irradiation of lithium blanket material. Further, a fusion reactor will produce only short lived radioactive waste products [28, 29].

During the fusion of deuterium and tritium an alpha particle is produced with a high energy neutron (figure 1.4). Moreover, this fusion requires low activation energy and thus low temperature as compared to other nuclear fusion reactions between H and T or H and D.

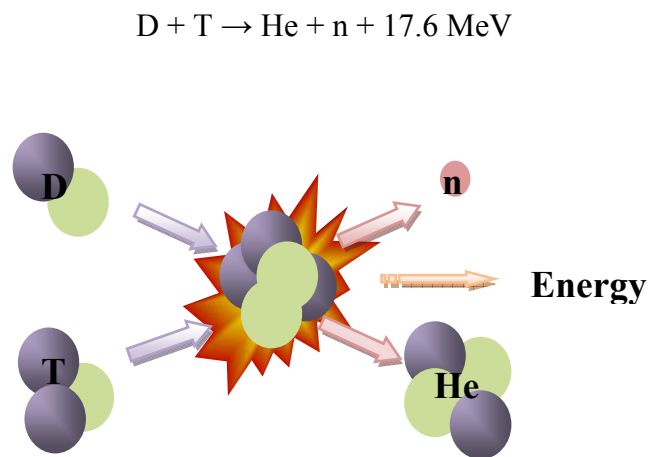


Figure1.4: Fusion Reaction using deuterium and tritium.

The International Thermonuclear Experimental Reactor (ITER) is envisaged with a view to demonstrate the possibility of generating electricity by fusion reaction. India is one of the participating countries in the ITER project financially and scientifically. Nuclear fusion research in India is primarily carried out in BARC and Institute of Plasma Research (IPR). Many research programmes are being pursued to develop Test Blanket Modules (TBM) in order to demonstrate the production and extraction of tritium [30-33]. ITER will be using lithium compounds for tritium breeding. Among the solid lithium compounds the ceramic matrices are preferred due to their more favourable physical characteristics in intense neutron fluxes and at high temperatures [34-36]. Lithium-containing ceramics such as Li_2O , LiAlO_2 , Li_4SiO_4 , Li_2ZrO_3 and Li_2TiO_3 have been considered as candidates for tritium breeding materials. The tritium breeder blanket serves two primary functions in the fusion reactor. One is breeding tritium and the second is converting the released energy into heat. Both the functions are very important for the successful operation of a fusion power reactor. The breeder materials should:

1. breed and release tritium,
2. possess physical and chemical stability at high temperature,
3. display compatibility with other blanket components, and
4. exhibit adequate irradiation behaviour. Studies revealed that Li_2TiO_3 is the most preferred material for TBM and therefore, it was developed and fabricated at BARC [37, 38].

1.2.4 Chemistry in nuclear fuel cycle:

Optimum utilization of fissile content in the nuclear fuels during reactor operation can result in increasing power production. Improving the fuel quality is one of the criteria to ensure longer residence time of fuel in the reactor. This in turn results in higher burn-up leading to enhanced power. Reactor physicists and fuel fabricators stipulate certain quality (specifications) to the nuclear fuel and other reactor materials for this purpose. In order to realise the smooth and efficient functioning of the reactor, the fuel should satisfy the specifications derived for it. The specification includes both physical and chemical qualities of the material. The chemical analyses pertaining to the Chemical Quality Control (CQC) process play a pivotal role in achieving the quality of the nuclear material fabricated into nuclear fuel. In addition to the nuclear fuels, strategically important nuclear materials like tritium generators [39] etc., also require determination of percentage and trace level components for their optimum performance during reactor irradiation. As India is involved in the International Test Experimental Reactor (ITER) project (a fusion based reactor programme) and DAE supports this programme by fabricating tritium breeders (Li_2TiO_3) employing different methods [38], the requirement for development of analytical methods for the analysis of tritium breeders for their chemical characterization need not be over emphasized.

Several analytical techniques are employed for the chemical characterization or CQC analysis of nuclear materials [40]. Among them, elemental determinators, ICP-AES [41], ICP-MS [42, 43], TIMS [44], alpha and gamma spectrometry [45, 46], XRD [47], electro analytical techniques, spectrophotometer etc. are some of the important techniques routinely employed for chemical characterisation analysis. In the recent past chromatographic techniques like High Pressure Liquid

Chromatography (HPLC) and Ion Chromatography (IC) have been introduced into the CQC analyses of nuclear materials [48]. Some of the techniques used for CQC measurements are described below:

1.2.4.1 Determination of major elements: Electroanalytical techniques are mainly used for the determination of U and Pu in nuclear fuel materials. The electroanalytical methods are capable of analysing the fuel samples with a precision better than 0.2 % [49, 50]. Complexometric titration using EDTA is employed for the determination of thorium in the Th containing fuels [51, 52]. Determination of Zr in metallic fuels is mainly carried out by gravimetric methods, where Zr is selectively precipitated as its mandelate complex in hydrochloric acid medium [53].

(i) Determination of metallic impurities: Every fuel has a list of specifications for different elements and other parameters with a view to achieve better performance of the fuel as well as to ensure the safe operation of the nuclear reactor. Table 1.3 lists out the specifications for metallic impurities for a variety of fuel materials meant for both thermal and fast reactors.

Atomic Emission Spectroscopy (AES):

DC Arc-AES: Analyses of metallics in the uranium containing fuels are being carried out by converting the uranium into U_3O_8 form. Subsequently a known amount of the sample is mixed with a carrier and loaded to a graphite electrode. The electrode is excited in a DC arc and its emission spectrum is recorded. Solid samples are analysed by using D. C. Arc as an excitation source [54, 55]. However D.C.-Arc method suffers from certain limitations including its poor precision. In the case of Pu bearing materials, a sample mixture of 100 mg (total) was prepared by mixing 5% AgCl, 35% Pu and pure U_3O_8 contributes the rest. While analysing the

plutonium carbide or mixed carbide fuels it is necessary to convert them into their oxide form prior to the analysis. D.C.-Arc method is useful in analysing a group of metallics which includes, Al, Be, Ca, Cd, Co, Cr, Cu, Fe, Li, Mg, Mn, Mo, Na, Ni, Pb, Si, Sn, Ta, V, W and Zn. Their limits of detection are in the range of 0.1 ppm to 100 ppm in nuclear materials. The technique requires precise matching of standard and samples to achieve better accuracy.

Table 1.3: Specification limits of metallics for thermal and fast reactor fuels.

Impurity	Thermal Reactors (ppm _w)			Fast Reactors (ppm _w)		
	UO ₂	PuO ₂	(U,Pu)O ₂	UO ₂	PuO ₂	(U,Pu)O ₂
Ag	1	10	25	1	10	25
Al	25	250	400	25	250	500
B	0.3	2	1	0.3	2	2
Be						10
Ca	50	500	250	50	500	100
Cd	0.2	6	1	0.2	6	1
Co		25	75		25	200
Cr	25	200	400	15	200	300
Cu	20	50	400	10	50	100
Fe	100	500	400	100	500	1000

Gd	0.1	1	1	0.1	1	
Mg	50	200	200	10	200	50
Mn	10	100	400	10	100	200
Mo	4	200	400	2	200	200
Na			400			100
Ni	20	200	400	20	200	500
Pb		200	400		200	200
Sn						10
V			400			100
W					200	200
Zn		200	400		200	100
Zr					100	

ICP-AES: This technique has good sensitivity and also capable of analysing the refractive matrices. In the case of ICP-AES analysis of nuclear fuels require pre-separation of matrix element(s) [56-58]. The chemical separation is carried out mainly by solvent extraction as it provides faster separation. Ion exchange separation is also used in some cases. Elements like Sm, Eu, Gd, and Dy have stringent specifications in the fuels and these elements can be determined with a precision better than 10% at 0.1 ppm. Although this technique is used for the determination of all metallic impurities, it is not recommended for some elements

like Mo, W etc. as they are expected to be lost partially during dissolution of the fuel samples. The use of chemical separation procedures can lead to possibility of contamination and loss of few analytes like Si, W, Sn, Mo etc.

Atomic Absorption Spectroscopy (AAS): AAS is an element specific technique and it requires a characteristic radiation source and a source to atomise the analyte. Atomisation can be achieved by using a flame or Electro Thermal Atomization (ETA). It is possible to analyse solid samples in ETA-AAS with better sensitivity [59]. Determination of all the metal impurities in AAS is a slower process and hence, one element is analysed at a time. Like atomic emission spectroscopy methods, AAS also requires prior separation of matrix element(s). The uranium containing fuels are analysed after the separation of uranium by solvent extraction with tributylphosphate (TBP) in HNO₃. ETA-AAS based methods have been developed for the analysis of Ag, Al, Ca, Cd, Co, Cr, Cu, Fe, Li, Mg, Mn, Na, Ni, Pb, Sb, Sn, and Zn in variety of nuclear materials. Compared to the D.C.Arc.-AES, the atomic absorption procedure, though longer, provides better sensitivity and precision.

ICP-MS: ICP-MS is one of the versatile analytical tools for carrying out trace and ultra-trace level analysis. It is a rapid and highly sensitive technique [60]. ICP-MS provides quantitative determination as well as isotopic ratios or composition. Therefore, it is possible to detect the isotopes that unnatural isotope abundances. Along with the multi-elemental capability it has very low limit of detection (LOD) i.e. in the range of 1-10 ppt. ICP-MS gives a precision of 5% or better at the concentration of ppb level, however, at time the method suffers from isobaric interferences and memory effects. One of the limitations of ICPMS analysis is that the dissolved solids in the sample solutions should not be more than 0.4%, and this

demands rigorous sample preparation procedure to the samples of low dissolved contents that are amenable to the ICP-MS analysis. ICP-MS coupled with laser ablation source is a good choice for the solid sample analysis.

Total Reflection X-ray Fluorescence (TXRF): TXRF, an advanced variant of Energy Dispersive X-ray Fluorescence (EDXRF) is a comparatively new technique of material characterization [61]. The geometrical improvements in TXRF help in achieving better detection in comparison to that of EDXRF. It has multi-elemental capability and can analyse most of the elements above $Z=11$. The LOD for the technique is relatively higher (in ppm range) as compared to AES, MS and AAS techniques. Therefore trace impurities present in ppm and above concentration range only can be quantified. The precision of measurements is up to 5%.

Nuclear analytical techniques: In nuclear analytical techniques the material under analysis is subjected to a nuclear reaction by irradiating them with either neutrons or protons followed by the measurement of emitted gamma energy. This technique is widely employed in the characterisation of many nuclear materials such as, zircalloys, stainless steels, Ni alloys, high purity aluminium and graphite and uranium oxide, U-Th mixed oxides, uranium ores and minerals etc. Instrumental neutron activation analysis (INAA) uses neutrons generated in the reactor and is a good technique for medium and high Z elements. Hence, it finds useful in the determination of trace metallic impurities. The detection limit for the method varies from ppb to ppm range depending upon the matrix being analysed. It is a non-destructive direct solid sample analysis technique and provides a good precision up to 1% [62, 63]. However requirement of reactor as the neutron source is one of the set back of the technique that restricts its use.

Spectrophotometry: Spectrophotometry is a simple and economically viable technique for the determination of many metallic and their species. Due to the availability of several multi-elemental techniques with good precision and sensitivity, spectrophotometry is less commonly used. However, it is widely used for the elemental specific analyses where the other workhorse techniques fail. The detection limits (LOD) for many methods lay in the ppb to ppm range. Interferences are the common problems with spectrophotometric methods and therefore, they require suitable masking reagents or other procedures to circumvent the interferences.

1.2.4.2 Isotopic composition analysis:

Isotopic composition of several elements in nuclear fuels and other nuclear materials are being carried out by thermal ionisation mass spectrometry (TIMS) [64, 65]. The isotopic composition of uranium and plutonium are analysed for every fuel material to ascertain the fissile element(s) content(s). Other important nuclear materials like boron, cadmium, gadolinium, zirconium, heavy water etc. are also analysed for the isotopic composition. In the case of plutonium and uranium, analytical methods based on gamma spectroscopy are also available for determining isotopic composition.

1.2.4.3 Determination of Non-metallics: Analyses of carbon, nitrogen, phosphorus, sulphur, chlorine, fluorine, hydrogen, moisture, total gas content etc. are some of non-metallic analyses. Quantification of carbon is based on the combustion method wherein the C present in the sample is converted into CO₂ at 1273K in a graphite or alumina crucible using copper or tungsten as an accelerator in presence of oxygen flow. The CO₂ thus formed is purified and detected by thermal conductivity or

infrared (IR) detection [66]. The oxygen present in the fuel is determined by inert gas fusion method. Sample is fused at 2773K in He/Ar flow in graphite crucible. The oxygen present in the sample forms CO which is determined by IR [67]. Nitrogen present in the sample can be determined by the inert gas fusion or Kjeldahl distillation methods [68]. In fusion method sample is fused in graphite crucible at 2773K. N₂ thus produced in the process is purified and determined by thermal conductivity measurements. Hydrogen is also determined by inert gas fusion method where the fusion is carried out at lower temperature of 2273K without any flux. After purification and separation using a GC column, hydrogen is determined by thermal conductivity [69]. Sulphur is determined by combustion to form SO₂, followed by IR detection or by a mass spectrometer [70].

Chlorine and fluorine in the samples are determined by a two-step method. The halides were separated by pyrohydrolysis technique followed by their quantification using spectrophotometry or ion chromatography [71]. During the pyrohydrolysis separation the solid sample is subjected to action of heat and moisture simultaneously in presence of a carrier gas. This converts the F and Cl into HF and HCl, respectively and they are trapped in a dilute NaOH solution. Pyrohydrolysis is the only separation technique available for separating chlorine and fluorine in low concentrations. Dissolution of samples using acids or fusion methods are not useful in determining the halides as the reagents contribute significant amount of these halides leading to introduction of high blank. Ion chromatography is being employed for the routine analysis of Cl and F in the fuels as the concentration of these halides normally found to be less than 10 ppm. Although a few nuclear analytical techniques have been reported for the determination of Cl and F in several nuclear materials, they do not find much use in the routine CQC measurements.

Boron, a non-metal, is included in the list of metallic impurities. The concentration of boron in the nuclear materials is often determined by D.C.Arc-AES method along with other metallic impurities. Alternatively, selective separation of boron using diols followed by spectrophotometric determination with curcumin as chromogenic agent is a sensitive method [72]. Nuclear analytical methods were also reported for the determination of boron in different matrices. Boron in many nuclear and other materials (solid samples) can be separated by pyrohydrolysis and trapped as boric acid in dilute NaOH [73]. The pyrohydrolysis distillate thus obtained can be analysed for boron content by IC, ICP-MS, ICP-AES, AAS and spectrophotometer. Table 1.4 lists the specification limits of non-metallics in several nuclear fuel materials.

Table1.4: Specifications for non metallics.

Elements	UO ₂	PuO ₂	(U,Pu)O ₂	(U,Pu)O ₂	(U,Pu)C	(U,Pu)C	
			(Thermal)	(Fast)	(Mark-1)	(Mark-2)	
O/M			1.98-2.02	1.98 ± 0.002)	± 1.025	± 1.025	±
C/M				0.02	0.005	0.005	
M₂C₃					5-20%	5-20%	
C	150 ppm	200 ppm	200 ppm	300 ppm	(4.8± 0.25)%	(4.8± 0.25)%	
N	200 ppm	200 ppm	100 ppm	200 ppm			

O					6500 ppm	5000 ppm
O+N					7500 ppm	6500 ppm
H		1 ppm	3 ppm			
S	300	300	50 ppm			
	ppm	ppm				
Cl	25 ppm	50 ppm	15 ppm	25 ppm	25 ppm	25 ppm
F	25 ppm	25 ppm	10 ppm	25 ppm	25 ppm	25 ppm
H₂O	5000		10 ppm	30 ppm		
	ppm					
B	10 ppm	10 ppm	1 ppm	3 ppm	4.5 ppm	4.5 ppm
B. Eq.		2 ppm	5.5 ppm	5.5 ppm	5.5 ppm	5.5 ppm

1.2.5 Scope of Present Investigations:

The CQC processes of various nuclear materials as mentioned above demand the development of new analytical methodologies. Improvement in the existing methodologies is also desirable for realizing higher accuracy and precision, low detection limit, high selectivity, simultaneous or multi-elemental analysis, minimum generation of analytical waste and minimum use of chemical reagents etc.

Analytical methods which can analyse directly the dissolved sample solutions are preferred as they eliminate the cumbersome sample preparation procedures. Few applications of CE and IC, where direct analysis of the dissolved sample solution

without employing matrix separation have been reported in literature [74, 75]. Such direct analyses not only avoid the pre-separation of matrix or pre-concentration of analytes but also useful in the absence of reference materials.

As discussed in the preceding sections that spectrometric techniques like AES, ICP-MS, AAS etc. have been used for the material characterisation analysis on routine basis. Electro-analytical techniques also find immense applications in the analysis of major components. However these methods sometime suffer from several limitations such as interferences, poor sensitivity, labour-intensive sample preparations etc. Chromatography methods offer simultaneous separation as well as quantification and therefore, chromatography techniques like ion chromatography, HPLC etc. are being introduced in the chemical characterisation analysis. Ion chromatography is a useful technique for the determination of common anions and cations whereas reversed phase ion interaction chromatography is used for the separation and determination of both transition and inner transition elements [76-79]. Moreover, the chromatography separations can be used for the speciation studies. For example chromatography methods can distinguish different metal oxidation states, such as Cr(III) and Cr(VI) and also Fe(II) and Fe(III) [80,81]. Different methods for the use of IC in nuclear industry have been reported in literature. Separation of fission products, trace impurities, lanthanides along with different actinides are some of them to be mentioned [82, 83] where ICP-MS was used as the detector. IC coupled to scintillation detector has also been used for alpha active actinide separation and determination [84, 85]. Ion interaction chromatography (IIC) has been used for determination of lanthanides, uranium, thorium and plutonium in irradiated fuel samples [86]. IC has been significantly contributing in analysing the distillates

obtained from pyrohydrolysis of fuel samples [73] for boron and halides. However considering the ability of the method its full potential has not been utilised.

Like ion chromatography, capillary electrophoresis (CE) is another technique which can be used for simultaneous separation and determination of cations and anions [87-90]. CE with indirect detection has been applied to the analysis of inorganic anions, cations, organic acids, alkali metals, amino acids, and nucleotides [91, 92]. Lanthanides, transition metal ions and alkali and alkali earth metals have been analysed in several materials [93-95]. However these methods have not been applied to the analysis of nuclear fuel or other nuclear materials. The method requires nano grams of sample injection, which can reduce radioactive waste significantly. One of the important advantages of the CE is it can be utilised for direct sample analysis without carrying out the matrix separation.

In spite of the unique features of IC and CE, not many applications were reported for the analysis of nuclear materials. Therefore, efforts have been made to utilise these techniques for nuclear material analysis independently and validate the results.

Pyrohydrolysis as a separation technique has found several applications like cement, soil, nanoparticles and nuclear material [96-99]. The term pyrohydrolysis was adopted to describe hydrolytic reactions whose equilibrium constants and higher reaction rates seem to be favoured at higher temperatures. During pyrohydrolysis the sample is heated at high temperature in presence of moist oxygen or a suitable carrier gas. Pyrohydrolysis finds many applications in the determination of halides at trace level concentrations in many complex matrices as it separates halides and boron directly from a solid matrix and provides an interference free clean distillate carrying out trace and ultra-trace level analysis [73,100]. Pyrohydrolysis has been

used to separate halides and B directly from a solid sample [73]. However the method has potential to be used for few other analytes specially metals. The simultaneous separation and determination of anions by IC is very special as similar sensitive and simultaneous analysis of anions is not possible with any other technique. Therefore Pyrohydrolysis and IC form a great combination and have significant potential for application in nuclear material sample analysis.

Analysis of halides and boron in environmental and plant samples involves tedious sample preparation procedures due to the presence of organic compounds. The analytical methods that have been developed for the analyses of nuclear materials involving initial pyrohydrolysis separation followed by analytical determinations can be extended for the analyses of environmental samples.

1.3 References:

1. N.M. A. Mohamed, A. Badawi, Prog. Nucl. Energy, 91, (2016)49.
2. B. R. T. Frost, R. Inst. Chem., Rev., 2(1969)163.
3. M. Jacoby, Chemical and Engineering News, 93(2015)44.
4. K. Anantharaman, V. Shivakumar, D. Saha, J. Nucl. Mater., 383(2008)119.
5. H. M. Mattys, Actinides Rev.,1(1968) 165.
6. J. F. Schumar, J. Nucl. Mater., 100 (I 98 I) 3 1.
7. B. W. Brook, A. Alonso, D. A. Meneley, J. Misak, T.Blees, J. B. van Erp, Sustainable Mater. Technol., 1 (2014)8.
8. F. Javidkia, M. Hashemi-Tilehnoee, V. Zabihi, Journal of Energy and Power Engineering, 5 (2011) 811.
9. A. Gopalakrishnan, Annual Review of Energy and the Environment, 27(2002)369.

10. R. Tongia, V. S. Arunachalam, *Current Science*, 75(1998)549.
11. P.K. Vasudev, *Electrical India*, 54(2014) 28.
12. A. Kakodkar, R.K. Sinha, M.L. Dhawan, IAEA-SM-353/54.
13. F. A. Settle, *J. Chem. Educ.*, 86 (2009)316.
14. R. C. Ewing, *MRS Bulletin*, 33(2008)338
15. Nuclear Fuel Cycle, <http://www.dae.nic.in>
16. H. Stehle, *J. Nucl. Mater.*, 153(1988)3.
17. K. Konno, T. Hirosawa, *J. Nucl. Sci. Technol.*, 39(2002)771.
18. G. A. Timofeev, V. Ya. Gabeskiria, G. A. Simakin, V. B. Mishenev, et. al.
J. Radioanal. Nucl. Chem., 51(1979) 377.
19. U. Basak, P.S. Kutty, S. Mishra, S.K. Sharma, et.al., *BARC News Letter*,
249(2003)191.
20. V.P. Sinha, G.P. Mishra, S. Pal, K.B. Khan, P.V. Hegde, G.J. Prasad, *J. Nucl. Mater.*, 383 (2008) 196.
21. V.P. Sinha, G. J. Prasad, P.V. Hegde, R. Keswani, C.B. Basak, S. Pal, G.P. Mishra, *J. Alloys Compd.* ,473 (2009) 238.
22. W. E. Lee, M. Gilbert, S. T. Murphy, R. W. Grimes, *J. Am. Chem. Soc.*,
96(2013)2005.
23. V. Troyanov, V. Popov, I. Baranaev, *Prog. Nucl. Energy*, 38(2001)267.
24. L. C. Walters, B. R. Seidel, J. Howard Kittel, *Nuclear Technology*,
65(1984) 179.
25. B. R. Seidel, L. C. Walters, Y. I. Chang, *JOM*, 39(1987)10.
26. T. Sofu, *Nucl. Eng. Technol.* 47(2015) 227.
27. G.J. Prasad, *BARC Newsletter*, 332(2013)v.

28. R. Murray, K. E. Holbert, Nuclear Energy: An Introduction to the Concepts, Systems, and Applications, Elsevier, 7th edition (2015)477.
29. T. J. Dolan, Nuclear Energy: Selected Entries from the Encyclopedia of Sustainability science and Technology, Springer (2012)305.
30. Editorial, Nature, 511(2014)383.
31. R. W. Conn, V. A. Chuyanov, N. Inoue, D. R. Sweetman, Scientific American, 266(1992)102.
32. Y. Shimomura, Phys. Plasmas 1 (1994) 1612.
33. John C. Wesley et. al. Phys. Plasmas 4(1997)2642.
34. G. Federici, C.H. Wu, A.R. Raffray, M.C. Billone, J. Nucl. Mater., 187(1992)1.
35. K. Tomabechi et. al., J. Nucl. Mater., 179(1991)1173.
36. Z. Wen, X. Wu, XiaogangXu, ZhonghuaGu, Fusion Eng. Des. 85(2010) 1551.
37. D. Mandal, M. R. K. Sheno, S. K. Ghosh, Fusion Eng. Des., 85(2010) 819.
38. T. V. VittalRao, Y.R. Bamankar, S. K. Mukerjee, S. K. Aggarwal, J. Nucl. Mater., 426(2013) 102.
39. Y. Shimomura, W. Spears, IEEE Transactions on Applied Superconductivity, 4(2)(2004)1369.
40. S. K. Patil, Materials Science Forum,48(1989)371.
41. M. Krachler, R. Alvarez-Sarandes, S. V. Winckel, J. Radioanal. Nucl. Chem., 304(2015)1201.
42. I. G. Alonso, J.F. Babelot, J. P. Glatz, O. Cromboom, L. Koch, Radiochim. Acta., 62(1993) 71.
43. A. M. Meeks, J. M. Giaquinto, J. M. Keller, , J. Radioanal. Nucl. Chem.,

- 234(1998)131.
44. D. Suzuki, F. Esaka, Y. Miyamoto, M. Magara, *Appl. Radiat. Isot.*, 96(2015) 52.
 45. Y.Y. Ebaid, *Rom. Journ. Phys.*, 55(2010) 69.
 46. A. M. Sanchez, F. V. Tome, J. D. Bejarano, M. J. Vargas, *Nucl. Instrum. Methods Phys. Res. Sect. A*, 313(1992)219
 47. G. C. Jain, K. B. Khan, S. Majumdar, H. S. Kamat, C. Ganguly, *Characterisation and Quality Control of Nuclear Fuels, CQCNF-2002*, Allied publication, pg. 376.
 48. A. Kelkar, A. Prakash, M. Afzal, J. P. Panakkal, H. S. Kamath, *J. Radioanal. Nucl. Chem.*, 284(2010)443.
 49. Mary Xavier, P. Nair, K. Lohithakshan, S. Marathe, H. Jain *J. Radioanal. Nucl. Chem.*, 48(1991)251.
 50. P. R. Nair, M. Xavier, S. K. Aggarwal, *Radiochimica Acta*, 97(2009)419.
 51. K. Chander, S. P. Hasilkar, A. V. Jadhav, H. C. Jain, *Journal of J. Radioanal. Nucl. Chem.*, 174(1993)127.
 52. V. N. Rao, G. G. Rao, *Fresenius Zeitschrift fur analytische Chemie*, 155(1957)334.
 53. G. W. C. Milner, A. P. Skewies, *AERE, C/R1126*.
 54. A. Sengupta, V.C. Adya, T. K. Seshagiri, S. K. Thulasidas, S. V. Godbole, V. Natarajan, *Journal of Research in Spectroscopy*, 2014 (2014)1.
 55. A.G.I. Dalvi, C. S. Deodhar, T. K. Seshagiri, M. S. Khalap, B. D. Joshi, *Talanta*, 25(1978)665.
 56. S. K. Thulasidas, M. Kumar, B. Rajeswari, B. A. Dhawale, S. V. Godbole, V. Natarajan, *Instrum. Sci. Technol.*, 43(2015)125.

57. E. A. Huff, D. L. Bowers, *Appl. Spectrosc.*, 44(1990)728.
58. V. C. Adya, A. Sengupta, S. K. Thulasidas, V. Natarajan, *J. Radioanal. Nucl. Chem.*, 307 (2016) 1489.
59. A. L. de Souza, M. E. Barboza Cotrim, M. A. Faustino Pires, *Microchem. J.*, 106(2013) 194.
60. S. F. Wolf, D. L. Bowers, J. C. Cunnane, *J. Radioanal. Nucl. Chem.*, 263(2005)581.
61. N.L. Misra, Sangita Dhara, S.K. Aggarwal, *BARC Newsletter*, 337(2014)1.
62. R. J. Rosenberg, R. Zilliacus, *J. Radioanal. Nucl. Chem.*, 169(1993)13.
63. R. Acharya, *BARC Newsletter*, 337(2014)9.
64. S. K. Aggarwal, G. Chourasya, R. K. Duggal, RadhikaRao, H. C. Jain, *Int. J. Mass Spectrom.*, 69(1986)137.
65. R. K. Webster, A. A. Smales, D. F. Dance, L. J. Slee, *Anal. Chim. Acta.* 24(1960)371.
66. D. Srivatsava, S. P. Garg, G. L. Goswami, *Journal of Nuclear Materials*, 161(1989)44.
67. K. V. Chetty, J. Radhakrshna, Y. S. Sayi, N. Balachander, et. al. *Radiochem. Radioanal. Letters*, 59(1983)161.
68. Z. Z. Yuan, Q. X. Dai, X. N. Cheng, K. M. Chen, *Material Characterisation*, 58(2007)87.
69. V. Venugopal, K. N. Roy, Ziley Singh, R. Prasad, D. Kumar, G. L. Goswami, *Proceedings of Seminar on Fast Reactor Fuel Cycle*, 1(1986)14.
70. Y. S. Sayi, P. S. Shankaran, C. S. Yadav, G. C. Chaparu, et. al. *Proc. Nat. Acad. Sci.* 72(A)(2002)241.

71. M. A. Mahajan, M. V. R. Prasad, H. R. Mhatre, R. M. Sawant, R. K. Rastogi, G. H. Rizvi, N. K. Chaudhuri, J. Radioanal. Nucl. Chem., Articles, 148(1991)93.
72. P. S. Ramajaneyulu, Y. S. Sayi, V. A. Raman, K. L. Ramakumar, J. Radioanal. Nucl. Chem., 274(2007)109.
73. S. Jeyakumar, V.V. Raut, K. L. Ramakumar, Talanta, 76(2008)1246.
74. Determination of Aluminum in Complex Matrices Using Chelation Ion Chromatography, Dionex, Application note, AN 69, 1991.
75. A. Riaz, B. Kim, D. S. Chung, Electrophoresis, 24(2003)2788.
76. R. Kadnar, Journal of Chromatography A 804(1998)217.
77. M. C. Bruzzoniti, E. Mentasti, C. Sarzanini, L. J. Kra, Analytica Chimica Acta, 322(1996)49.
78. H. Lu, S. Mou, J. M. Riviello, J Chromatogr A., 857(1999)343.
79. Determination of Inorganic Anions in Drinking Water by Ion Chromatography, DIONEX, Application Note 133.
80. R.A. Mohamed, A.M. Abdel-Lateef, H.H. Mahmoud, A.I. Helal, Studies in Chemical Process Technology (SCPT) 1(2013)75.
81. M. M. Wolle, T. Fahrenholz, G.M. MizanurRahman, Matt Pamuku, H.M. Kingston, D. Browne, Journal of Chromatography A, 1347(2014) 96.
82. M. Betti, Journal of Chromatography A, 789 (1997)369.
83. J. I.G. Alonsot, F. Sena, P. Arbore, M. Betti, L. Koch, J. Anal. At. Spectrom., 10(1995)381.
84. S. H. Reboul, E. H. Borai, R. A. Fjeld, Analytical and Bioanalytical Chemistry, 374(2002)1096.
85. E.H. Boraia, A.S. Mady, Applied Radiation and Isotopes, 57(2002)463.

86. P. Kumar, P. G. Jaison, V. M. Telmore, S. Paul, S. K. Aggarwal, International Journal of Analytical Mass Spectrometry and Chromatography, 1(2013)72.
87. W. R. Barger, R. L. Mowery, J. R. Wyatt, Journal of Chromatography A, 680(1994)659.
88. Y. F. Fung, K. M. Lau, Electrophoresis, 22(2001)2192.
89. M. Turnes Carou, P. Lopez Mahia, S. Muniategui Lorenzo, E. Fernandez Fernandez, D. Prada Rodriguez, J Chromatogr A. 918(20014)11.
90. B. Westergaard, H. C. B. Hansen, O. K. Borggaard, Analyst, April 123(1998)721.
91. Q. Dong, W. Jin, J. Shan, Electrophoresis. 23(2002)559.
92. P. Zhu, S. Wang, J. Wang, L. Zhou, P. Shi, J Chromatogr B, 1008(2016)156.
93. F. Foret, S. Fanali, A. Nardi, P. Bocek, Electrophoresis, 11(1990)780.
94. D. F. Swaile, M. J. Sepaniak, Anal. Chem., 63(1991)179.
95. K. Bachmann, J. Boden, I. Haumann, Journal of Chromatography A, 626(1992)259.
96. Y. Noguchi, L. Zhang, T. Maruta, L. N. Kiba, AnalyticaChimicaActa, 640(2009)106.
97. M. Langenauer, U. Krahenbuhl, AnalyticaChimicaActa, 274, (1993)253.
98. F. G. Antes, J. S.F. Pereira, M. S.P. Enders, C. M.M. Moreira, et. al., Microchemical Journal, 101 (2012) 54.
99. S. K. Sahoo, Y. Muramatsu, S. Yoshida, H. Matsuzaki, W. Ruhm, J. Radiat. Res. 50(2009)325.
100. Ticiane Taflik, J. Braz. Chem. Soc., 23(2012)488.

Chapter: 2

Principles of Experimental Techniques

2.1 Introduction:

A number of analytical instruments have been employed during the course of current investigations. Some of these techniques are common to more than one investigation. For example, pyrohydrolysis followed by ion chromatography has been employed for determination of halogens in U-Zr and U-Pu-Zr samples described in Chapter-3, for Mo in U-Mo samples described in Chapter-4 and for simultaneous determination of BO_3^- , F^- , Cl^- and MoO_4^{2-} ions in nuclear materials. Ion chromatography and Capillary electrophoresis has been employed for the determination of Li in U-Li samples described in Chapter-5. Chapter-6 describes application of Capillary Zone Electrophoresis (CZE) for the determination of Fe in Uranium matrix. Lastly ion chromatography has once again been employed for optimising washing procedure to be used for removal of chloride and nitrate from Li_2TiO_3 . Instead of describing the principles of these techniques each time in subsequent individual chapters, general description is given in this Chapter. The experimental details, as applicable are given in the respective Chapters.

In addition, a number of other techniques have also been employed as supporting tools to generate the requisite information on the samples investigated. These techniques were employed primarily for getting more information to interpret the experimental observations for drawing meaningful conclusions. This information includes XRD data, and other trace elemental techniques such as TGA, AAS, ICP-AES. Details of such techniques are also given in this Chapter.

2.2 Chromatography

Chromatography is a separation technique that separates components of complex mixtures on the basis of their retention behaviour on a stationary phase in presence of a mobile phase. It is defined as the physical method of separation where the analytes are distributed or partitioned between two immiscible phases viz. stationary and mobile phases. Modern chromatographic techniques are coupled with suitable detection systems and thereby they offer sequential separation as well as quantification of analytes from a single sample aliquot. In all chromatographic separations a mobile phase is passed through an immiscible stationary phase, which is fixed. The analytes in the sample distribute themselves between the mobile and stationary phases. Due to the flow of mobile phase the weakly retained components move ahead of strongly retained components [1-3]. The mobile phase entering the column is called eluent whereas the eluent emerging from the end of the column is called eluate and the process of passing mobile phase through a chromatography column is called elution.

2.2.1 Types of Chromatography

Chromatography can be divided into several types based on the basis of the mechanism of interaction between the solute and the stationary phase, as shown in Figure 2.1.

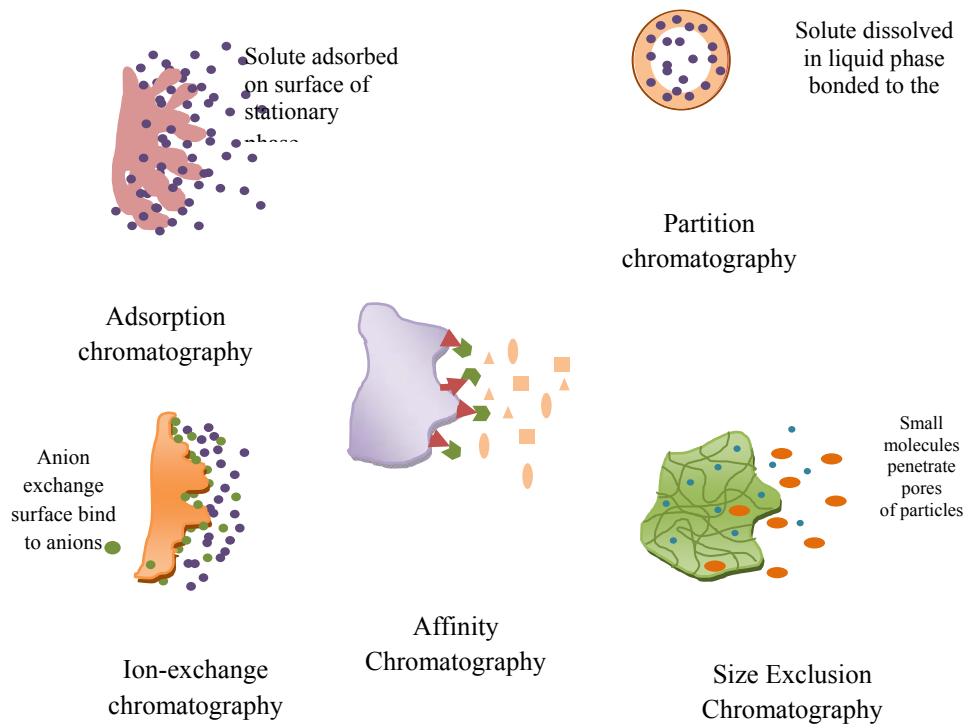


Figure 2.1: Major types of Chromatography

Adsorption chromatography: The retention of solute on the stationary phase is due to the adsorption. Stationary phase is a solid surface whereas mobile phases can be a liquid or a gas [4].

Partition chromatography: The retention mechanism in this case is similar to solvent extraction. Solute is partitioned between a mobile phase (liquid or gas) and a stationary liquid phase adsorbed on solid surface [5].

Ion-exchange chromatography: Anions or cations of analytes in the sample aliquot during elution get exchanged with their corresponding counter ions on the stationary solid phase due to the ion exchange mechanism. Stationary phase is usually a resin suitably modified as an ion exchanger and the mobile phase is a liquid [6].

Size exclusion chromatography: Size-exclusion chromatography (SEC), also called gel-filtration or gel-permeation chromatography (GPC), uses stationary phase impregnated with porous particles of varying size to separate molecules of different sizes. It is generally used to separate biological molecules, and to determine molecular weights and molecular weight distributions of polymers. Molecules that are smaller than the pore size can enter the particles and therefore have a longer path and longer transit time than larger molecules that cannot enter the particles [7].

Affinity chromatography: This technique utilises specific interactions between one kind of solute molecule and a second molecule that is immobilized to the stationary phase [8].

Chromatographic techniques are also classified on the basis of the physical states of both stationary and mobile phases used.

Gas-liquid chromatography (GLC): Solid or a liquid adsorbed on a solid support is the stationary phase and the mobile phase is always a gas.

Gas-solid chromatography (GSC): The mobile phase is a gas whereas the stationary phase is a solid.

Liquid-liquid chromatography (LLC): Stationary phase is liquid adsorbed on solid and mobile phase is liquid.

Liquid-solid chromatography (LSC): Stationary phase is a solid whereas mobile phase is a liquid.

2.2.2 Ion-Exchange Chromatography:

The ion exchange chromatography separation is mainly based on the differences in the ion exchange affinities of the sample ions towards the fixed ions of the stationary ion exchange resin. Hence, depending upon the affinities of the ions they will have different retention times, which is defined as the time in which an ion or a species is retained inside the column. In anion exchangers, positively charged groups are fixed on the stationary phase, which attracts solute anions whereas in the case of cation exchangers, fixed negatively charged ions on the stationary phase attract the cations of the solute. In general, ion exchangers favour the binding of ions of higher charge density [9].

Generally the ion exchange resins are the polymers and co-polymers of organic compounds. Polystyrene based ion exchangers are synthesised by the copolymerization of styrene and divinylbenzene (DVB). The DVB content is varied from 1 to 16% to increase the extent of cross-linking. The phenyl rings are substituted with appropriate functional groups to obtain cation exchange or anion exchange resins. For instance, substitution of sulfonate group was performed to obtain the cation exchange resin whereas a quarternary ammonium group is introduced to obtain an anion exchanger.

2.2.2.1 Ion Exchange equilibria:

The law of mass action can be used to treat ion-exchange equilibria [10]. For example, when a dilute solution containing metal ions is passed through a column packed with a sulfonic acid resin, the following equilibrium is established (fig. 2.2):

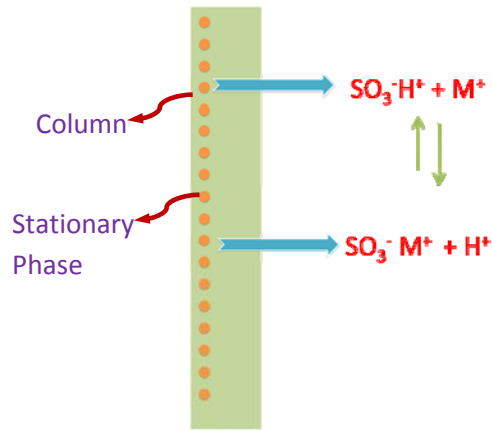


Figure 2.2: Schematic representation of Ion Exchange mechanism.



for which the equilibrium constant K_r is given by

$$K_r = \frac{[M]_{res}[H]^{n}_{aq}}{[M]_{aq}[H]^{n}_{res}} \quad \text{-----} \quad (2)$$

Polyvalent ions are much more strongly retained than singly charged species. Within a given group of ions having same charge, the differences among values for K appear to be related to the size of the hydrated ion as well as other properties. Therefore, for a typical sulfonated cation-exchange resin, values of equilibrium constant for univalent ions decrease in the order Ag^{+} , Cs^{+} , Rb^{+} , K^{+} , NH_4^{+} , Na^{+} , H^{+} , Li^{+} . For divalent cations the order is Ba^{2+} , Pb^{2+} , Sr^{2+} , Ca^{2+} , Ni^{2+} , Cd^{2+} , Cu^{2+} , Co^{2+} , Zn^{2+} , Mg^{2+} , UO_2^{2+} .

Analyte ions with different selectivity coefficients for a specific combination of resin and eluent anion will be separated due to different degrees of interaction with the stationary phase. The mechanism for anion exchange separation is analogous.

2.2.2.2 Conductivity detection:

Ion chromatography coupled with conductivity detector became a powerful tool for the quantification of ions after the development of low-exchange capacity columns. Improvement in the sensitivity of detection as well as very low limit of detection limit (LOD) was achieved after the introduction of suppression technology. The suppression technique is employed for reducing the conductivity of the mobile phase after the column and before the detector.

Electrical conductivity measures the ability of a solution to conduct an electric current between two electrodes across which an electric field has been applied. The conductance of a solution (g) is commonly expressed by the SI unit Siemens (S), and is the reciprocal of the resistance (R) measured in ohm (Ω).

$$g = 1/R \quad \text{-----} \quad (3)$$

Conductivity detectors are simple devices consisting of a detection cell with two electrodes, which can either be in contact with the stream of eluent. Conductivity detection is the natural choice for IC, since the separated analytes are electrically conducting. The conductance signal depends on the electrolyte concentration (C) of the ionic species present (both eluent and analyte ions, either + or -) and their limiting equivalent ionic conductances (λ).

In suppressor-based ion chromatography, the ion-exchange column is followed by a suppressor column, or a suppressor membrane, that converts an ionic eluent into a

non-ionic species that does not interfere with the conductometric detection of analyte ions [11].

Currently, several other detector types such as spectrophotometer and electrochemical detectors are available for ion chromatography.

2.2.3 Terms used in chromatography separations:

The mechanism of chromatography separations is understood by Column theory. Following are important factors that control the separation of analytes on the column.

- (i) **Column dead time (t_0):** it is the time necessary for a non-retained component to pass through the column. And the volume of mobile phase corresponding to the dead time is known as dead volume (V_0).
- (ii) **Retention time (t_R):** It is the time taken for an analyte to emerge out of the column after its retention on the column in which the components reside inside the column. This includes the dead time of the column.
- (iii) **Resolution (R):** Resolution is the measure of how a peak is separated with respect to its neighbouring peaks. The resolution R of two neighboring peaks is defined as the quotient of the difference in the absolute retention times and the arithmetic mean of their peak widths w at the respective peak base.

$$R = (t_{R2} - t_{R1}) / [(w_1 + w_2) / 2] \quad \text{-----} \quad (4)$$

where t_{R2} and t_{R1} are the retention times for components 1 and 2 respectively, w_1 and w_2 are their corresponding peak widths.

(iv) **Selectivity (α):** the selectivity is defined as the ratio of the solute retention times of two different components.

$$R = (t_{R2} - t_0) / (t_{R1} - t_0) \quad \text{-----} \quad (5)$$

The selectivity is a thermodynamic quantity and at constant temperature, it is determined by the properties of the stationary phase.

The selectivity of the column is due to several factors, e.g., the support material and the chemical structure of the ion exchange group.

The selectivity factor (α) of two analyte ions A and B eluting close to each other is the measure of how well these ions are separated, and is calculated according to:

$$\alpha = k'_B / k'_A \quad \text{-----} \quad (6)$$

where k'_A and k'_B are the retention factors for the first and the last eluted ion, respectively.

(v) **Retention factor (k'):** it is also known as Capacity factor. It is the product of the phase ratio Φ between stationary and mobile phase in the separator column and the Nernst distribution coefficient, K .

$$k' = K \times (V_s / V_m) \quad \text{-----} \quad (7)$$

$$K = C_s / C_m \quad \text{-----} \quad (8)$$

where K is Nernst distribution coefficient, V_s is volume of the stationary phase, V_m is volume of mobile phase, C_s and C_m are solute concentrations in the stationary and mobile phase respectively.

Practically k' for any peak of a component is measured as

$$k' = (t_R - t_0) / t_0 \quad \dots\dots\dots (9)$$

Number of Theoretical Plates (N)

A chromatography column does not contain anything resembling physical distillation plates or other similar features. Theoretical plate numbers are indirect measure of peak width for a peak at a specific retention time. The number of theoretical plates is a mathematical concept and can be calculated using Equation,

$$N = 16L^2/w_{1/2} \quad \text{-----} \quad (10)$$

(Where L is the column length and $w_{1/2}$ is width of peak at half peak height).

Columns with high plate numbers are considered to be more efficient, that is, have higher column efficiency, than columns with a lower plate count. A column with a high number of theoretical plates will have a narrower peak at a given retention time than a column with a lower N number [12].

2.2.4 Plate Height Equation:

Another measure of column efficiency is the height equivalent to a theoretical plate denoted as H . It is calculated using Equation, $H = L/N$ and usually reported in millimetres (Where L is the column length and N is number of theoretical plates of the column). The column efficiency is considered as high when the number of theoretical plates is more per unit length of the column.

Plate height, H , is proportional to the variance of a chromatographic band. The smaller the plate height, the narrower the band. The Van-Deemter equation tells us how the column and flow rate affect the plate height:

$$H = A + B/u_x + Cu_x \quad \text{-----} \quad (11)$$

Where u_x is the linear flow rate and A , B , and C are constants for a given column and stationary phase. Changing the column and stationary phase changes A (*Eddy diffusion*), B (*longitudinal diffusion*), and C (*resistance to mass transfer*).

A - Eddy diffusion:

The mobile phase moves through the stationary phase which is packed under high pressure. Solute molecules will take different paths through the stationary phase at random. This will cause broadening of the solute band, because different paths are of different lengths.

B - Longitudinal diffusion:

The concentration of the analyte is less at the edges of the band than at the center. Analyte diffuses out from the centre to the edges. This causes band broadening. If the velocity of the mobile phase is high then the analyte spends less time on the column, which decreases the effects of longitudinal diffusion.

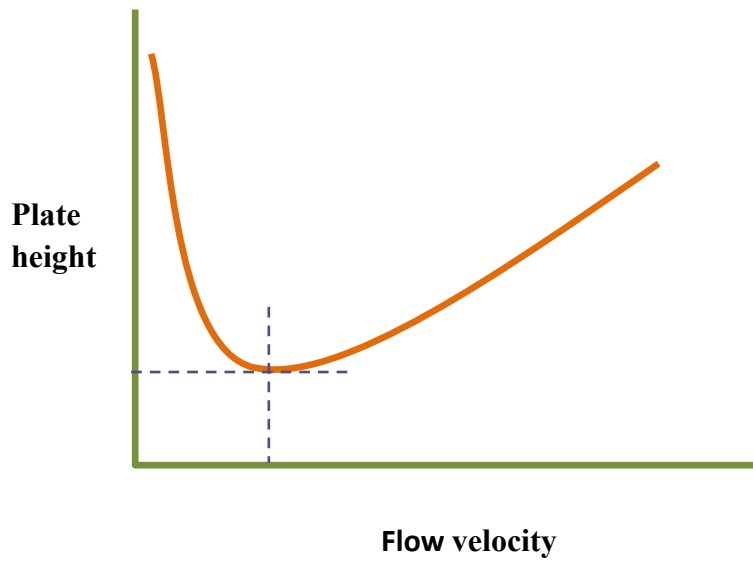


Figure 2.3: A typical Van Deemter plot.

C - Resistance to mass transfer:

The analyte takes a certain amount of time to equilibrate between the stationary and mobile phase. If the velocity of the mobile phase is high, and the analyte has a strong affinity for the stationary phase, then the analyte in the mobile phase will move ahead of the analyte in the stationary phase. The band of analyte is broadened. The higher the velocity of mobile phase, the worse the broadening becomes.

For each peak in the chromatogram, the capacity factor, k' , is defined as,

$$k' = (t_2 - t_0) / t_0 \quad \text{-----} \quad (12)$$

The separation factor (α) is defined as the ratio of the retention factors (k),

$$\alpha = \frac{k'_2}{k'_1} \quad \text{-----} \quad (13)$$

It is useful to relate the resolution to the number of plates in the column, the selectivity factor and the retention factors of the two solutes;

$$R = \frac{\sqrt{N}}{4} \times \frac{(\alpha-1)}{\alpha} \times \frac{k_2'}{1+k_2'} \quad \text{-----} \quad (14)$$

To obtain high resolution, the three terms must be maximised. An increase in N, the number of theoretical plates, by lengthening the column leads to an increase in retention time and increased band broadening - which may not be desirable. Instead, to increase the number of plates, the height equivalent to a theoretical plate can be reduced by reducing the size of the stationary phase particles.

Other experimental parameters which can affect the resolution are,

- (i) Changing mobile phase composition
- (ii) Changing column temperature
- (iii) Changing composition of stationary phase

Using special chemical effects (such as incorporating a species which complexes with one of the solutes into the stationary phase) etc.

2.2.5 Instrumentation:

The schematic shown below (Fig. 2.4) represents an ion chromatography system. The sample is introduced into the system via a sample loop on the injector. When in the inject position the sample is pumped onto the column by the eluent and the sample ions are then attracted to the charged stationary phase of the column. The

eluent elutes the retained ions which then go through the detector (which is most commonly conductivity) and are depicted as peaks on a chromatogram.



Figure 2.4: Block diagram for an Ion Chromatography system.

Figure-2.5 represents an IC system designed for analysis of radioactive samples. Some parts of the system which are in direct contact with the active samples, viz. sample injector, column, suppressor and detector are detached from the main system

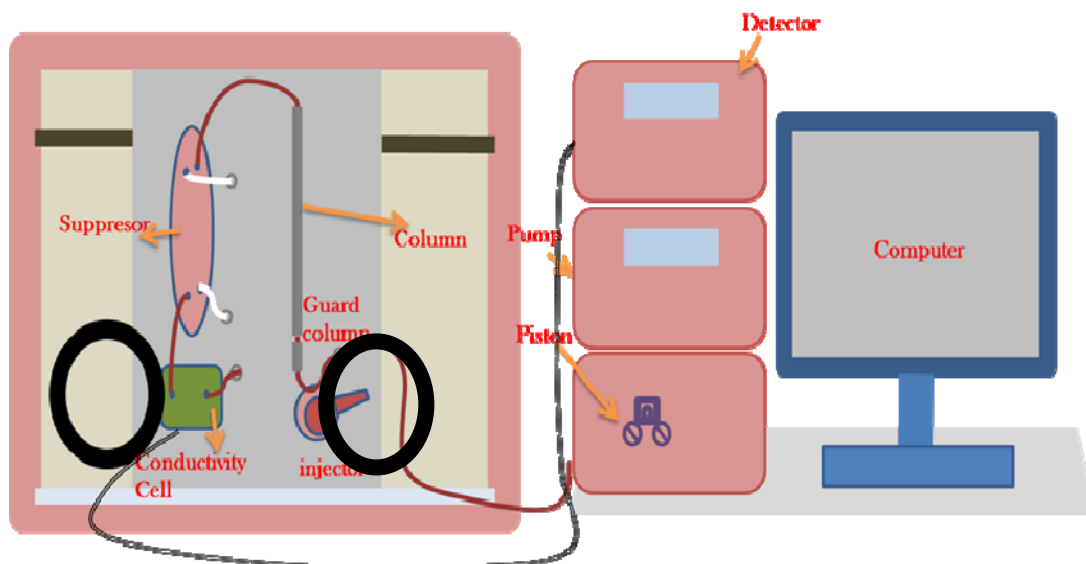


Figure 2.5: Schematic representation of an Ion Chromatography system designed for radioactive samples.

and are installed in a fume hood. The fume hood is under suction and the air of fumehood is passed through HEPA filters before getting released to atmosphere. The liquid waste collected in fume hood are disposed as per the standard procedures of radioactive liquid wastes.

Studies described in this dissertation utilised the ion chromatography for determining various anions like F^- , Cl^- , NO_3^- , MoO_4^{2-} etc. The separations were carried out on anion exchange columns with suppressor conductivity detection.

2.3 Capillary Electrophoresis:

Capillary electrophoresis (CE) is a rapid separation technique and it turned to be a good analytical tool by coupling suitable detectors. CE separates ions based on their electrophoretic mobility caused by application of potential (applied voltage). The electrophoretic mobility is dependent upon the charge of the ion, the viscosity, and the radius of the ion or molecular species. The rate at which the particle moves is directly proportional to the applied electric field, the greater the field strength, the faster the mobility. Neutral species are not affected, only ions move with the electric field. If two ions are the same size, the one with greater charge will move faster than the one with lesser charge. For the ions of same charge, the ion with small size will have faster migration rate as it will experience less friction in the medium. The capillary electrophoresis has some advantages over other separation techniques such as fast separation, very small sample size and separations with high resolution. CE is a useful technique because there is a large range of detection methods available [12].

Employing a capillary in electrophoresis had solved some common problems in traditional electrophoresis. For example, the narrow dimensions of the capillaries

greatly increased the surface to volume ratio, which eliminated overheating by the application of high voltages.

2.3.1 Electrophoretic Mobility:

Electrophoresis is the process in which sample ions move under the influence of an applied voltage. The ion experiences a force that is equal to the product of the net charge and the electric field strength. It is also affected by a drag force that is equal to the product of, the translational friction coefficient, and the velocity. This leads to the expression for electrophoretic mobility [14]:

$$\mu_{EP} = \frac{q}{f} = \frac{q}{6\pi\eta r} \quad \text{-----} \quad (15)$$

Where f stands for a spherical particle is given by the Stokes' law; η is the viscosity of the solvent, and r is the radius of the atom. The rate at which these ions migrate is dictated by the charge to mass ratio. The actual velocity of the ions is directly proportional to E, the magnitude of the electrical field and can be determined by the following equation:

$$v = \mu_{EP} E \quad \text{-----} \quad (16)$$

This relationship shows that a greater voltage will quicken the migration of the ionic species.

2.3.2 Electro osmotic Flow:

The electro osmotic flow (EOF) is caused by applying high-voltage to an electrolyte, which is filled in a capillary. The flow of electro osmotic flow is explained on the basis of an electrical double theory. According to this mechanism, $-\text{SiOH}$ of the silica releases a proton to become SiO^- ions when a buffer solution having pH more than 3 is allowed to pass through the silica capillary. Hence, the capillary wall then has a negative charge, which develops a double layer of cations attracted to it. The inner cation layer is stationary, while the outer layer is free to move along the capillary. The applied electric field causes the free cations to move toward the cathode creating a bulk flow, which is known as electro osmotic flow. The rate of the electroosmotic flow [14] is governed by the following equation:

$$\mu_{EOF} = \frac{\epsilon}{4\pi\eta} E\zeta \quad \text{-----} \quad (17)$$

Where, ϵ is the dielectric constant of the solution, η is the viscosity of the solution, E is the field strength, and ζ is the zeta potential. Because the electrophoretic mobility is greater than the electroosmotic flow, negatively charged particles, which are naturally attracted to the positively charged anode, will separate out as well.

2.3.3 Instrumentation:

A typical CE system consists of a high-voltage power supply, a sample introduction system, a capillary tube, a detector and an output device. Each side of the high voltage power supply is connected to an electrode as shown in the Figure 2.6. These electrodes help to induce an electric field to initiate the migration of the sample from the anode to the cathode through a capillary tube. The capillary is made of fused

silica and is sometimes coated with polyimide. Each end of the capillary tube is dipped in a vial containing the electrode and a background electrolytic solution. There is usually a small window near the cathodic end of the capillary for UV-VIS detection.

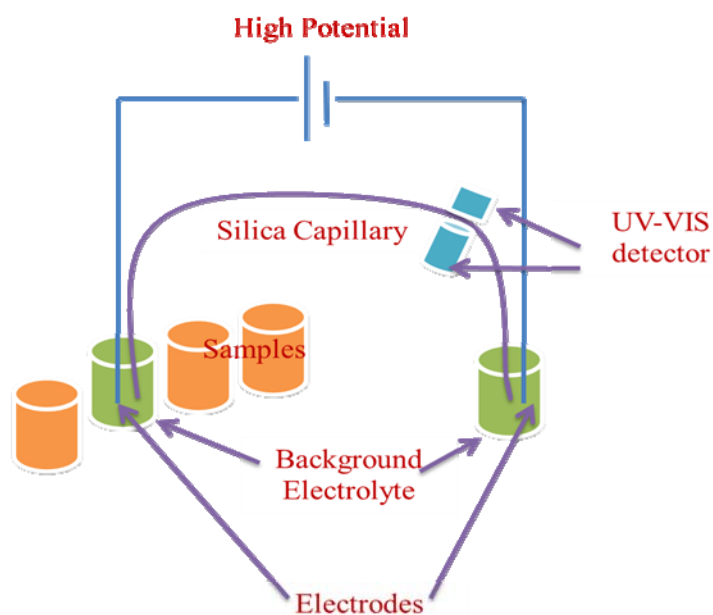


Figure 2.6: Capillary Electrophoresis instrumentation.

There are six types of capillary electrophoresis available [15] and they are (i) capillary zone electrophoresis (CZE), (ii) capillary gel electrophoresis (CGE) (iii), micellarelectrokinetic capillary chromatography (MEKC), (iv) capillary electro chromatography (CEC), (v) capillary isoelectric focusing (CIEF), and (vi) capillary isotachopheresis (CITP).

2.3.4 Capillary Zone Electrophoresis (CZE):

In CZE analytes move in the EOF but separate into bands because of differences in their electrophoretic mobilities, μ . Differences in μ make each analyte's overall migration velocity slightly different, and difference in migration velocity is

responsible for the separation. As it was discussed earlier in the presence of an applied electric field, the diffuse layer migrates towards the negatively charged cathode creating an electrophoretic flow (μ_{ep}) that drags bulk solvent along with it. Anions in solution are attracted to the positively charged anode, but get swept to the cathode as well. Cations with the largest charge-to-mass ratios separate out first, followed by cations with reduced ratios, neutral species, anions with smaller charge-to-mass ratios, and finally anions with greater ratios. The electroosmotic velocity can be adjusted by altering pH, the viscosity of the solvent, ionic strength, voltage, and the dielectric constant.

In liquid chromatography the separations are carried out on a packed and there the peak broadening is being explained on the basis of van Deemter equation, which accounts the broadening due to three phenomena namely multiple flow paths, longitudinal diffusion, and finite rate of mass transfer. In capillary electrophoresis, there is no stationary phase. Therefore, the only fundamental source of broadening under ideal conditions is longitudinal diffusion.

The present thesis reports about the developed CZE methods for determining Fe in uranium matrices and Li in Li-Al alloys. The method that deals with the determination of Fe in U matrices utilised chloride as the complexing agent in the BGE. In the CZE method for the determination of Li in Li-Al alloy was developed by using Imidazole as the co-ion.

2.4 X-ray powder diffraction analysis (XRD):

XRD is perhaps the most widely used X-ray based analytical technique for characterizing materials. As the name suggests, the sample is usually in a powdery form. The positions and the intensities of the peaks are used for identifying the

underlying structure (or phase) of the material [16]. The three-dimensional structure of crystalline materials is defined by regular, repeating planes of atoms that form a crystal lattice. When a focused X-ray beam interacts with these planes of atoms, part of the beam is transmitted, part is absorbed by the sample, part is refracted and scattered, and part is diffracted. X-rays are diffracted by each structure differently, depending on what atoms make up the crystal lattice and how these atoms are arranged. When an X-ray beam hits a sample and is diffracted, we can measure the distances between the planes of the atoms that constitute the sample by applying Bragg's Law, named after William Lawrence Bragg, who first proposed it in 1921. Bragg's Law is:

$$n\lambda = 2d \sin\theta, \quad \text{-----} \quad (18)$$

where the integer n is the order of the diffracted beam, λ is the wavelength of the incident X-ray beam, d is the distance between adjacent planes of atoms (the d-spacings), and θ is the angle of incidence of the X-ray beam. We can measure the d-spacings. The geometry of an XRD unit is designed to accommodate this measurement. The characteristic set of d-spacings generated in a typical X-ray scan provides a unique fingerprint of the material or materials present in the sample. When properly interpreted, by comparison with standard reference patterns and measurements, this fingerprint allows for identification of the material.

Instrumentation: In XRD, X-rays are generated within a sealed tube which is under vacuum. A filament present inside the tube is heated by applying current and the filament emits electrons. Moreover, higher the current the greater the number of electrons emitted from the filament. A high voltage, typically 15-60 kilovolts, is applied within the tube. This high voltage accelerates the electrons, which then hit a

target, commonly made of copper. When these electrons hit the target, X-rays are produced. The wavelength of these X-rays is characteristic of that target. These X-rays are collimated and directed onto the sample, which is in fine powder form. A detector detects the X-ray signal; the signal is then processed either by a microprocessor or electronically, converting the signal to a count rate [17].

The XRD technique was utilized during various studies to understand the various structural transformations occur during their pyrohydrolysis. The structural information obtained from the XRD is vital in interpreting the mechanism of pyrohydrolysis for the material under investigation.

2.5 Thermogravimetric Analysis:

Thermogravimetric analysis (TGA) measures the change in weight of a material as a function of temperature (or time) under a controlled atmosphere. TGA is widely employed for the measurement of a material's thermal stability, moisture, solvent content, and composition of components (in percentile level) in a compound [18]. A TGA analysis is performed by gradually raising the temperature of a sample in a furnace as its weight is measured on an analytical balance that remains outside of the furnace. In TGA, mass loss is observed if a thermal event involves loss of a volatile component. Chemical reactions, such as combustion, involve mass losses. A plot of sample weight versus temperature or time is used to illustrate the thermal transitions in the material.

The studies described in this dissertation, TGA was utilised specially to understand the chemistry of volatilization of MoO_3 in moist atmosphere at different temperatures.

2.6. Inductively Coupled Plasma Atomic Emission Spectrometry:

Atomic emission spectrometry (AES) is a method of chemical analysis that uses the intensity of light emitted from a flame, plasma, arc, or spark at a particular wavelength to determine the quantity of an element in a sample. The wavelength of the atomic spectral line gives the identity of the element while the intensity of the emitted light is proportional to the number of atoms of the element. Inductively coupled plasma atomic emission spectroscopy (ICP-AES) uses ICP to produce excited atoms and ions that emit electromagnetic radiation at wavelengths characteristic of a particular element. Advantages of ICP-AES are excellent limit of detection and linear dynamic range, multi-element capability, low chemical interference and a stable and reproducible signal. Disadvantages are spectral interferences (many emission lines), cost and operating expense and the fact that samples typically must be in a liquid solution [19,20].

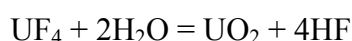
The ICP-AES technique has been used in the studies of this thesis to validate the results obtained by the developed methods by comparing the values obtained from ICP-AES.

2.7 Pyrohydrolysis:

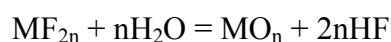
Pyrohydrolysis is one of the separation techniques where the analytes are directly separated from the solid materials without dissolving them. Pyrohydrolysis is based on the principle where the decomposition solid materials in presence of heat and water vapour. During the simultaneous action of heat and steam, the analytes are

converted into their volatile form and get extracted through the flow of steam, which is subsequently condensed and collected in the form of distillate.

Domange and Wohlhuter [21] had determined the equilibrium constant for the reaction



in the range 200° to 500° C. They concluded that higher temperatures favour the formation of the hydrolysis products, the equilibrium constant being 1.36×10^{-1} at 250°C. and an estimated value of 1.93 at 1000°C. Warf et al [22] extended the observations of Domange and Wohlhuter and postulated that in the case of a general equation



the free energy of formation is expected to become more negative with rising temperatures, because the standard entropy of 2 moles of hydrogen fluoride is roughly twice that of 1 mole of steam.

A plot of Free energy formation and the temperature for different metal halides [23] is shown in Figure 2.7. It is seen that as the temperature increases the ΔG becomes more and more negative. The end product is the halogen acid and the corresponding metal oxide. It leads to the conclusion that quantitative release of halogen from the solid matrix is facilitated through opening of the solid matrix and conversion of the metal halide to metal oxide. Besides high temperature, for effective interaction of moisture with metal halide to occur the sample should preferably be in the powder form to offer large surface area. The kinetics of release of halogens is thus directly related to the kinetics of formation of metal oxide.

After extensively investigating different metal halide systems, Warf et al[22] classified them into a rapidly hydrolyzable group and a slowly hydrolyzable group. The first included AlF_3 , BiF_3 , MgF_2 , ThF_4 , UF_4 , UF_3 , UO_2F_2 , VF_3 , ZnF_2 , ZrF_4 , ZrOF_2 , and the rare earth fluorides.

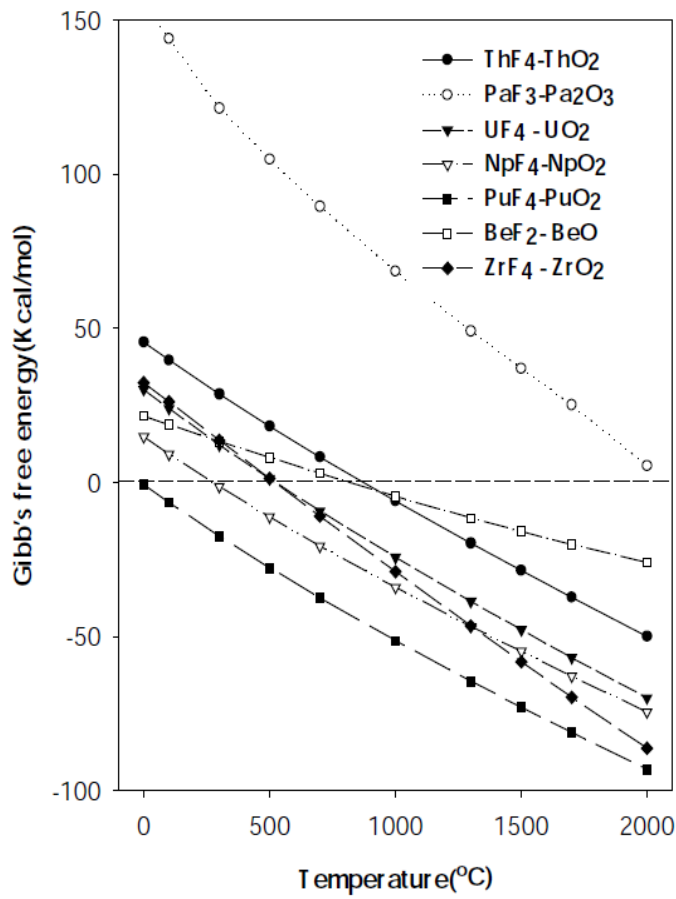


Figure 2.7:Gibb's free energies of formation of various compounds [23].

The second group included the fluorides of the alkali metals, the alkaline earth metals, and beryllium. Those in the first group were hydrolyzed quantitatively in 20 minutes or less at 1273K.

The volatile halogen acids are collected in a PVC bottle containing dilute NaOH (trapping solution) and this solution is known as pyrohydrolysis distillate. The pyrohydrolysis distillates obtained are subsequently analysed by selective instrumental methods for quantifying the analytes. Similarly boron can be separated in the form of boric acid from several materials [24-26].

Pyrohydrolytic separation mainly depends on (i) temperature of pyrohydrolysis (ii) carrier gas flow rate (iii) sample mass and (iv) time (duration) of pyrohydrolysis.

(i) Pyrohydrolysis temperature: Temperature is an important parameter as the material under pyrohydrolysis is needed to be decomposed or brought changes in the volume of the material either by physical or chemical means. For organics as well as easily pulverisable materials, a moderate temperature range between 673 and 973K is chosen. However, refractory materials which are highly resistive for the action of heat require quite high temperature (more than 1273K).

(ii) Carrier gas choice and flow rate: The carrier gas selection and its flow rate are important parameters in pyrohydrolysis. It indirectly helps in improving the sensitivity of the analytical determination. Most of the pyrohydrolysis are carried out with oxygen as carrier gas except for the cases where oxygen may cause unwanted or unfavourable reactions. For instance, pyrohydrolysis of uranium carbide or plutonium carbide or mixed uranium and plutonium carbide is carried out with

Argon gas (inert gas) due to their pyrophoric nature. The flow rate of steam is controlled by the carrier gas flow rate and therefore, it directly controls the condensed distillate volume. Typically the pyrohydrolysis distillate collection volume is kept around 25 mL in 30 minutes collection. This is very important to have appreciable concentrations of the analytes in the distillate.

(iii) Mass of the sample: A sample mass of 10 mg to 5g are taken for pyrohydrolysis. For a given sample, the sample mass is decided by considering the concentration range of analytes present in the sample.

(iv) Time of pyrohydrolysis: Time of pyrohydrolysis is the most important one as it decides the recoveries of analytes. Depending upon the pyrohydrolysis temperature and the concentration of the analytes the separation kinetics is varied. Therefore, the time of pyrohydrolysis needed to be optimized for each matrix. For example the uranium or plutonium carbides are pyrohydrolysed for only 15-20 minutes for the complete recovery of chlorine and fluorine whereas in certain ceramic and refractive materials like zirconia, thoria etc. is pyrohydrolysed for few hours.

Literature survey shows a variety of samples like geological samples, coal, organic materials, nano particles, cement, nuclear materials etc. [27-31] are regularly analysed for their halide contents after pyrohydrolysis separation. The basic design of the pyrohydrolysis apparatus is presented in the Figure 2.8. Depending on the materials to be pyrohydrolysed some modifications in the apparatus are also being incorporated.

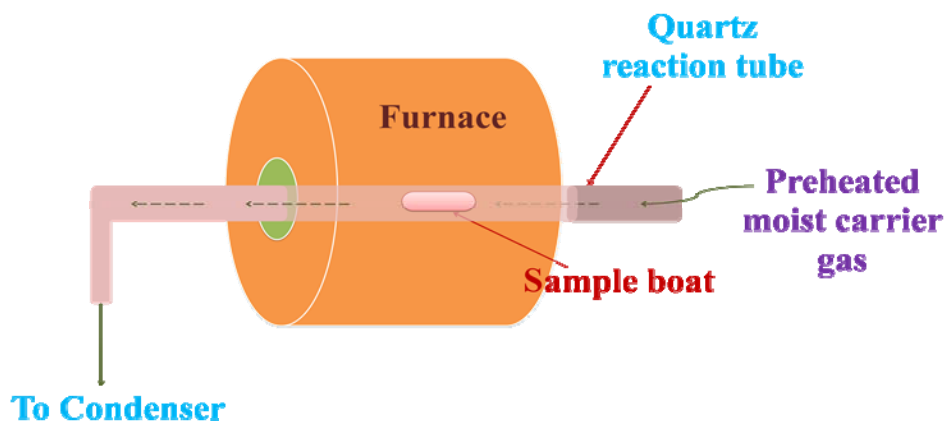


Figure 2.8: Basic Pyrohydrolysis instrument.

In order to carry out the pyrohydrolysis of radioactive materials, the apparatus is housed inside an active glove box. This limits the free handling or operation of the PH apparatus and from the safety point of view, it poses many challenges. Therefore, many modifications have been incorporated in the system to carry out the operations and handling easier and safe. In addition, to increase the sample through-put during routine sample analyses, necessary changes were incorporated in the design with a view to carry out the sample loading and unloading is easier and safe. These requirements resulted in advance pyrohydrolysis system as depicted in Figure-2.9. The main features of the design are, (i) pre-heater for the carrier gas is not required as the same furnace where the sample is heated is utilized for heating moist carrier gas. (ii) The furnace is movable, which helps in easy access to the reaction tube. (iii) The combination of outer and inner reaction tube allow easy and fast loading of sample boat. (iv) The overall space occupied is reduced significantly.

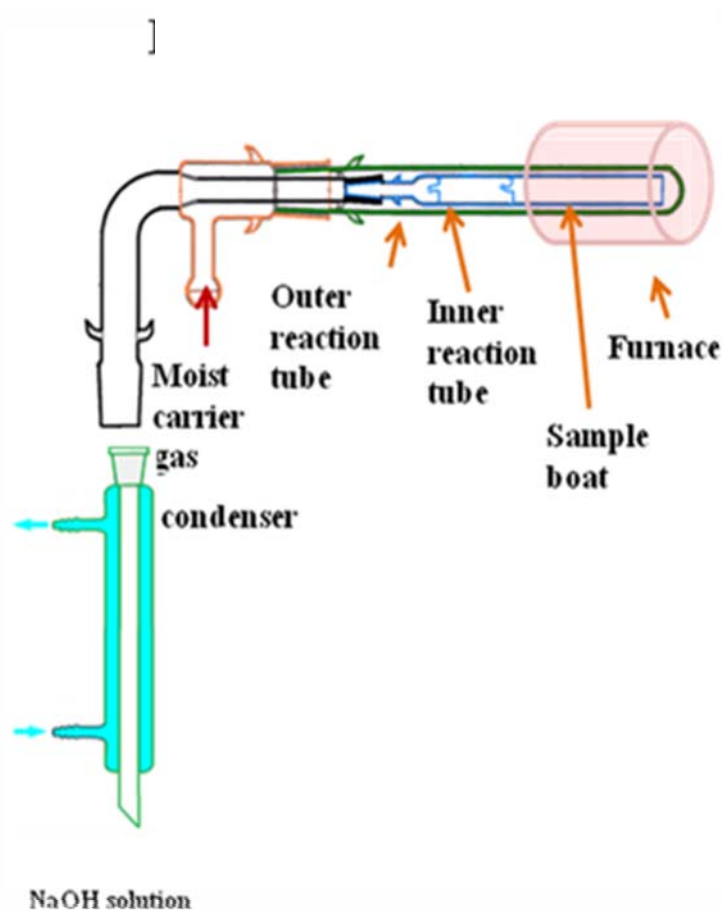


Figure 2.9: The modified Pyrohydrolysis apparatus for Glove Box operation.

Pyrohydrolysis was used for clean sample preparation. Studies were carried out to understand the pyrohydrolysis behaviour of U-Zr and U-Pu-Zr alloy samples. A novel method was also developed where Mo was separated directly from U matrix using pyrohydrolysis. For analysing environmental samples pyrohydrolysis was used to provide a simultaneous separation of B, F, Cl and Mo.

2.8 References:

1. C. F. Poole, The essence of Chromatography, Elsevier, (2003)1.
2. J. M. Miller, Chromatography Concepts and Contrast, Wiley, 2nd edition (2005)35.
3. D. A. Skoog, J. J. Leary, Principles of Instrumental Analysis, Saunders College Publisher, 4th edition(1991)579.
4. J. Cazes, Encyclopedia of Chromatography, Volume-1, Taylor and Francis, (2005)21.
5. J. Cazes, Encyclopedia of Chromatography, Volume-1, Taylor and Francis, (2005)296.
6. J. Cazes, Encyclopedia of Chromatography, Volume-1, Taylor and Francis, (2005)859.
7. J. Cazes, Encyclopedia of Chromatography, Volume-1, Taylor and Francis, (2005)11.
8. J. Cazes, Encyclopedia of Chromatography, Volume-1, Taylor and Francis, (2005)33.
9. J. S. Fritz, D. T. Gjerde, Ion Chromatography, 3rd edition, Wiley VCH, (2000)4.
10. P. R. Haddad, P. E. Jackson, Ion Chromatography Principles and Applications, Elsevier (1999)1.
11. J. Weiss, Ion Chromatography, Second Edition, VCH (1995)291.
12. L. R. Snyder, J. J. Kirkland, Introduction to Modern Chromatography, 2nd edition(1979)15.
13. H. Whatley, Clinical and Forensic Applications of Capillary Electrophoresis, chapter 2, (2001)22.

14. S. E. Y. Li, *Capillary Electrophoresis Principles, practice and applications*, Elsevier (1992)12.
15. C. M. Johnson, A. P. McKeown, M. R. Euerby, *Capillary Electrochromatography*, Elsevier, Volume 62(2001)87.
16. Y. Waseda, E. Maturba, K. Shinoda, *X-ray Diffraction Crystallography*, springer(2011)107.
17. A. A. Bunaciua, E. G. Udristoiub, H. Y. Aboul-Eneinc, *Crit. Rev. Anal. Chem.*, 45(2015)289.
18. R. Bottom, *Principles and Applications of Thermal Analysis*, Blackwell Publishing (2008)87.
19. K. L. Linge, *Geostand. Geoanal. Res.*, 29(2005)7.
20. M. Thompson, *Handbook of Inductively Coupled Plasma Spectrometry*, Blackie & Sons Ltd. (1989)43.
21. (6) Domange, L., and Wohlhuter, M., *Compt, rend*, 228, 1591(1949).
22. James C. Warf, W. D. Cline, and Ruth D. Tevebaugh, *Anal. Chem.*, 26(1954), 342
23. Mun-Sik Woo, Sung-Chan Hwang, Jun-Bo Shim, Young-Ho Kang and Jae-Hyung Yoo, Paper presented at OECD Nuclear Energy Agency Seventh Information Exchange Meeting on Actinide and Fission Product Partitioning and Transmutation, 14-16 October 2002, Jeju (Korea).
24. M. A. Mahajan, M. V. R. Prasad, H. R. Mhatre, R. M. Sawant, et al., *J. Radioanal. Nucl. Chem.*, 148(1991), 93.
25. S. Jeyakumar, V. V. Raut, K. L. Ramakumar, *Talanta*, 76(2008)1246.
26. S. Jeyakumar, V. G. Mishra, M. K. Das, V. V. Raut, R.M. Sawant, K. L. Ramakumar, *Radiochim. Acta*; 102(2014)291.

27. J. E. Rae, S.A. Malik, *Chemosphere* 33(1996)2121.
28. M. Bettinelli, S. Spezia, C. Minoia, A. Ronchi, *At. Spectrosc.* 23(2002)105.
29. F.G. Antes, F. A. Duarte, J. N.G. Paniz, M. F. P. Santos, et. al., *At. Spectrosc.* 29(2008)157.
30. Y. Muramatsu, Y. Takada, H. Matsuzaki, S. Yoshida, *Quat. Geochronol.* 3(2008)291.
31. Y. Nogushi, L. Zhang, T. Maruta, T. Yamane, N. Kiba, *Anal. Chim. Acta*, 640(2009) 106.

Chapter: 3

Direct Extraction of Molybdenum from Solid Uranium Matrices Employing Pyrohydrolysis and Its Determination by Ion Chromatography

3.1 Introduction:

Uranium is used as a nuclear fuel both in ceramic (UO_2) and alloy forms. Both the types of fuels have their own advantages and disadvantages. Depending upon their composition and properties they are considered suitable for different reactors. Molybdenum is an alloying element for metallic fuels such as U-Mo, U-TRU-Mo (TRU, trans-uranium elements such as Np, Pu, and Am), and so on. These alloys are advantageous due to their γ phase stability of U [1]. Presence of Mo in ceramic fuel causes creep resistance (results in swelling of fuel pellets and causes adverse effects on the integrity of clad material). Hence, the presence of Mo even at a trace level concentration is undesirable in oxide or mixed oxide fuels of U and Pu. Another important factor is the oxygen potential of the Mo/MoO₂ couple which is very close to that of the stoichiometric UO₂ [2] and can affect the o/m ratio of UO₂. Therefore, separation and determination of Mo in nuclear fuels in the concentration range of trace to percent levels is an important requirement.

Methods that are being used in the chemical characterisation of nuclear materials for the determination of Mo in U or U-Pu matrices involve dissolution of the material in appropriate acid media followed by solvent extraction or ion exchange separations [3-7]. These methods are laborious and generate radioactive liquid wastes. Unless precautions are taken there may be loss of Mo during the sample preparation steps.

This loss of Mo leads to erroneous determination of Mo. Such loss was encountered while determining Mo in ammonium diuranate (ADU) [8]. Therefore, it is desirable to have a sample preparation procedure that does not lead to loss of Mo and also brings reduction in the radioactive waste generation.

Pyrohydrolysis (PH) is a separation method which separates the analyte(s) directly from the solid matrix and do not use any organic reagent or acids. PH is a well-known technique for separating halogens and boron from several solid matrices [9-15]. The pyrohydrolysis conditions or separation parameters governing recoveries of the analytes depend on the matrix and also the nature of the analyte [16, 17]. Pyrohydrolysis is widely used for separating non-metals such as halogens, boron, and sulphur, and its application for separating metals or metal species has not been explored and reported so far.

Several studies (18-20) indicate that MoO_3 , the more stable oxide of Mo has higher vapour pressure. In addition, the volatilisation of Mo is enhanced when the atmosphere contains moisture [20, 21]. This implies the feasibility of separating Mo quantitatively from solid matrices by making use of associated vapour chemistry of Mo. Present investigations are aimed at exploring the feasibility of adapting pyrohydrolysis for separating molybdenum from uranium based nuclear materials.

3.2 Experimental Section:

3.2.1 Reagents:

For the preparation of synthetic standards, U metal and UO_2 (nuclear grade, Bhabha Atomic Research Centre (BARC), Mumbai, India) and Mo metal powder and MoO_3 (>99.95% Alfa Aesar, Heysham, U.K.) were used. The standard solutions of F^- , Cl^- ,

NO_3^- , and SO_4^{2-} were prepared by dissolving their respective Na salts (>99.9%, Merck, Darmstadt, Germany). Standard solutions of MoO_4^{2-} were prepared by dissolving $(\text{NH}_4)_6\text{Mo}_7\text{O}_{24}$ (>99.98%, Sigma-Aldrich, St. Louis, MO, USA) in high purity water. All other reagents were of analytical grade. For the preparation of all solutions and production of steam, high purity water (18.2 M Ω ·cm) obtained from a Milli-Q system (Millipore, Billerica, MA, USA) was used.

3.2.2 Preparation of Standards Containing Mo:

In order to study the recovery of Mo by pyrohydrolysis, in-house standards with known Mo contents were prepared. Since the real samples can have different chemical forms of uranium matrix, the standards were prepared in metal (U-metal) as well as in the oxide form (UO_2). The standards were prepared in the concentration range between 100 and 5000 ppm. Two U–Mo alloys having 500 and 5000 ppm of Mo were prepared by Arc melting method [22]. Two different mixed oxide ($\text{UO}_2 + \text{MoO}_3$) working standards, each with 100 and 500 ppm of Mo, were prepared by mixing calculated amounts of MoO_3 and UO_2 powders. The powders were ground thoroughly for about 3 h to get homogeneity. In addition, UMoO_6 was synthesized by following a reported procedure [23].

3.2.3 Instrumentation:

An all-quartz pyrohydrolysis apparatus was used [24]. The description of the apparatus was given in the chapter 2. A 150 mm length Liebig condenser with chilled water (~278K) circulation was used. A commercial ion chromatograph (IC; DX-500 model; Dionex, Sunnyvale, CA, USA) consisting of a gradient pump (GP-50), ED-40 conductivity detector, and an anion self-regenerator suppressor (ASRS-II) was used for obtaining the chromatograms., IonPac AS16 (250 × 4 mm) along

with its guard column, IonPac AG16 (50 × 4 mm). The TG analyses were carried out on a TGA-DTA Instrument (Netzsch STA 409 PC, NETZSCH-Geratebau GmbH, Germany). XRD patterns were recorded using Rigaku MiniFlex-600 X-ray diffractometer.

3.2.4 IC Analysis of Mo:

Since during pyrohydrolysis the volatile form of Mo i.e. MoO_4^{2-} will be trapped in a dilute solution of NaOH, there is a need to develop an ion chromatography separation method for separating MoO_4^{2-} ion along with other common anions. In the basic medium Mo exist as MoO_4^{2-} . Using ion chromatography the MoO_4^{2-} ion can be separated on an anion exchange column. An ion exchange column, Ionpac AS16 was selected owing to its high capacity and good selectivity. Dilute NaOH solutions in the concentration range between 10 and 35 mM were used as mobile phases as the sample is in NaOH medium. It was observed that a mobile phase of 15 mM NaOH at a flow rate of 1 mL min^{-1} was found to be optimum for separating the MoO_4^{2-} ion from the other common anions. Figure 1 shows a typical chromatogram obtained for a standard solution containing MoO_4^{2-} ion. The limit of detection (LOD) of the method was calculated on the basis of the S/N ratio = 3 method, and it was found to be 80 ppb for Mo.

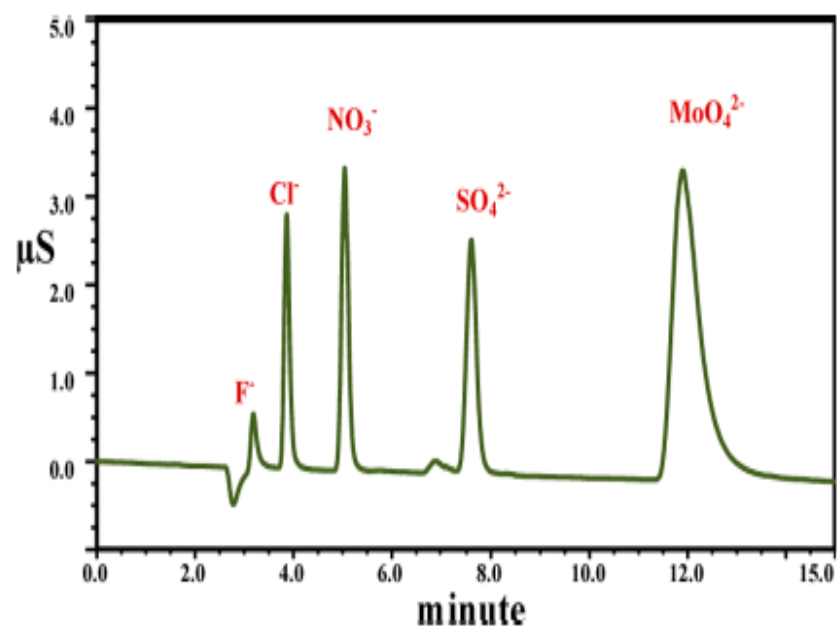


Figure 3.1: Chromatogram of an anion mix standard containing F⁻ (0.5 ppm), Cl⁻ (1.0 ppm), NO₃⁻ (2.0 ppm), SO₄²⁻ (2.0 ppm), and MoO₄²⁻ (10.0 ppm): column, IonPac AS-16; eluent, 15 mM NaOH; flow rate, 1 mL min⁻¹.

3.3 Results and Discussion:

The feasibility of separating Mo from uranium matrices using pyrohydrolysis was explored with a view to determining Mo accurately in uranium. To start with, a thermogravimetryanalysis (TGA) was carried to understand the vapour chemistry of MoO₃. During TGA moist atmosphere condition was maintained to know the effect of moisture on the loss of MoO₃ at high temperatures. TGA of MoO₃ using Ar carrier gas with and without water vapour at elevated temperatures may provide information relevant to the vaporization of Mo under the conditions similar to pyrohydrolysis. The reported TGA studies on MoO₃ have shown loss of MoO₃ by increasing temperature [25], however, TGA studies on the effect of water vapour on the vaporization of MoO₃ under isothermal conditions were not reported.

3.3.1 Thermogravimetric Analysis:

For this purpose, ~ 3 mg of the sample (MoO_3) was heated at a rate of 298K min^{-1} to the desired temperature, and thereafter, it was kept constant. At first TGA was performed at 1073K with Ar by keeping its flow rate at 100 mL min^{-1} (Figure 2.2 a). The atmosphere maintained was dry.

To perform a similar analysis in moist conditions the Ar carrier gas was passed through boiling water, which saturated the Ar with moisture. The weight loss curve with this moist condition is shown in Figure 2.2 b.

In case of the dry Ar atmosphere the weight loss of MoO_3 was $\sim 21\%$ whereas the weight loss was around 43% when the experiment was performed in moist Ar. This observation was similar to the observation of enhanced vapour pressure of MoO_3 due to presence of moisture atmosphere [21] and reconfirms the fact that the presence of water enhances the volatilization of MoO_3 .

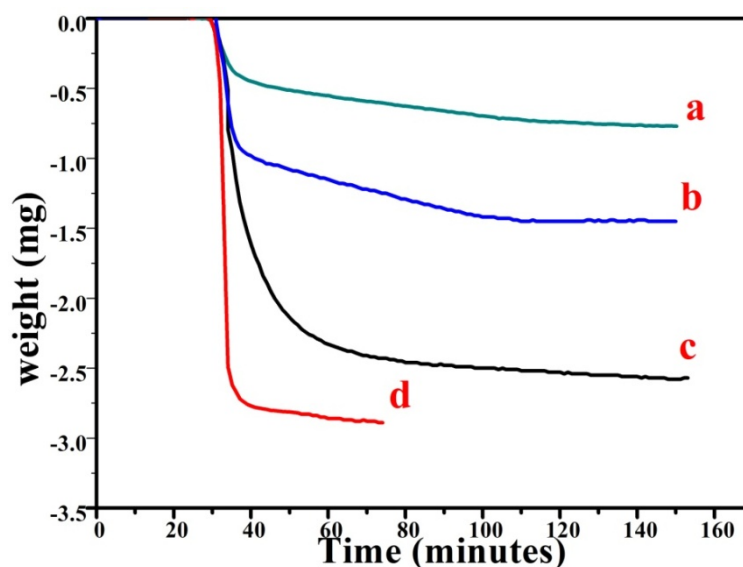


Figure 3.2: Isothermal thermograms of ~ 3 mg of MoO_3 at different temperatures and carrier gas conditions: (a) 1073K in dry Ar carrier gas; (b) 1073K in moist Ar carrier gas; (c) 1273K in moist Ar carrier gas; (d) 1473K in moist Ar carrier gas.

The moist Ar condition was further explored at 1273K as well as 1473K and the thermograms obtained were shown in Figure 2.2 c and d, respectively. The weight loss of MoO₃ was found to be 83% at 1273K whereas the same was 96% at 1473K. The results indicate that the rate of vaporisation of MoO₃ is temperature dependent. Since the apparatus used for pyrohydrolysis is made up of quartz, pyrohydrolysis should not be carried out above 1273K for longer duration especially for the routine kind of work. In view of this, the TGA time of analysis was increased to 200 min at 1273K and under this condition 97% weight loss of MoO₃ was observed.

3.3.2 Pyrohydrolysis of Mo Containing Standards:

Though the TGA studies showed more than 97% volatilisation of MoO₃ in moist Ar at higher temperatures, it is necessary to maintain conditions during pyrohydrolysis which favours formation of MoO₃ (In U matrices Mo can be present in forms other than MoO₃, which are not volatile). In view of this during pyrohydrolysis moist oxygen was used as the carrier gas. During the pyrohydrolysis of sample in moist oxygen the Mo may undergo following changes:

- (i) Oxidation of Mo to its oxide, MoO₃(s)
- (ii) Volatilization of MoO₃(s) to MoO₃(g) and
- (iii) Dissolution of MoO₃(g) in water vapour due to formation of MoO₃·H₂O, which would drastically enhance the volatilization of MoO₃

MoO₃ Standards:

In order to study the pyrohydrolysis of Mo containing uranium materials, synthetic standards were prepared. Two synthetic mixed oxide standards (UO₂ + MoO₃) having 100 and 500 ppm of Mo were prepared and subjected to pyrohydrolysis for

different time durations. Sample masses of ~1g and 0.5 g were taken for 100 ppm and 500 ppm standards, respectively. A plot of Mo recovered as a function of time is shown in Figure 2.3a. Though quantitative recovery of Mo was realized in the both standards, the time of pyrohydrolysis required for achieving the quantitative recovery in each case was different.

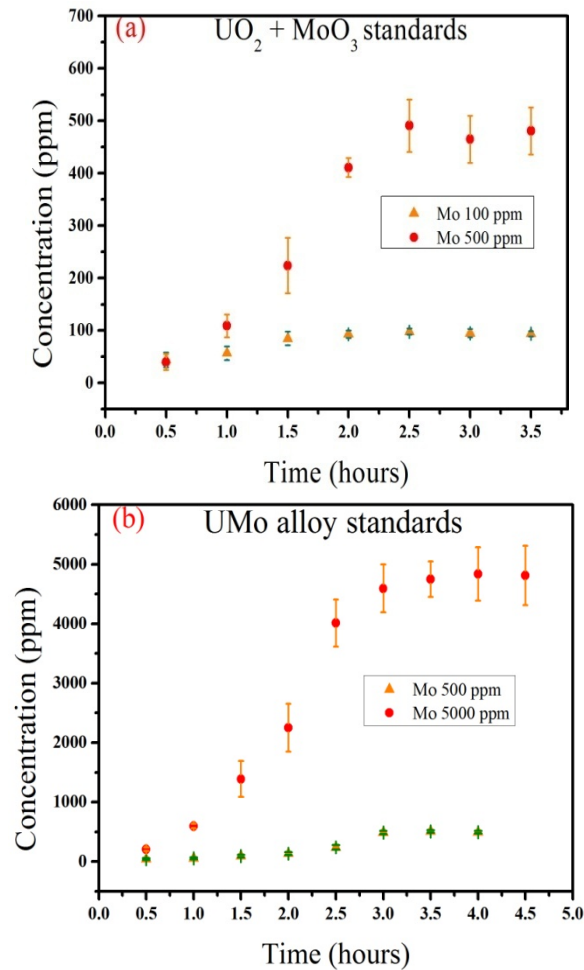


Figure 3.3. Recovery curve in moist O₂ carrier gas (a) for UO₂ + MoO₃ mixture standard containing 100 and 500 ppm Mo and (b) for UMo alloy standard containing 500 and 5000 ppm Mo.

Table 3.1. Minimum Time Required for Recovery of Mo Better than 95%, from Alloy and Oxide Standards.

standard	Mo (ppm)	sample weight (g)	time (h) of PH for >95% recovery
UO₂ + MoO₃	100	1.0	2.0
	500	0.5	2.5
UMo alloy	500	0.5	3.0
	5000	0.5	3.5

Alloy Standards: In addition to the oxides, two more synthetic standards of U-Mo alloy (500 and 5000 ppm of Mo) were also prepared and pyrohydrolyzed. A sample mass of ~0.5g of each standard was pyrohydrolysed. The Mo recovery as a function of time is shown in Figure 2.3b. Table 1 lists out the comparison of time required for pyrohydrolysis of oxide and alloy standards.

3.3.3 Kinetics of Mo Separation:

Following are the important observations made during the Pyrohydrolysis of standards

- i. The time required for the quantitative separation of Mo depends upon the concentration of Mo and the sample mass.
- ii. Although the carrier gas flow rate during PH was kept nearly 20 times higher than TGA, the time of pyrohydrolysis in all of the cases was observed to be longer than expected.

The probable reasons for these observations could be the slow vaporization of MoO_3 in uranium matrix and/or the formation of non-volatile Mo compounds due to solid state reactions. It is necessary to investigate the cause for this slow kinetics and to take necessary action for improving the kinetics of separation.

Vaporization Kinetics: To understand the vaporisation of MoO_3 in U matrix under pyrohydrolysis conditions, a synthetic mixed oxide standard containing 20% Mo by weight was subjected to pyrohydrolysis for different time durations, i.e., 1/2, 1.0, 1 1/2, and 2.0 h, in moist O_2 atmosphere at 1273K.

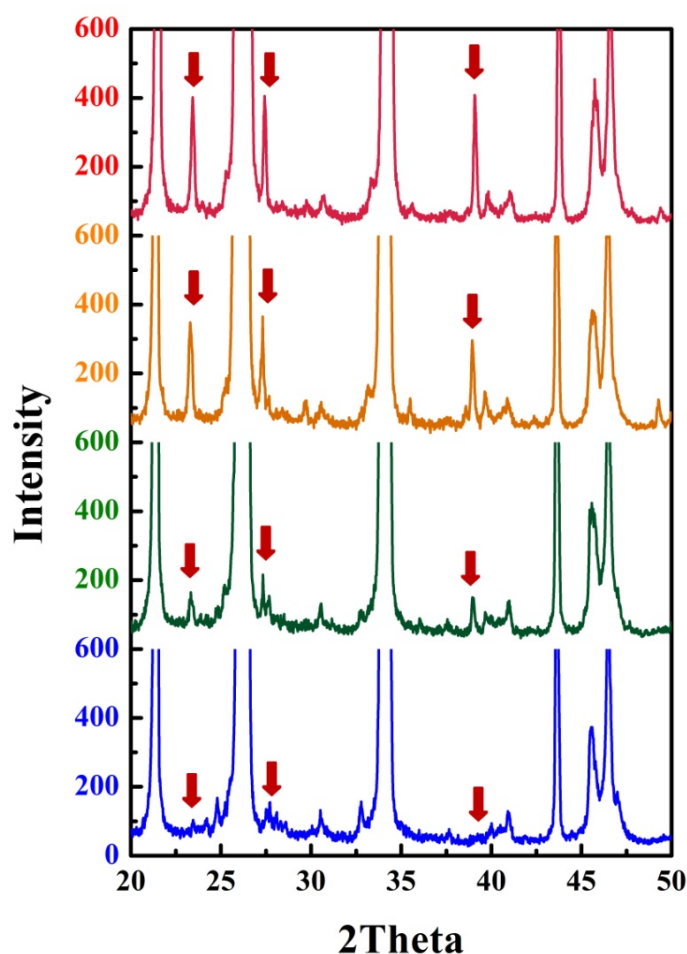


Figure 3.4. XRD patterns of UO_2 and MoO_3 mixture recorded after (a) 1/2, (b) 1, (c) 1 1/2, and (d) 2 h of pyrohydrolysis. The downward arrow symbol indicates a few major peaks for MoO_3 .

The materials obtained after pyrohydrolysis in each case were subjected to XRD analysis, and Figure 3.4 shows an overlay of the recorded XRD patterns. As the XRD patterns shows with peaks corresponding to vaporization of MoO_3 decreases with time. It can also be observed in 2 hrs the content was below the detection limit of XRD. This indicates the vaporization is prompt enough, even when the Mo content is quite high.

Formation of Non-volatile Compounds: In the present case, U and Mo can form compounds such as UMo_2O_8 , U_2MoO_8 , UMoO_5 , and UMoO_6 [27]. Reported studies

show that UMo_2O_8 , U_2MoO_8 , and UMoO_5 under oxygen atmosphere and in the temperature range of 760–796K are converted to UMoO_6 . The reported decomposition temperatures for UMoO_6 were found to be different in different literatures 1200K [26] and 1400K [27]. It may be possible that UMoO_6 is formed during pyrohydrolysis (temp \sim 1223K) and remains un-decomposed. This can affect the separation kinetics. Therefore, it becomes necessary to understand the behaviour of UMoO_6 during PH. For this purpose, UMoO_6 was synthesized [22] and it was pyrohydrolyzed for 2½ h. XRD analyses of UMoO_6 before and after pyrohydrolysis confirmed the complete conversion of UMoO_6 to U_3O_8 (Figure 3.5).

Since the formation of UMoO_6 could not be ascertained for the delay in pyrohydrolysis, the possibility of local condensation of $\text{MoO}_3 \cdot \text{H}_2\text{O}$ vapour on parts of the reaction tube (relatively at lower temperature) was considered. This was investigated by heating the parts of the apparatus which are at lower temperatures. After heating the apparatus externally the recovery increased considerably. This indicates that there is reversible local condensation responsible for the slower recovery of Mo.

To improve the kinetics of separation, a short reaction tube was incorporated in the PH apparatus which provides a shorter path length as well as relatively higher temperature as it was closer to the furnace. The modified apparatus brought quantitative recovery of Mo within 2½ h irrespective of the Mo content in the samples.

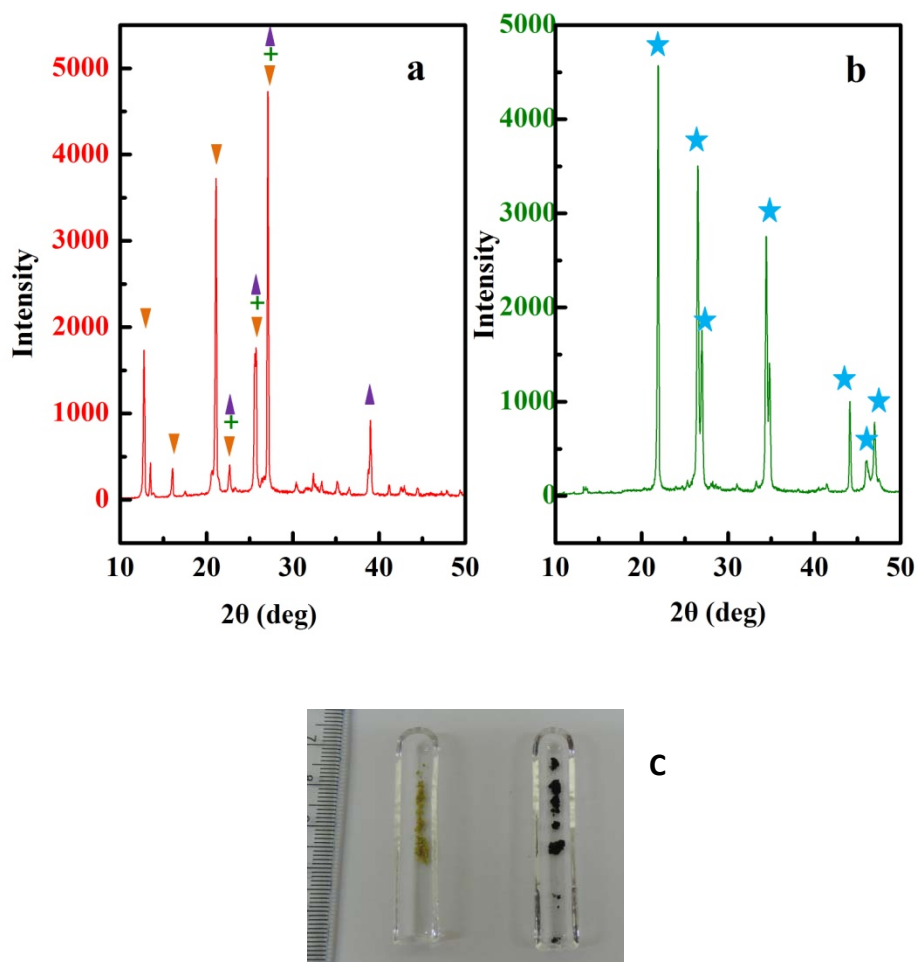


Figure 3.5: XRD patterns of (a) UMoO₆ powder and (b) U₃O₈ formed after pyrohydrolysis of UMoO₆ (all peaks are characteristic to U₃O₈): carrier gas, moist O₂; time, 2½ h; temperature, 1273K. (c) The picture of UMoO₆ before and after pyrohydrolysis.

3.3.4 Optimization of Pyrohydrolysis Conditions:

Pyrohydrolysis at 1573K: It may be recalled that the TGA studies showed that the rate of volatilization of MoO₃ increases with temperature. Pyrohydrolysis was carried out at 1573K by varying the time of pyrohydrolysis. Results showed quantitative extraction of Mo within 1½ h. During the study it was also observed

that continuous operation of the quartz PH apparatus for about 20 h (in 2 days) showed visible effects of devitrification.

Optimization of Sample Mass: For U-Mo alloy standard having 5000 ppm of Mo the standard deviation in the recovery of Mo was varied from 3 to 12% while the sample mass was increased from 50 to 1000 mg. Therefore it was concluded that for samples containing higher concentration of Mo it is important to keep sample mass low in order to get good precision. For mixed oxide standard having 100 ppm of Mo showed acceptable precision only when the sample mass was above 250 mg. This is because of the concentration of Mo in the distillate becomes less than the detection limit of IC. The analysis of samples containing low Mo requires high sample mass (~1000 mg) during PH.

Therefore, depending upon the expected concentration of Mo in the sample, the sample size for pyrohydrolysis would vary between 50 and 1000 mg

Optimized Pyrohydrolysis Conditions:

Based on the results, the optimum pyrohydrolysis conditions are as follows:

- (i) Sample mass, 50–1000 mg (depends on Mo content)
- (ii) PH temperature, 1273 K or more
- (iii) Time duration of PH, 2½ h or more for 1423 K
- (iv) Carrier gas flow rate, 2 L min⁻¹
- (v) Trapping agent, 5 mL of 25 mM NaOH.

3.3.5 Method Validation and Sample Analysis:

A certified reference material (CRM) of U_3O_8 (ILCE-4, Department of Atomic Energy (DAE), Mumbai, India) was analysed for its Mo content [28]. The Mo content in this standard is certified as 47.1 ± 8.7 ppm. The CRM was also analysed by ICP-AES method (without heating) and the results obtained are listed in Table 3.2.

Method was extended to the real samples of ammoniumdiuranate (ADU) samples containing enriched uranium were analysed. The determination of Mo in these enriched U containing ADU samples is important because:

- i. During enrichment process, the Mo present in the form of MoF_6 is also in the vapour phase and gets enriched in the U-235 phase. This may result in Mo concentrations more than expected.
- ii. The existing method for the determination of Mo in ADU involves heating of the sample to $800^\circ C$, which may cause loss of Mo as ADU has significant amount of moisture.

This loss of Mo from ADU due to the heating of ADU prior to its dissolution was confirmed by carrying out separate analyses of ADU with and without heating. In first analysis, the existing procedure involving the heating of ADU to 1073K and converting into the matrix into U_3O_8 . Further the oxide was dissolved in nitric acid and it was treated with TBP to extract the U matrix. The remaining aqueous sample was analysed by ICP-AES for Mo content. In the second analysis, the same procedure was followed except the heating step. The results obtained from both the analyses are given in Table 3.2. It is seen from the results that heating step caused significant loss of Mo. In a separate analysis the same sample was analysed by

following the developed method in which the Mo was separated by pyrohydrolysis and the distillate was analysed by IC and ICP-AES. The values obtained from IC as well as ICP-AES were listed in the Table 3.2.

Table 3.2. Comparison of results obtained for ADU Samples by the Developed Method, Solvent Extraction Followed by ICP-AES, and Pyrohydrolysis followed by ICP-AES Methods.

Sample	Concentration of Mo (ppm)				
	Certified	ICP-AES ¹ (ppm)	ICP-AES ² (ppm)	PH distillate by ICP-AES (ppm)	PH distillate by IC (ppm)
ADU-1		20 ± 6	35 ± 5	38 ± 4	37 ± 2
ADU-2		17 ± 5	38 ± 4	40 ± 5	41 ± 3
ADU-3		-	-		52 ± 3
ILCE-IV	47.1 ± 8.7		45 ± 5		42 ± 2

¹Conventional procedure, ADU heated to 850 °C, dissolved in HNO₃, U separated by TBP, and aqueous phase analyzed for Mo content.

²ADU directly dissolved in HNO₃ to avoid Mo loss due to heating, separated by TBP, and the aqueous phase analyzed for Mo content.

3.4 Conclusion:

The present study explored the feasibility of separating Mo in uranium matrices using pyrohydrolysis for the first time. A simple, green, and eco-friendly pyrohydrolysis separation of Mo directly from the solid matrices without the use of acids and other organic reagents was developed. The pyrohydrolysis separation

followed by ion chromatography determination was successfully applied to ADU samples having enriched uranium.

3.5 References:

1. V. P. Sinha, G. J. Prasad, P. V. Hegde, R. Keswani, C. B. Basak, S. Pal, G. P. Mishra, *J. Alloys Compd.* 473(2009)238.
2. P. Martin, M. Ripert, G. Carlot, P. Parent, C. Laffon, *J. Nucl. Mater.* 326(2004)132.
3. S. F. Marsh, *Anal. Chem.* 39(1967) 696.
4. T. Sato, H. Watanabe, H. Suzuki, *Hydrometallurgy* 23(1990)297.
5. P. C. Rout, K. Sarangi, *Hydrometallurgy* 133(2013)149.
6. R. E. Lewis, *Int. J. Appl. Radiat. Isot.* 22(1971)603.
7. A. G. C. Nair, S. K. Das, S. M. Deshmukh, S. Prakash, *Radiochim. Acta* 57(1992)29.
8. M. K. Saxena, P. Kumar, S. B. Deb, K. L. Ramakumar, *Nuclear and Radiochemistry Symposium Proceeding; Bhabha Atomic Research Centre (BARC): Mumbai, India, 2005; pp 487.*
9. F. G. Antes, F. A. Duarte, J. N. G. Paniz, , M. F. P. Santos, R. C. L. Guimaraes, E. M. M. Flores, V. L. Dressler, *At. Spectrosc.* 29(2008)157.
10. V. L. Dressler, D. Pozebon,, E. L. M. Flores, J. N. G. Paniz, E. M. M. Flores, *J. Braz. Chem. Soc.* 14(2003)334.
11. Y. Noguchi, L. Zhang, T. Maruta, T. Yamane, N. Kiba, *Anal. Chim. Acta* 640(2009) 106.
12. Y. Muramatsu, Y. Takada, H. Matsuzaki, S. Yoshida, *Quat. Geochronol.* 3(2008)291.

13. F. G. Antes, J. S. F. Pereira, M. S. P. Enders, C. M. M. Moreira, E. I. Muller, E. M. M. Flores, V. L. Dressler, *J. Microchem.* 101(2012)54.
14. C. C. Muller, T. S. Nunes, A. L. H. Muller, V. L. Dressler, E. M. M. Flores, E. I. Muller, *J. Braz. Chem. Soc.* 26(2015)110.
15. R. M. Sawant, M. A. Mahajan, P. Verma, D. Shah, U. K. Thakur, K. L. Ramakumar, V. Venugopal, *Radiochim. Acta.* 95(2009)585.
16. J. C. Warf, W. D. Cline, R. D. Tevebaugh, *Anal. Chem.* 26(1954)342.
17. S. Jeyakumar, V. V. Raut, K. L. Ramakumar, *Talanta* 76(2008)1246.
18. G. R. Smolik, D. A. Petti, S. T. J. Schuetz, *Nucl. Mater.* 283-287(2000)1458.
19. A. P. V. Soares, M. F. Portel, A. Kiennemann, L. Hilaire, *Chem. Eng. Sci.* 58(2003) 1315.
20. C. K. Gupta, *Extractive Metallurgy of Molybdenum*; CRC Press: Boca Raton, FL, USA(1992) 238.
21. K. U. Rempel, A. A. Migdisov, A. E. Williams-Jones, *Geochim. Cosmochim. Acta* 70(2006) 687.
22. N. T. Kim-Ngan, I. Tkach, S. Maskova, L. Havela, A. Warren, T. Scott, *Adv. Nat. Sci.: Nanosci. Nanotechnol.* 4(2013)035006.
23. M. Keskar, N. D. Dahale, K. J. Krishnan, *Nucl. Mater.* 393(2009)328.
24. M. A. Mahajan, M. V. R. Prasad, H. R. Mhatre, R. M. Sawant, R. K. Rastogi, G. H. Rizvi, N. K. J. Chaudhuri, *Radioanal. Nucl. Chem.* 148(1991)93.
25. T. Nagai, N. Sato, S. Kitawaki, A. Uehara, T. Fujii, H. Yamana,; M. J. Myochin, *Nucl. Mater.* 433(2013)397.
26. S. R. Bharadwaj, S. R. Dharwadkar, M. S. Chandrasekharaiah, *Thermochim. Acta* 79(1984)377.

27. E. V. Suleimanov, A. V. Golubev, E. V. Alekseev, C. A. Geiger, W. Depmeier, V. G. Krivovichev, *J. Chem. Thermodyn.* 42(2010)873.
28. DAE-Interlaboratory Comparison experiment (ILCE) for trace metal assay of uranium - Phase 4, Document; Bhabha Atomic Research Centre (BARC): Mumbai, India, 2002.

Chapter: 4

Studies on U-Zr and U-Pu-Zr Alloys for Determination of Cl and F Using Pyrohydrolysis

4.1 Introduction:

Metallic fuels are being considered for future Indian fast reactors program. This is mainly because of the advantages associated with these fuels. Unlike oxide fuel, metallic fuel with its higher breeding ratio and shorter doubling time will be able to produce more plutonium to help commission many more nuclear power reactors. It may be mentioned that to meet the increasing energy demand, the country has embarked on a major programme to generate additional 20,000 MW of nuclear power by 2020 and the target is to have 30GW by 2020. This can be achieved only if many nuclear power plants are commissioned. And for this to happen, sufficient nuclear fuel should be available. Oxide fuel with only 1.1 breeding ratio produces very little extra plutonium compared to metallic fuel with a breeding ratio of 1.4-1.5. Hence the doubling time is more in the case of oxide and least for metallic fuel. The doubling time for metallic fuel is ten years while it is thirty years in the case of oxide fuel. It is judicious to have a fuel cycle with shorter doubling time.

The other important advantages are:

- i. High thermal conductivity
- ii. heavymetal density
- iii. ease of fabrication
- iv. Possibility of Pyro-process for recycling [1, 2].

In view of this, the long term Indian Fast Reactor programme will be based on metallic fuels [3].

Use of U or U-Pu as metallic fuel has few limitations such as their unfavourable melting during fabrication and formation of low melting compounds with the stainless steel clad materials. U-Zr and U-Pu-Zr alloy fuels are the material of choice due to their higher solidus temperature and higher eutectic with T91 clad. The fabrication of these materials and their test-irradiation in FBTR is an ongoing project in BARC. Like any other nuclear fuel the presence of F and Cl may cause problems to the integrity of fuel cladding due to their corrosive nature [4–6]. Since these halides cause depassivation of clad surface and corrosion, F and Cl have stringent specification limits in various types of fuels. Hence, their concentration in the fuels needed to be controlled [7]. The chemical reagents that are used in the processes of fabrication and reprocessing are the major sources for Cl and F and they get added into the nuclear materials as impurities. It is known that during fabrication of alloys the impurities can be easily picked up by the highly reactive molten metallic components. It is important to have sensitive and reliable methods for the analysis of chlorine and fluorine at various stages of fabrication of U-Zr and U-Pu-Zr alloys.

In pyrohydrolysis the halides are separated using either moist argon or oxygen as carrier gas and by heating the matrix at high temperature. The chlorine and fluorine released from the solid sample are in the form of HCl and HF, respectively. The HCl and HF thus formed are carried away by the moist carrier gas which is subsequently trapped in a dilute NaOH solution (pyrohydrolysis distillate).

Once the distillate is available, suitable analytical techniques are employed for the determination of individual analytes. The determination of halogen using

pyrohydrolysis separation followed by ion chromatography in various matrices can be found in [10–24].

In our laboratory also, pyrohydrolysis technique followed by ion chromatography is being routinely employed for this purpose. Necessary analytical methodologies have been developed by optimising experimental conditions for quantitative extraction of halogens from different nuclear fuel matrices such as U_3O_8 , $(U, Pu)O_2$, $(U, Pu)C$, ThO_2 etc. The present study investigates different pyrohydrolysis conditions to understand the behaviour of U-Zr and U-Pu-Zr matrices for realising quantitative extraction of chlorine and fluorine.

4.2: Experimental Section:

4.2.1 Pyrohydrolysis setup:

All quartz pyrohydrolysis set up consisting of two concentric tubes was used for pyrohydrolysis purpose. The outer tube has an inlet and serves as a pre-heater for moist carrier gas. The inner tube houses the sample boat and it is attached to gas outlet. The gas outlet tube is cooled by a condenser. The condensate is collected in a bottle containing dilute NaOH. A schematic diagram of the pyrohydrolysis set up is presented elsewhere [22].

4.2.2 Ion chromatography system:

A commercial (Dionex DX-500) ion chromatography system consisting of an IP-20 isocratic pump, anion self-regenerator suppressor in external recycle mode, ED-40 conductivity detector with a DS3 stabilizer has been used for obtaining all the chromatograms. Samples were introduced through a 100 μ l loop fitted with a Rheodyne injector. Separation of anions were achieved on an analytical column

(Dionex, Ion PacAS16, 250x4mm) coupled with its guard column (AG16, 50x4 mm). A software viz. Chromeleon was used for instrument control as well as for data collection and processing. Other IC details are provided in the literature [22].

4.2.3 XRD instrument: The oxidized product of U-Zr samples were analysed using Rigaku MINIFLEX 600 X-ray diffractometer (θ - 2θ geometry) using $\text{CuK}\alpha$ radiation ($\lambda = 1.5406 \text{ \AA}$) with a scan rate of 1° min^{-1} was used. The oxidized products of U-Pu-Zr alloy were characterized by using $\text{CuK}\alpha$ ($\lambda = 1.54184 \text{ \AA}$) radiation employing Diano X-ray diffractometer (Diano Corporation, Wobmn, MA) and graphite monochromater. The instrument is housed in a glove box to handle the radioactive material.

4.2.4 Thermoanalyzer: Mettler Thermo Analyzer (model: TGA/SDTA851e/MT5/LF1600) in flowing dry air at heating rate of $10^\circ\text{C}/\text{min}$ up to 1000°C . Thermo analyzer was calibrated from the weight loss obtained for the decomposition of 100mg of $\text{CuSO}_4 \cdot 5\text{H}_2\text{O}$ to CuO , while heating at 1000°C in air.

4.2.5 Alloy fabrication and characterization:

U-Zr and U-Pu-Zr alloys were fabricated in the Radiometallurgy Division, BARC, using arc melting method [23,24]. The U and Pu contents in the U-Zr and U-Pu-Zr alloys were determined by electro analytical methods (bi-amperimetry whereas the concentration of Zr was determined by gravimetric method. The determined weight percentage of U, Pu and Zr are given in Table 4.1. The metallic impurities in these alloys are determined by ICP-MS and ICP-AES [25, 26].

Table 4.1: Chemical analysis of U, Pu and Zr from U-Zr and U-Pu-Zr alloy.

Material	wt. % Zr	wt. % U	wt. % Pu
U-Pu-Zr	4.7	76.1	19.1
U-Zr	6.1	93.8	-

Table 4.1: Chemical analysis of U, Pu and Zr from U-Zr and U-Pu-Zr alloy.

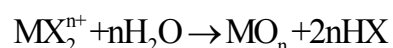
4.2.6 Pyrohydrolysis procedure:

The alloys were pyrohydrolysed with moist Ar and moist O₂, separately. The condensed aqueous phase or distillate was collected in 5ml of 25mM NaOH solution (trapping solution). The distillate thus collected during pyrohydrolysis was diluted to 25 ml and was subjected to ion chromatography analysis.

4.3 Results and discussion:

Owing to the pyrophoric nature of Pu-alloys and mixed carbide fuels, the pyrohydrolysis is generally carried out in Ar atmosphere to avoid the vigorous reactions between the pyrophoric alloys and O₂/H₂O and also to release analytes in a controlled manner. The halides present in the alloy matrices are mainly in form of metal halides (MX_n).

The chemical reaction responsible for the release of halides from the matrix is,



The reaction occurs at 1173K or above since the free energy for the reaction is favourably negative at high temperatures. James C Warf et al. [18] have reported the

pyrohydrolysis of UF_4 , UF_3 , UO_2F_2 , ZrF_4 , and ZrOF_2 . However; the pyrohydrolysis of Pu-alloys have not been much investigated. Therefore, this study was directed to investigating pyrohydrolysis of U-Zr and U-Pu-Zr alloys and quantification of fluorine and chlorine contents employing ion chromatography. As reference materials of U-Zr and U-Pu-Zr with certified fluorine and chlorine contents were not available, Initially the pyrohydrolysis was carried out with Ar as a carrier gas [20] maintaining experimental conditions same as were followed for UO_2 , $(\text{U,Pu})\text{O}_2$ samples. However with a view to achieving maximum recovery the F and Cl from the alloy matrices, the pyrohydrolytic behavior of U-Zr alloys were studied by pyrohydrolysing the materials for different time intervals in moist argon. Figure 4.1 depicts the results.

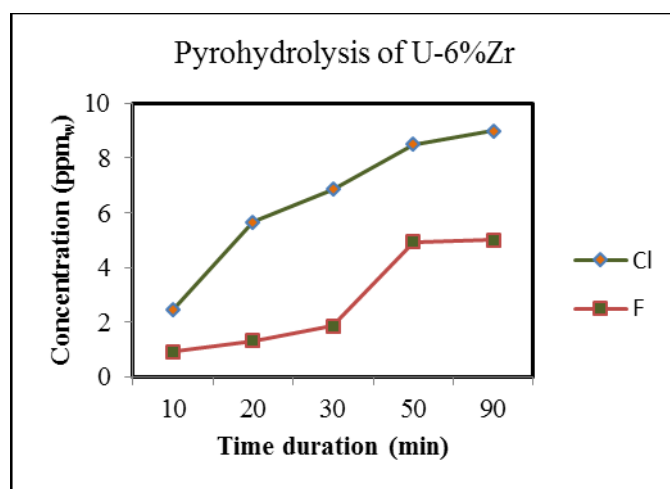


Figure 4.1 Pyrohydrolysis of U-6%Zr sample. (Conditions: 1173K moist Ar)

From the figure following observations could be drawn:

- i. Pyrohydrolysis conditions used for UO_2 and $(\text{U,Pu})\text{O}_2$ samples can also be used for pyrohydrolysing alloy samples
- ii. The results for both fluorine and chlorine show tendency to saturate

- iii. However the time taken to reach saturation or maximum concentration value is higher than in the case of UO_2 and $(\text{U,Pu})\text{O}_2$ samples.

From the above observations following preliminary conclusions could be drawn:

- a. The pyrohydrolysis of alloy samples is also thermodynamically feasible. This suggests that the chemical processes occurring in the case of UO_2 and $(\text{U,Pu})\text{O}_2$ samples may be occurring in the case of alloy samples also.
- b. The kinetics of the conversion process seems to be slow in the case of alloy samples.

To confirm these preliminary conclusions,

Although it is known that the kinetics of separation can be enhanced by using a suitable accelerator such as U_3O_8 or V_2O_5 [29], in the present case the uranium in the sample initially gets oxidised and acts as an in-situ accelerator and therefore no external accelerator was added.

In order to understand the reason behind the slow extraction as well as the extraction mechanism, it is necessary to observe the changes in the material during pyrohydrolysis. Therefore, the pyrohydrolysed products obtained at different time intervals were analysed by X-ray powder diffraction method. The XRD patterns of the oxidized product of U-Zr alloy under different duration of heating at 1173K in moist Ar atmospheres are shown in Figure 4.1. The different identified products formed during pyrohydrolysis are summarized in table 4.3. The XRD pattern of U-Zr alloy heated in moist Ar atmosphere for 10 min (Figure4.1a) indicated X-ray lines similar to UO_2 (FCC phase). No lines due to ZrO_2 were observed in XRD pattern

indicating the solubility of ZrO_2 in UO_2 . Recent studies showed that up to 35 mole % of ZrO_2 can be dissolved in UO_2 under mild oxidizing conditions at 1673K [30,31].

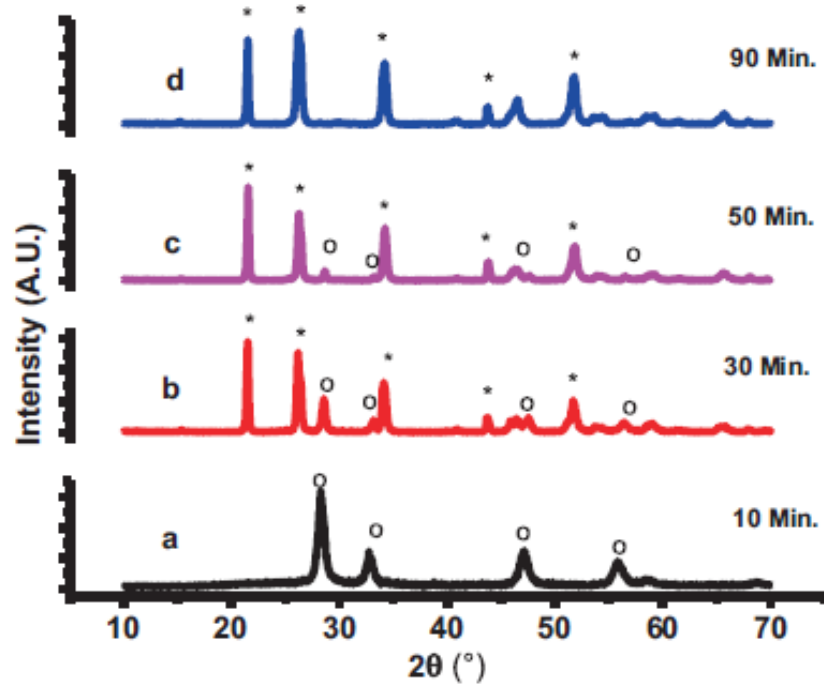


Figure 4.2: XRD patterns of pyrohydrolysed products of U-Zr alloy heated in moist Ar atmosphere at 1173K for (a) 10 min., (b) 30 min., (c) 50 min. and (d) 90 min. (o and * represent UO_2 and $\alpha-U_3O_8$, respectively).

Table 4.2: The summary of products identified by XRD on heat treatment of U-Zr alloy.

Starting material	Heat treatment	End product identified by XRD	Lattice parameter of FCC solid solution (Å)
U-Zr alloy	Dry air/1000°C/10°C /min	($\alpha-U_3O_8$)ss orthorhombic	-

U-Zr alloy	Moist Ar/900°C/ 10 min	(U, Zr)O _{2+x} FCC	5.458 (2)
U-Zr alloy	Moist Ar/900°C/ 30 min	(α -U ₃ O ₈) orthorhombic + (U,Zr)O _{2+x} FCC	- 5.410 (3)
U-Zr alloy	Moist Ar/900°C/ 50 min	(α -U ₃ O ₈) orthorhombic +(U, Zr)O _{2+x} FCC	- 5.410 (3)
U-Zr alloy	Moist Ar/900°C/ 90 min	(α -U ₃ O ₈)ss orthorhombic	-

XRD pattern of the U-Zr alloy heated in moist Ar atmosphere for 30 min (Figure 4.1b) showed the lines due to U₃O₈+UO₂ phase indicating incomplete oxidation of the alloy. XRD pattern shown in Figure 4.1c clearly reveals U₃O₈ as a major phase and FCC phase corresponding to UO₂ as a minor phase in the 50 minutes heated material. The weak lines due to UO₂ indicate that even 50 min heating is not sufficient to oxidize alloy sample completely to U₃O₈. The XRD obtained for the material pyrohydrolysed for 90 minutes showed the complete oxidation of uranium to U₃O₈ (Figure 4.1d). Since the volume of the material expands during the oxidation and this condition is favourable for separating the halides and the same is confirmed by the recoveries obtained for Cl and F. Since the oxidation of uranium is slow for the first 30 minutes of pyrohydrolysis, it is possible to use moist oxygen instead of moist Ar carrier gas. The use of moist oxygen will enhance the rate of oxidation; however, a controlled oxidation is necessary in case the rate of oxidation is high. Hence, similar investigation was repeated with moist oxygen carrier gas instead of moist Ar and the results obtained were listed in Table 4.4. Interestingly, it was observed that a maximum recovery of both chlorine and fluorine were obtained

even before 30 min. As seen from the Table 4.4, the percentage recovery of Cl and F from U-Zr alloy matrix is close to 100% when the samples are heated in moist O₂ atmosphere for 30 min. Between F and Cl, the recovery of Cl is faster than F as reported earlier [18]. These observations indicate that the chlorine and fluorine pyrohydrolysis extraction kinetics is determined by the formation of U₃O₈, however, it needs to be investigated.

Table 4.3: Pyrohydrolysis data for U-6wt%Zr alloys sample for varying time using moist oxygen as a carrier gas.

Duration of pyrohydrolysis (min)	Recovery of F (%)	Recovery of Cl (%)
10	96.7 ± 14.0	100.1 ± 7.1
20	99.2 ± 8.1	98.8 ± 5.3
30	100.0 ± 5.2	100 ± 3.7
50	101.0 ± 2.3	99.2 ± 3.8

To investigate the oxidation behaviour of U-Zr alloy in oxygen atmosphere, a study was carried out using thermogravimetric (TG), differential thermal analysis (DTA) and differential thermogravimetric analysis (DTG) simultaneously. Figure 4.2 shows TG and DTA plots for oxidation of U-Zr alloy in dry air. The analysis of TG and DTG data indicate that the oxidation of alloy takes place in single step in the temperature range of 473 to 773K. The XRD pattern for the pyrohydrolysed product obtained at 1273K was similar to that of U₃O₈. Thermogravimetric study showed

that the oxidation of the alloy was completed before it reached 1173K and got converted into U_3O_8 . This clearly shows that the complete oxidation of U-Zr alloy is necessary for the quantitative extraction of Cl and F from the matrix. However, in the case of the pyrohydrolysed samples in moist Ar obtained at different time intervals at 1173K showed that the complete recovery of Cl and F was possible only when the alloy was pyrohydrolysed for at least 90 minutes.

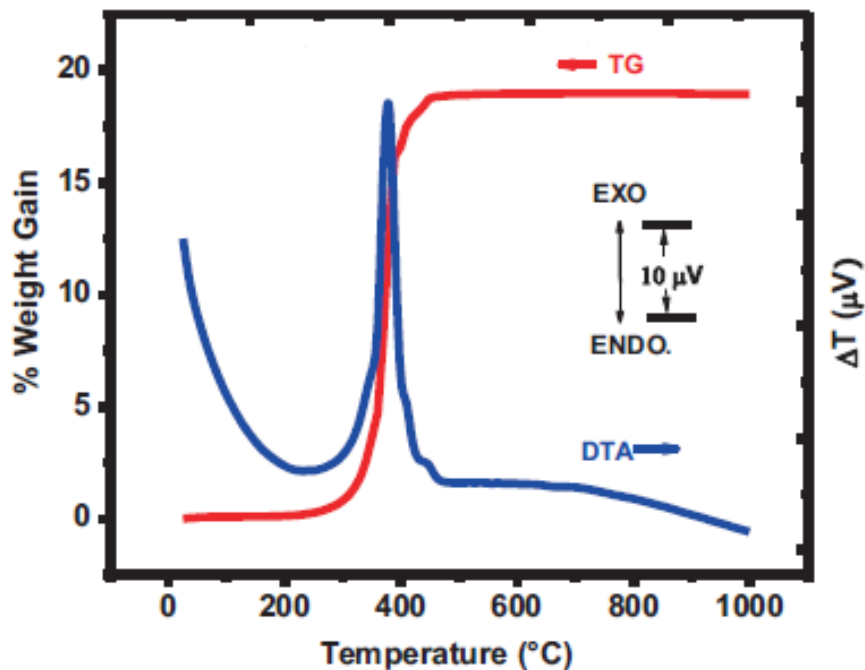


Figure 4.3: TG and DTA of U-Zr alloy in dry air with a heating rate of 10K/min.

All the above observations can be attributed to the density variations of the alloy during the oxidation process. It is known that U metal is thermodynamically unstable. While in contact with air and on heating U metal forms a hyperstoichiometric oxide represented as UO_{2+x} and when the exposure proceeds, phase transformation to U_4O_9 , U_3O_7 and finally U_3O_8 will take place at 773K. During this oxidation process,

the crystal structure will also change from FCC (UO_2) to orthorhombic (U_3O_8). The density calculated from X-ray data is 8.34 g/cc for U_3O_8 compared with 10.96 g/cc for UO_2 and this decrease in density resulted by the formation of U_3O_8 phase (~36% increase in unit cell volume for conversion of UO_2 to U_3O_8). This micro structural change can break up the material and lead to a large macroscopic expansion.

Based on the results obtained for U-Zr alloys, further studies were extended to U-Pu-Zr alloy. U-Pu-Zr alloys were also analyzed in moist oxygen atmosphere. Pyrohydrolysis of the U-Pu-Zr alloy samples was carried out by varying time of pyrohydrolysis at 1173K and the data are given in Table 4.5.

Table 4.4: Pyrohydrolysis data for U-19 wt% Pu-4.7 wt% Zr alloy sample for varying pyrohydrolysis time, with moist oxygen as carrier gas.

Duration of pyrohydrolysis (min)	U-Pu-Zr alloy	
	Moist O_2	
	Recovery of F (%)	Recovery of Cl (%)
10	91.5 ± 10.1	96.6 ± 5.1
20	99.6 ± 9.8	99.6 ± 6.7
30	100.0 ± 5.5	100.0 ± 4.7

Table 4.5 shows that heating of 30 minutes is sufficient for the quantitative recovery of Cl and F. The XRD pattern obtained for U-Pu-Zr alloy after heating in moist oxygen atmosphere was shown in Figure 4.3. The summary of products identified by XRD on heat treatment in moist oxygen atmosphere is given in Table 4.6. Though the concentration of U_3O_8 is more than the FCC phase of PuO_2 in the product phase, peaks due to U_3O_8 and $(\text{Pu}, \text{Zr})\text{O}_2$ were observed for U-Pu-Zr. The solubility of

ZrO₂ in actinide oxide increases with decrease in size of actinide ion [28] and it is reported that the solubility of ZrO₂ in PuO₂ is around 77 mol% at 1673K.

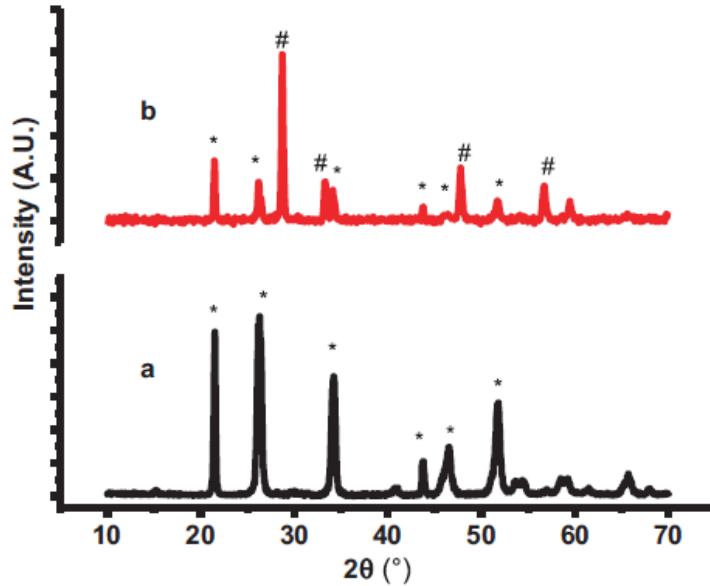


Figure 4.4: XRD patterns of pyrohydrolysed product of (a) U-Zr and (b) U-Pu-Zr alloy heated in moist oxygen atmosphere at 900°C for 30 min. (* and # represent (α -U₃O₈)ss and (PuO₂)ss, respectively)

Table 4.5: The summary of products identified by XRD on heat treatment of U-Zr and U-Pu-Zr alloys.

Starting material	Heat treatment	End product identified by XRD	Lattice parameter of FCC solid solution (Å)
U-Zr alloy	MoistO ₂ /900°C/30 min	(α -U ₃ O ₈)ss	-
U-Pu-Zr alloy	MoistO ₂ /900°C/30 min	(α -U ₃ O ₈)ss orthorhombic + FCC (Pu, Zr)O ₂	5.386 (1)

The above study has revealed that in moist oxygen, U present in the alloy gets converted into U₃O₈ in 10 min of pyrohydrolysis. An in-house working standard of

uranium oxide (UO_2) with known concentration of chloride and fluoride was used for validating the method and recovery calculations. Analysis of this standard was carried out prior to sample analysis to ensure the recoveries of F and Cl and a recovery of 95% was obtained. Replicate analysis of the sample showed good reproducibility of values.

Since the determination of chloride and fluoride was carried out by ion chromatography, the IC separation conditions were optimised. After studying the effect of eluent concentration on the retention of chloride and fluoride, the eluent was fixed as 13mM NaOH at flow rate of 1 mL/min. Limit of detections (LOD) calculated for chloride and fluoride were 20 ppb and 10 ppb, respectively.

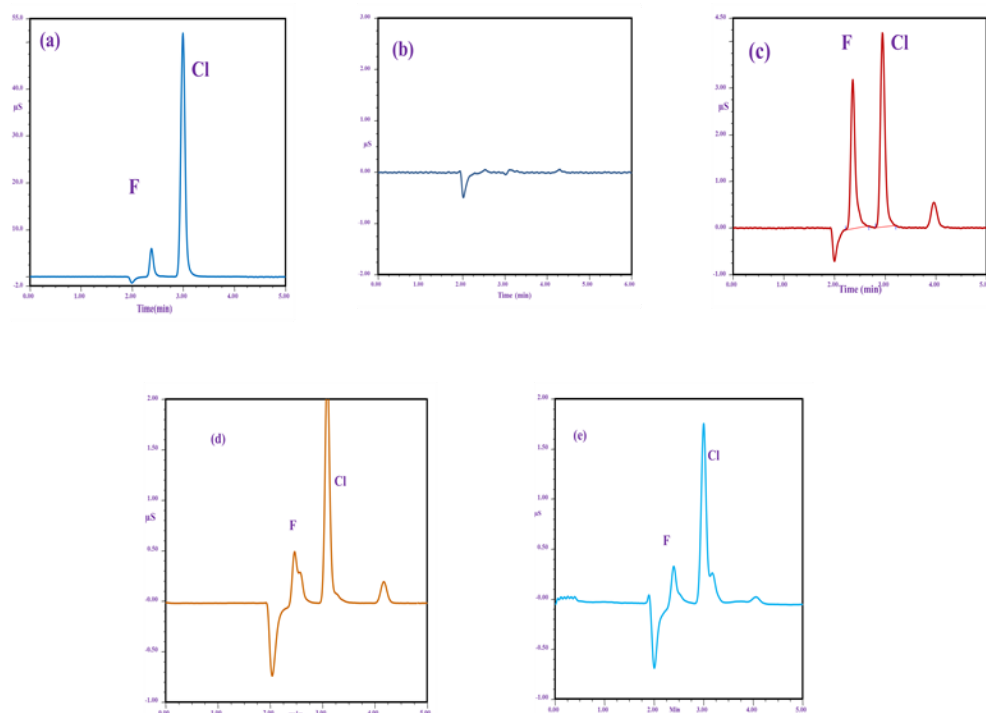


Figure 4.5: Chromatograms for different distillates analysed by IC. (a) standard solution, (b) blank run, (c) U_3O_8 standard (d) U-Zr sample and (e) U-Pu-Zr samples.

The optimised IC separation conditions could successfully be used for the analyses of the samples and the IC results obtained for samples are listed in Table 4.7. The reproducibility of measurement (precision in the measurement) was better than 5% at 0.1 ppm of both chloride and fluoride.

Table 4.6: F and Cl content of some routine samples analysed by pyrohydrolysis using moist oxygen.

Pyrohydrolysis followed by IC		
Samples aliquots	F content (ppm)	Cl content (ppm)
U-Zr alloy-1	4.1 ± 0.4	4.8 ± 0.3
U-Zr alloy-2	3.6 ± 0.4	9.2 ± 0.4
U-Zr alloy-3	5.0 ± 0.3	8.3 ± 0.5
U-Pu-Zr alloy-1	8.1 ± 0.6	25.8 ± 0.13
U-Pu-Zr alloy-2	2.9 ± 0.2	6.4 ± 0.4
U-Pu-Zr alloy-3	1.0 ± 0.2	4.3 ± 0.4
U-Pu-Zr alloy-4	1.6 ± 0.3	3.8 ± 0.5

4.4 Conclusions:

A pyrohydrolysis method for the separation of Cl and F in U-Zr and U-Pu-Zr alloys was developed. Extensive investigation on the pyrohydrolysis behaviour of the alloys revealed that the complete recovery of both chlorine and fluorine by pyrohydrolysis is possible only after converting the uranium into U₃O₈. The relevance between oxidation of uranium to U₃O₈ was confirmed by carrying out the XRD and TG/DTA studies. Pyrohydrolysis with moist oxygen facilitated the formation of U₃O₈ in minimum time of heating and also facilitated the quantitative

release of halides. The developed method was successfully employed for the routine analysis of real samples.

4.5 References:

1. G. L. Hoffman, L. C. Walters, T. H. Bauger, *Progress. Nucl. Energ.*, 31(1997)83.
2. A.Riyas, P. Mohankrishnan, *Ann. Nucl. Energy*, 35(2008) 87.
3. S. C. Chetal, P. Chellapandi, P. Puthiyavinayagam, S. Raghupathy, V. Balasubramanian, P. Selvaraj, P.Mohanakrishnan,*Asian Nuclear Prospects*, 7 (2011) 64.
4. M. V.Ramaniah, *PureAppl. Chem.*, 54 (1982) 889.
5. S. H.Shann, D. R. Olander, *J. Nucl. Mater.*, 113 (1983) 234.
6. S. V. Elinson, N. A.Zemlyanukhina, I. V. Pavlova, V. P. Filatkina, V. T. Tsvetkova, *Radiokhimiya*, 23 (1981)753.
7. Y. S.Sayi, K. L. Ramkumar, V. Venugopal, *IANCAS bulletin*, 3 (2008)180.
8. H. H. Willard, O. B. Winter, *Ind. Eng. Chem. (Anal Ed.)*, 5(1933)7.
9. R. D.Dabeka, A. D. McKenzie, *J. Assoc. Off. Anal. Chem.*, 64(1981)1021.
10. M. Bettinelli, S. Spezia, C.Minoia, A. Ronchi, *At. Spectrosc.*, 23(2002)105.
11. F. G. Antes, F. A. Duarte, J. N.G. Paniz, M. F. P.Santos, R. C. L. Guimaraes, , E. M. M. Flores, V. L.Dressler, *At. Spectrosc.*, 29(2008)157.
12. V. L. Dressler, D. Pozebon, E. L. M. Flores, J. N. G. Paniz, E. M. M. Flores, J. *Braz. Chem. Soc.*, 14(2003)334.

13. Y. Muramatsu, Y. Takada, H. Matsuzaki, S. Yoshida, *Quat. Geochronol.*, 3(2008)291.
14. M. Boniface, N. Jendrzewski, P. Agrier, M. Coleman, F. Pineau, M. Javoy, *Chem. Geol.*, 242(2007)187.
15. Y. Nogushi, L. Zhang, T. Maruta, T. Yamane, N. Kiba, *Anal. Chim. Acta* 640(2009)106.
16. J. E. Rae, S. A. Malik, *Chemosphere*, 33(1996) 2121.
17. G. A. Fabiane, J. S. F. Pereira, M. S. P. Enders, C. M. M. Moreira, E. I. Muller, E. M. M. Flores, *Microchem. J.*, 101(2012)54.
18. J. C. Warf, W. D. Cline, R. D. Tevebaugh, *Anal. Chem.*, 26(1954)342.
19. M. Iwasaki, N. Ishikawa, *J. Nucl. Sci. and Tech.*, 20 (1983) 400.
20. R. M. Sawant, M. A. Mahajan, P. Verma, D. Shah, U. K. Thakur, K. L. Ramkumar, V. Venugopal, *Radiochim. Acta*, 95(2007)585.
21. M. A. Mahajan, M. V. R. Prasad, H. R. Mhatre, R. M. Sawant, R. K. Rastogi, G. H. Rizvi, N. K. Chaudhuri, *J. Radioanal. Nucl. Chem.* 148(1991)93.
22. R. M. Sawant, M. A. Mahajan, D. Shah, U. K. Thakur, K. L. Ramkumar, *J. Radioanal. Nucl. Chem.*, 287(2011)423.
23. T. R. G. Kutty, S. Kaity, C. B. Basak, Arun Kumar, R. P. Singh, *Nucl. Eng. Desn.*, 250(2012)125.
24. S. Kaity, J. Banerjee, K. Ravi, R. Keswani, T. R. G. Kutty, Arun Kumar, G. J. Prasad, *J. Nucl. Mater.*, 433(2013)206.

25. A. Saha, S. B. Deb, B. K. Nagar, M. K. Saxena, *Atomic Spectroscopy*, 34(2013)125.
26. A. Sengupta, V. C Adya, *Atomic Spectroscopy*, 34(2013)207.
27. V. R. Wiederkehr, G. W. Goward, *Anal. Chem.*, 31(1959)2102.
28. S. Jeyakumar, V. V.Raut, K. L. Ramakumar, *Talanta*, 76(2008)1246.
29. R. H. Powell, O. Menis, *Anal. Chem.*, 30(1958)1546.
30. N. K. Kulkarni, K. Krishnan, U. M. Kasar, S. K.Sali, S. K. Aggarwal, *J. Nucl. Mater.*, 384(2009)81.
31. G. A. Rama Rao, V. Venugopal, D. D.Sood, *J. Nucl.Mater.*, 209(1994)161.
32. S. K. Sali, N. K. Kulkarni, D. G. Phal, S. K. Aggarwal, V. Venugopal, *J. Am. Cer. Soc.*, 93(2010)3437.
33. D. F. Corroll, *J. Am. Cer. Soc.*, 46(1963)194.

Chapter: 5

Development of Ion Chromatography and Capillary Electrophoresis Methods for the Determination of Li in Li–Al Alloy

5.1 Introduction:

Lithium aluminium alloy is used as a target material for producing tritium by the nuclear reaction ${}^6\text{Li}(n,\alpha)\text{T}$. Li is alloyed with Al to reduce the high reactivity of Li with air and moisture [1]. In addition Al is having low neutron absorption cross-section and helps in dissipating heat. The material has potential for its use in fusion reactor, where tritium produced from Li diffuses out from solid matrix and get into the plasma of the reactor to fuse with deuterium. Li-Al alloy has advantages over pure Li such as high melting point (973K) and greater vapour pressure of tritium from the matrix [2].

For the use of the Li-Al material as a target for tritium production or for use in fusion reactor, it is important to know the exact Li content in addition to ${}^6\text{Li}$ abundance, and this would enable to ensure the calculated performance of the reactor. Therefore, certification of lithium content in Li–Al alloy demands an accurate and precise method.

The methods available for Li determination in Li-Al alloy are based on Atomic Absorption Spectrometry (AAS) and Inductively Coupled Plasma–Atomic Emission Spectrometry (ICP-AES) [3]. However, the literature shows that these methods suffer from few limitations. For instance, in AAS the Al matrix causes incomplete

atomization of Li if not separated. On the other hand in the ICP-AES the Al matrix affects the signal intensity of Li lines. This demands the separation of Al matrix prior to the sample analysis by these methods. It may be required to use the standard addition method in the absence of matrix matched standards. Electrochemical techniques may not be amenable due to lack of suitable redox valence states for alkali elements. Chromatography techniques have found extensive applications in elemental separations. There is a scope for developing a simple and rapid Ion Chromatography method where direct sample analysis without any matrix separation step is possible. Ion chromatography (IC) has found several applications for the determination of alkali and alkaline earth metals in different matrices [4–7]. Ion chromatography provides online separation as well as determination. This feature along with the flexibility of optimizing several parameters helps in modifying the separation scheme to suit the analysis of analyte(s) in complex matrices.

Capillary Electrophoresis (CE) is yet another efficient separation technique where the analytes can be separated rapidly by controlling some parameters without resorting to matrix isolation [8]. Many applications of CE have been reported for the determination of alkali metal determination [7–13]. Since IC and CE are complementary to each other, in the absence of a suitable matrix matched certified reference materials both ion chromatography and capillary electrophoresis methods can be used to validate the results obtained from each other. The validation is acceptable because separation in each method is based on different physico-chemical parameters. The present study is aimed at developing analytical procedures for the determination of Li using both ion chromatography and capillary electrophoresis, without resorting to matrix separation.

5.2 Experimental:

5.2.1 Instrumentation:

IC separations were performed on a commercial IC system (DX-500 Dionex) consisting of a gradient pump (GP-50), conductivity detector (ED-40) and a cation self-regenerating suppressor (CSRS) for suppressing background conductivity of the mobile phase. IC separations were carried out on a cation exchange column CS12 (Dionex). Capillary electrophoresis (CE) instrument, CEC-770 model (Prince Technology Netherlands), was employed and it is equipped with diode array detector. Silica capillaries of dimension (50 μm i.d. and 60 cm total length) were used throughout the study.

5.2.2 Reagents:

Methane sulphonic acid (MSA), imidazole (99.9 % purity) and stock solutions of standard alkali metal used were of Sigma-Aldrich make. Rest of the solutions were prepared using A.R. grade reagents. All the solutions were prepared in high purity water obtained from the Milli-Q Academy apparatus.

5.2.3 Sample preparation:

Prior to dissolution, the alloy samples were washed repeatedly with acetone to remove organic contaminants. Accurately weighed ($\sim 0.1\text{g}$) sample was boiled in concentrated nitric acid (5ml) till complete dissolution. In order to bring the medium of sample in 1% nitric acid the dissolved solution was heated to near dryness and 1% nitric acid was added.

5.3 Results and discussion:

5.3.1 Ion Chromatography Studies:

Direct sample injection of the dissolved sample without separation of the matrix is possible when the analyte of interest gets eluted ahead of the matrix element. Such separation is possible on a cation exchange column (order of the elution is Li followed by the matrix element Al). Since Al in the solution is in its +3 oxidation state and therefore is retained for longer time. However complete elution of Al from the column takes long time which curtails fast turn around time for multiple analyses. Therefore there is a scope to reduce the time of analysis in order to increase the sample throughput. To achieve this, a high capacity cation exchange column was selected (carboxylic acid functional group) along with its guard column. The separator column has a total capacity of 3.36 meq. In order to optimize the concentration of the eluent (MSA), separation was carried by varying the concentration of MSA. Based on the separation obtained, it was observed that 20 mM of MSA was found optimum. Elution of alkali and alkaline elements and NH_4^+ was performed with low concentration MSA. At this concentration of MSA and the flow rate, the matrix element Al has strong retention. Figure 5.1 shows a chromatogram of Alkali metal ion standards for the optimised elution conditions.

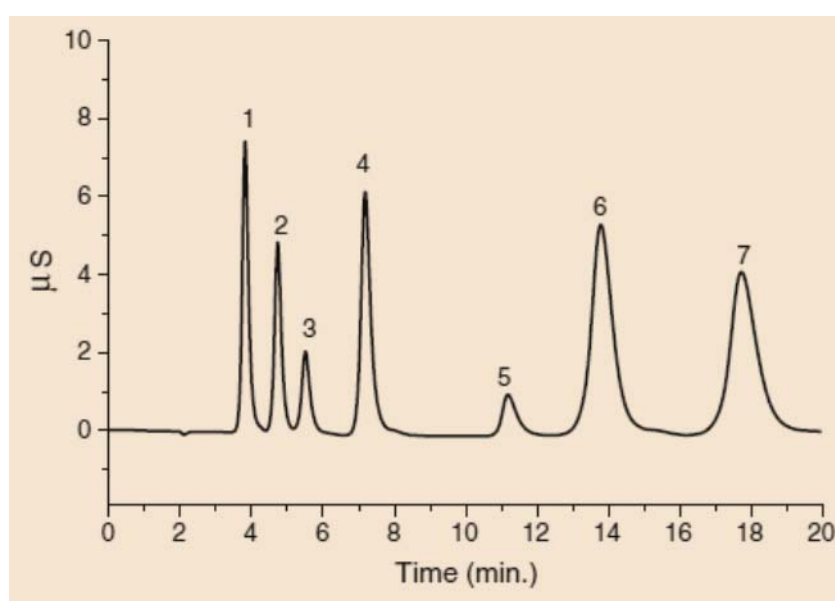


Figure 5.1: A standard sample chromatogram. Peaks 1–7 are (1) Li (2 mg/L), (2) Na (2 mg/L), (3) NH₄⁺, (4) K (5 mg/L), (5) Cs (5 mg/L), (6) Mg (3 mg/L) and (7) Ca (5 mg/L). Column: Ion Pac CS12; Eluent: 20 mM MSA; Flow rate 1ml/min.

Li was separated from Li-Al matrix using the optimised conditions. At this MSA concentration separation of Li was good without any interference from a solution having around 2.0 g/L of Al matrix (Li/Al ~ 500 to 1000).

0.1g of the sample is dissolved and diluted to 100 ml. Considering the 25µL injection volume around 2.7 µmoles of Al was injected into the column. After performing 25 sample runs the column is loaded with around 62.5 µmoles of Al, which is around 2% of the total capacity of the cation exchange column (3.36 meq). Therefore, presence of Al does not affect the separation of Li. Chromatogram of a typical sample run is given in Fig. 5.2.

After every 25 sample injections, the column was thoroughly washed with higher concentration of MSA (0.2M) to remove the matrix element Al.

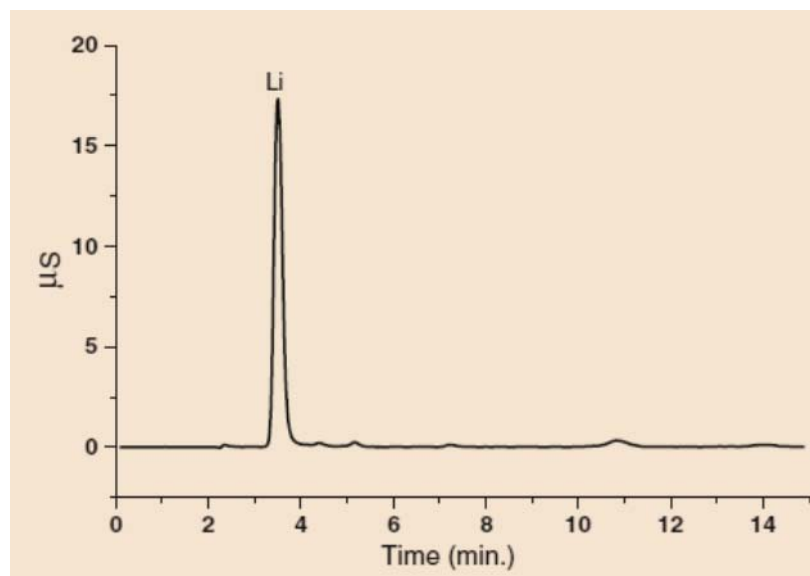


Figure 5.2: A typical sample chromatogram obtained for a sample Column: Ion Pac CS12; Eluent: 20 mM MSA. Flow rate 1mL/min. Detection Suppressed Conductivity.

The precision of the method is found to be 4.5 % at 0.3 mg/L of Li. The LOD for Li is 25 ng/L, which was calculated on the basis of $S/N = 3$ method. Calibration plot was constructed by using Li standards in the concentration range between 0.5–25 mg/L and it showed a regression coefficient better than 0.999.

5.3.2 Capillary electrophoresis studies:

The capillary electrophoresis separation of Li from Li-Al alloys without any pre-matrix separation poses two challenges.

- (i) Due to the higher charge of Al (Al^{3+}) it is expected to appear before Li in the electrogram. An early appearance of matrix peak can mask the analyte peak or disturb the base line. This causes erroneous determination of Li.
- (ii) Li^+ ion do not absorb in the UV-Vis region which is necessary for detecting trace Li^+ .

The first problem can be addressed by using a complexing agent, which is selective for Al ion. The complexing agent forms a complex with Al^{3+} as this reduces the charge density of Al ion. Therefore the Al matrix peak would appear after the analyte peak. The second problem is generally circumvented by using a co-ion in the back ground electrolyte (BGE). The co-ion is a molecule which absorbs either in UV or in Visible region, and provides a base line absorption for the BGE. When the analyte species appear in the detector due to the dilution of co-ion the baseline absorption decreases causing detection of analyte as a negative peak. Both the requirements were met using imidazole as the co-ion. Imidazole is one of the most suitable molecules used for the analysis of alkali metals as it has appreciable absorbance at 214 nm with $(0.44 \text{ m}^2/\text{kV}/\text{s})$ similar to alkali metal ions [9]. Imidazole is known to have significant complexation with Co(III), V(III) and Fe(III) [14–16], therefore, it can form complex with Al (III).

Therefore, 20 mM imidazole solution at pH 2 was chosen as BGE. For achieving better sensitivity a high potential is applied. However, generation of high current due to higher conductivity of BGE is the limiting factor. Hence it is important to maintain the BGE ionic strength as low as possible, as it can affect the joule heating significantly. Buffers that are used in the BGE are the important contributors in increasing ionic strength. Thus, use of any buffer was avoided and frequent replacement of BGE was practiced to avoid any variation in pH. With this final BGE having 20 mM Imidazole at pH 2 without any buffer, several runs were performed to optimize the applied potential. For the sample matrix under study and selected BGE composition, 20 kV of potential was found to be suitable for desired results. The electropherogram showing separation of K^+ , Na^+ , Ca^{2+} , Mg^{2+} , and Li (Fig. 5.3). Under the same separation condition the Al peak could not be observed up to 10 min.

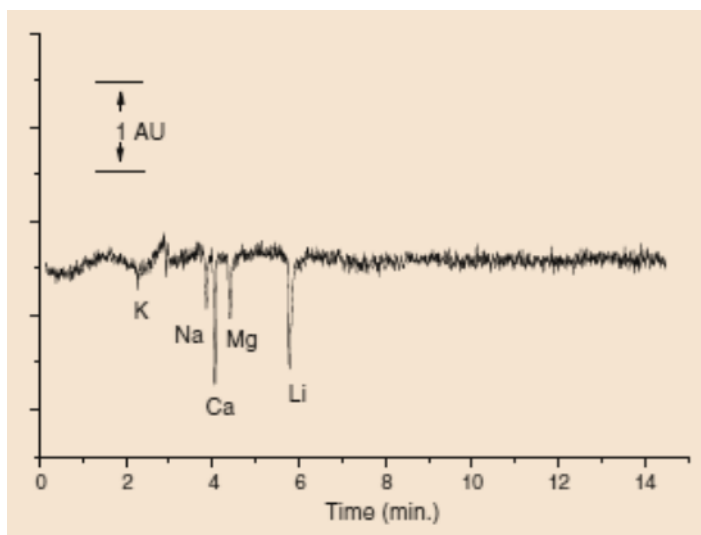


Figure 5.3: Capillary 50 μ m (i.d.) 960 cm (total length), BGE 20 mM Imidazole pH 2 Sample: (K, Na, Ca, Mg, Li) Li 1 mg/L others 0.5 mg/L.

A typical electropherogram obtained for a Li–Al alloy sample is shown in Fig. 5.4. A calibration plot was constructed with series of Li standards in the concentration range of 1–15 mg/L with regression coefficient of 0.981. It was possible to get further improvement in the regression coefficient. In CE the peak time reproducibility is relatively poor (as compared to IC), which causes variation in the peak area. To overcome the effect a plot of peak area/peak time versus Li concentration for the same concentration range was prepared, which showed an improved regression coefficient of 0.994 (Fig. 5.5). The ratio of peak area to peak time provided a correction for the variation in peak area because of small changes in peak time. The improved calibration was used for the quantitative determination of Li in samples. The limit of detection (LOD) of Li is 120 ng/L.

Several Li–Al alloy samples were analysed following the developed IC and CE methods and the results of Li contents are reported in Table 5.1.

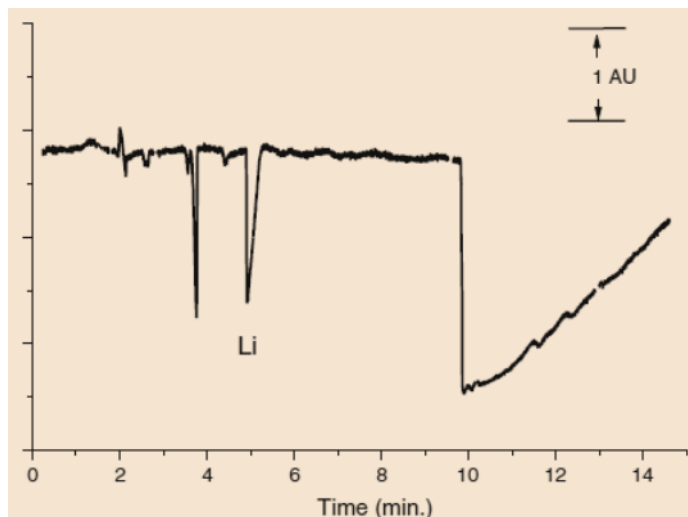


Figure 5.4: Capillary 50 μm (i.d.) and 60 cm (total length), BGE 20 mM Imidazole pH 2, Sample: (real sample having 2.1 mg/L Li)

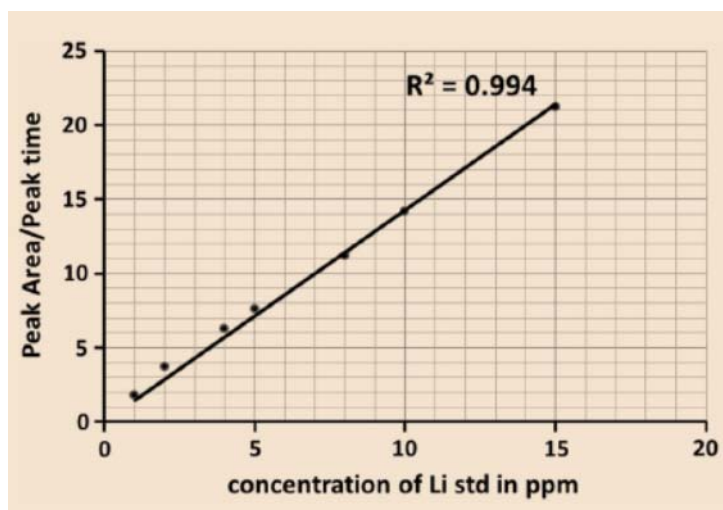


Figure 5.5: Calibration plot of peak area/peak time versus Li concentration.

Table 5.1: Comparison of Li percentage determined by CE and IC in Li–Al alloy samples.

Sample	IC (%Li)	CE (%Li)
1.	3.2 ± 0.02	3.3 ± 0.2
2.	4.7 ± 0.02	4.5 ± 0.2
3.	4.1 ± 0.02	4.1 ± 0.2
4.	4.3 ± 0.02	4.0 ± 0.2

5.4 Conclusion:

An IC method was developed for the determination of Li in Li-Al alloy. High capacity column along with a weak eluent was used to obtain interference free separation and determination with good precision and sensitivity. On the other hand selective complexation of imidazole with Al ion was used successfully in the CE method to push the matrix after analyte peak. In view of no interference from Al, samples were analyzed without any matrix separation. Both CE and IC methods produced results which were comparable and thus validate each other. Better sensitivity and lower standard deviation showed superiority of IC method over the CE method, though the latter has an advantage of faster analysis than IC.

5.5 References:

1. P. L. Carconi, S. Caradio, A. Moauro, J. Radioanal. Nucl. Chem., 151(1991)357.
2. J. R. Powell, F. T. Miles, A. Aronson, H. E. Winsche, Studies of fusion reactor blankets with minimum radioactive inventory and with tritium breeding in solid lithium compounds: a preliminary report Department of Applied Science, Brookhaven National Laboratory associated Universities Inc., Upton, New York, (1973).
3. S. P. Mirjana, Z. P. Nebojsa, M. Momir J. Anal.At.Spectrom., 4(1989)587.
4. R. R. Singh, N. M. Abbas J.Chromatogr. A, 733 (1996) 93.
5. N. Ulrike, T. Hansjorg J.Chromatogr.A, 920(2001) 201.
6. O. Zerbinati, F. Balduzzi, V. Dell'Oro, J. Chromatogr. A, 88(2000)645.
7. A. Kelker, A. Prakash, A. Mohmad, J. P. Pannakal, H. S. Kamat J. Radioanal. Nucl. Chem. 28(2011)595.
8. J. C. Reijenga, J. Radioanal. Nucl. Chem., 163(1992) 155.
9. W. Beck, H. Engelhardt, Chromatographia, 33(1992) 313
10. J. P. Pascali, D. Sorio, F. Bortolotti, F. Tagliaro, Anal.Bioanal. Chem., 396(2010) 2543.
11. E. X. Vrouwe, R. Luttge, W. Olthuis, A. Berg Electrophoresis, 15(2005) 3032
12. K. Fukushi, S. Minami, M. Kitakata, M. Nishijima, K. Yokota, S. Takeda, S. Wakida, Anal.Sci. 22(2006) 1129.
13. G. L. Klunder, J. E. Andrews, M. N. Church, J. D. Spear, R. E. Russo, P. M. Grant, B. D. Andresen, J. Radioanal. Nucl. Chem., 236(1998) 14.

14. Z. Kosrow, M. Akbar, F. Naser, F. Khalil, M. Wahid, Turk. J. Chem. 27(2003)71.
15. H. Podsiadły Polyhedron 27(2008)1563.
16. S. Staffan, Pure.Appl. Chem. 69(1997) 1549.

Chapter: 6

Rapid Separation and Quantification of Iron in Uranium Nuclear

Matrix by Capillary Zone Electrophoresis (CZE)

6.1. Introduction:

Determination of trace elements in nuclear materials is imperative as the performance of the materials depends on their chemical purity [1]. While developing new nuclear materials, it is necessary to analyse the raw materials as well as the products obtained at different stages of manufacturing for their metallic impurities. In the case of new nuclear fuel development, chemical characterisation of the product material at different process stages is desirable to account for the addition of impurities, if any. Fe and Ca are two common metallic impurities getting added up in the nuclear fuel through the process equipment [2]. Presence of these elements beyond the specified limit is undesirable. Moreover, the concentration of Fe in the fuel enables the fabricator to take adequate measures to achieve the desired purity.

Several analytical methods are available for the determination of iron in nuclear materials. The methods involving ICP-AES [3,4], ICP-MS [5], spectrophotometry [6], ion chromatography [7,8] and HPLC [9] are well known. These instrumental methods are associated with laborious and time consuming sample preparation steps as they require matrix separation prior to the instrumental analysis. While following such separation procedures, it is necessary to have a reference material to assess the recovery of analytes from the matrix. However, in the case of nuclear materials availability of reference materials is limited. Development of an analytical method for the direct instrumental analysis of the dissolved fuel samples without separating

matrix will be advantageous. This chapter deals with the development of a simple, and rapid method to for determination of Fe in nuclear fuel samples.

Capillary Zone Electrophoresis (CZE) is a powerful separation method. It can provide high speed of separation, high separation efficiency and resolving power with very small sample size. Though CZE has not been widely used for the analysis of nuclear materials, many studies have been reported in the literature where the CZE analyses of inorganic substances for common cations and anions [10-15]. Further few CE methods have been reported for the determination of metallic or cations in non-aqueous media [16,17] using partial or complete complexation techniques [18,19]. CZE in hyphenation with ICP-MS [20-22] or using quantitative microchip [23] were also used in determining very low concentrations of the metal ions. Despite the increased applications to inorganic materials, the application of CE in nuclear industry is somewhat limited [24, 25].

The separation in CZE is based on the differential electrophoretic mobility of charged compounds. The difference in charge-to-mass ratio varies the mobility of the analytes and the separation is achieved. However, in the case of transition metal cations their mobilities are almost similar due to their similar size and identical charge. This causes difficulty in their separation. Therefore, for the CZE separation of transition metals is being achieved by incorporating the following approaches [26]:

- (i) addition of a complexing agent to the carrier electrolyte [27,28]
- (ii) addition of a complexing ligand to the sample solution before introduction into the capillary [29].

Applications of CZE for the determination of iron in water, electroplating baths and cyanide complexes have been reported [30-34]. In the case of Fe, separation of Fe(II) and Fe(III) after complexing with o-phenanthroline and EDTA has been reported [35]. Another study reports the separation of Fe(III) as its DTPA complex [36]. However these reported methods cannot be adopted for the analysis of Fe in nuclear fuel samples as these ligands also form an anionic complex with U(VI), which has higher charge density than the Fe complex. For instance, with EDTA Fe(III) and U(VI) form $(\text{Fe-EDTA})^-$ and $(\text{UO}_2\text{-EDTA})^{2-}$ complexes, respectively [33, 37]. Hence the order of separation in CZE will be U followed by Fe and with this elution order injecting the dissolved uranium samples directly into the capillary will result a large peak of U matrix, which will mask the Fe peak. This demands the reversal of EOF (Electro Osmotic Flow) towards the detector direction. A common practice for achieving the reversal of EOF direction is coating the capillary with cetyltrimethyl ammonium bromide (CTAB) in alkaline pH BGE (Background Electrolyte). However, this coating method cannot be adopted in the case of uranium and iron separation as the basic pH medium of BGE will cause the hydrolysis of metal ions. Hence, alternatively, complexation with chloride was considered for the separation of iron in uranium matrix as the chloride complexes of uranium and iron are favourable for the desired separation.

The present study is aimed at developing a CZE method for the separation and quantification of iron in uranium matrix without employing pre-separation of uranium matrix. Direct analysis of the dissolved sample will lead to significant reduction in the analysis time and such analysis is helpful in analysing the process control samples.

6.2. Experimental:

6.2.1. Instrumentation:

Separations were performed on a commercial capillary electrophoresis apparatus (Prince Technologies, CEC-770, Netherlands) equipped with a photodiode array detector. Fused silica capillaries of 50 μm i.d. and 60 cm long were used. A capillary having 75 μm i.d. and 60 cm long was also used. Sample was injected in hydrodynamic mode by applying 50 mbar pressure for 0.2 minutes duration on the sample vial at which, a sample volume of 1.5 nL would get injected. System DAX software was used for data acquisition. Direct UV detection was performed at 214 nm. All the experiments were conducted at room temperature (25-27°C). A pH meter (Eutech, Tutor-model, Malaysia) was used for measuring the pH of the solutions.

6.2.2. Reagents and Solutions

Standard stock solution of Fe(III) was prepared by dissolving $\text{Fe}(\text{NO}_3)_3 \cdot 9\text{H}_2\text{O}$ (99.99%, Aldrich Chemicals, USA) in 0.01N HNO_3 . Subsequently, the working standards were made from the stock by appropriate dilutions. High purity HCl and HNO_3 acids (suprapure, MERCK, Germany) were used for the sample and electrolyte preparations. Potassium chloride (GR grade, MERCK, Germany) was used. Nuclear grade UO_2 (NFC, India) was used for the preparation of standard uranium solution and the concentration of U was obtained from biamperometric determination [38]. All solutions, electrolytes and standard solutions were prepared with ultrapure water (18 M Ω) obtained from a MilliQ-Academic System (Millipore, India).

6.2.3. Procedure for Conditioning Capillary and Sample Injection:

The capillary used was first washed with 0.2 M NaOH for 15 min and then with water for 10 min followed by rinsing with BGE for 15 min. About 1.5nL of the sample solution was injected into the capillary hydrodynamically by applying 50 mbar pressure for 0.2min. A potential of 15 kV was applied during the sample run and in between two sample runs, the capillary was again rinsed with BGE for 5 min.

6.3. Results and Discussion:

Although the capillary zone electrophoresis (CZE) applications involve samples containing analytes in comparable concentration, this study is an attempt to analyse the Fe in trace concentration in presence of high concentration of uranium. Such direct analysis is advantageous as it provides hassle free sample preparation. Since the dissolved uranium sample solution has high ionic strength, the direct injection of sample into the capillary can cause difficulties like:

(i) peak broadening (ii) variation in the EOF (iii) poor precision on the migration time and (iv) poor separation efficiency.

Despite these difficulties, direct separation of trace analytes in presence of bulk matrix is feasible in CZE provided the method satisfies two conditions:

(i) the analyte and the matrix elements should have large difference in their relative mobilities and (ii) the mobility of the analyte should be faster than matrix element.

Under these conditions, the analyte reaches the detector much earlier than the matrix element and therefore, it can be free from matrix effects. In the present case, since both uranyl and ferric ions (in their hydrated form) had little difference in their charge densities, it is difficult to separate them under normal conditions and addition

of a complexing agent is essential for their separation. As discussed earlier the organic ligands that had been used in the metal ions separations in CZE [30-36, 39] may not be suitable in the present study. Hence, complexation of these metal ions with chloride was considered because chloride forms different types of complexes with UO_2^{2+} and Fe^{3+} ions. Both uranyl and ferric ions form cationic complexes but of different charge densities. Moreover, the chloride medium enables the direct detection of selected metal ions [40,41] including iron.

The uranyl ion predominantly forms UO_2Cl^+ complex at lower concentrations of chloride ion (<0.5 M) [42,43] when the pH is between 2 and 3. When the concentration of chloride exceeds 5 M, it forms anionic complexes. Similarly, Fe(III) can form both cationic and anionic complexes with chloride such as FeCl^{2+} , FeCl_2^+ , FeCl_3 and FeCl_4^- . At lower concentrations of chloride, Fe(III) forms predominantly FeCl_2^+ [44]. The formation constants (log values) for the UO_2Cl^+ and FeCl^{2+} complexes are 0.17 and 1.52, respectively. This indicates that the Fe^{+3} has more affinity towards chloride complex formation [43,45] than UO_2^{2+} .

Therefore, with low chloride concentration it is possible to have UO_2Cl^+ and FeCl_2^+ complexes, which had different mobility due to difference in their charge differences. Therefore complexation with chloride can bring the desired separation in CZE. Since the divalent transition metal ions such as Zn(II), Cu(II), Cd(II), Mn(II) etc., [46] form either anionic or neutral chloride complexes [47] and hence, they do not interfere with Fe(III). The absorbance of the peak for iron as FeCl_2^+ complex was measured at 214 nm [45].

6.3.1. Optimization of Background Electrolyte:

A combination of HCl and KCl was considered for BGE. The role of HCl in BGE is to prevent the hydrolysis of iron, uranium and their chloride complexes by providing acidic pH whereas the KCl ensures the stability of the chloride complexes formed. All the separations were carried out with 15 kV applied voltage.

Initially the separation behaviour was investigated at different pH conditions, for this separation of Fe(III) was performed in BGE with 10^{-2} , 10^{-3} , 10^{-4} and 10^{-5} M HCl solutions corresponding to pH 2, 3, 4 and 5 without KCl. This has been carried out with a view to obtaining a BGE with minimum ionic strength possible so that effect of joule heat can be minimized. While carrying out the CZE separation, the standard iron solutions were also prepared in the respective HCl solutions in order to have almost identical composition in the BGE as well as in the standards.

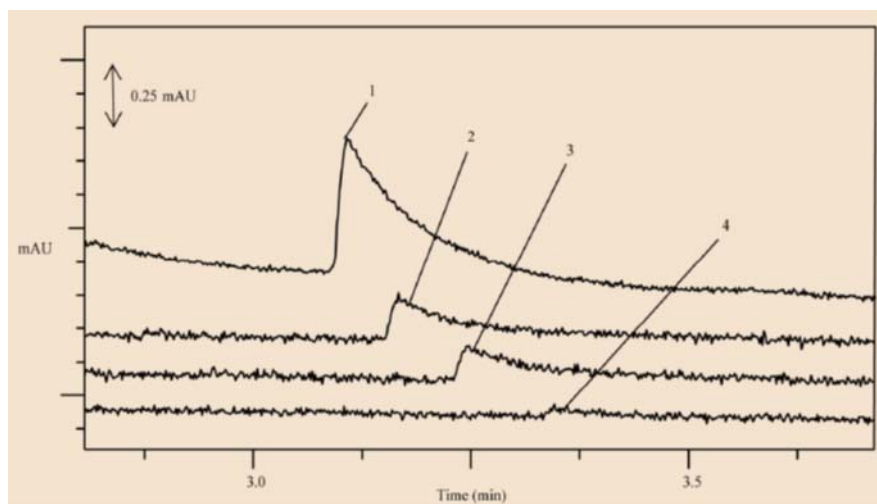


Figure 6.1. Electropherograms obtained for a standard iron solution ($25 \text{ mg}\cdot\text{L}^{-1}$) with BGEs of different pH.

- (1) 10^{-2} M HCl BGE corresponding to pH 2;
- (2) 10^{-3} M HCl BGE corresponding to pH 3;
- (3) 10^{-4} M HCl BGE corresponding to pH 4 and
- (4) 10^{-5} M HCl BGE corresponding to pH 5,

Conditions: Capillary: $60 \text{ cm} \times 50 \mu\text{m}$, Applied voltage: 15 kV. Detection: direct UV

Figure 6.1 shows the overlay of electropherograms obtained for each carrier electrolyte which shows that decreasing the pH of the carrier electrolyte decreased the migration time of Fe(III). The change in migration time in this case may be possibly due to,

- i. At higher pH the silanol group of the capillary provides negatively charged sites which retain the free metal ions of iron for longer time.
- ii. At higher pH solutions complex formation is not significant due to lower concentrations of chloride.
- iii. The hydrolysis of Fe(III) and its chloride complexes may occur and form neutral species [44].

Since the above observations are due to varying concentrations of chloride (as concentration of HCl varies), it is necessary to investigate at constant chloride concentration. Also it is necessary to study the influence of pH on the separation at a fixed chloride concentration and the effect of chloride concentration at fixed pH condition. For this purpose, three sets of solutions corresponding to pH 2, 3 and 4 were prepared. In each set, the pH was maintained by keeping a fixed concentration of HCl but the total chloride content was varied from 30 to 100 mM by adding KCl.

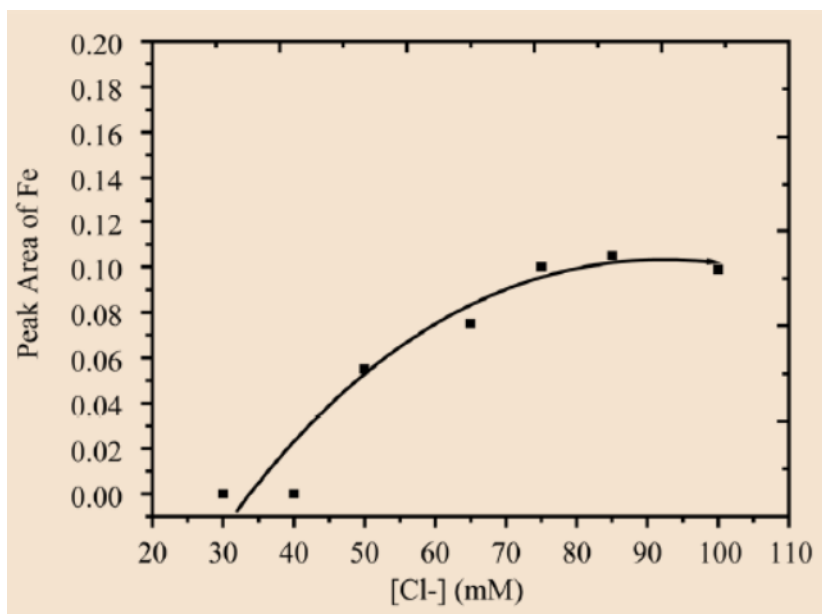


Figure 6.2. Effect of total chloride concentration on the peak area of iron obtained with pH 2. (BGEs were of 10⁻² M HCl (fixed) and varying amounts of KCl). Capillary: 60 cm × 50 μ m, Applied voltage: 15 kV; Detection: direct UV at 214nm.

It was observed (Fig. 6.2) that for pH 2 BGE the sensitivity of Fe peak increased with increasing chloride concentration and it was saturated when the chloride concentration was 75 mM chloride (10mM HCl + 65mM KCl). Increasing the chloride concentration above 75 mM caused only marginal changes in the peak areas. On the other hand, at higher pH and chloride concentrations the base line was noisy and could not be used for analysis. It is expected that during the CZE separation a little change in the pH of the electrolyte due to applied potential and protonation of silanol groups. The effect of this slight pH variations was studied with electrolytes of pH 1.8, 2.0 and 2.2. However, it was found that under these three pH conditions the variations in peak time and peak area were within $\pm 1\%$. Based on the observations, a BGE of 10mM HCl and 65mM KCl (pH 2) was found as optimum BGE composition.

With the optimized BGE condition the uranyl ion (as UO_2Cl^+) appeared much later than iron peak. On the other hand the transition, alkali and alkaline earth metal cations could not be detected even up to 60 minutes and this could be due to the formation of their anionic complexes, which are moving either with low mobility or in opposite direction. The peaks of Fe(III) and U(VI) were confirmed by injecting the standard mixture solutions of different concentrations.

6.3.2. Optimization of Applied Voltage:

In CZE the number of theoretical plates (N) can be expressed as [48],

$$N = \mu \exp(V/2D_s)$$

where N is efficiency, μ is constant, V is applied voltage and D_s is the diffusion coefficient. The above equation shows that higher efficiency of separation may be achieved by applying higher potential. Hence the effect of applied potential on the separation between Fe(III) and U(VI) was studied between 5 and 30 kV. It was observed that when the applied potential is 20kV the change in the mobility and reproducibility of Fe and U peaks was significant and the resolution between Fe and U at higher voltages were found to be poor. A plot of current Vs applied voltage showed that the current and voltage was non linear beyond 18 kV. This indicates that the capillary is unable to dissipate the Joule heat generated in the capillary at this high voltage. Therefore, an applied voltage of 15 kV was fixed for further separation. Figure 6.3 shows typical electropherograms obtained for Fe(III) of different concentrations under the optimized conditions.

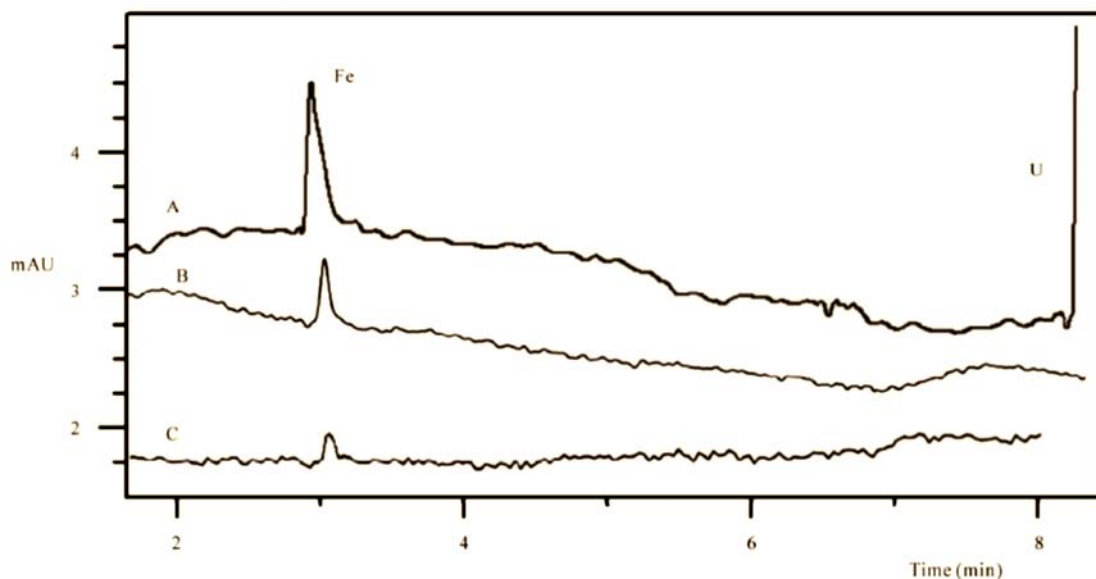


Figure 6.3. Electropherograms obtained for a standard solution of Fe(III) and Uranium. (A) Fe(III) (5 $\mu\text{g/mL}$) + U(VI) (80,000 $\mu\text{g/mL}$) standard solution; (B) Fe(III) standard solution (1 $\mu\text{g/mL}$); (C) Fe(III) (0.08 $\mu\text{g/mL}$) standard solution. BGE: 10 mM HCl in 65 mM KCl (pH 2), Conditions: Capillary: 60 cm \times 50 μm , Applied voltage: 15 kV. Detection: direct UV at 214 nm.

6.3.3. Matrix element tolerance:

Since the separation is aimed at determining iron in presence of matrix uranium, the tolerance of uranium was studied. For this purpose, 50 ppm Fe standard was taken in varying amounts of U(VI) (0.1-90 mg of U/mL) and they were analysed for the Fe. The values obtained are tabulated in Table 6.1 and it showed overall precision and accuracy better than 5%. The data also show a good recovery of Fe in presence of bulk uranium.

Table 6.1: Recoveries of spiked iron in uranium solutions of various concentrations.

No.	Uranium (ppm)	Fe spiked in U solution (ppm)	Fe determined by CE (ppm)	% of recovery
1.	10	50	48.6 ± 2.4	97.2
2.	1000	50	48.3±2.7	96.6
3.	10000	50	51.9±2.9	103.8
4.	50000	50	47.9±3.1	95.8
5.	75000	50	52.3±2.6	104.6
6.	90000	50	51.8±2.8	103.6

6.3.4. Validation of Method:

The possible interferences from transition metal ions was studied and it was observed that the metal ions like Cu(II), Pb(II), Ni(II), Zn(II), Mn(II), Co(II), Cd(II), Cr(III), alkali, alkaline earth metals (300 ppm each) did not interfere at Fe peak. Hence, the CZE separation is highly specific for Fe(III).

A linear calibration plot was constructed using the Fe(III) standards in the concentration range of 1-50 ppm. The linear correlation coefficient obtained in this case was 0.9995. The limit of detection (LOD) for Fe(III) was calculated and it was found to be 0.1 ppm. The absolute LOD is 9×10^{-14} g, where the sample volume was 1.5 nL. An electrogram obtained for 0.08 ppm of iron, which is very close to the detection limit was also shown in Figure5.3.

The reproducibility of peak area and peak time was studied with two standards viz. Std-1 (5 ppm of Fe alone) and Std-2 (5 ppm of Fe(III) and 80 ppm of U(VI)). Ten consecutive run of the standards provided a precision better than 2% on peak area whereas a precision of 1% was obtained on the peak time of Fe(III). However, replicate analyses (n = 20) of a 1 ppm iron standard solution under the optimized conditions brought about a precision of 3.5%.

6.4. Analysis of Certified Reference Materials:

To check the accuracy of the developed procedure, two reference materials of U_3O_8 viz. ILCE-4 and ILCE-5 (CRM-DAE) [49] were used and analysed. Accurately weighed quantities (0.3 - 0.4 g) of the reference materials were dissolved in 5 mL of high purity Conc. HNO_3 and the solution was heated to near dryness and the process was repeated twice or thrice until the sample is completely dissolved. Further 3.5 mL of 0.01 N HCl (pH 2) acid solution was added at warm condition. The pH of adjusted using 0.01 N HCl solution, if required. Prior to sample injection, the solution was transferred into a standard volumetric flask and made up to 5 mL using 0.01 N HCl. The nitric acid dissolution helped in maintaining the higher oxidation states of Fe and U. The sample preparation step completes within 30 minutes as it does not involve any separations. Table 6.2 compares the results obtained for the two reference materials and the values obtained by this method are in good agreement with the certified values.

Table 6.2: Comparison between iron determination via the developed method and certified method.

No.	Reference standard code	Concentration of Fe (ppm)		
		mean	certified	% deviation
1.	ILCE-IV	163.5 ± 2.8	170	3.8
2.	ILCE-V	275.2 ± 2.9	290	5.4

6.5. Real Sample Analysis:

The method was applied to nine uranium fuel samples from an advanced fuel fabrication facility. The samples are either in metallic or oxide form of uranium. Samples were dissolved by following the procedure as described above for the standard reference materials. Dilutions of the samples were carried out as per the requirement to bring Fe concentration to the linearity range. Table 6.3 lists the typical iron contents determined in the samples. An electropherogram obtained for a sample is presented in Fig. 6.4.

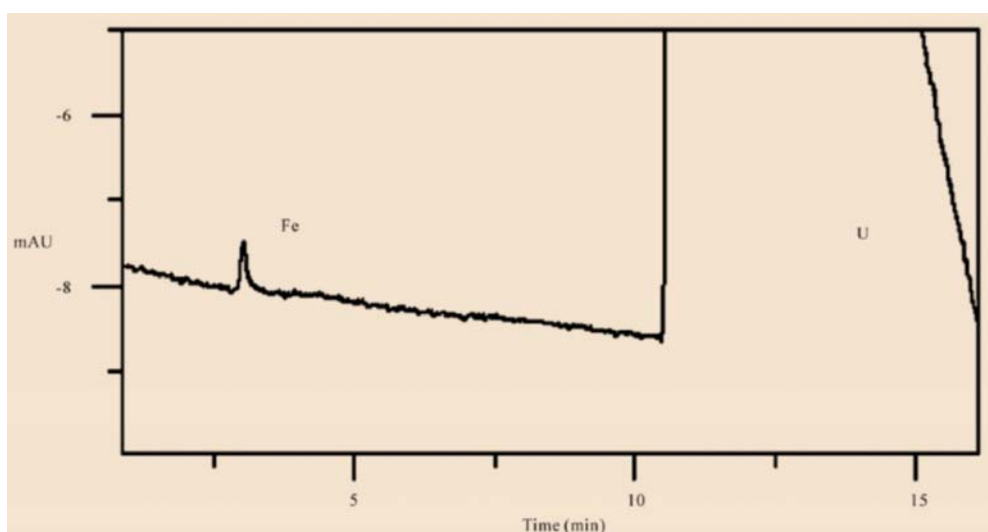


Figure 6.4: A typical electropherogram obtained for a sample solution.

Table 6.3: Results obtained for the samples.

Sample Code	Fe (ppm)
M1	882 ± 52
M2	1311 ± 70
M3	753 ± 37
M4	801 ± 36
M5	913 ± 46
U1	318 ± 19
U2	723 ± 33
U3	626 ± 29
U4	389 ± 18

6.6. Advantages of the CZE Method:

The method developed for the determination of Fe in U matrix by CZE brought following advantages:

- (i) specific for iron
- (ii) shows high tolerance for uranium matrix
- (iii) simple sample preparation procedure
- (iv) rapid separation

(v) provides good precision and better recovery of Fe

(vi) generation of minimum analytical waste

6.7 Conclusions

A rapid, reproducible and simple CZE method for the determination of iron in uranium matrix was developed. For the desired separation chloride complexation of both the species were explored. The capability of the method for determining iron with high background of the matrix element was proved by analyzing matrix match reference materials. The method was applied successfully to the determination of iron in different uranium fuel samples.

6.8 References:

1. M. V. Ramaniah, *Pure Appl. Chem.*, 54(1982)889.
2. H. C. Bailly, D. Menessier, C. Prunier, "The Nuclear Fuel of Pressurized Water Reactors and Fast neutron Reactors: Design and Behavior," Lavoisier Publishing Inc., Paris, 1999.
3. K. S. Rao, T. Balaji, T. P. Rao, Y. Babu and G. R. K.Naidu, *Spectrochim.Acta, Part B*, 57(2002) 1333
4. M. Gopalakrishnan, K. Radhakrishnan, P. S. Dhani, V. T.Kulkarni, M. V. Joshi, A. B. Patwardhan, A. Ramanujam, J. N. Mathur, *Talanta*, 44(1997)69.
5. H. Vanhoe, C. Vandecasteele, J. Versieck, R. Dams, *Anal. Chem.*, 61(1989)1851.
6. Z. Marczenko and M. Balcerzak, *Separation, Preconcentration and Spectrophotometry in Inorganic Analysis*, Elsevier, (2000)226.

7. A. Kelkar, A. Prakash, M. Afzal, J. P. Panakkal H. S.Kamath, J.Radioanal. Nucl. Chem., 284(2010)443.
8. V. V. Raut, M. K. Das, S. Jeyakumar, K. L. Ramakumar, Proceedings SESTEC-2008, Delhi, 12-14 March 2008.
9. R. M. Cassidy, S. Elchuk, J. Liq. Chromatogr. Related Technol., 4, (1981)379.
10. S. Hjerten, Chromatographic Reviews, 9(1967)122.
11. A. K. Malik, Methods MolBiol, 328(2008)21.
12. J. S. Fritz, J.Chromatogr. A, 884(2000)261.
13. A. R. Timerbaev, Electrophoresis, 25(2004)4008.
14. A. R. Timerbaev, Electrophoresis, 28(2007)3420.
15. A. R. Timerbaev, Electrophoresis, 31(2010)192.
16. F. Qu, J. Lina, J.Chromatog. A, 1068(2005)169.
17. F. Qu, J. Lin, Z. Chen, J.Chromatogr. A, 1022(2004)217.
18. E. Naujalis and A. Padarauskas, J.Chromatogr. A, 977(2002)135.
19. J. Gao, X. Sun, W. Yang, H. Fan, C. Li, X. Mao, J.Chil. Chem. Soc., 53(2008)431.
20. B. H. Li, X. P. Yan, J. Sep. Sci., 30(2007)916.
21. J. E. Sonke, V. J. M. Salters, J.Chromatog.A, 1159(2007)63.
22. R. Kautenburger, H. P. Beck, J.Chromatogr. A, 59(2007)75.
23. E. X. Vrouwe, R. Luttge, W. Olthuis, A. van den Berg, J.Chromatogr. A, 1102(2006) 287.
24. G. L. Klunder, J. E. Andrews, P. M. Grant, B. D. Andresen, R. E. Russo, Anal. Chem., 69(1997)2988.
25. B. Kuczewski, C. M. Marquardt, A. Seibert, H. Geckeis, J. V. Kratz, N. Trautmann, Anal.Chem., 75(2003)6769.

26. A. R. Timerbaev, J. Capillary Electrophor., 1(1995)14.
27. F. Foret, S. Fanali, A. Nardi and P. Bocek, Electrophoresis, 11(1990) 780.
28. Y. Shi and J. S. Fritz, J.Chromatogr. A, 640(1993)473.
29. A. R. Timerbaev, O. P. Semenova, O. M. Petrukhin, J.Chromatogr. A, 943(2002)263.
30. S. Pozdniakova, A. Padaruskas, G. Schwedt, Anal.Chim.Acta, 351(1997)41.
31. B. Y. Deng, C. J. Zeng, W. T. Chan, Spectros.Spect.l Anal., 25(2005) 1868.
32. P. Blatny, F. Kvasnicka, E. Kenndler, J.Chromatogr. A, 757(1997)297.
33. B. Baraj, M. Martinez, A. Sastre and M. Aguilar, J.Chromatogr. A, 695(1995)103.
34. G. Owens, V. K. Ferguson, M. J. McLaughlin, I. Singleton, R. J. Reid, F. A. Smith, Environ. Sci. Technol., 34(2000) 885.
35. S. Schaffer, P. Gared, C. Dezael and D. Richard, J.Chromatogr. A, 740(1996)151.
36. W. Buchberger, S. Mulleder, Mikrochim.Acta, 119(1995)103.
37. P. Kuban, P. Kuban, V. Kuban, J.Chromatogr. A, 836(1999)75.
38. M. Xavier, P. R. Nair, K. V. Lohithakshan, S. G. Marathe, H. C. Jain, J.Radioanal. Nucl. Chem., 148(1991)251.
39. I. Ali, V. K. Gupta, H. Y. Aboul-Enein, Electrophoresis, 26(2005)3988.
40. B. Baraj, A. Sastre, A. Merkoci, M. Martinez, J.Chromatogr. A, 718(1995)227.
41. B. Baraj, A. Sastre, M. Martinez, K. Spahiu, Anal.Chim.Acta, 319(1996)191.
42. C. Hennig, K. Servaes, P. Nockemann, K. V. Hecke, L. V.Meervelt, J. Wouters, L. Fluyt, C. Gorller-Walrand, R.V. Deun, Inorg.Chem., 47(2008)2987.
43. C. Hennig, J. Tutschku, A. Rossberg, G. Bernhard, A.C. Scheinost, Inorg. Chem., 44(2005)6655.

44. N. J. Welham, K. A. Malatt and S. Vukcevic, *Hydrometallurgy*, 57(2000)209.
45. W. Liu, B. Etschmann, J. Brugger, L. Spiccia, G. Foran, B. McInnes, *Chem. Geol.*, 231(2006) 326.
46. W. Walkowlak, D. Bhattacharyya, R. B. Grieves, *Anal. Chem.*, 48(1976) 975.
47. J. Bjerrum, *Acta Chem. Scand. Ser. A*, 41(1987)328.
48. H. Engelhardt, W. Beck and T. Schmitt, "Capillary Electrophoresis," Friedrich Vieweg&SohnVerlagsgesellschaftmbH, Braunschweig/Wiesbaden, 1996.
49. DAE-Interlaboratory Comparison Experiment (ILCE) for Trace Metal Assay of Uranium, Phase-II Experiments: Development of Certified U₃O₈ Reference Materials, Document, BARC, India, February 2002.

Chapter : 7

Application of Ion chromatography for Optimizing Washing Procedure for Removal of Chloride and Nitrate from Li_2TiO_3 Microspheres using LiOH Solution.

7.1 Introduction:

For the International Thermonuclear Experimental Reactor (ITER) programme different types of Li compounds have been considered as Test Blanket Material (TBM) for tritium breeding. In these materials tritium is generated due to the nuclear reaction with neutrons: ${}^6\text{Li}(n,\alpha){}^3\text{T}$. Tritium formed in the breeder matrix will be recovered by purging with helium. For the purpose of producing tritium, many ceramic lithium compounds such as Li_2O , LiAlO_2 , Li_2ZrO_3 , Li_2TiO_3 and Li_4SiO_4 are under consideration. Among them Li_2TiO_3 has relatively better chemical stability and tritium recovery at lower temperatures. Although it can be fabricated by various methods [1-5], the sol-gel based processes have several advantages over the other methods. In BARC synthesis of Li_2TiO_3 (Lithium enriched to 60% in Li-6) is being carried out by following an internal gelation technique of sol-gel process[6]. Lithium nitrate and TiOCl_2 are the starting materials for the synthesis. It is seen the final product Li_2TiO_3 microspheres is getting contaminated with significant quantities of nitrate and chloride from the feed materials. Presence of nitrate and chloride are not desirable because, they cause cracking of microspheres during sintering at high temperatures. Therefore, in order to improve the fabrication procedure to obtain nitrate and chloride free product, it was planned to wash the product with enriched LiOH solution. The washing with enriched LiOH is necessary in order to avoid

leaching of Li from the final matrix and also to avoid dilution of ${}^6\text{Li}$ due to the isotopic exchange with ${}^7\text{Li}$. Only minimum quantities of ${}^6\text{LiOH}$ should be used to conserve this precious material. Therefore the enriched LiOH has to be used judiciously. In order to decide the total volume of ${}^6\text{LiOH}$ required, it is necessary to know the total nitrate and chloride contents in the microspheres and also the quantities of Cl^- and NO_3^- removed during each washing cycle. The amount of impurities removed in the washed solutions will help in deciding the washing program which will use minimum LiOH. The wash solutions were analysed for the concentrations of chloride and nitrate. Various methods were reported for the analysis of Cl^- and NO_3^- . Ion Chromatography is widely used for determination of chloride and nitrate in different types of matrices [7-11]. Optimization of various IC parameters to realize good separation between nitrate and chloride and their determination is necessary as the samples are of high ionic strength.

In addition to the determination of chloride and nitrate in wash solutions it is also important to analyse the finished product to confirm the removal of impurities. It is important to certify the chloride impurity in the product as chloride is corrosive in nature. This necessitates the determination of chlorine in the final product of Li_2TiO_3 as a part of its chemical characterization. In general the impurity analyses in various matrices are carried out using an appropriate method after the dissolution of the sample. However, for the analysis of trace impurities, the dissolution of the sample can lead to high background and blank contributions. In view of these, non-destructive analysis (NDA) methods are always preferred [12]. In addition to this Li_2TiO_3 is difficult to dissolve.

Pyrohydrolysis is a well known separation technique mainly used to separate halides directly from a solid sample. The separated analytes are collected in a dilute NaOH.

The distillate collected is clean and interference free, which can be used for trace level analysis. The final determination of halides can be carried out by suitable methods such as, spectrophotometry or ion chromatography etc. [13-21]. In addition to halides, nitrogen from the sample is also separated but their separation is not quantitative, however qualitative information regarding the presence of nitrogen in the sample can be obtained. The present study is aimed at (i) proposing a simple IC method for the determination of chloride and nitrate in LiOH washing solutions, (ii) developing a washing strategy to minimise the volume of LiOH and (iii) developing a pyrohydrolysis- ion chromatography combined method for the determination of chlorine in the Li_2TiO_3 microspheres.

7.2 Experimental:

7.2.1 Materials and reagents:

Analytical grade LiCl, LiNO_3 , hexamethylenetetramine (HMTA), urea, TiCl_4 and LiOH were used for the synthesis of Li_2TiO_3 . Standard solutions of chloride and nitrate were prepared by dissolving their respective Na salts of 99.9% purity. NaOH (99.9% purity) was used for the preparation of mobile phase. All reagents were obtained from Merck, Germany. For the preparation of all solutions and production of steam, high purity deionised water (18.2 M Ω cm) obtained from a Milli-Q water system (Millipore, USA) was used.

7.2.2 Instrumentation:

A quartz pyrohydrolysis (PH) apparatus was used. The details of the pyrohydrolysis apparatus was described elsewhere [22]. A commercial ion chromatograph (DX-500 model; Dionex, USA) consisting of a gradient pump (GP-50), ED-40 conductivity

detector and an anion self-regenerating suppressor (ASRS-II) was used for obtaining the chromatograms. Samples were introduced through a Rheodyne injector fitted with a 50- μ L loop. Ion chromatographic separations were carried out separately on two analytical columns, viz. IonPac AS16 (250 \times 4 mm) and IonPac AS18 (250 \times 4 mm) along with their respective guard columns, IonPac AG16 (50 \times 4 mm) and AG18 (50 \times 4 mm) respectively.

7.3 Results and Discussion:

For optimisation of process parameters, initial experiments were carried out using natural Li bearing compounds. This has been done to conserve the more expensive enriched Li-6 bearing compounds. The optimised parameters were then used for the enriched material.

7.3.1 Preparation and washing of Li_2TiO_3 :

Lithium titanate microspheres were prepared by using the internal gelation process [6]. By mixing 3 M HMTA/urea solution, 3 M TiOCl_2 and 3 M $\text{LiCl}/\text{LiNO}_3$ solutions with Li to Ti mole ratio as $\text{Li}:\text{Ti} = 2:1$, a feed solution was prepared. This feed solution in the form of droplets was dispersed in hot silicone oil, where Li_2TiO_3 microspheres are formed. The microspheres formed are first washed with CCl_4 and then with LiOH . The washing with LiOH was required for removal of nitrate and chloride, which are responsible for cracking of microsphere during drying and heating steps. To stop the leaching of Li from the microspheres washings were performed with 1.55 M LiOH . In this work washing processes were carried out batch wise with minimum volume of LiOH solution (Li-natural) and the generated washing effluents were reused with a view to reduce the total volume of LiOH solution actually required. The amount of nitrate and chloride in the washing

solutions obtained in each step helped in planning a washing strategy for Li_2TiO_3 microspheres so as to realise minimum volume of LiOH .

7.3.2 Sample preparation for IC analysis

Each washing effluent was sampled and filtered through 0.2 μm filter paper to remove the microspheres. Since the washing solutions were reused during the entire process, the solutions obtained from the initial washings had higher concentrations of chloride and nitrate. Therefore, the samples were diluted appropriately to bring the Cl^- and NO_3^- concentrations within the dynamic calibration range (100 ppb to 10 ppm) of IC analysis.

7.3.3 Ion chromatographic analysis:

IC can facilitate the simultaneous separation and determination of different anions especially halides, nitrate, sulphate etc. The samples have high ionic strength and varying concentrations of the analytes. This necessitates the selection of appropriate eluent as well as analytical column. Because the sample contains a large amount of OH^- ions hydroxide eluent was preferred over the carbonate.

For the selection of separator column, two anion exchange columns viz. IonPac AS16 and IonPac AS18. Both columns have been selected based on the column chemistry as well as differences in their column capacities. Standard solutions of fluoride, chloride, nitrate and sulphate were prepared in 1.5 M LiOH and injected into the IC. [Figures 7.1 (a) and (b) show plots of retention time vs. NaOH concentration for IonPac AS18 and IonPac AS16, respectively.] It can be seen that for a given concentration of the eluent, the AS16 column offers faster elution than IonPac AS18 column. Figure 7.2 shows the chromatograms obtained with both

IonPac AS16 and AS18 columns using 15mM and 40mM NaOH eluents respectively. Although the chloride peak appeared at the same time with both the columns, the IonPac AS16 column provided a better resolution between chloride and nitrate compared to the IonPac AS- 18 column. Based on the observations, the IonPac AS16 column along with 15 mM NaOH eluent at a flow rate of 1 mL/min was identified as suitable for the elution of chloride and nitrate.

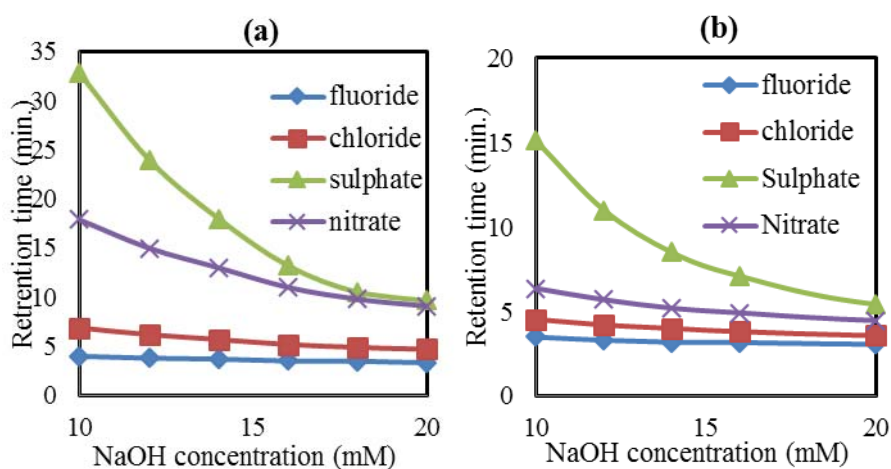


Fig. 7.1: Effect of [NaOH] on the retention times of various anions.

(a) IonPac AS18 column and (b) IonPac AS16 column.

Calibration plots were constructed for both Cl^- and NO_3^- in the concentration range of 0.1 to 10 ppm. The linear regression coefficient obtained for the plots corresponding to Cl^- and NO_3^- are 0.998 and 0.995 respectively. The limit of detection (LOD) for chloride and nitrate were calculated as 25 and 40 ppb, respectively. The precision of the measurements was better than 5% (RSD) at 0.3 ppm of Cl^- and 0.5 ppm of NO_3^- (Figure 4).

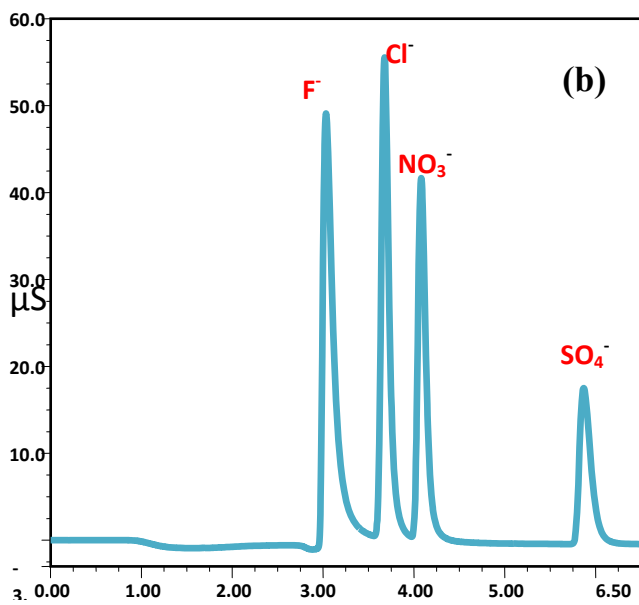
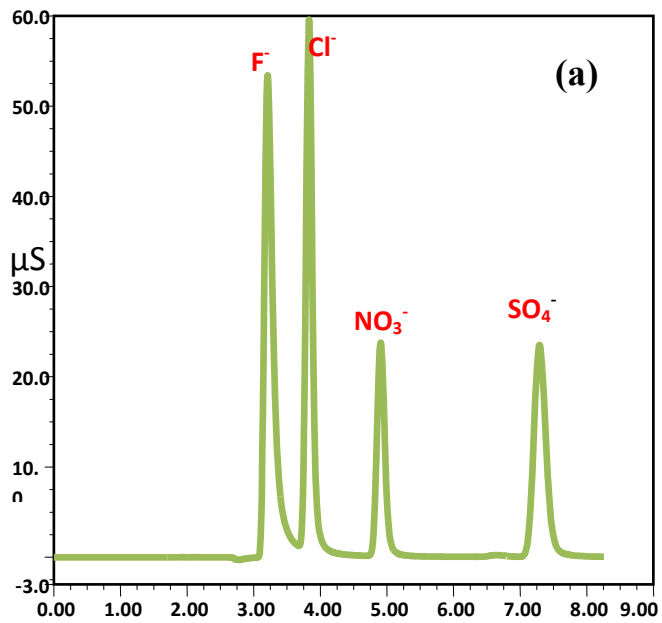


Figure 7.2: Standard chromatograms obtained for standard with F^- , Cl^- , NO_3^- and SO_4^{2-} (10.0 ppm each). (a) Column: AS16 column, Eluent: 15 mM NaOH. (b) Column: AS18 column, Eluent: 40 mM NaOH.

7.3.4 Reduction in volume and recycling of LiOH washing effluent:

A single batch of lithium titanate microspheres weighing about 200g was prepared using internal gelation process. Further it was divided into four parts (A, B, C and D). Part A was digested at 60°C in LiOH solution (50 ml) for 18 hrs and the supernatant was filtered. The filtered effluent is labelled as effluent A₁ and it cannot be reused as it contains large quantities of chemicals leached out during digestion. Further the microspheres were given three washes of LiOH, with the washings labelled as A₂, A₃ and A₄ and the effluents produced were kept for their reuse as these solutions contain less impurities compared to A₁. However, the other three parts of the microspheres viz. B, C and D were also digested but not with fresh LiOH. Further a systematic washing plan was envisaged by knowing the level of impurities present in each washing effluent as shown in Figure 7.6. For instance, the effluent A₂ would be reused as B₁, which means it would be used for digesting the microsphere part B. Similarly A₃ would act as B₂, the second wash of B₂ and so on. Each wash had a volume of 50 mL and therefore, the total volume of LiOH wash solution required as per the wash plan was 350 mL against the actual requirement of 800 mL (similar level of impurities were removed using single wash of 800ml LiOH). Therefore the developed washing procedure significantly reduced the volume of fresh LiOH solution. The concentration of chloride and nitrate were analysed and Figure 7.7 shows a bar graph depicting the concentrations of chloride and nitrate in each washing. The figure indicates the reduction in the concentrations of chloride and nitrate sequentially.

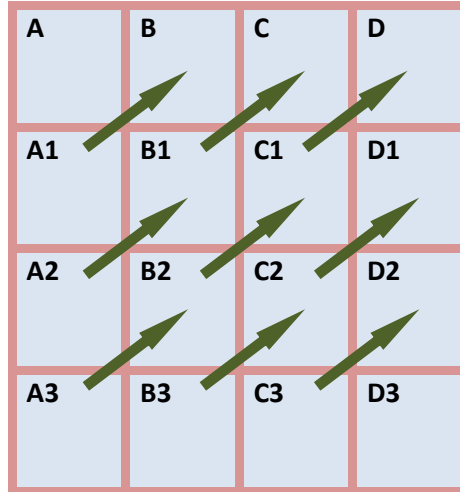


Figure 7.3 The optimised reuse of LiOH washing solution. A, B, C, and D are different Li_2TiO_3 lots, the numbers 1, 2, 3 represent no. of washing. The washing solution containing lower impurity are reused for samples containing higher impurities

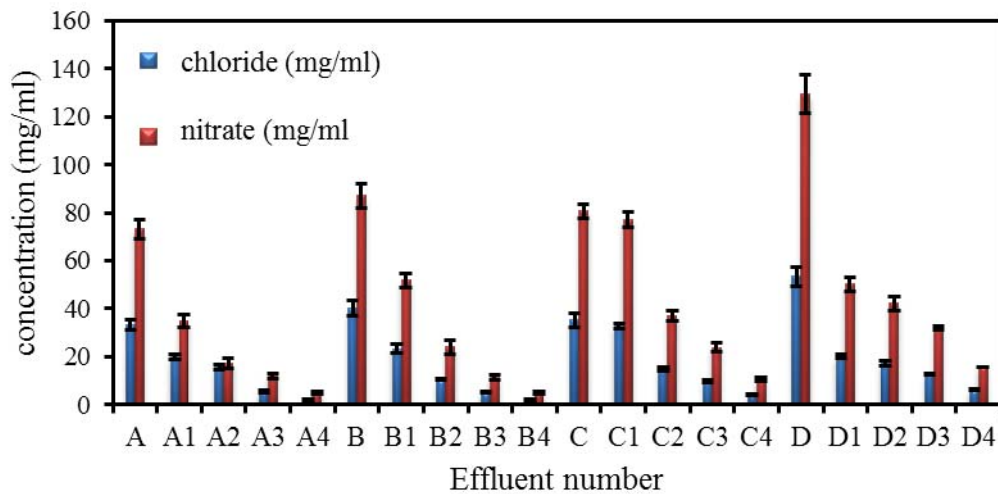


Figure 7.4: Concentration of chloride and nitrate in wash solutions collected at different steps of optimised washing method.

The optimised process parameters were used for washing enriched Li_2TiO_3 material to be used as TBM for ITER. It was possible to reduce the consumption of enriched LiOH by more than 50% (350 mL against 800 mL).

7.3.5 Determination of chlorine Li_2TiO_3 microspheres:

The determination of chlorine in the finished product, Li_2TiO_3 microspheres was carried out to ensure the efficient washing to certify the final product. This determination was carried out using pyrohydrolysis extraction of chlorine followed by ion chromatography determination combined method. Around 0.5 g of Li_2TiO_3 microspheres were pyrohydrolysed at 1273K with moist oxygen as the carrier gas. The carrier gas flow rate was maintained as 1.5 litres/min and the condensed distillate was collected in 5 mL of 15 mM NaOH . The distillate was further analysed by IC for chloride and nitrate contents.

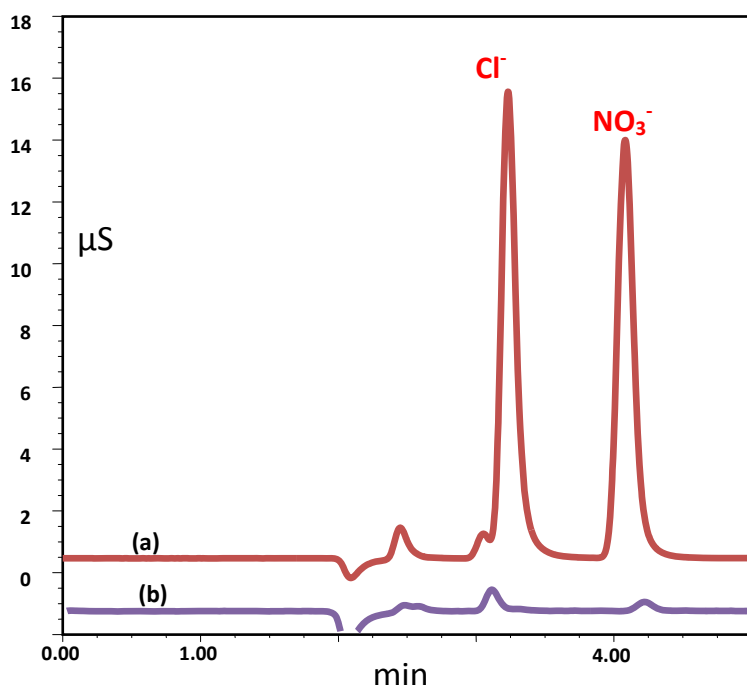


Figure 7.5: Chromatograms obtained for the Li_2TiO_3 pyrohydrolysis distillates (a) before washing (initial product) (b) after washing.

The maximum recovery of chlorine was confirmed by pyrohydrolysing different aliquots of the sample of the same lot for different time intervals. It was observed that 45 minutes of pyrohydrolysis could extract chlorine as HCl completely. Pyrohydrolysis could not extract all the nitrogen oxides. This is because nitrogen can form different species during pyrohydrolysis, these species have different solubility and pyrohydrolysis behaviour. However, the amount of nitrate present in the pyrohydrolysis distillate indicates presence or absence of nitrate in the sample as well as it provides the concentration semi-quantitatively. Table 7.1 summarizes the typical concentrations of chloride in the real samples.

Table 7.1 chlorine obtained for real samples of Li₂TiO₃ finished products.

Sample code	Chlorine(µg/g)
LiT-1	6.2 ± 0.4
LiT-2	4.9 ± 0.5
LiT-3	17.8± 1.3
LiT-4	13.1± 0.8

7.4 Conclusions

1. A washing procedure for Li_2TiO_3 microspheres for the removal of the Cl^- and NO_3^- contamination using LiOH solution was established.
2. The proposed washing procedure achieved significant reduction in the total volume of LiOH required and this would help in the judicious use of enriched LiOH solution.
3. The chlorine concentration in the washed product for is CQC certification has been realised by developing a PH-IC combined method.

7.5 References:

1. W. Xiangwei, W. Zhaoyin, H. Jinduo, X. Xiaoxiong, A. Bin Li, M. Deptula, Fusion Eng Des., 83(2008)112.
2. A. Deptuła, M. Brykała, W. Ladaa, T. Olczaka, B. Sartowska, A. G. Chmielewski, et al., Fusion Eng. Des., 84(2009)681.
3. X. Wu, Z. Wen, X. Xu., J. Nucl. Mater., 393(2009)186.
4. K. Tsuchiya, H. Kawamura, K. Fuchinoue., J. Nucl. Mater., 258(1998)1985.
5. J. R. Dahn, S. U. Von, M. W. Juzkow., J. Electrochem. Soc., 138(1991)2.
6. T. V. Vittal Rao, Y. R. Bamankar, S. K. Mukerjee., J. Nucl. Mater. 426(2012)102.
7. R. Michalski, I. Kurzyca, Pol. J. Environ.Stud., 15(2006)5.
8. N. Gros, Water., 5(2013)659.
9. M. Zhou, D. Guo, Microchem. J., 65(2000)221.

10. J. Morales, S. Ligbel, J. Mesa, *J. Chromatogr. A.*, 884(2000)185.
11. M. Neal, C. Neal, H. Wickham, *Hydrol. Earth Syst. Sci.*, 11(2007)294.
12. S. Chhillar, R. Acharya, T. Vittal Rao, Y. Bamankar, S. Mukerjee, P. Pujari, J. *Radioanal. Nucl. Chem.*, 298(2013)1597.
13. F. Antes, F. Duarte, J. N. Paniz, M. Santos, R. C. L. Guimaraes, E. Flores, *At.Spectrosc.*, 29(2008)157.
14. H. Kusuno, H. Matsuzaki, T. Nagata, et al., *Nucl. Instrum. Methods Phys. Res. Sect. B.*, 361(2015)414.
15. Y. Noguchi, L. Zhang, T. Maruta, *Anal. Chim. Acta.* 640(2009)106.
16. Y. Muramatsu, Y. Takada, H. Matsuzaki, *Quat. Geochronol.* 3(2008)291.
17. S. N. Thieli, C. M. Cristiano, B. Paua, A. L. H. Muller, M. F. Mesko, P. A. Mello, et. al. *Anal. Methods.*, 7(2015)2129.
18. V. G. Mishra, S. K. Sali, D. J. Shah, *Radiochim. acta.*, 102(2014)895.
19. R.M. Sawant, M. A. Mahajan, D. J. Shah, *J. Radioanal. Nucl. Chem.*, 287(2011)423.
20. R. M. Sawant, M. A. Mahajan, P. Verma, D. J. Shah, U. K. Thakur, K. L. Ramakumar, et al., *Radiochim. Acta.*, 95(2007)585.
21. S. Jeyakumar, V. Raut, K. L. Ramakumar. *Talanta.*, 76(2008)1246.
22. M. Mahajan, M. Prasad, H. Mhatre, R. M. Sawant, R. Rastogi, G. Rizvi, N. Chaudhari, *J. Radioanal. Nucl. Chem.*, 148(1991).

Chapter: 8

Development of Ion Chromatographic Method for the Simultaneous Separation and Determination of B, Cl and Mo in Plant and Soil Samples

8.1 Introduction:

Boron, chlorine and molybdenum along with copper, iron, manganese and zinc are important micronutrients for plants [1]. Boron plays an important role in N-metabolism, photosynthesis and cellular differentiation and development. Chlorine plays a vital role in maintaining the cell charges. Mo is important for enzyme function and N₂ fixation. On the other hand, in many cases, these micronutrients become toxic when their concentration exceeds certain limit. The micronutrient elements are available for the plants through soil. Analyses of plant and soil samples for the determination of these micronutrients are helpful in various studies relevant to both diagnostic and monitoring [2]. The concentration of micronutrient elements is also helpful as it is correlated to plant growth and yield of crops [3-5]. There are different analytical methods available for the analysis of micronutrients. Most of the methods are based on the extraction of micronutrient(s) into an aqueous phase [6] followed by instrumental analysis. However, the separation procedures followed are not amenable to simultaneous analyses as they are mostly element specific. For example, separate procedures for the extraction of B, Cl and Mo are reported in the literature [7]. The method for extracting boron uses HCl as one of the reagents and hence, it is not possible to determine Cl in the extract. Similarly the extraction of Mo uses several reagents, which causes problems in the determination of Cl and B.

Distilled water and ranex-30 solution is often used for extracting chloride, which cannot extract boron, Mo etc. Since these extraction procedures use concentrated acids for sample digestion, ion chromatographic analysis of anions become impractical [7,8].

Pyrohydrolysis, a simple separation technique, is being employed for the separation of boron, chlorine, fluorine, molybdenum etc. directly from the solid matrices without their dissolution [9, 10]. The separated species are trapped in a dilute NaOH solution. Though the organic matrices like plant samples are easily combustible at high temperatures, they need extra care during the pyrohydrolysis as the organic matrices are prone to cause flare. This demands a controlled heating pattern of the organic samples during pyrohydrolysis so as to prevent the analyte loss. The main advantage of pyrohydrolytic separation is that the distillate obtained from pyrohydrolysis has much lower ionic contents compared to the dissolved solution and therefore, the distillate is more amenable for ion chromatographic analysis. Since the non-metallic elements like Cl, B etc are present in anionic form in the distillate their simultaneous separation by IC is feasible. The pyrohydrolysis and IC combination methods have been successfully employed for the analysis of carbon nano tubes, coals and graphite [11-13] samples, which suggests the feasibility of employing pyrohydrolysis for the plant samples. Many studies have been reported on the pyrohydrolysis separation of halides and B in carbon compounds [14-16]. In addition to the extraction of non-metals by pyrohydrolysis, feasibility of separating Mo in solid uranium matrices have been reported [10]. Hence, there is a scope of applying pyrohydrolysis for the simultaneous separation of B, Cl and Mo from plant and soil samples. For this purpose, it is necessary to identify the various pyrohydrolysis conditions. The present study deals with developing a pyrohydrolysis

method for the simultaneous separation of B, Cl and Mo. In order to find the optimum pyrohydrolysis conditions, the determination of these analytes recovered under PH conditions needed to be carried out. For this, initially an IC method was developed for carrying out simultaneous separation and determination of B, Cl and Mo. Ion chromatography is the best choice for their simultaneous determination because these three analytes are in ionic form in the solution. Moreover, the procedures for their individual separation and determination has been reported in the literatures.

The IC has been used for simultaneous determination of nitrate, chloride sulphate and phosphate in plant extracts [17]. B has been determined using IC by converting it to tetrafluoroborate [18] or by using mannitol as a complexing agent [19]. In addition to this Mo in form of molybdate has been determined in different environmental samples [20, 21]. However, there is no IC method reported for their simultaneous analysis and hence, it is proposed to develop an IC method in the present work.

For the separation and determination of anions, diluted solutions of NaOH or carbonate/ bicarbonate are being used as eluents. Ion chromatography separation and determination of boron has been carried out by adding d-mannitol as a complexing agent in the eluent [9]. The determination of B by IC requires mannitol because the complex of B and mannitol has lower de-protonation constant as compared to boric acid. The lower pKa helps in getting B in anionic form during column separation and in detector (after passing through suppressor). In order to support the development of pyrohydrolysis method (for simultaneous separation of B, Cl and Mo from plant and soil samples), ion chromatographic studies were carried out to understand the effect of mannitol (as a part of eluent) on retention and sensitivity of Mo, and the

observation were employed in developing a gradient method for the simultaneous detection of B, Cl and Mo.

8.2 Experimental:

8.2.1 Reagents and materials:

The standard solutions of F^- , Cl^- , NO_3^- and SO_4^{2-} were prepared by dissolving their respective Na salts of 99.9% purity (Merck, Germany). Standard solutions of MoO_4^{2-} were prepared by dissolving $(NH_4)_6Mo_7O_{24}$ (99.98% pure, Sigma-Aldrich, USA). Standard boron solution was prepared by dissolving known amount of boric acid (Merck Germany). For the eluent the GR grade NaOH and d-mannitol, of Merck Germany make were used. The $NaHCO_3$ used was AR grade (Thomas Baker, India). For the preparation of all solutions and production of steam, high purity deionised water (18.2 M Ω .cm) obtained from a Milli-Q water system (Millipore, USA) was used.

8.2.2 Apparatus and instrument:

All quartz pyrohydrolysis set up consisting of two concentric tubes was used for pyrohydrolysis purpose. The outer tube has an inlet and serves as pre-heater for moist carrier gas. The inner tube houses the sample boat and it is attached to gas outlet. The gas outlet tube is cooled by condenser. The condensate is collected in a bottle containing dilute NaOH.

A commercial ion chromatograph (Dionex, model ICS-5000) consisting of a self-regenerator suppressor (ASRS-II) and a conductivity detector was used. Samples were introduced through a 50 μ l loop fitted with a Rheodyne injector. Separation of anions was achieved with anion columns viz. IC-Pak anion (Waters) and Ion Pac

AS16 (Dionex). A software namely Chromeleon was used for instrument control, data collection and data processing.

8.2.3 Samples:

Rice plant and soil samples were obtained from the experimental gamma field at Trombay.

8.3 Result and Discussion:

8.3.1 Separation studies:

One of our earlier studies showed that while separating boron along with halides the sensitivity of B peak was strongly dependent on the concentration of d-mannitol present in the eluent [9]. Based on this, an eluent consisting of HCO_3^- and d-mannitol was considered for separating boron as borate ion along with other anions. An anion exchange column, IC Pak Anion (Waters) was considered.

Chromatograms were obtained by injecting a standard solution having mixture of anions viz. fluoride, chloride, nitrate, sulphate and molybdate by taking the eluents as 17.5mM HCO_3^- with varying mannitol concentration from zero to 0.56M. Following observations were made from the chromatograms.

- i. Retention times of all anions did not change with change in the d-mannitol concentration in the eluent. Figure 8.1(a) as can be observed in figure 1(a), the retention times of all the anions are nearly same.
- ii. Although there is no change in the retention time of Mo peak while increasing the d-mannitol concentration in the eluent, the sensitivity of molybdate peak decreased significantly (Fig. 8.1(b)).

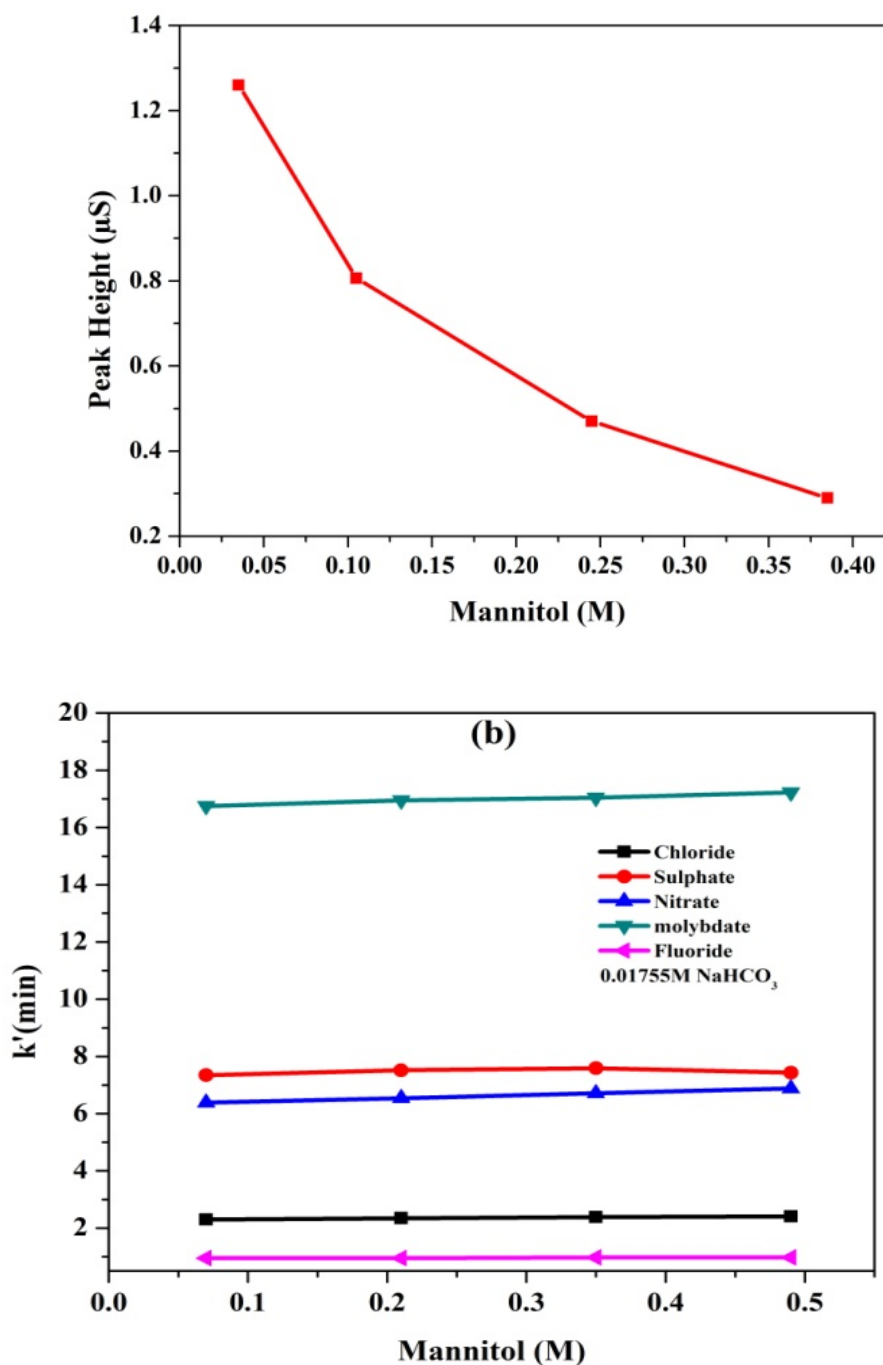
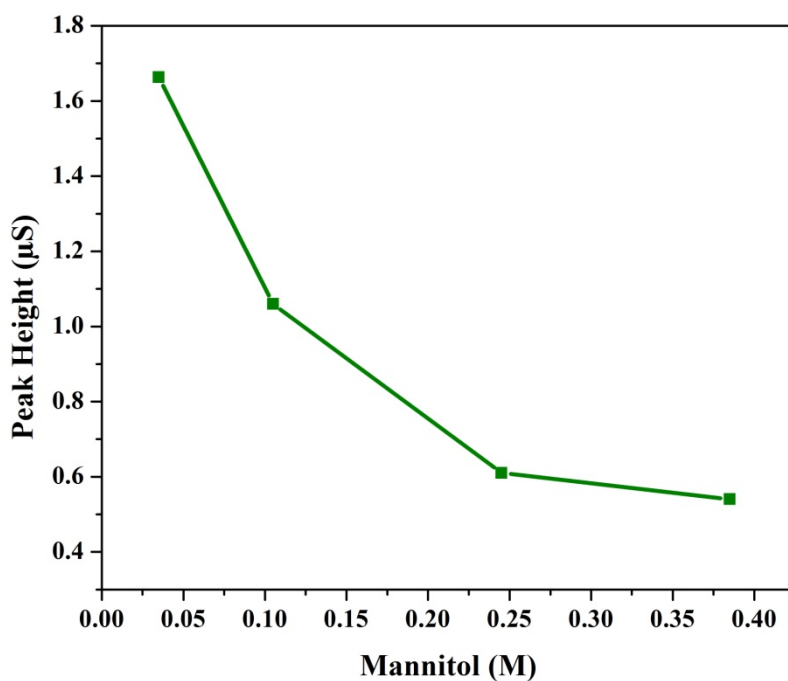


Figure 8.1: (a) Peak height of molybdate peak (20ppm) (b) retention time of anions; Column: IC-Pak anion, Eluent: NaHCO_3 (0.01755M) and d-mannitol (concentration varied), flow rate 1 ml/min.

One possible reason for the effect of mannitol on molybdate peak sensitivity is complex formation between Mo and mannitol. However, in the event of such complex formation, the charge density of the Mo-complex is expected to vary and

hence its retention time. However, there was no effect of mannitol concentration on the retention time of molybdenum peak. Further to understand the role of chemistry of stationary phase on the sensitivity of molybdate peak, a similar study was carried out on Ion Pac AS-18 (dionex) analytical column. The observations were similar to that of the previously used IC Pak column. Figure 8.2 shows the observation of decreasing Mo peak sensitivity and no change in the retention times of anions due to increasing concentration of mannitol. Hence, the stationary phase has no role on the sensitivity of Mo peak.



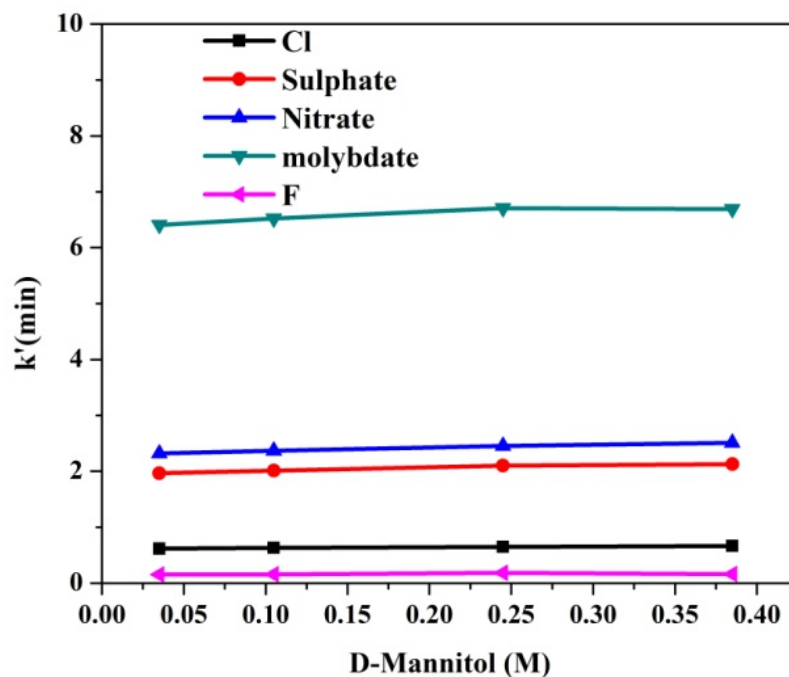


Figure 8.2: (a) Peak height of molybdate peak (20ppm) (b) retention time of anions; Column: Ion Pac AS16, Eluent: NaHCO_3 (0.01755M) and d-mannitol (concentration varied), flow rate 1 ml/min.

Further it was proposed to investigate the problem by changing the eluent combination. Instead of bicarbonate-mannitol eluent, sodium hydroxide-mannitol combination was considered. Since the IC Pak anion column is not compatible with the eluents having pH more than 12, the separation with NaOH-mannitol was carried out on Ion Pac As-18 column. During all the separations, the NaOH concentration was kept constant at 30 mM and d-mannitol concentration was varied from 0 to 0.56M. Following observations were made.

- i. The retention times of all the anions under study increased gradually while increasing the d-mannitol concentration in the eluent (Fig.8.3).
- ii. Since the retention time of Mo varied significantly by increasing the mannitol concentration, the relation between sensitivity of Mo peak against

concentration of mannitol could not be correlated.

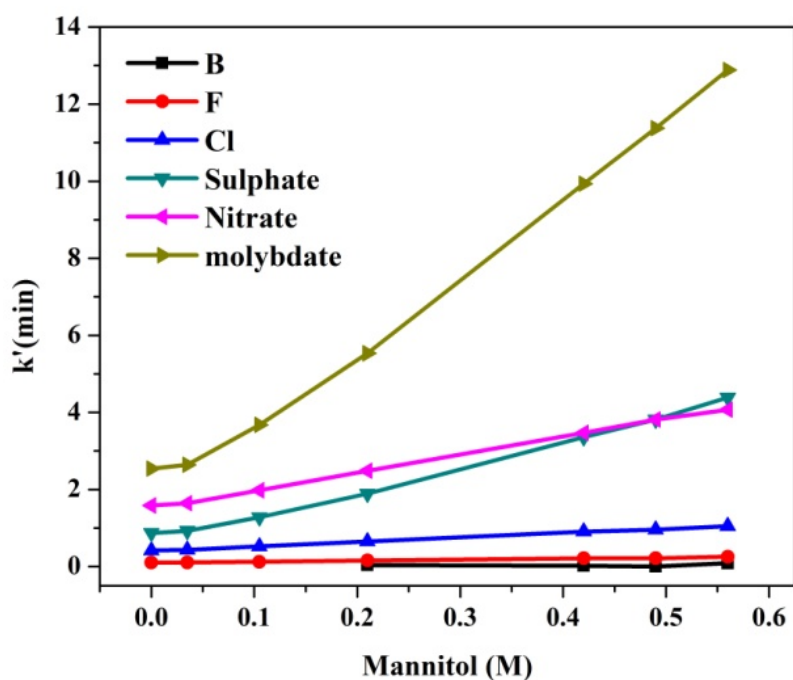


Figure 8.3: Retention time of anions; Column: Ion Pac AS16, Eluent: NaOH (30mM) and d-mannitol (concentration varied), flow rate 1 ml/min.

In order to study the effect of d-mannitol on molybdate sensitivity in NaOH combination eluent, a sensitivity study was carried out without using the separation column (flow injection mode). During this experiment the eluent composition was varied by changing the mannitol concentration and a molybdenum standard solution was injected. The peak height of Mo peak decreased systematically with increasing d-mannitol (figure 8.4).

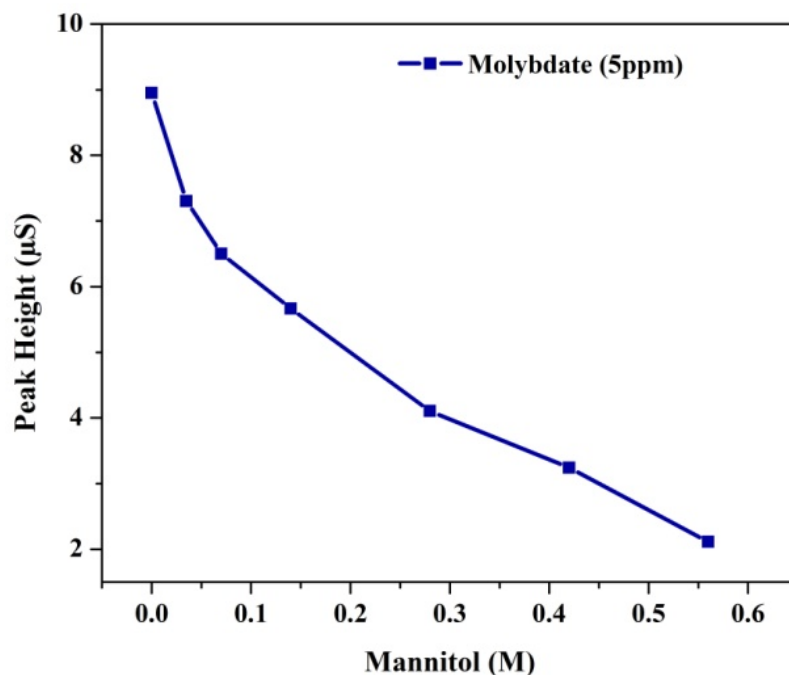


Figure 8.4: (a) Peak height of molybdate peak (5ppm); No separation Column, Eluent: NaOH (30mM) and d-mannitol (concentration varied), flow rate: 0.1ml/min.

The observations from the above experiments infer that the effect of sensitivity and change in the retention time while using NaOH eluent are due to the role of mannitol.

However, the observations could not explain the following:

- i. Why there is no change in the retention time of Mo when HCO_3^- was used in the eluent and it decreased only the sensitivity?
- ii. Why does NaOH-mannitol combination cause changes both in retention time and sensitivity of Mo peak?

8.3.2 Explanation:

Molybdate anion-d-mannitol complex was studied and reported in the literature [23]. The study presented speciation diagrams wherein it was seen that a fraction of Mo was present in different forms as a function of $\log[\text{H}^+]$. It can be observed that a

complexation of Mo and mannitol is favoured at lower pH (higher $[H^+]$). From the speciation diagram it is understood that in the presence of high concentration of mannitol and at pH 8 or above the dominant form of Mo is molybdate. Whereas at $pH \leq 3$ a complex is formed and it consists of two mannitol, one Mo and three protons. On increasing the pH the complex undergoes deprotonation.

In order to correlate the pH of the mobile phases and complex formation between Mo and mannitol, the pH of the mobile phases were measured at two points viz. one at the column out-let and the other at suppressor out-let. For a 50mM NaOH the pH was 13.1 and for 50 mM HCO_3^- pH was 8.8.

Both in NaOH and $NaHCO_3$ mobile phases the pH of eluents in the column is above 8, and at this pH conditions Mo exists predominantly as molybdate. Therefore the separation of Mo occurs as un-complexed molybdate ion.

On the other hand the pH conditions of these eluents after suppressor were found to be 7.5 (NaOH) and 4.4 ($NaHCO_3$), respectively. And as per the speciation diagram of Mo and mannitol [23], the conditions are favourable for complex formation between Mo and d-mannitol. Therefore, formation of the complex takes place after the suppressor and prior to reaching the detector. This causes the decrease in sensitivity of detection with increasing d-mannitol in eluents of NaOH and $NaHCO_3$. Hence the out-come of the experiment shows that (i) retention behaviour of molybdate and other common anions were not altered while increasing the d-mannitol concentration in the carbonate eluent as the pH of the eluent inside the column is more than 7 and at this condition, molybdate does not form complex with d-mannitol (ii) retention behaviour of molybdate and other common anions were changed (increase in retention time) when the d-mannitol concentration was increased in the NaOH eluent

and (iii) the detection sensitivity (suppressed conductivity) of molybdate was found to be decreasing with increasing d-mannitol concentration in the eluents of both carbonate and hydroxide.

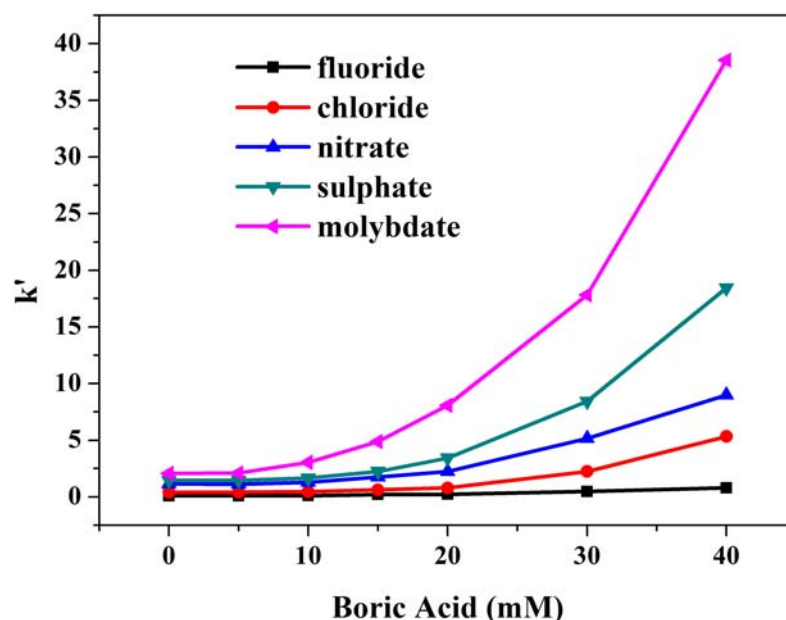


Figure 8.5: Retention time of anions; Column: Ion Pac AS16, Eluent: NaOH (30mM) and boric acid (concentration varied), flow rate 1 ml/min.

It is necessary to investigate the question why retention times of molybdate and other common anions are changing while increasing d-mannitol concentration in the NaOH eluent and it did not occur in carbonate eluent. To understand the role of mannitol on the retention time, mannitol was replaced with boric acid in the mobile phase. The boric acid was considered in place of mannitol because it is weak acid ($pK_{a1} = 9.1$) and it has been used as weak eluent for separating anions [24]. The concentration of boric acid was varied between 0 and 55 mM in the eluent whereas NaOH concentration was remain constant throughout the experiment. Figure 8.5 depicts the retention trends obtained due to increasing boric acid concentration in the eluents. The trend shows that the behaviour of boric acid was same as d-mannitol up

to 15 mM i.e. the retention times of all anions including the molybdate. When the boric acid concentration was more than 15 mM, the retention times of all anions remain unchanged; as it happened with carbonate eluents. The unchanged retention times of anions can be explained as follows. Boric acid being a weak acid, (stronger than mannitol) initial addition of boric acid neutralised the NaOH, which reduced the strength of NaOH and thereby, the retention time increased. After the neutralisation of NaOH, a buffer was formed and further addition of boric acid could not cause any change in hydroxide concentration.

The Pka^1 of d-mannitol is 13.0 [25]. This shows that when eluent pH is above 12 (possible in the case of NaOH) significant fraction (more than 10%) of d-mannitol is present in de-protonated form. The mannitol concentrations are in molar range whereas NaOH concentration is in millimolar range in the mobile phase. Hence a significant amount of dissociated d-mannitol is available in the mobile phase which can neutralise the NaOH eluent and reduce the strength of the eluent, which causes increase in the retention times of all the anions.

The dissociation (deprotonation) of d-mannitol does not occur in the bicarbonate mobile phase as the pH of bicarbonate eluent is less than 9. Therefore in presence of $NaHCO_3$, mannitol in the eluent remains as a neutral molecule and cannot affect the retention time of anions.

8.3.3 Development of gradient elution procedure:

Based on the results of the above investigations it is obvious that presence of d-mannitol in the eluent is undesirable as it reduces the detection sensitivity. On the other hand the presence of d-mannitol is crucial for the separation and detection boron as borate ion. In view of this, a gradient elution method was developed to

achieve the simultaneous separation and detection of B and Mo along with other common anions. A concentration gradient elution procedure was incorporated where the d-mannitol concentration was brought to zero in the eluent prior to the elution of molybdate peak. The final optimized gradient elution program is mentioned in table 8.1.

Table 8.1: The optimized gradient elution program for simultaneous separation and determination of B, Cl and Mo. Column: Ion Pac AS16, flow rate 1 ml/min.

Time (min.)	NaOH (mM)	Mannitol (M)
0	5	0.56
5	5	0.385
8	10	0.14
12	20	0
20	30	0

8.3.4 Sample Analysis:

Different parts of rice plants viz. root, stem and leaves were cut and dried at 353K. Each sample was pyrohydrolysed in moist oxygen carrier gas at 1373K for 2 h. The distillate was collected in 5mM NaOH. The separation and determination of B, Cl and Mo was carried out by following the developed IC method. During pyrohydrolysis it was observed that the plant samples completely burned and no traces of the sample remain in the sample boat. The results obtained for the samples are listed in Table 2. It was found that the Mo content in the samples was below the IC detection limit and therefore the distillates were analysed for Mo by ICP-AES.

However, two rice plants that were grown in the laboratory conditions with Mo stress. Mo was added in the soil in form of ammonium molybdate. These samples were subjected to pyrohydrolysis and the distillates were analysed. In these two samples molybdate peaks were detected and quantified (Table 2). The Cl, B, and Mo were also analysed by the conventional method and results are reported in table 8.2. When the soil samples were pyrohydrolysed it was possible to detect the B, Cl and Mo using the IC method developed. However the results of different aliquots of the same sample were not reproducible. This indicates that during pyrohydrolysis the complete recovery of analytes is not possible during the pyrohydrolysis.

Table 8.2: The concentration of B, Cl and Mo obtained in dried plant samples and Soil PH distillates by the developed IC method and their comparison with conventional methods.

Sample	B (mg/kg)			Cl (mg/kg)		Mo (mg/kg)		
	Ph-IC	PH-ICP-AES	Conventional ¹	PH-IC	Conventional ²	Ph-IC	PH-ICP-MS	Conventional ³
Leaf	56 ± 9	51 ± 5	41 ± 8	121 ± 9	112 ± 14	0.9 ± 0.2*	1.2 ± 0.3	-
Stem	83 ± 8	76 ± 7	-	623 ± 34	561 ± 42	0.7 ± 0.3*	0.9 ± 0.2	0.8 ± 0.2
root	23 ± 4	-	-	12 ± 4	-	1.2 ± 0.4*	-	-
Soil	22 ± 15	31 ± 15	-	625 ± 30	-	32 ± 2	-	-

* the samples were concentrated ~50 times by vacuum evaporation.

¹ dried 2 g leaf, ash at 773 K, dissolved in 20% HCl, diluted, filtered and B determined by ICPAES.

² dried 2 g plant sample, extraction with hot water, filtered and Cl determined by IC.

³ dried 2 g stem, ash at 773 K, organic matrix destroyed using H₂SO₄ and H₂O₂, diluted (5 ml), filtered and Mo determined by AAS.

8.4 Conclusion:

Effect of d-mannitol on anions during IC separation was studied in detail and it was found that presence of mannitol effects the Mo peak sensitivity. Depending on the observations a gradient elution IC method was developed for the analysis of PH distillates. The PH-IC method was used successfully to determine B, Cl and Mo

simultaneously in plant samples. For the soil samples the Pyrohydrolytic procedure followed could not provide complete recovery.

8.5 References:

1. Ross M. Welch & Larry Shuman, *Critical Reviews in Plant Science*, 14(1995)49.
2. Raul A. Sperotto, Felipe K. Ricachenevsky, Lorraine E. Williams, Marta W. Vasconcelos and Paloma K. Menguier, Editorial, Published on 05 September 2014, *Front. Plant Sci.* doi: 10.3389/fpls.2014.00438.
3. Rajeev Gopal, Yogesh K. Sharma, Arvind K. Shukla, *Journal of Plant Nutrition*, 39(2016)463.
4. Jeanine M. Davis, Douglas C. Sanders, Paul V. Nelson, Laura Legnick, Wade J. Sperry, *J. Amer. Soc. Hort. Sci.* 128(3)(2003)441.
5. Ranjit Chatterjee, Subhendu Bandyopadhyay, *Journal of Saudi Society of Agricultural Sciences*, in press. doi.org/10.1016/j.jssas.2015.11.001
6. B. Zygmunt and J. Namiesnik, *Journal of Chromatographic Science*, 41(2003)109.
7. *Hand book of Reference Methods for Plant Analysis*, Edited by Yash P. Kalra, 1998 by Taylor & Francis Group.
8. *Ion Chromatography in Environmental Analysis*, Peter E. Jackson, *Encyclopedia of Analytical Chemistry*, R. A. Meyers (Ed.), pp. 2779–2801.
9. S. Jeyakumar, Vaibhavi V Raut, K. L. Ramakumar, *Talanta* 76(2008)1246.

10. Vivekchandra G. Mishra, Uday K. Thakur, Dipti J. Shah, Neeraj K. Gupta, Subbiah Jeyakumar, Bhupendra S. Tomar, and Karanam L. Ramakumar, *anal. Chem.*, 87(2015)10728.
11. Bingxian Peng, Daishe Wu, Jinhu Lai, Huayun Xiao, Ping L, *Fuel* 94 (2012) 629.
12. Fabiane G. Antes, Juliana S.F. Pereira, Michele S.P. Enders, Clarissa M.M. Moreira, Edson I. Müller, Erico M.M. Flores, Valderi L. Dressler, *Microchemical Journal* 101 (2012) 54.
13. Thieli Schaefer Nunes, Cristiano Cabral Muller, Paula Balestrin, Aline Lima Hermes Muller, Marcia Foster Mesko, Paola de Azevedo Melloa and Edson Irineu Muller, *Anal. Methods*, 7(2015)2129.
14. The F, Cl, Br and I Contents of Reference Glasses BHVO-2G, BIR-1G, BCR-2G, GSD-1G, GSE-1G, NIST SRM 610 and NIST SRM 612, Michael A. W. Marks, Mark A. Kendrick, G. Nelson Eby, Thomas Zack and Thomas Wenze, *Geostandards and Geoanalytical Research* · June 2016.
15. Vivekchandra Guruprasad Mishra, Sanjay KrishnaraoSali, DiptiJayesh Shah, Uday Kumar Thakur, Ramesh MahadeoSawant, Bhupendra Singh Tomar, *Radiochim. Acta* 2014; 102(10): 895–901.
16. Vaibhavi Vishwajeet Raut, Subbiah Jeyakumar, Dipti Jayesh Shah, Uday Kumar Thakur, Bhupendra Singh Tomar, Karanam Lakshminarayana Ramakumar, *Analytical Sciences*, 31 (2015)219.

17. Mahmoud Kalbasi, M. Ali Tabatabai, *Communications in Soil Science and Plant Analysis* 16(1985)787.
18. C. J. Hill and R. P. Lash, *Anal Chem.*, 52(1980)24.
19. Andrea Tapparo, Paolo Pastore and G. Giorgio Bombi, *Analyst*, 123(1993)1771.
20. Yasuo Nakashima, Yoshinori Inoue, Takahisa Yamamoto, WakaKamichatani, SigehiroKagaya, Atsushi Yamamoto, *Analytical Sciences*, 28(2012)1113.
21. Harish C. Mehra and William T. Frankenberger, Jr., *Analyst*, 114(1989)707.
22. H. Dale Pennington, *Hortscience* 26(1991)1496.
23. Lage Pettersson, *Acta Chemica Scandinavica* (1972) 4067.
24. Hu W., Haddad P. R., Tanaka K., Sato S., Mori M., Xu Q., Ikedo M., Tanaka S., *J. Chromatogr A*. 1039(2004)59.
25. E. GAidamauskas, E. Norkus, J. Vaiciuniene, D. C. Cranes, T. Vuorinen, J. Jaciauskiene, and G. Baltrunas, *Carbohydrate Research*, 340(2005)1553.

**DEVELOPMENT OF ANALYTICAL METHODOLOGY
FOR TRACE ELEMENTS IN
NUCLEAR/ENVIRONMENTAL SAMPLES USING
CHROMATOGRAPHY TECHNIQUES**

By
VIVEKCHANDRA GURUPRASAD MISHRA
(CHEM01201104010)

**Bhabha Atomic Research Centre,
Mumbai**

*A thesis submitted to the
Board of Studies in Chemical Sciences
In partial fulfillment of requirements
for the Degree of
DOCTOR OF PHILOSOPHY
of
HOMI BHABHA NATIONAL INSTITUTE*



March, 2017

STATEMENT BY AUTHOR

This dissertation has been submitted in partial fulfillment of requirements for an advanced degree at Homi Bhabha National Institute (HBNI) and is deposited in the Library to be made available to borrowers under rules of the HBNI.

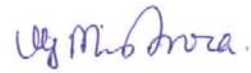
Brief quotations from this dissertation are allowable without special permission, provided that accurate acknowledgement of source is made. Requests for permission for extended quotation from or reproduction of this manuscript in whole or in part may be granted by the Competent Authority of HBNI when in his or her judgment the proposed use of the material is in the interests of scholarship. In all other instances, however, permission must be obtained from the author.



Vivekchandra G. Mishra

DECLARATION

I, hereby declare that the investigation presented in the thesis has been carried out by me. The work is original and has not been submitted earlier as a whole or in part for a degree / diploma at this or any other Institution / University.



Vivekchandra G. Mishra

List of Publications arising from the thesis

Journal

1. Direct extraction of molybdenum from solid uranium matrices employing pyrohydrolysis, a reagent free green separation method and its determination by Ion Chromatography.

Vivekchandra Guruprasad Mishra, Uday Kumar Thakur, Dipti Jayesh Shah, Neeraj Kumar Gupta, Subbiah Jeyakumar, Bhupendra Singh Tomar, Karanam Lakshminarayana Ramakumar

Anal. Chem. 87(2015)10728.

2. Simultaneous determination of borate, chloride and molybdate in pyrohydrolysis distillates of plant and soil samples by ion chromatography.

Vivekchandra Guruprasad Mishra, Mrinal Kanti Das, Dipti Jayesh Shah, Subbiah Jeyakumar, Bhupendra Singh Tomar, Karanam Lakshminarayana Ramakumar

J. Chromatogr. A 1532(2018)144-149.

3. Application of Ion chromatography for optimizing washing procedure for removal of Chloride and Nitrate from Li_2TiO_3 microspheres using LiOH solutions.

Vivekchandra G. Mishra, U. K. Thakur, T. V. Vittal Rao, Y. R. Bamankar, Dipti J. Shah, S. Jeyakumar, B. S. Tomar and K. L. Ramakumar

J. Res. Anal. 2(1)(2016)35.

4. Studies on U-Zr and U-Pu-Zr alloys for determination of Cl and F using pyrohydrolysis.

Vivekchandra Guruprasad Mishra, Sanjay Krishnarao Sali, Dipti Jayesh Shah, Uday Kumar Thakur, Ramesh Mahadeo Sawant, and Bhupendra Singh Tomar.

Radiochim. Acta 102(2014)895.

5. Development of ion chromatography and capillary electrophoresis methods for the determination of Li in Li-Al alloy.

V. G. Mishra, M. K. Das, V. V. Raut, S. Jeyakumar, R. M. Sawant, B. S. Tomar, and K. L. Ramakumar

J. Radioanal. Nucl. Chem. 300(2014)125.

6. Rapid Separation and Quantification of Iron in Uranium Nuclear Matrix by Capillary Zone Electrophoresis (CZE).

Vivekchandra Mishra, Mrinal Kanti Das, Subbiah Jeyakumar, Ramesh Mahadeo Sawant, Karanam Lakshminarayana Ramakumar.

Am. J. Anal. Chem., 2(2011)46.

Conferences

1. Extraction of Molybdenum from uranium matrix employing Pyrohydrolysis: A novel approach.

V.G. Mishra, U. K. Thakur, D. J. Shah, N. K. Gupta, S. Jeyakumar, B. S. Tomar and K. L. Ramakumar.

Proceedings of DAE -BRNS National Symposium on Nuclear and Radiochemistry 2015, 9-13 Feb, 2015, 409.

2. Feasibility study on the simultaneous separation and analysis of B, Cl, F, and Mo in the Pyrohydrolysis extract of Uranium samples employing ion chromatography.

V. G. Mishra, M.K. Das, D. J. Shah, S. Jeyakumar, B. S. Tomar and K. L. Ramakumar.

Proceedings of DAE-BRNS National Symposium on Nuclear and Radiochemistry 2015, 9-13 Feb, 2015, 415.

3. Determination of Chloride and Nitrate in LiOH solutions used for washing Li_2TiO_3 microspheres employing Ion Chromatography.

U. K. Thakur, **V. G. Mishra**, T. V. Vittal Rao, Y. R. Bamankar, D. J. Shah, S. Jeyakumar, B. S. Tomar

Proceedings of DAE-BRNS National Symposium on Nuclear and Radiochemistry 2015, 9-13 Feb, 2015, 413.

4. Determination of Lithium-Aluminium Alloy by Capillary Electrophoresis.

V.G. Mishra, M. K. Das, S. Jeyakumar, R. M. Sawant, B. S. Tomar, and K. L. Ramakumar

Proceedings of DAE-BRNS National Symposium on Nuclear and Radiochemistry 2013, 19-23 Feb, 2013, 445.

5. Separation and Quantification of Lithium in Aluminium Matrices using Ion Chromatography

V.G.Mishra, M.K.Das, B.K.Nagar, S.Jeyakumar, R.M.Sawant, B.S.Tomar and K.L.Ramakumar

Proceedings of DAE-BRNS Biennial Symposium on Emerging Trends in Separation Science and Technology 2012, 27 Feb-Mar 01, Mumbai, 159.

6. Study on pyrohydrolysis extraction and determination of Cl, F in U-Zr and U-Pu-Zr alloys.

D. J. Shah, **V. G. Mishra**, U. K. Thakur, R. M. Sawant, and B. S. Tomar

Proceedings of DAE-BRNS Biennial Symposium on Emerging Trends in Separation Science and Technology, Mumbai, February 25-28, 2014,104.

7. XRD study on pyrohydrolysed U-Zr and U-Pu-Zr alloys for halide extraction

U. K. Thakur, S. K. Sali, D. J. Shah, **V. G. Mishra**, R. M. Sawant, and B. S. Tomar

Proceedings of DAE-BRNS Biennial Symposium on Emerging Trends in Separation Science and Technology, Mumbai, February 25-28, 2014,106.

8. Separation and Determination of Iron from Uranium Matrix by Capillary Zone Electrophoresis (CZE).

V. G. Mishra, M. K. Das, S. Jeyakumar, R. M. Sawant, and K. L. Ramakumar.

Proceedings of DAE-BRNS Biennial Symposium on Emerging Trends in Separation Science and Technology 2010, IGCAR, Kalpakkam, March 1-4, 2010, 461.

Vivekchandra G. Mishra

Dedicated to.....

My Grandmother

Late Smt. Ramarati Mishra

&

My Parents

Smt. Kishori Devi Mishra

Shri Guru Prasad Mishra

Acknowledgment

I extend my sincere gratitude to all who put their efforts and spent time for me to get successful completion of the work, without whose support this would have been impossible.

It is my pleasure to thank my guide **Dr. K. L. Ramakumar**, for his continuous encouragement and motivation in mentoring me throughout the course of this thesis work. I would like to express the gratitude to my senior and technology advisor **Dr. S. Jeyakumar**, who has equally motivated and supported me during the entire period of work. I thank him for all the care, advice and encouragement he has given to me. Any words will not be sufficient to thank them for their support and contribution.

I also want to express my heartfelt thanks to my Head of Division and Chairman of Doctoral Committee, **Dr. B. S. Tomar**, for his cooperation and concern during the entire course of my PhD work. His guidance and suggestions helped in improving my work greatly. I also want to extend my thanks to all the other members of Doctoral Committee, **Dr. R. K. Verma, Dr. Sangita D. Kumar** and **Dr. G. G. Pandit** for their invaluable suggestions and insightful comments provided during the doctoral committee meetings. I am thankful to them for their strong support and cooperation throughout the course of my PhD program.

I sincerely thank all my lab mates, specially, **Smt Dipti J. Shah, Shri. Uday Kumar Thakur and Shri Mrinal Kanti Das**, who made me to carry the work in pleasant and effortless environment to keep me all the time comfortable in finishing the jobs. Without their kind support and keen contributions the work would have not been at its shape as it is now. I am grateful to all my friends for their emotional support, entertainment and being a great company all the time.

Last but always at the close to heart, I am fortunate to have blessings, love, support and encouragement from **my parents and family** who made me stable and studious at all odd and even happenings. I thank **Mayank, Mridula and Saket** who made all my time after office hours so joyful and cherishing and to come again as fresh as every time.

Above all I thank the almighty for enabling me to complete the task.

Vivekchandra G. Mishra

CONTENTS

<i>Synopsis</i>	I
<i>List of figures</i>	XIII
<i>List of tables</i>	XX
<i>Chapter-1- Introduction</i>	1-29
1.1 Basics of nuclear energy	1
1.2 Indian Nuclear Program	1
1.2.1 Nuclear fuel cycle	3
1.2.2 Types of nuclear fuels	4
1.2.3 Fusion Energy	9
1.2.4 Chemistry in nuclear fuel cycle	11
1.2.4.1 Determination of major elements	12
1.2.4.2 Isotopic composition analysis	17
1.2.4.3 Determination of Non-metallics	17
1.2.5 Scope of Present Investigations	20
1.3 References	23
<i>Chapter-2- Principles of Experimental Techniques</i>	30-60

2.1	Introduction	30
2.2	Chromatography	31
2.2.1	Types of Chromatography	31
2.2.2	Ion-Exchange Chromatography	34
2.2.2.1	Ion Exchange equilibria	34
2.2.2.2	Conductivity detection	36
2.2.3	Terms used in chromatography separations	37
2.2.4	Plate Height Equation	39
2.2.5	Instrumentation	42
2.3	Capillary Electrophoresis	44
2.3.1	Electrophoretic Mobility	45
2.3.2	Electro osmotic Flow	45
2.3.3	Instrumentation	46
2.3.4	Capillary Zone Electrophoresis (CZE)	47
2.4	X-ray powder diffraction analysis (XRD)	48
2.5	Thermogravimetric Analysis	50
2.6	Inductively Coupled Plasma Atomic Emission	51

Spectrometry	
2.7 Pyrohydrolysis	51
2.8 References	58
<i>Chapter-3- Direct Extraction of Molybdenum from Solid Uranium</i>	61-79
<i>Matrices Employing Pyrohydrolysis and Its Determination by Ion Chromatography</i>	
3.1 Introduction	61
3.2 Experimental Section	62
3.2.1 Reagents	62
3.2.2 Preparation of Standards Containing Mo	63
3.2.3 Instrumentation	63
3.2.4 IC Analysis of Mo	64
3.3 Results and Discussion	65
3.3.1 Thermogravimetric Analysis	65
3.3.2 Pyrohydrolysis of Mo Containing Standards	67
3.3.3 Kinetics of Mo Separation	70
3.3.4 Optimization of Pyrohydrolysis Conditions	73
3.3.5 Method Validation and Sample Analysis	75

3.4 Conclusion 76

3.5 References 77

Chapter-4-Studies On U-Zr And U-Pu-Zr Alloys For Determination of Cl And F Using Pyrohydrolysis 80-97

4.1 Introduction 80

4.2 Experimental Section 82

4.2.1 Pyrohydrolysis setup 82

4.2.2 Ionchromatography system 82

4.2.3 XRD instrument 83

4.2.4 Thermoanalyzer 83

4.2.5 Alloy fabrication and characterization 83

4.2.6 Pyrohydrolysis procedure 84

4.3 Results and discussion 84

4.4 Conclusions 94

4.5 References 95

Chapter-5-Development of Ion Chromatography and Capillary Electrophoresis Methods for the Determination of Li in Li-Al Alloy 98-109

5.1	Introduction	98
5.2	Experimental	99
5.2.1	Instrumentation	100
5.2.2	Reagents	100
5.2.3	Sample preparation	100
5.3	Results and discussion	100
5.3.1	Ion Chromatography Studies	100
5.3.2	Capillary electrophoresis studies	103
5.4	Conclusion	107
5.5	References	107
<i>Chapter-6-Rapid Separation and Quantification of Iron in Uranium Nuclear Matrix by Capillary Zone Electrophoresis (CZE)</i>		110-128
6.1	Introduction	110
6.2	Experimental	113
6.2.1	Instrumentation	113
6.2.2	Reagents and Solutions	113
6.2.3	Procedure for Conditioning Capillary and Sample Injection	114

6.3	Results and Discussion	114
6.3.1	Optimization of Background Electrolyte	116
6.3.2	Optimization of Applied Voltage	120
6.3.3	Matrix element tolerance	120
6.3.4	Validation of Method	121
6.4	Analysis of Certified Reference Materials	122
6.5	Real Sample Analysis	123
6.6	Advantages of the CZE Method	125
6.7	Conclusions	125
6.8	References	125
	<i>Chapter-7-Application of Ion chromatography for optimizing washing procedure for removal of Chloride and Nitrate from Li₂TiO₃ microspheres using LiOH solution.</i>	129-141
7.1	Introduction	129
7.2	Experimental	131
7.2.1	Materials and reagents	131
7.2.2	Instrumentation	131
7.3	Results and Discussion	132

7.3.1 Preparation and washing of Li_2TiO_3	132
7.3.2 Sample preparation for IC analysis	133
7.3.3 Ion chromatographic analysis	133
7.3.4 Reduction in volume and recycling of LiOH washing effluent	136
7.3.5 Determination of chlorine Li_2TiO_3 microspheres	138
7.4 Conclusions	140
7.5 References	140
<i>Chapter-8-Development of ion chromatographic method for the simultaneous separation and determination of B, Cl and Mo in plant and soil samples</i>	142-159
8.1 Introduction	142
8.2 Experimental	145
8.2.1 Reagents and materials	145
8.2.2 Apparatus and instrument	145
8.2.3 Samples	146
8.3 Result and Discussion	146
8.3.1 Separation studies	146

8.3.2 Explanation	151
8.3.3 Development of gradient elution procedure:	154
8.3.4 Sample Analysis	155
8.4 Conclusion	156
8.5 References	157

SYNOPSIS

Limited uranium resources and abundant thorium resources in the country prompted Dr. H.J. Bhabha, the initiator of Indian atomic energy program to envision a three stage nuclear energy program for sustained growth of nuclear power program. This obviously requires closed nuclear fuel cycle involving reprocessing of spent fuel from the first stage to fuel the second and third stages. The Department of Atomic Energy (DAE), India, is pursuing an indigenous power program linking the fuel cycle of Pressurized Heavy Water Reactor (PHWR), Liquid Metal Cooled Fast Breeder Reactors (LMFBR) and ^{232}Th - ^{233}U based advanced reactors [1-3]. Optimum utilization of fissile content in the nuclear fuels during reactor operation can result in increasing power production. Improving the fuel quality is one of the criteria to ensure longer residence time of fuel in the reactor. This in turn results in higher burn-up leading to enhanced power. Reactor physicists and fuel fabricators stipulate certain quality (specifications) to the nuclear fuel and other reactor materials for this purpose. In order to realize the smooth and efficient functioning of the reactor, the fuel should satisfy the specifications derived for it. The specification includes both physical and chemical qualities of the material. The chemical analyses pertaining to the Chemical Quality Control (CQC) process play a pivotal role in achieving the quality of the material fabricated. The CQC analyses mainly involve the analysis of feed (also known as starting materials) materials, intermediate and the finished products [4-7]. In addition to the nuclear fuels, strategically important nuclear materials like tritium generators [8] etc., are also require determination of percentage and trace level components for their optimum performance during reactor irradiation.

Nuclear energy is generated either by fission or fusion. Fusion energy is generated by fusing two light atoms, which are mostly the hydrogen isotopes. The waste generated during fusion will largely be either helium or water [8]. India is involved in the International Test Experimental Reactor (ITER) project (a fusion based reactor program) and DAE supports this program by fabricating tritium breeders (Li_2TiO_3) employing different methods [9]. This necessitates the development of analytical methods for the analysis of tritium breeders for their chemical characterization.

Several analytical techniques are employed for the chemical characterization or CQC analysis of nuclear materials [4]. Among them, elemental determinators, Inductively Coupled Plasma- Atomic Emission Spectroscopy (ICP-AES) [10], Inductively Coupled Plasma-Mass Spectrometry ICP-MS [11-12], Thermal Ionization Mass Spectrometry (TIMS) [13], alpha and gamma spectrometry[14,15], X-ray Diffraction (XRD) [16], electro analytical techniques, spectrophotometer etc are some of the important techniques routinely employed for chemical characterization analysis. In the recent past chromatographic techniques like High Pressure Liquid Chromatography (HPLC) and Ion Chromatography (IC) have been introduced into the CQC analyses of nuclear materials [17]. However, the CQC processes of various nuclear materials demand the development of new analytical methodologies. Improvement in the existing methodologies is also attempted with a view to improving accuracy and precision, low detection limit, high selectivity, simultaneous or multi-elemental analysis, minimum generation of analytical waste and minimum use of chemical reagents etc.

Chromatography is a physical method of separation wherein the analytes are separated due to their differential distribution between two immiscible phases. The major advantage of chromatographic techniques is that they offer simultaneous

separation and quantification. Ion chromatography is used for separating both cation and anion species wherein the separation occurs due to their different affinities toward the ion exchange process on the stationary phase [18] whereas, HPLC is mainly employed for the separation of organic as well as neutral molecules. Capillary Electrophoresis (CE) is a simple, rapid and high efficient separation method and is employed for separating ions as well as neutral molecules. Unlike HPLC and IC, separation in CE is achieved by applying an electric field which causes differential velocities of the ions or molecules due to their electrophoretic migration. The separation is carried out inside a thin capillary of 50 - 100 μm diameter and a length of 0.5 to 1 meter and the separation is complete within few minutes. CE is considered as a complementary technique to IC [19] and hence, both IC and CE are being used for separating several ions in a wide range of sample matrices.

Analytical methods which can analyze directly the dissolved sample solutions are preferred as they eliminate the cumbersome sample preparation procedures. Few applications of CE and IC, where direct analysis of the dissolved sample solution without employing matrix separation have been reported in literature [20,21]. Such direct analyses not only avoid the pre-separation of matrix or pre-concentration of analytes but also useful in the absence of reference materials. In the present study, efforts have been made to develop analytical methods for the direct analysis using IC and CE.

Pyrohydrolysis is a physical method of separation where the analyte is removed from the matrix by converting it into a volatile species. It is widely employed for separating halides from various nuclear materials. During pyrohydrolysis the sample

is heated at high temperature in presence of moist oxygen or a suitable carrier gas. Chlorine, fluorine and boron are separated in the form of hydrochloric, hydrofluoric and boric acids, respectively. Pyrohydrolysis separates halides and boron directly from a solid matrix and produces a clean sample solution, which is favorable in carrying out trace and ultra-trace level analysis [22,23]. Therefore, pyrohydrolysis finds many applications in the determination of halides at trace level concentrations in many complex matrices. Analysis of halides and boron in environmental and plant samples involves tedious sample preparation procedures due to the presence of organic compounds. The analytical methods that have been developed for the analyses of nuclear materials involving initial pyrohydrolysis separation followed by analytical determinations can be extended for the analyses of environmental samples. In this thesis, the analysis of environmental samples like soil and plants using pyrohydrolysis and ion chromatography have been reported.

In spite of the unique features of IC and CE, not many applications were reported for the analysis of nuclear materials. Therefore, efforts have been made to utilize these techniques for nuclear material analysis independently and validate the results. The present thesis is divided into eight chapters and the brief description of each chapter is given below.

CHAPTER ONE: This chapter discusses the need for high quality nuclear materials and the importance of their Chemical Quality Control (CQC) analysis. It also recounts the effect of the concentration of the specified elements (specification limits) on the performance of the nuclear material or fuel. It also discusses about the analytical techniques employed in the CQC analysis and emphasizes the need for developing new analytical methods with a view to achieving better accuracy and precision specially while determining the trace and ultra trace constituents (both

metallic and non-metallic impurities). It highlights the importance and advantages on the use of chromatographic methods like IC and CE in the CQC analysis of nuclear materials.

CHAPTER TWO: This chapter deals with the experimental part of the studies reported in the thesis. It describes the basic principles of the techniques employed. Special emphasis has been given to ion chromatography and capillary electrophoresis separations. Pyrohydrolysis is basically a non-instrumental separation technique which has been exploited employing an in-house designed equipment. Details of this technique have been discussed along with IC and CE. Other techniques like X-Ray Diffraction (XRD), Thermo Gravimetry (TG), Inductively Coupled Plasma -Atomic Emission Spectrometry (ICP-AES) were also used to obtain supportive information required for the investigation. The usefulness of these techniques in the present studies has been described in this chapter.

CHAPTER THREE: This chapter deals with the direct separation of molybdenum from solid uranium matrices employing pyrohydrolysis and its determination by ion chromatography. Pyrohydrolysis (PH) is a well-established technique for the direct extraction of non-metals like halides and boron from solid matrices without acid digestion and use of chemical reagents. However, PH extraction of metals or metal species has not been reported. This is for the first time the pyrohydrolysis separation of a metal, Mo in the form of MoO_4^{2-} was reported. Systematic studies were carried out to understand the high temperature chemistry of Mo and its oxides. It has been shown that MoO_3 volatilization is enhanced drastically in presence of moist atmosphere [24]. The volatilization behavior of MoO_3 in presence of moist Ar at 950°C was carried out with TG to explore the feasibility of PH extraction of Mo. To understand the mechanism and kinetics of the separation, the XRD patterns were

attained for the material after pyrohydrolysing at different time intervals. The study brings out the need for the suitable modification of the PH apparatus to improve the recovery of Mo. The Mo in the distillate was determined by IC. The developed method was extended to the analysis of Mo in ADU samples on routine basis.

CHAPTER FOUR: This chapter discusses the determination of chlorine and fluorine in U-Zr and U-Pu-Zr alloys using pyrohydrolysis separation followed by IC determination. U-Zr and U-Pu-Zr alloys are being considered as fuel for fast breeder reactors due to improved breeding possibilities associated with metallic fuel [25]. These newly developed materials have specification limits for Cl and F and hence, there is a need for developing an analytical method for the determination of chlorine and fluorine in U-Zr and U-Pu-Zr alloys. The study reports the pyrohydrolysis of the materials as well as the optimization of various pyrohydrolysis conditions required for the maximum recovery of Cl and F. The samples were pyrohydrolysed for different time intervals and their XRD patterns were recorded. The XRD data helped in understanding the mechanism of pyrohydrolysis and to optimize the time of pyrohydrolysis. This chapter also deals with the analysis of the real samples.

CHAPTER FIVE: This chapter discusses the development of ion chromatography (IC) and capillary electrophoresis (CE) methods for the determination of Li in Li-Al alloy. The Li-Al alloy is irradiated in reactor for the production of tritium (${}^6\text{Li}(n,\alpha)\text{T}$). The Li content in Li-Al alloy is about 4%. The common analytical methods employed for the determination of Li are ICP-AES and Atomic Absorption Spectroscopy (AAS). However, these techniques could not be utilized for certifying Li in Li-Al alloy because of certain inherent difficulties [26] (such as interferences are observed in AES and signal suppression is observed in AAS due to Al matrix). Hence, an IC method for the determination of Li in Li-Al alloy was developed.

Although IC is capable of separating the alkali and alkaline earth metals, presence of large amount of Al matrix may cause difficulty in separating Li. Since Al^{3+} ions will have strong retention on the ion exchange column than Li^+ , elution of Li^+ ahead of Al^{3+} ion is desirable for the determination of Li. A weak strength mobile phase to elute Li is the choice to realize this. otherwise it would get eluted along with un-retained components. Using the weak-strength eluent also helps in retaining Al^{3+} on the column. Therefore, IC separation was carried out on a high capacity cation exchange column with methane sulphonic acid (MSA) as eluent with a view to retaining Al on the column. While using MSA (20 mM MSA) as eluent, Li is eluted in reasonable time whereas Al^{3+} is retained on the column and it would not get eluted unless the mobile phase strength is increased five times. The developed procedure showed high tolerance for Al and provided a precision better than 0.2% (RSD). In the absence of a certified reference material to check the accuracy of the results, another method based on capillary electrophoresis was developed independently and the results obtained by this method were compared. Unlike IC the elution order in CE separation is Al followed by Li. This is because the tri-positive charged Al moves ahead of singly charged Li. However, for the purpose of analytical determination of Li such separation is not acceptable as the bulk Al peak significantly affects the recovery of Li. To reverse the elution order, imidazole was used as a co-ion, which forms complex with the metal cations also enables the indirect detection of cations. Imidazole forms complex with Al selectively and reduces its charge density, which resulted the appearance of Al peak after Li in the electrogram. Moreover the developed method showed high tolerance for Al matrix. The results obtained from both IC and CE were compared. IC provided better

sensitivity and precision, whereas CE has the advantages like fast analysis, low sample volume, and reduction in waste generation.

CHAPTER SIX: This chapter deals with the development of a Capillary Zone Electrophoresis (CZE) method for the determination of iron in uranium matrix without employing the pre-separation of uranium. Iron is a common contaminant picked up by the product material from various process equipments. In order to control the process to obtain the desired quality of the end product, it is necessary to check the Fe contents in both unfinished and finished products. This demands a rapid as well as reliable method for the determination of Fe. For this purpose, a CE method was developed as the dissolved sample solution can be injected directly into CE and the total analysis time is few minutes. However, while developing direct CE method for separating Fe from U matrices, the following conditions are to be considered (i) the Fe peak should appear before uranium, (ii) sufficient resolution between the Fe and U peak so that matrix is tolerated and (iii) the Fe peak should be interference-free from other transition metals. Hence, to realize the separation with the above conditions, CE separation was carried in the form of chloride complexes of Fe and U [27,28]. Uranium and iron form positively charged chloride complexes. The iron-chloride complex has higher positive charge density than uranium-chloride complex which is responsible for the separation as well as to provide the required elution order (iron peak is followed by uranium). Moreover, the chloride medium brings the advantage of interference free determination of Fe as the other transition metals form either anionic or neutral complexes [29]. The developed method was validated by analyzing ILCE (IV) and (V) reference materials and the results for Fe were within 5 % of certified value. Several other samples were also analyzed and reported.

CHAPTER SEVEN: This chapter discusses the application of ion chromatography for optimizing washing procedure to be used for removal of chloride and nitrate from Li_2TiO_3 microspheres using lithium hydroxide as wash solution. Li_2TiO_3 is proposed for Test Blanket Material (TBM) for International Thermonuclear Experimental Reactor (ITER). Li_2TiO_3 were produced through wet process where the microspheres are contaminated with chloride and nitrate. Subsequently chloride and nitrate were removed by washing with LiOH. Since the proposed Li_2TiO_3 contains 60% enriched ^6Li , washing is carried out with $^6\text{LiOH}$ to avoid depletion in the ^6Li content of Li_2TiO_3 . Therefore, the entire washing process is required to be completed with minimum volume of $^6\text{LiOH}$. The present work describes the ion chromatographic (IC) determination of Cl^- and NO_3^- in LiOH wash solutions at different washing stages. Based on the results, a procedure was for the repeated use of LiOH, which significantly reduces the volume of LiOH otherwise required. The final chlorine content of Li_2TiO_3 was determined by IC after its pyrohydrolysis extraction. The results obtained for the washing solutions helped in arriving at a washing procedure wherein maximum impurities could be extracted with minimum washing solution of LiOH.

CHAPTER EIGHT: This chapter reports an ion chromatographic method for the simultaneous separation and determination of borate, fluoride, chloride and molybdate ions, which is useful in the chemical characterization of nuclear fuels and environmental samples (plant and soil). Though the pyrohydrolysis separation of Mo from uranium matrix was discussed in chapter three, the present study deals with the simultaneous separation of Mo B, F and Cl as molybdate, borate, fluoride and chloride ions and their subsequent IC separation and determination. For the determination of boron by IC, use of mannitol in the eluent is necessary to convert

the weak H_3BO_3 into a strong anion complex form, which is amenable for the anion exchange separation [23]. During the IC separation, it was observed that MoO_4^{2-} peak area decreased with increasing mannitol concentration. In general, the decrease in peak area could be due to the effect of complexation, however, such effect should cause change in retention time of the analyte which was not observed in this case. Proper investigation was carried out to understand this behavior of mannitol and molybdate. The retention behaviors of these ions was studied on different anion exchange columns as well as with different mobile phase compositions. The study resulted in many interesting observations and based on results obtained, the unusual behavior was explained on the basis of complexation of Mo with mannitol at different pH and deprotonation of mannitol.

References:

1. http://www.barc.gov.in/about/anushakti_sne.html.
2. P. K. Vasudev, *Electrical India*, 54(2014)28.
3. G. Gopalkrishnan, *Annual Review of Energy and Environment*, 27(2002)369.
4. S. K. Patil, *Materials Science Forum*, 48(1989)371.
5. N. K. Rao, H. C. Shri, K. K. Katiyar, U. C. Sinha, et. al., *J. Nucl. Mater.*, 81(1979)171.
6. N. Kondal Rao, *J. Nucl. Mater.*, 106(1982)273.
7. B. Laxminarayanan, P. S. A. Narayanan, *Characterisation and Quality Control of Nuclear Fuels*, CQCNF-2002, Allied publication, pg. 578.
8. Y. Shimomura, W. Spears, *IEEE Transactions on Applied Superconductivity*, 14(2)(2004)1369.
9. T. V. Vittal Rao, Y. R. Bamankar, S. K. Mukerjee, *J Nucl Mater.*, 426(2012)102.

10. M. Krachler, R. Alvarez-Sarandes, S. V. Winckel, J. Radioanal. Nucl. Chem., 304(2015)1201.
11. I. G. Alonso, J.F. Babelot, J. P. Glatz, O. Cromboom, L. Koch, Radiochim. Acta., 62(1993) 71.
12. A. M. Meeks, J. M. Giaquinto, J. M. Keller, , J. Radioanal. Nucl. Chem., 234(1998)131.
13. D. Suzuki, F. Esaka, Y. Miyamoto, M. Magara, Appl. Radiat. Isot., 96(2015) 52.
14. Y.Y. Ebaïd, Rom. Journ. Phys., 55(2010) 69.
15. A. M. Sanchez, F. V. Tome, J. D. Bejarano, M. J. Vargas, Nucl. Instrum. Methods Phys. Res. Sect. A, 313(1992)219.
16. G. C. Jain, K. B. Khan, S. Majumdar, H. S. Kamat, C. Ganguly, Characterisation and Quality Control of Nuclear Fuels, CQCNF-2002, Allied publication, pg. 376.
17. A. Kelkar, A. Prakash, M. Afzal, J. P. Panakkal, H. S. Kamath, J. Radioanal. Nucl. Chem., 284(2010)443.
18. P. R. Haddad and P. E. Jackson, Journal Of Chromatography Library - volume 46, Ion Chromatography Principles and Applications.
19. S. E. Y. Li, Journal Of Chromatography Library- volume 52, Capillary Electrophoresis Principles, practice and applications.
20. Determination of Aluminum in Complex Matrices Using Chelation Ion Chromatography, Dionex, Application note, AN 69, 1991.
21. A. Riaz, B. Kim, D. S. Chung, Electrophoresis, 24(2003)2788.
22. Ticiane Taflik, J. Braz. Chem. Soc., 23(2012)488.
23. S. Jeyakumar, V. V. Raut, K. L. Ramakumar, Talanta, 76(2008) 1246.

24. K. U. Rempel, A. A. Migdisov, A. E. Williams-Jones, *Geochim. Cosmochim. Acta.*, 70(2006) 687.
25. S. C. Chetal, P. Chellapandi, P. Puthiyavinayagam, S. Raghupathy, Balasubramanian, et. al. *Asian Nuclear Prospects*, 7(2011)64.
26. S.P. Mirjana, Z. P. Nebojsa, M. Momir, *J Anal At Spectrom.*, 4(1989)587.
27. C. Hennig, K. Servaes, P. Nockemann, et. al. *Inorganic Chemistry*, 47(2008)2987.
28. C. Hennig, J. Tutschku, A. Rossberg, G. Bernhard and A. C. Scheinost, *Inorganic Chemistry*, 44(2005) 6655.
29. J. Bjerrum, *Acta Chem. Scand. Series A*, 41(1987)328.

List of Figures

Fig. 1.1	Indian three stage nuclear program	3
Fig.1.2	Nuclear fuel cycle	4
Fig.1.3	Metallic fuels designed for FBR.	8
Fig.1.4	Fusion Reaction using deuterium and tritium	9
Fig. 2.1	Major types of Chromatography	32
Fig. 2.2	Schematic representation of Ion Exchange mechanism	35
Fig. 2.3	A typical Van Deemter plot	41
Fig. 2.4	Block diagram for an Ion Chromatography system	43
Fig. 2.5	Schematic representation of an Ion Chromatography system designed for radioactive samples	44
Fig. 2.6	Capillary Electrophoresis instrumentation	47
Fig. 2.7	Gibb's free energies of formation of various compounds	53
Fig. 2.8	Basic Pyrohydrolysis instrument	56
Fig. 2.9	The modified Pyrohydrolysis apparatus for Glove Box operation	57

- Fig. 3.1** Chromatogram of an anion mix standard containing F⁻ (0.5 ppm), Cl⁻ (1.0 ppm), NO₃⁻ (2.0 ppm), SO₄⁻² (2.0 ppm), and MoO₄²⁻ (10.0 ppm): column, IonPac AS-16; eluent, 15 mMNaOH; flow rate, 1 mL min⁻¹. 65
- Fig. 3.2** Isothermal thermograms of ~3 mg of MoO₃ at different temperatures and carrier gas conditions: (a) 1073K in dry Ar carrier gas; (b) 1073K in moist Ar carrier gas; (c) 1273K in moist Ar carrier gas; (d) 1473K in moist Ar carrier gas. 66
- Fig. 3.3** Recovery curve in moist O₂ carrier gas (a) for UO₂ + MoO₃ mixture standard containing 100 and 500 ppm Mo and (b) for UMo alloy standard containing 500 and 5000 ppm Mo. 68
- Fig. 3.4** XRD patterns of UO₂ and MoO₃ mixture recorded after (a) 1/2, (b) 1, (c) 1 1/2, and (d) 2 h of pyrohydrolysis. The downward arrow symbol indicates a few major peaks for MoO₃ 71
- Fig. 3.5** XRD patterns of (a) UMoO₆ powder and (b) U₃O₈ formed after pyrohydrolysis of UMoO₆ (all peaks are characteristic to U₃O₈): carrier gas, moist O₂; time, 2 1/2 h; temperature, 1273K. (c) The picture of UMoO₆ before and after pyrohydrolysis. 73

- Fig. 4.1** Pyrohydrolysis of U-6%Zr sample. (Conditions: 900⁰C moist Ar) 85
- Fig. 4.2** XRD patterns of pyrohydrolysed products of U-Zr alloy heated in moist Ar atmosphere at 900⁰C for (a) 10 min., (b) 30 min., (c) 50 min. and (d) 90 min. (o and * represent UO₂ and α -U₃O₈, respectively). 87
- Fig. 4.3** TG and DTA of U-Zr alloy in dry air with a heating rate of 10⁰C/min 90
- Fig. 4.4** XRD patterns of pyrohydrolysed product of (a) U-Zr and (b) U-Pu-Zr alloy heated in moist oxygen atmosphere at 900⁰C for 30 min. (* and # represent (α -U₃O₈)_{ss} and (PuO₂)_{ss}, respectively) 92
- Fig. 4.5** Chromatograms for different distillates analysed by IC. (a) standard solution, (b) blank run, (c) U₃O₈ standard (d) U-Zr sample and (e) U-Pu-Zr samples. 94
- Fig. 5.1** A standard sample chromatogram. Peaks 1–7 are (1) Li (2 mg/L), (2) Na (2 mg/L), (3) NH₄⁺, (4) K (5 mg/L), (5) Cs (5 mg/L), (6) Mg (3 mg/L) and (7) Ca (5 mg/L). Column: Ion Pac CS12; Eluent: 20 mM MSA; Flow rate 1 ml/min. 102

- Fig. 5.2** A typical sample chromatogram obtained for a sampleColumn: Ion Pac CS12; Eluent: 20 mM MSA. Flow rate 1mL/min. Detection Suppressed Conductivity. 103
- Fig. 5.3** Capillary 50 μm (i.d.) 9 60 cm (total length), BGE 20 mM Imidazole pH 2 Sample: (K, Na, Ca, Mg, Li) Li 1 mg/L others 0.5 mg/L. 105
- Fig. 5.4** Capillary 50 μm (i.d.) and 60 cm (total length), BGE 20 mM Imidazole pH 2, Sample: (real sample having 2.1 mg/L Li) 106
- Fig. 5.5** Calibration plot of peak area/peak time versus Li concentration. 106
- Fig. 6.1** Electropherograms obtained for a standard iron solution ($25 \text{ mg}\cdot\text{L}^{-1}$) with BGEs of different pH. 116
- Fig. 6.2** Effect of total chloride concentration on the peak area of iron obtained with pH 2. (BGEs were of 10⁻² M HCl(fixed) and varying amounts of KCl). Capillary: 60 cm \times 50 μm , Applied voltage: 15 kV; Detection: direct UV at 214nm. 118
- Fig. 6.3** .Electropherograms obtained for a standard solution of Fe(III) and Uranium. (A) Fe(III) (5 $\mu\text{g}/\text{mL}$) + U(VI) (80,000 $\mu\text{g}/\text{mL}$) standard solution; (B) Fe(III) standard solution (1 $\mu\text{g}/\text{mL}$); (C) Fe(III) (0.08 $\mu\text{g}/\text{mL}$) standard 120

solution. BGE: 10 mM HCl in 65 mM KCl (pH 2),
Conditions: Capillary: 60 cm × 50 μm, Applied voltage:
15 kV. Detection: direct UV at 214 nm.

- Fig. 6.4** A typical electropherogram obtained for a sample solution. 124
- Fig.7.1** Effect of [NaOH] on the retention times of various anions. 134
(a) IonPac AS18 column and (b) IonPac AS16 column.
- Fig.7.2** Standard chromatograms obtained for standard with F⁻, Cl⁻, NO₃⁻ and SO₄²⁻ (10.0 ppm each). (a) Column: AS16 column, Eluent: 15 mM NaOH. (b) Column: AS18 column, Eluent: 40 mM NaOH. 135
- Fig.7.3** The optimised reuse of LiOH washing solution. A, B, C, and D are different Li₂TiO₃ lots, the numbers 1, 2, 3 represent no. of washing. The washing solution containing lower impurity are reused for samples containing higher impurities 137
- Fig.7.4** Concentration of chloride and nitrate in wash solutions collected at different steps of optimised washing 137

method.

- Fig.7.5** Chromatograms obtained for the Li_2TiO_3 pyrohydrolysis distillates (a) before washing (initial product) (b) after washing. 138
- Fig.8.1** (a) Peak height of molybdatepeak(20ppm) (b) retention time of anions; Column: IC-Pak anion, Eluent: NaHCO_3 (0.01755M) and d-mannitol (concentration varied), flow rate 1 ml/min. 147
- Fig.8.2** (a) Peak height of molybdatepeak(20ppm) (b) retention time of anions; Column: Ion Pac AS16, Eluent: NaHCO_3 (0.01755M) and d-mannitol (concentration varied), flow rate 1 ml/min. 149
- Fig.8.3** Retention time of anions; Column: Ion Pac AS16, Eluent: NaOH (30mM) and d-mannitol (concentration varied), flow rate 1 ml/min. 150

Fig.8.4 (a) Peak height of molybdate peak (5ppm); No separation Column, Eluent: NaOH(30mM) and d-mannitol (concentration varied), flow rate:0.1ml/min. 151

Fig.8.5 Retention time of anions; Column: Ion Pac AS16, Eluent: NaOH(30mM) and boric acid(concentration varied), flow rate 1 ml/min. 153

List of Tables

Table.1.1	Different ceramic fuels and their composition used for Indian nuclear reactors.	6
Table.1.2	Breeding ratio and doubling time comparison of different nuclear fuels.	8
Table.1.3	Specification limits of metallics for thermal and fast reactor fuels.	14
Table.1.4	Specifications for non metallics.	20
Table.3.1	Minimum Time Required for Recovery of Mo Better than 95%, from Alloy and Oxide Standards.	69
Table.3.2	Comparison of results obtained for ADU Samples by the Developed Method, Solvent Extraction Followed by ICP-AES, and Pyrohydrolysis followed by ICP-AES Methods.	76
Table.4.1	Chemical analysis of U, Pu and Zr from U-Zr and U-Pu-Zr alloy.	84
Table.4.2	The summary of products identified by XRD on heat	88

	treatment of U-Zr alloy.	
Table.4.3	Pyrohydrolysis data for U-6wt%Zr alloys sample for varying time using moist oxygen as a carrier gas.	89
Table.4.4	Pyrohydrolysis data for U-19 wt% Pu-4.7 wt% Zr alloyssample for varying pyrohydrolysis time, with moist oxygen as carrier gas.	91
Table.4.5	The summary of products identified by XRD on heat treatment of U-Zr and U-Pu-Zr alloys.	92
Table.4.6	F and Cl content of some routine samples analysed by pyrohydrolysis using moist oxygen.	94
Table.5.1	Comparison of Li percentage determined by CE and IC in Li-Al alloy samples.	107
Table.6.1	Recoveries of spiked iron in uranium solutions of various concentrations.	121
Table.6.2	Comparison between iron determination via the developed method and certified method.	123
Table.6.3	Results obtained for the samples.	124

Table.7.1	chlorine obtained for real samples of Li_2TiO_3 finished products.	139
Table.8.1	The optimized gradient elution program for simultaneous separation and determination of B, Cl and Mo. Column: Ion Pac AS16, flow rate 1 ml/min.	155
Table.8.2	The concentration of B, Cl and Mo obtained in dried plant samples and Soil PH distillates by the developed IC method and their comparison with conventional methods.	156

Chapter: 1

Introduction

1.1 Basics of nuclear energy:

Nuclear energy is produced either by nuclear fission or nuclear fusion. In practice the nuclear energy or power is generated by carrying out nuclear fission in a nuclear reactor. The nuclear fuel materials have fissile isotopes such as ^{235}U , ^{233}U and ^{239}Pu . [1, 2]. Nuclear fuels contain both fissile and fertile isotopes, which on interaction with neutrons undergo fission. In every fission process two or three neutrons are produced and they help the self-sustaining chain reaction which releases energy with a controlled rate in a nuclear reactor. ^{235}U and ^{239}Pu are the commonly used fissile isotopes in nuclear reactors. Among the uranium isotopes ^{235}U is a naturally available fissile material whereas it's another fissile isotope, ^{233}U is not available in nature. ^{233}U is obtained by the neutron irradiation of thorium (Th) in a nuclear reactor. Thorium nuclei absorb neutrons and get converted into ^{233}U . Plutonium (^{239}Pu), another fissile material formed due to the irradiation of ^{238}U with neutrons. Thus ^{238}U and ^{232}Th are also valuable nuclear resources, and are called fertile materials, [3-6] as they can be converted into fissile material for fuelling nuclear reactors.

1.2 Indian Nuclear Program:

Nuclear Energy is an important and perhaps inevitable option for the country for its energy security in the long run. Nuclear energy is needed not only for producing electricity but also for meeting non-electricity energy needs. In comparison to other fossil fuels, nuclear power requires less quantities of fuel. No other source of energy

can produce such an amount of power from a very small quantity of material [7,8]. Moreover it is also a green source of energy. To utilise the large abundant of thorium in India, Dr. Homi J. Bhabha envisaged a three-stage Indian nuclear power program in 1954 [9-11].

Stage 1: In the first stage natural uranium is used in pressurized heavy water reactors (PHWR) to produce electricity and ^{239}Pu . PHWR uses natural uranium as fuel and heavy water as moderator and coolant. Plutonium produced is separated from the spent fuel in plutonium reprocessing plants.

Stage 2: The second stage deals with the fast reactor technology. In the second stage the plutonium obtained from the first stage is mixed with uranium (as a mixed-oxide (MOX) or as metallic fuel) and used in the Fast Breeder Reactors. The fast breeder reactors will fission plutonium for power and breed more plutonium from the ^{238}U . Thorium will also be used in the reactor to produce ^{233}U .

Stage 3: The third stage of Indian nuclear programme envisages utilisation of thorium in place of uranium for power generation. Advanced heavy water reactors (AHWR) will be used in this stage. Power will be generated from the ^{232}Th - ^{233}U fuel aided by plutonium. Currently this stage is still in the research stage [12]. Bhabha Atomic Research Centre is developing an advance heavy water reactor that will use both thorium ^{233}U and thorium-plutonium mixed oxide as fuel.

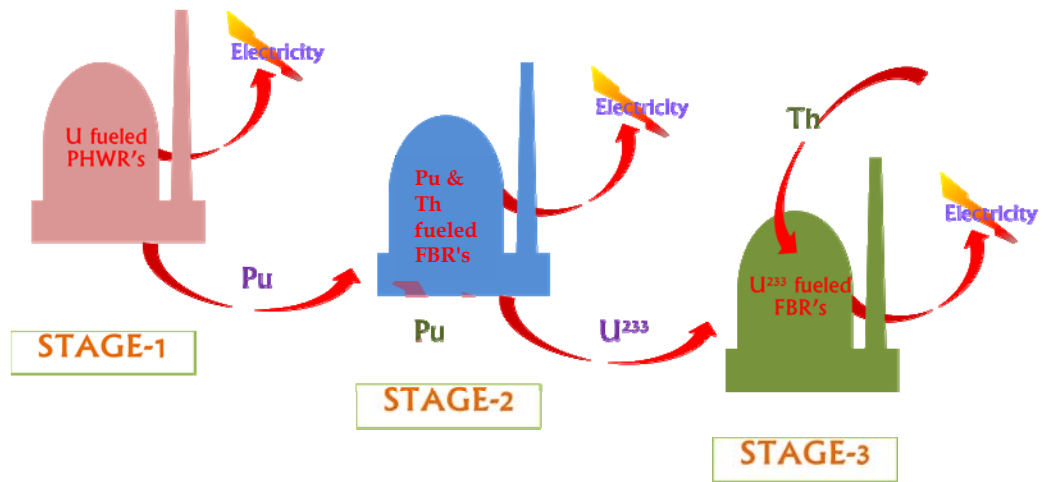


Figure 1.1: Indian three stage nuclear program

1.2.1 Nuclear fuel cycle:

The nuclear fuel cycle consists of mining, separation, refining, purifying, utilising as fuel and ultimately disposing of the nuclear waste generated. The nuclear fuel cycle, include a series of stages through which nuclear fuel progresses. The nuclear fuel cycle is divided into two parts namely front end and back end. The front end of the fuel cycle deals with all the processes (right from mining to fabrication) that are involved before the use of fuel in the reactor. The back end fuel cycle consists of reprocessing of the spent fuel and recovery procedures. If spent fuel is not reprocessed, the fuel cycle is referred to as an open fuel cycle (or a once-through fuel cycle); if the spent fuel is reprocessed, it is referred to as a closed fuel cycle [13, 14]. India is following close end fuel cycle [15] and following are the various processes. Figure 1.2 depicts the close end fuel cycle that India follows.

- (i) Uranium extraction from uranium ore, and conversion to yellowcake
- (ii) Conversion of yellow cake into uranium hexafluoride (UF₆)
- (iii) Enrichment to increase the concentration of U²³⁵ in UF₆

- (iv) Fuel fabrication to convert enriched UF_6 into fuel for nuclear reactors
- (v) Use of the fuel in reactors
- (vi) Interim storage of spent nuclear fuel
- (vii) Reprocessing (or recycling) of high-level waste
- (viii) Final disposal of high level waste.

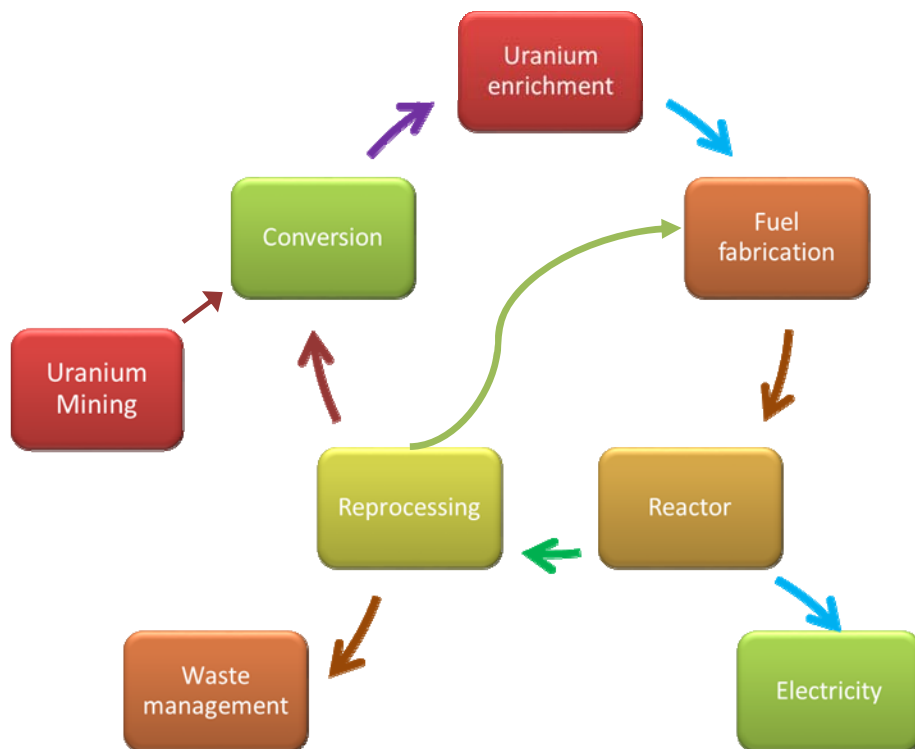


Figure 1.2: Nuclear fuel cycle

1.2.2 Types of nuclear fuels:

Typically, depending on the nature of nuclear reactor, different types of fuels are used. These are classified as, (i) ceramic fuels (ii) intermetallic fuels (iii) metallic fuels (iv) composite fuels and (v) advance fuels.

(i) Ceramic Fuels: The ceramic fuels are categorised into oxide and non- oxide ceramic fuels. The oxide fuels are oxides of U, Pu and mixed oxides of U and Pu (eg. UO_2 , and $(\text{U,Pu})\text{O}_2$) whereas the materials like $(\text{U,Pu})\text{C}$ and $(\text{U,Pu})\text{N}$ are known as non-oxide ceramic fuels.

Uranium oxide and mixed oxide fuels: Natural UO_2 is used as fuel in PHWR which uses heavy water as coolant and moderator. The boiling water reactor (BWR) and pressurised water reactor (PWR) use light water as coolant and moderator. As light water (H_2O) has somewhat higher absorption cross section for thermal neutrons, to compensate for their loss, UO_2 with some enrichment (up to 3% U-235 as against natural abundance of 0.72%) is employed. MOX fuels with 0.4% and 4% Pu are also being tested in combination with UO_2 in PHWR and BWR, respectively to realise higher energy output without significant changes in the reactor design.

The oxide fuels are chemically stable and compatible with water. They also show high temperature and high irradiation resistance. In addition to this, India has expertise on the fabrication of oxide fuel and complete knowledge on the oxide fuel performance in the reactor. Due to the above advantages of the oxide fuels and their compatibility with liquid Na, MOX fuels are the preferred choice for FBRs [16-18]. The proposed AHWR reactor designed for Th utilization will be using mixed oxide fuels of U, Pu and Th. Table 1.1 lists out the use of different ceramic fuels in various Indian nuclear reactors.

Table1.1: Different ceramic fuels and their composition used for Indian nuclear reactors.

Reactor	PHWR	BWR	PFBR	FBTR
Fuel composition	0.4%PuO ₂ (inside 7 pins)	UO ₂ of different enrichment,	(U _{0.79} Pu _{0.21})O ₂ (Inside)	(U _{0.3} Pu _{0.7})C (MKI)
	Nat.UO ₂ (outside 12 pins)	Low 0.9%	(U _{0.72} Pu _{0.28})O ₂ (outside)	(U _{0.45} Pu _{0.55})C (MKII)
		Med 1.55%		
		High 3.25%		

Non-oxide ceramic fuels (Carbide and Nitride): The non-oxide ceramic fuels have certain advantages such as better thermal conductivity, denser fissile content and better breeding ratio over the oxide fuels. The Fast breeder test reactor at Kalpakkam utilises the mixed carbides of U and Pu, (U,Pu)C, as fuel [19]. Since the FBTR core is smaller in size it requires fuel with high fissile content, mixed carbide fuel, it was considered for FBTR. However, due to their pyrophoric nature, their handling and fabrication call for enhanced safety requirements.

(ii) Intermetallic fuels: Uranium intermetallic fuels such as U–Al, U–Si, and U–Mo are mainly used in research and test reactors for neutron production [20, 21]. As compared to ceramic fuels intermetallic fuels can achieve higher densities thereby requiring lower fuel inventories. APSARA research reactor at Bhabha Atomic Research Centre was using U-Al based intermetallic fuel which is now modified to U-Si based intermetallic fuel to reduce the U enrichment requirements.

(iii) Composite fuels: Composite fuels consist of a fissile element phase dispersed in an inert matrix [22]. Composite fuels are of two types; cermet fuels and cercer fuels. Cermet fuels consist of ceramic fuel particles dispersed in a metallic matrix whereas the Cer-cer fuels consist of ceramic fuel particles dispersed in a ceramic matrix [23]. Cermet fuel cores are most often metallurgically bonded to the cladding material to improve heat transfer from the fuel core to the coolant. The composite fuels are generally considered for the research and test reactors, however, due to the higher fissile density, better thermal conductivity and possibility of improving breeding ratio these fuels are also being considered for fast breeder reactors. These fuels are also being considered for irradiation and power production from plutonium and minor actinides.

Metallic fuel: Metallic fuels have higher densities of fissile and fertile materials and high thermal conductivity. They are capable of providing high breeding ratio. Hence, they are considered to be suitable for fast reactors [24-27]. Table 1.2 gives a summary of some metallic fuels and their breeding ratio and doubling time. Metallic fuels are known to cause problems due to high swelling. Such problems were circumvented by reducing the fuel smear density to ~ 75% and by fission gas release before fuel-cladding contact. Mechanically bonded U-Pu binary fuels as well as sodium bonded U-Pu-Zr alloys (figure 1.3) are being considered as the most suitable metallic fuel compositions due to their solidus temperatures and compatibility with stainless steels. The spent metallic fuels can be reprocessed by pyro-process recycling method, which was economically more attractive than the PUREX method of reprocessing. Few metallic fuels were put into FBTR for test purposes and also to understand their behavior. It is expected that India would go for its fast reactor

program based on metallic fuels in future to achieve significant growth in nuclear power.

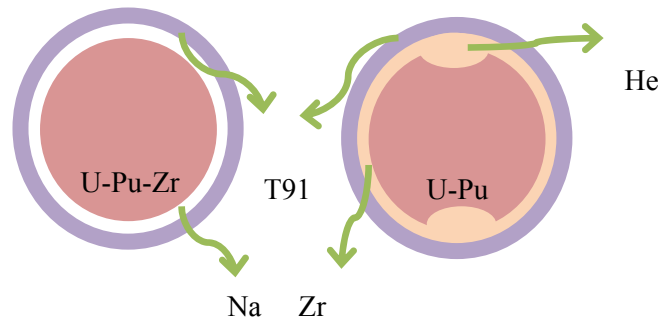


Figure 1.3: Metallic fuels designed for FBR.

Table 1.2: Breeding ratio and doubling time comparison of different nuclear fuels.

Fuel Material	U-Pu Oxide	U-Pu Carbide	U-Pu-10% Zr	U-Pu-6% Zr	U-Pu with 150 μ Zr liner
Breeding Ratio	1.09	1.19	1.36	1.47	1.56
Doubling time (y)	40	20	9.4	7.2	7

1.2.3 Fusion Energy:

Fusion can provide large amounts of energy and does not cause any adverse effects on the environment. One of the most prominent nuclear fusion reactions is that between deuterium and tritium. The former can be obtained from the seawater whereas the latter is obtained by the neutron irradiation of lithium blanket material. Further, a fusion reactor will produce only short lived radioactive waste products [28, 29].

During the fusion of deuterium and tritium an alpha particle is produced with a high energy neutron (figure 1.4). Moreover, this fusion requires low activation energy and thus low temperature as compared to other nuclear fusion reactions between H and T or H and D.

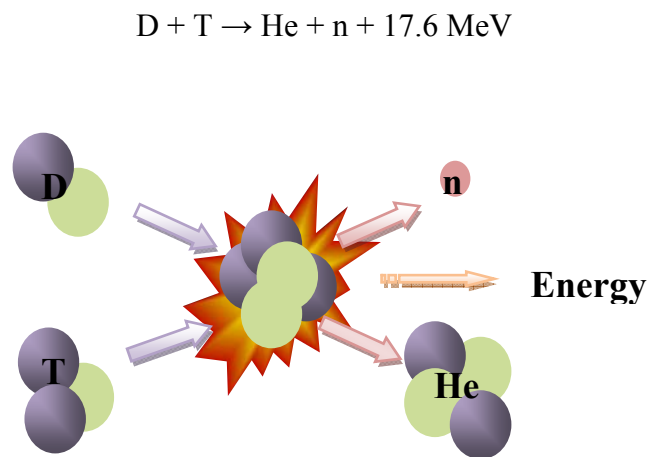


Figure1.4: Fusion Reaction using deuterium and tritium.

The International Thermonuclear Experimental Reactor (ITER) is envisaged with a view to demonstrate the possibility of generating electricity by fusion reaction. India is one of the participating countries in the ITER project financially and scientifically. Nuclear fusion research in India is primarily carried out in BARC and Institute of Plasma Research (IPR). Many research programmes are being pursued to develop Test Blanket Modules (TBM) in order to demonstrate the production and extraction of tritium [30-33]. ITER will be using lithium compounds for tritium breeding. Among the solid lithium compounds the ceramic matrices are preferred due to their more favourable physical characteristics in intense neutron fluxes and at high temperatures [34-36]. Lithium-containing ceramics such as Li_2O , LiAlO_2 , Li_4SiO_4 , Li_2ZrO_3 and Li_2TiO_3 have been considered as candidates for tritium breeding materials. The tritium breeder blanket serves two primary functions in the fusion reactor. One is breeding tritium and the second is converting the released energy into heat. Both the functions are very important for the successful operation of a fusion power reactor. The breeder materials should:

1. breed and release tritium,
2. possess physical and chemical stability at high temperature,
3. display compatibility with other blanket components, and
4. exhibit adequate irradiation behaviour. Studies revealed that Li_2TiO_3 is the most preferred material for TBM and therefore, it was developed and fabricated at BARC [37, 38].

1.2.4 Chemistry in nuclear fuel cycle:

Optimum utilization of fissile content in the nuclear fuels during reactor operation can result in increasing power production. Improving the fuel quality is one of the criteria to ensure longer residence time of fuel in the reactor. This in turn results in higher burn-up leading to enhanced power. Reactor physicists and fuel fabricators stipulate certain quality (specifications) to the nuclear fuel and other reactor materials for this purpose. In order to realise the smooth and efficient functioning of the reactor, the fuel should satisfy the specifications derived for it. The specification includes both physical and chemical qualities of the material. The chemical analyses pertaining to the Chemical Quality Control (CQC) process play a pivotal role in achieving the quality of the nuclear material fabricated into nuclear fuel. In addition to the nuclear fuels, strategically important nuclear materials like tritium generators [39] etc., also require determination of percentage and trace level components for their optimum performance during reactor irradiation. As India is involved in the International Test Experimental Reactor (ITER) project (a fusion based reactor programme) and DAE supports this programme by fabricating tritium breeders (Li_2TiO_3) employing different methods [38], the requirement for development of analytical methods for the analysis of tritium breeders for their chemical characterization need not be over emphasized.

Several analytical techniques are employed for the chemical characterization or CQC analysis of nuclear materials [40]. Among them, elemental determinators, ICP-AES [41], ICP-MS [42, 43], TIMS [44], alpha and gamma spectrometry [45, 46], XRD [47], electro analytical techniques, spectrophotometer etc. are some of the important techniques routinely employed for chemical characterisation analysis. In the recent past chromatographic techniques like High Pressure Liquid

Chromatography (HPLC) and Ion Chromatography (IC) have been introduced into the CQC analyses of nuclear materials [48]. Some of the techniques used for CQC measurements are described below:

1.2.4.1 Determination of major elements: Electroanalytical techniques are mainly used for the determination of U and Pu in nuclear fuel materials. The electroanalytical methods are capable of analysing the fuel samples with a precision better than 0.2 % [49, 50]. Complexometric titration using EDTA is employed for the determination of thorium in the Th containing fuels [51, 52]. Determination of Zr in metallic fuels is mainly carried out by gravimetric methods, where Zr is selectively precipitated as its mandelate complex in hydrochloric acid medium [53].

(i) Determination of metallic impurities: Every fuel has a list of specifications for different elements and other parameters with a view to achieve better performance of the fuel as well as to ensure the safe operation of the nuclear reactor. Table 1.3 lists out the specifications for metallic impurities for a variety of fuel materials meant for both thermal and fast reactors.

Atomic Emission Spectroscopy (AES):

DC Arc-AES: Analyses of metallics in the uranium containing fuels are being carried out by converting the uranium into U_3O_8 form. Subsequently a known amount of the sample is mixed with a carrier and loaded to a graphite electrode. The electrode is excited in a DC arc and its emission spectrum is recorded. Solid samples are analysed by using D. C. Arc as an excitation source [54, 55]. However D.C.-Arc method suffers from certain limitations including its poor precision. In the case of Pu bearing materials, a sample mixture of 100 mg (total) was prepared by mixing 5% AgCl, 35% Pu and pure U_3O_8 contributes the rest. While analysing the

plutonium carbide or mixed carbide fuels it is necessary to convert them into their oxide form prior to the analysis. D.C.-Arc method is useful in analysing a group of metallics which includes, Al, Be, Ca, Cd, Co, Cr, Cu, Fe, Li, Mg, Mn, Mo, Na, Ni, Pb, Si, Sn, Ta, V, W and Zn. Their limits of detection are in the range of 0.1 ppm to 100 ppm in nuclear materials. The technique requires precise matching of standard and samples to achieve better accuracy.

Table 1.3: Specification limits of metallics for thermal and fast reactor fuels.

Impurity	Thermal Reactors (ppm _w)			Fast Reactors (ppm _w)		
	UO ₂	PuO ₂	(U,Pu)O ₂	UO ₂	PuO ₂	(U,Pu)O ₂
Ag	1	10	25	1	10	25
Al	25	250	400	25	250	500
B	0.3	2	1	0.3	2	2
Be						10
Ca	50	500	250	50	500	100
Cd	0.2	6	1	0.2	6	1
Co		25	75		25	200
Cr	25	200	400	15	200	300
Cu	20	50	400	10	50	100
Fe	100	500	400	100	500	1000

Gd	0.1	1	1	0.1	1	
Mg	50	200	200	10	200	50
Mn	10	100	400	10	100	200
Mo	4	200	400	2	200	200
Na			400			100
Ni	20	200	400	20	200	500
Pb		200	400		200	200
Sn						10
V			400			100
W					200	200
Zn		200	400		200	100
Zr					100	

ICP-AES: This technique has good sensitivity and also capable of analysing the refractive matrices. In the case of ICP-AES analysis of nuclear fuels require pre-separation of matrix element(s) [56-58]. The chemical separation is carried out mainly by solvent extraction as it provides faster separation. Ion exchange separation is also used in some cases. Elements like Sm, Eu, Gd, and Dy have stringent specifications in the fuels and these elements can be determined with a precision better than 10% at 0.1 ppm. Although this technique is used for the determination of all metallic impurities, it is not recommended for some elements

like Mo, W etc. as they are expected to be lost partially during dissolution of the fuel samples. The use of chemical separation procedures can lead to possibility of contamination and loss of few analytes like Si, W, Sn, Mo etc.

Atomic Absorption Spectroscopy (AAS): AAS is an element specific technique and it requires a characteristic radiation source and a source to atomise the analyte. Atomisation can be achieved by using a flame or Electro Thermal Atomization (ETA). It is possible to analyse solid samples in ETA-AAS with better sensitivity [59]. Determination of all the metal impurities in AAS is a slower process and hence, one element is analysed at a time. Like atomic emission spectroscopy methods, AAS also requires prior separation of matrix element(s). The uranium containing fuels are analysed after the separation of uranium by solvent extraction with tributylphosphate (TBP) in HNO_3 . ETA-AAS based methods have been developed for the analysis of Ag, Al, Ca, Cd, Co, Cr, Cu, Fe, Li, Mg, Mn, Na, Ni, Pb, Sb, Sn, and Zn in variety of nuclear materials. Compared to the D.C.Arc.-AES, the atomic absorption procedure, though longer, provides better sensitivity and precision.

ICP-MS: ICP-MS is one of the versatile analytical tools for carrying out trace and ultra-trace level analysis. It is a rapid and highly sensitive technique [60]. ICP-MS provides quantitative determination as well as isotopic ratios or composition. Therefore, it is possible to detect the isotopes that unnatural isotope abundances. Along with the multi-elemental capability it has very low limit of detection (LOD) i.e. in the range of 1-10 ppt. ICP-MS gives a precision of 5% or better at the concentration of ppb level, however, at time the method suffers from isobaric interferences and memory effects. One of the limitations of ICPMS analysis is that the dissolved solids in the sample solutions should not be more than 0.4%, and this

demands rigorous sample preparation procedure to the samples of low dissolved contents that are amenable to the ICP-MS analysis. ICP-MS coupled with laser ablation source is a good choice for the solid sample analysis.

Total Reflection X-ray Fluorescence (TXRF): TXRF, an advanced variant of Energy Dispersive X-ray Fluorescence (EDXRF) is a comparatively new technique of material characterization [61]. The geometrical improvements in TXRF help in achieving better detection in comparison to that of EDXRF. It has multi-elemental capability and can analyse most of the elements above $Z=11$. The LOD for the technique is relatively higher (in ppm range) as compared to AES, MS and AAS techniques. Therefore trace impurities present in ppm and above concentration range only can be quantified. The precision of measurements is up to 5%.

Nuclear analytical techniques: In nuclear analytical techniques the material under analysis is subjected to a nuclear reaction by irradiating them with either neutrons or protons followed by the measurement of emitted gamma energy. This technique is widely employed in the characterisation of many nuclear materials such as, zircalloys, stainless steels, Ni alloys, high purity aluminium and graphite and uranium oxide, U-Th mixed oxides, uranium ores and minerals etc. Instrumental neutron activation analysis (INAA) uses neutrons generated in the reactor and is a good technique for medium and high Z elements. Hence, it finds useful in the determination of trace metallic impurities. The detection limit for the method varies from ppb to ppm range depending upon the matrix being analysed. It is a non-destructive direct solid sample analysis technique and provides a good precision up to 1% [62, 63]. However requirement of reactor as the neutron source is one of the set back of the technique that restricts its use.

Spectrophotometry: Spectrophotometry is a simple and economically viable technique for the determination of many metallic and their species. Due to the availability of several multi-elemental techniques with good precision and sensitivity, spectrophotometry is less commonly used. However, it is widely used for the elemental specific analyses where the other workhorse techniques fail. The detection limits (LOD) for many methods lay in the ppb to ppm range. Interferences are the common problems with spectrophotometric methods and therefore, they require suitable masking reagents or other procedures to circumvent the interferences.

1.2.4.2 Isotopic composition analysis:

Isotopic composition of several elements in nuclear fuels and other nuclear materials are being carried out by thermal ionisation mass spectrometry (TIMS) [64, 65]. The isotopic composition of uranium and plutonium are analysed for every fuel material to ascertain the fissile element(s) content(s). Other important nuclear materials like boron, cadmium, gadolinium, zirconium, heavy water etc. are also analysed for the isotopic composition. In the case of plutonium and uranium, analytical methods based on gamma spectroscopy are also available for determining isotopic composition.

1.2.4.3 Determination of Non-metallics: Analyses of carbon, nitrogen, phosphorus, sulphur, chlorine, fluorine, hydrogen, moisture, total gas content etc. are some of non-metallic analyses. Quantification of carbon is based on the combustion method wherein the C present in the sample is converted into CO₂ at 1273K in a graphite or alumina crucible using copper or tungsten as an accelerator in presence of oxygen flow. The CO₂ thus formed is purified and detected by thermal conductivity or

infrared (IR) detection [66]. The oxygen present in the fuel is determined by inert gas fusion method. Sample is fused at 2773K in He/Ar flow in graphite crucible. The oxygen present in the sample forms CO which is determined by IR [67]. Nitrogen present in the sample can be determined by the inert gas fusion or Kjeldahl distillation methods [68]. In fusion method sample is fused in graphite crucible at 2773K. N₂ thus produced in the process is purified and determined by thermal conductivity measurements. Hydrogen is also determined by inert gas fusion method where the fusion is carried out at lower temperature of 2273K without any flux. After purification and separation using a GC column, hydrogen is determined by thermal conductivity [69]. Sulphur is determined by combustion to form SO₂, followed by IR detection or by a mass spectrometer [70].

Chlorine and fluorine in the samples are determined by a two-step method. The halides were separated by pyrohydrolysis technique followed by their quantification using spectrophotometry or ion chromatography [71]. During the pyrohydrolysis separation the solid sample is subjected to action of heat and moisture simultaneously in presence of a carrier gas. This converts the F and Cl into HF and HCl, respectively and they are trapped in a dilute NaOH solution. Pyrohydrolysis is the only separation technique available for separating chlorine and fluorine in low concentrations. Dissolution of samples using acids or fusion methods are not useful in determining the halides as the reagents contribute significant amount of these halides leading to introduction of high blank. Ion chromatography is being employed for the routine analysis of Cl and F in the fuels as the concentration of these halides normally found to be less than 10 ppm. Although a few nuclear analytical techniques have been reported for the determination of Cl and F in several nuclear materials, they do not find much use in the routine CQC measurements.

Boron, a non-metal, is included in the list of metallic impurities. The concentration of boron in the nuclear materials is often determined by D.C.Arc-AES method along with other metallic impurities. Alternatively, selective separation of boron using diols followed by spectrophotometric determination with curcumin as chromogenic agent is a sensitive method [72]. Nuclear analytical methods were also reported for the determination of boron in different matrices. Boron in many nuclear and other materials (solid samples) can be separated by pyrohydrolysis and trapped as boric acid in dilute NaOH [73]. The pyrohydrolysis distillate thus obtained can be analysed for boron content by IC, ICP-MS, ICP-AES, AAS and spectrophotometer. Table 1.4 lists the specification limits of non-metallics in several nuclear fuel materials.

Table 1.4: Specifications for non metallics.

Elements	UO ₂	PuO ₂	(U,Pu)O ₂	(U,Pu)O ₂	(U,Pu)C	(U,Pu)C	
			(Thermal)	(Fast)	(Mark-1)	(Mark-2)	
O/M			1.98-2.02	1.98 ± 0.002)	± 1.025	± 1.025	±
C/M				0.02	0.005	0.005	
M ₂ C ₃					5-20%	5-20%	
C	150 ppm	200 ppm	200 ppm	300 ppm	(4.8± 0.25)%	(4.8± 0.25)%	
N	200 ppm	200 ppm	100 ppm	200 ppm			

O					6500 ppm	5000 ppm
O+N					7500 ppm	6500 ppm
H		1 ppm	3 ppm			
S	300	300	50 ppm			
	ppm	ppm				
Cl	25 ppm	50 ppm	15 ppm	25 ppm	25 ppm	25 ppm
F	25 ppm	25 ppm	10 ppm	25 ppm	25 ppm	25 ppm
H₂O	5000		10 ppm	30 ppm		
	ppm					
B	10 ppm	10 ppm	1 ppm	3 ppm	4.5 ppm	4.5 ppm
B. Eq.		2 ppm	5.5 ppm	5.5 ppm	5.5 ppm	5.5 ppm

1.2.5 Scope of Present Investigations:

The CQC processes of various nuclear materials as mentioned above demand the development of new analytical methodologies. Improvement in the existing methodologies is also desirable for realizing higher accuracy and precision, low detection limit, high selectivity, simultaneous or multi-elemental analysis, minimum generation of analytical waste and minimum use of chemical reagents etc.

Analytical methods which can analyse directly the dissolved sample solutions are preferred as they eliminate the cumbersome sample preparation procedures. Few applications of CE and IC, where direct analysis of the dissolved sample solution

without employing matrix separation have been reported in literature [74, 75]. Such direct analyses not only avoid the pre-separation of matrix or pre-concentration of analytes but also useful in the absence of reference materials.

As discussed in the preceding sections that spectrometric techniques like AES, ICP-MS, AAS etc. have been used for the material characterisation analysis on routine basis. Electro-analytical techniques also find immense applications in the analysis of major components. However these methods sometime suffer from several limitations such as interferences, poor sensitivity, labour-intensive sample preparations etc. Chromatography methods offer simultaneous separation as well as quantification and therefore, chromatography techniques like ion chromatography, HPLC etc. are being introduced in the chemical characterisation analysis. Ion chromatography is a useful technique for the determination of common anions and cations whereas reversed phase ion interaction chromatography is used for the separation and determination of both transition and inner transition elements [76-79]. Moreover, the chromatography separations can be used for the speciation studies. For example chromatography methods can distinguish different metal oxidation states, such as Cr(III) and Cr(VI) and also Fe(II) and Fe(III) [80,81]. Different methods for the use of IC in nuclear industry have been reported in literature. Separation of fission products, trace impurities, lanthanides along with different actinides are some of them to be mentioned [82, 83] where ICP-MS was used as the detector. IC coupled to scintillation detector has also been used for alpha active actinide separation and determination [84, 85]. Ion interaction chromatography (IIC) has been used for determination of lanthanides, uranium, thorium and plutonium in irradiated fuel samples [86]. IC has been significantly contributing in analysing the distillates

obtained from pyrohydrolysis of fuel samples [73] for boron and halides. However considering the ability of the method its full potential has not been utilised.

Like ion chromatography, capillary electrophoresis (CE) is another technique which can be used for simultaneous separation and determination of cations and anions [87-90]. CE with indirect detection has been applied to the analysis of inorganic anions, cations, organic acids, alkali metals, amino acids, and nucleotides [91, 92]. Lanthanides, transition metal ions and alkali and alkali earth metals have been analysed in several materials [93-95]. However these methods have not been applied to the analysis of nuclear fuel or other nuclear materials. The method requires nano grams of sample injection, which can reduce radioactive waste significantly. One of the important advantages of the CE is it can be utilised for direct sample analysis without carrying out the matrix separation.

In spite of the unique features of IC and CE, not many applications were reported for the analysis of nuclear materials. Therefore, efforts have been made to utilise these techniques for nuclear material analysis independently and validate the results.

Pyrohydrolysis as a separation technique has found several applications like cement, soil, nanoparticles and nuclear material [96-99]. The term pyrohydrolysis was adopted to describe hydrolytic reactions whose equilibrium constants and higher reaction rates seem to be favoured at higher temperatures. During pyrohydrolysis the sample is heated at high temperature in presence of moist oxygen or a suitable carrier gas. Pyrohydrolysis finds many applications in the determination of halides at trace level concentrations in many complex matrices as it separates halides and boron directly from a solid matrix and provides an interference free clean distillate carrying out trace and ultra-trace level analysis [73,100]. Pyrohydrolysis has been

used to separate halides and B directly from a solid sample [73]. However the method has potential to be used for few other analytes specially metals. The simultaneous separation and determination of anions by IC is very special as similar sensitive and simultaneous analysis of anions is not possible with any other technique. Therefore Pyrohydrolysis and IC form a great combination and have significant potential for application in nuclear material sample analysis.

Analysis of halides and boron in environmental and plant samples involves tedious sample preparation procedures due to the presence of organic compounds. The analytical methods that have been developed for the analyses of nuclear materials involving initial pyrohydrolysis separation followed by analytical determinations can be extended for the analyses of environmental samples.

1.3 References:

1. N.M. A. Mohamed, A. Badawi, Prog. Nucl. Energy, 91, (2016)49.
2. B. R. T. Frost, R. Inst. Chem., Rev., 2(1969)163.
3. M. Jacoby, Chemical and Engineering News, 93(2015)44.
4. K. Anantharaman, V. Shivakumar, D. Saha, J. Nucl. Mater., 383(2008)119.
5. H. M. Mattys, Actinides Rev.,1(1968) 165.
6. J. F. Schumar, J. Nucl. Mater., 100 (I 98 I) 3 1.
7. B. W. Brook, A. Alonso, D. A. Meneley, J. Misak, T.Blees, J. B. van Erp, Sustainable Mater. Technol., 1 (2014)8.
8. F. Javidkia, M. Hashemi-Tilehnoee, V. Zabihi, Journal of Energy and Power Engineering, 5 (2011) 811.
9. A. Gopalakrishnan, Annual Review of Energy and the Environment, 27(2002)369.

10. R. Tongia, V. S. Arunachalam, *Current Science*, 75(1998)549.
11. P.K. Vasudev, *Electrical India*, 54(2014) 28.
12. A. Kakodkar, R.K. Sinha, M.L. Dhawan, IAEA-SM-353/54.
13. F. A. Settle, *J. Chem. Educ.*, 86 (2009)316.
14. R. C. Ewing, *MRS Bulletin*, 33(2008)338
15. Nuclear Fuel Cycle, <http://www.dae.nic.in>
16. H. Stehle, *J. Nucl. Mater.*, 153(1988)3.
17. K. Konno, T. Hirosawa, *J. Nucl. Sci. Technol.*, 39(2002)771.
18. G. A. Timofeev, V. Ya. Gabeskiria, G. A. Simakin, V. B. Mishenev, et. al. *J. Radioanal. Nucl. Chem.*, 51(1979) 377.
19. U. Basak, P.S. Kutty, S. Mishra, S.K. Sharma, et.al., *BARC News Letter*, 249(2003)191.
20. V.P. Sinha, G.P. Mishra, S. Pal, K.B. Khan, P.V. Hegde, G.J. Prasad, *J. Nucl. Mater.*, 383 (2008) 196.
21. V.P. Sinha, G. J. Prasad, P.V. Hegde, R. Keswani, C.B. Basak, S. Pal, G.P. Mishra, *J. Alloys Compd.* ,473 (2009) 238.
22. W. E. Lee, M. Gilbert, S. T. Murphy, R. W. Grimes, *J. Am. Chem. Soc.*, 96(2013)2005.
23. V. Troyanov, V. Popov, I. Baranaev, *Prog. Nucl. Energy*, 38(2001)267.
24. L. C. Walters, B. R. Seidel, J. Howard Kittel, *Nuclear Technology*, 65(1984) 179.
25. B. R. Seidel, L. C. Walters, Y. I. Chang, *JOM*, 39(1987)10.
26. T. Sofu, *Nucl. Eng. Technol.* 47(2015) 227.
27. G.J. Prasad, *BARC Newsletter*, 332(2013)v.

28. R. Murray, K. E. Holbert, Nuclear Energy: An Introduction to the Concepts, Systems, and Applications, Elsevier, 7th edition (2015)477.
29. T. J. Dolan, Nuclear Energy: Selected Entries from the Encyclopedia of Sustainability science and Technology, Springer (2012)305.
30. Editorial, Nature, 511(2014)383.
31. R. W. Conn, V. A. Chuyanov, N. Inoue, D. R. Sweetman, Scientific American, 266(1992)102.
32. Y. Shimomura, Phys. Plasmas 1 (1994) 1612.
33. John C. Wesley et. al. Phys. Plasmas 4(1997)2642.
34. G. Federici, C.H. Wu, A.R. Raffray, M.C. Billone, J. Nucl. Mater., 187(1992)1.
35. K. Tomabechi et. al., J. Nucl. Mater., 179(1991)1173.
36. Z. Wen, X. Wu, XiaogangXu, ZhonghuaGu, Fusion Eng. Des. 85(2010) 1551.
37. D. Mandal, M. R. K. Sheno, S. K. Ghosh, Fusion Eng. Des., 85(2010) 819.
38. T. V. VittalRao, Y.R. Bamankar, S. K. Mukerjee, S. K. Aggarwal, J. Nucl. Mater., 426(2013) 102.
39. Y. Shimomura, W. Spears, IEEE Transactions on Applied Superconductivity, 4(2)(2004)1369.
40. S. K. Patil, Materials Science Forum,48(1989)371.
41. M. Krachler, R. Alvarez-Sarandes, S. V. Winckel, J. Radioanal. Nucl. Chem., 304(2015)1201.
42. I. G. Alonso, J.F. Babelot, J. P. Glatz, O. Cromboom, L. Koch, Radiochim. Acta., 62(1993) 71.
43. A. M. Meeks, J. M. Giaquinto, J. M. Keller, , J. Radioanal. Nucl. Chem.,

- 234(1998)131.
44. D. Suzuki, F. Esaka, Y. Miyamoto, M. Magara, *Appl. Radiat. Isot.*, 96(2015) 52.
 45. Y.Y. Ebaid, *Rom. Journ. Phys.*, 55(2010) 69.
 46. A. M. Sanchez, F. V. Tome, J. D. Bejarano, M. J. Vargas, *Nucl. Instrum. Methods Phys. Res. Sect. A*, 313(1992)219
 47. G. C. Jain, K. B. Khan, S. Majumdar, H. S. Kamat, C. Ganguly, *Characterisation and Quality Control of Nuclear Fuels, CQCNF-2002*, Allied publication, pg. 376.
 48. A. Kelkar, A. Prakash, M. Afzal, J. P. Panakkal, H. S. Kamath, *J. Radioanal. Nucl. Chem.*, 284(2010)443.
 49. Mary Xavier, P. Nair, K. Lohithakshan, S. Marathe, H. Jain *J. Radioanal. Nucl. Chem.*, 48(1991)251.
 50. P. R. Nair, M. Xavier, S. K. Aggarwal, *Radiochimica Acta*, 97(2009)419.
 51. K. Chander, S. P. Hasilkar, A. V. Jadhav, H. C. Jain, *Journal of J. Radioanal. Nucl. Chem.*, 174(1993)127.
 52. V. N. Rao, G. G. Rao, *Fresenius Zeitschrift fur analytische Chemie*, 155(1957)334.
 53. G. W. C. Milner, A. P. Skewies, *AERE, C/R1126*.
 54. A. Sengupta, V.C. Adya, T. K. Seshagiri, S. K. Thulasidas, S. V. Godbole, V. Natarajan, *Journal of Research in Spectroscopy*, 2014 (2014)1.
 55. A.G.I. Dalvi, C. S. Deodhar, T. K. Seshagiri, M. S. Khalap, B. D. Joshi, *Talanta*, 25(1978)665.
 56. S. K. Thulasidas, M. Kumar, B. Rajeswari, B. A. Dhawale, S. V. Godbole, V. Natarajan, *Instrum. Sci. Technol.*, 43(2015)125.

57. E. A. Huff, D. L. Bowers, *Appl. Spectrosc.*, 44(1990)728.
58. V. C. Adya, A. Sengupta, S. K. Thulasidas, V. Natarajan, *J. Radioanal. Nucl. Chem.*, 307 (2016) 1489.
59. A. L. de Souza, M. E. Barboza Cotrim, M. A. Faustino Pires, *Microchem. J.*, 106(2013) 194.
60. S. F. Wolf, D. L. Bowers, J. C. Cunnane, *J. Radioanal. Nucl. Chem.*, 263(2005)581.
61. N.L. Misra, Sangita Dhara, S.K. Aggarwal, *BARC Newsletter*, 337(2014)1.
62. R. J. Rosenberg, R. Zilliacus, *J. Radioanal. Nucl. Chem.*, 169(1993)13.
63. R. Acharya, *BARC Newsletter*, 337(2014)9.
64. S. K. Aggarwal, G. Chourasya, R. K. Duggal, RadhikaRao, H. C. Jain, *Int. J. Mass Spectrom.*, 69(1986)137.
65. R. K. Webster, A. A. Smales, D. F. Dance, L. J. Slee, *Anal. Chim. Acta.* 24(1960)371.
66. D. Srivatsava, S. P. Garg, G. L. Goswami, *Journal of Nuclear Materials*, 161(1989)44.
67. K. V. Chetty, J. Radhakrishna, Y. S. Sayi, N. Balachander, et. al. *Radiochem. Radioanal. Letters*, 59(1983)161.
68. Z. Z. Yuan, Q. X. Dai, X. N. Cheng, K. M. Chen, *Material Characterisation*, 58(2007)87.
69. V. Venugopal, K. N. Roy, Ziley Singh, R. Prasad, D. Kumar, G. L. Goswami, *Proceedings of Seminar on Fast Reactor Fuel Cycle*, 1(1986)14.
70. Y. S. Sayi, P. S. Shankaran, C. S. Yadav, G. C. Chaparu, et. al. *Proc. Nat. Acad. Sci.* 72(A)(2002)241.

71. M. A. Mahajan, M. V. R. Prasad, H. R. Mhatre, R. M. Sawant, R. K. Rastogi, G. H. Rizvi, N. K. Chaudhuri, J. Radioanal. Nucl. Chem., Articles, 148(1991)93.
72. P. S. Ramajaneyulu, Y. S. Sayi, V. A. Raman, K. L. Ramakumar, J. Radioanal. Nucl. Chem., 274(2007)109.
73. S. Jeyakumar, V.V. Raut, K. L. Ramakumar, Talanta, 76(2008)1246.
74. Determination of Aluminum in Complex Matrices Using Chelation Ion Chromatography, Dionex, Application note, AN 69, 1991.
75. A. Riaz, B. Kim, D. S. Chung, Electrophoresis, 24(2003)2788.
76. R. Kadnar, Journal of Chromatography A 804(1998)217.
77. M. C. Bruzzoniti, E. Mentasti, C. Sarzanini, L. J. Kra, Analytica Chimica Acta, 322(1996)49.
78. H. Lu, S. Mou, J. M. Riviello, J Chromatogr A., 857(1999)343.
79. Determination of Inorganic Anions in Drinking Water by Ion Chromatography, DIONEX, Application Note 133.
80. R.A. Mohamed, A.M. Abdel-Lateef, H.H. Mahmoud, A.I. Helal, Studies in Chemical Process Technology (SCPT) 1(2013)75.
81. M. M. Wolle, T. Fahrenholz, G.M. MizanurRahman, Matt Pamuku, H.M. Kingston, D. Browne, Journal of Chromatography A, 1347(2014) 96.
82. M. Betti, Journal of Chromatography A, 789 (1997)369.
83. J. I.G. Alonsot, F. Sena, P. Arbore, M. Betti, L. Koch, J. Anal. At. Spectrom., 10(1995)381.
84. S. H. Reboul, E. H. Borai, R. A. Fjeld, Analytical and Bioanalytical Chemistry, 374(2002)1096.
85. E.H. Boraia, A.S. Mady, Applied Radiation and Isotopes, 57(2002)463.

86. P. Kumar, P. G. Jaison, V. M. Telmore, S. Paul, S. K. Aggarwal, International Journal of Analytical Mass Spectrometry and Chromatography, 1(2013)72.
87. W. R. Barger, R. L. Mowery, J. R. Wyatt, Journal of Chromatography A, 680(1994)659.
88. Y. F. Fung, K. M. Lau, Electrophoresis, 22(2001)2192.
89. M. Turnes Carou, P. Lopez Mahia, S. Muniategui Lorenzo, E. Fernandez Fernandez, D. Prada Rodriguez, J Chromatogr A. 918(20014)11.
90. B. Westergaard, H. C. B. Hansen, O. K. Borggaard, Analyst, April 123(1998)721.
91. Q. Dong, W. Jin, J. Shan, Electrophoresis. 23(2002)559.
92. P. Zhu, S. Wang, J. Wang, L. Zhou, P. Shi, J Chromatogr B, 1008(2016)156.
93. F. Foret, S. Fanali, A. Nardi, P. Bocek, Electrophoresis, 11(1990)780.
94. D. F. Swaile, M. J. Sepaniak, Anal. Chem., 63(1991)179.
95. K. Bachmann, J. Boden, I. Haumann, Journal of Chromatography A, 626(1992)259.
96. Y. Noguchi, L. Zhang, T. Maruta, L. N. Kiba, AnalyticaChimicaActa, 640(2009)106.
97. M. Langenauer, U. Krahenbuhl, AnalyticaChimicaActa, 274, (1993)253.
98. F. G. Antes, J. S.F. Pereira, M. S.P. Enders, C. M.M. Moreira, et. al., Microchemical Journal, 101 (2012) 54.
99. S. K. Sahoo, Y. Muramatsu, S. Yoshida, H. Matsuzaki, W. Ruhm, J. Radiat. Res. 50(2009)325.
100. Ticiane Taflik, J. Braz. Chem. Soc., 23(2012)488.

Chapter: 2

Principles of Experimental Techniques

2.1 Introduction:

A number of analytical instruments have been employed during the course of current investigations. Some of these techniques are common to more than one investigation. For example, pyrohydrolysis followed by ion chromatography has been employed for determination of halogens in U-Zr and U-Pu-Zr samples described in Chapter-3, for Mo in U-Mo samples described in Chapter-4 and for simultaneous determination of BO_3^- , F^- , Cl^- and MoO_4^{2-} ions in nuclear materials. Ion chromatography and Capillary electrophoresis has been employed for the determination of Li in U-Li samples described in Chapter-5. Chapter-6 describes application of Capillary Zone Electrophoresis (CZE) for the determination of Fe in Uranium matrix. Lastly ion chromatography has once again been employed for optimising washing procedure to be used for removal of chloride and nitrate from Li_2TiO_3 . Instead of describing the principles of these techniques each time in subsequent individual chapters, general description is given in this Chapter. The experimental details, as applicable are given in the respective Chapters.

In addition, a number of other techniques have also been employed as supporting tools to generate the requisite information on the samples investigated. These techniques were employed primarily for getting more information to interpret the experimental observations for drawing meaningful conclusions. This information includes XRD data, and other trace elemental techniques such as TGA, AAS, ICP-AES. Details of such techniques are also given in this Chapter.

2.2 Chromatography

Chromatography is a separation technique that separates components of complex mixtures on the basis of their retention behaviour on a stationary phase in presence of a mobile phase. It is defined as the physical method of separation where the analytes are distributed or partitioned between two immiscible phases viz. stationary and mobile phases. Modern chromatographic techniques are coupled with suitable detection systems and thereby they offer sequential separation as well as quantification of analytes from a single sample aliquot. In all chromatographic separations a mobile phase is passed through an immiscible stationary phase, which is fixed. The analytes in the sample distribute themselves between the mobile and stationary phases. Due to the flow of mobile phase the weakly retained components move ahead of strongly retained components [1-3]. The mobile phase entering the column is called eluent whereas the eluent emerging from the end of the column is called eluate and the process of passing mobile phase through a chromatography column is called elution.

2.2.1 Types of Chromatography

Chromatography can be divided into several types based on the basis of the mechanism of interaction between the solute and the stationary phase, as shown in Figure 2.1.

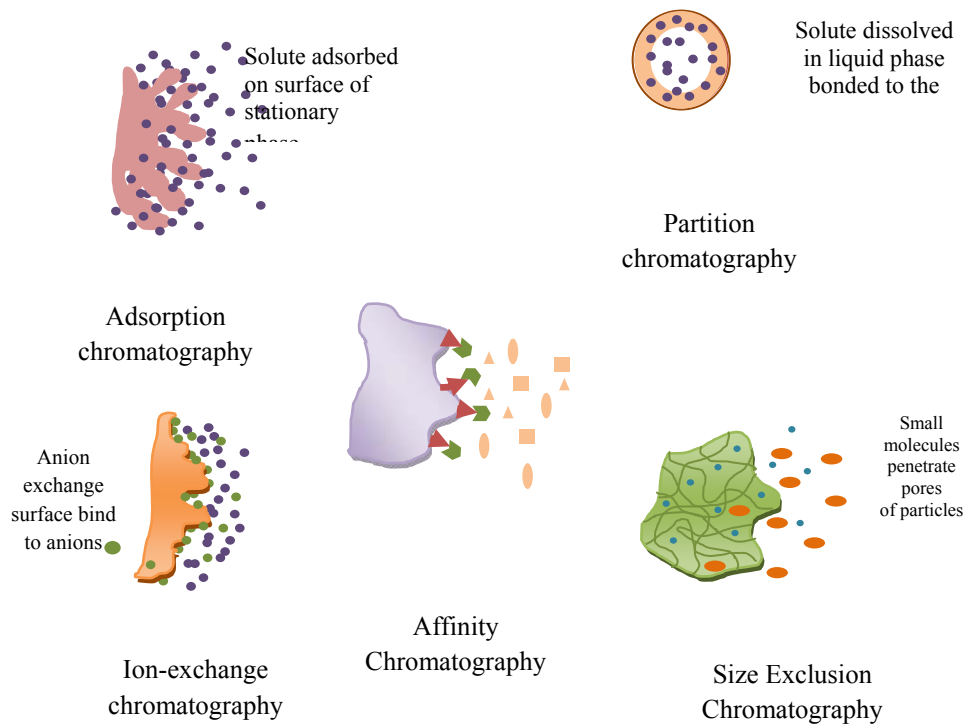


Figure 2.1: Major types of Chromatography

Adsorption chromatography: The retention of solute on the stationary phase is due to the adsorption. Stationary phase is a solid surface whereas mobile phases can be a liquid or a gas [4].

Partition chromatography: The retention mechanism in this case is similar to solvent extraction. Solute is partitioned between a mobile phase (liquid or gas) and a stationary liquid phase adsorbed on solid surface [5].

Ion-exchange chromatography: Anions or cations of analytes in the sample aliquot during elution get exchanged with their corresponding counter ions on the stationary solid phase due to the ion exchange mechanism. Stationary phase is usually a resin suitably modified as an ion exchanger and the mobile phase is a liquid [6].

Size exclusion chromatography: Size-exclusion chromatography (SEC), also called gel-filtration or gel-permeation chromatography (GPC), uses stationary phase impregnated with porous particles of varying size to separate molecules of different sizes. It is generally used to separate biological molecules, and to determine molecular weights and molecular weight distributions of polymers. Molecules that are smaller than the pore size can enter the particles and therefore have a longer path and longer transit time than larger molecules that cannot enter the particles [7].

Affinity chromatography: This technique utilises specific interactions between one kind of solute molecule and a second molecule that is immobilized to the stationary phase [8].

Chromatographic techniques are also classified on the basis of the physical states of both stationary and mobile phases used.

Gas-liquid chromatography (GLC): Solid or a liquid adsorbed on a solid support is the stationary phase and the mobile phase is always a gas.

Gas-solid chromatography (GSC): The mobile phase is a gas whereas the stationary phase is a solid.

Liquid-liquid chromatography (LLC): Stationary phase is liquid adsorbed on solid and mobile phase is liquid.

Liquid-solid chromatography (LSC): Stationary phase is a solid whereas mobile phase is a liquid.

2.2.2 Ion-Exchange Chromatography:

The ion exchange chromatography separation is mainly based on the differences in the ion exchange affinities of the sample ions towards the fixed ions of the stationary ion exchange resin. Hence, depending upon the affinities of the ions they will have different retention times, which is defined as the time in which an ion or a species is retained inside the column. In anion exchangers, positively charged groups are fixed on the stationary phase, which attracts solute anions whereas in the case of cation exchangers, fixed negatively charged ions on the stationary phase attract the cations of the solute. In general, ion exchangers favour the binding of ions of higher charge density [9].

Generally the ion exchange resins are the polymers and co-polymers of organic compounds. Polystyrene based ion exchangers are synthesised by the copolymerization of styrene and divinylbenzene (DVB). The DVB content is varied from 1 to 16% to increase the extent of cross-linking. The phenyl rings are substituted with appropriate functional groups to obtain cation exchange or anion exchange resins. For instance, substitution of sulfonate group was performed to obtain the cation exchange resin whereas a quarternary ammonium group is introduced to obtain an anion exchanger.

2.2.2.1 Ion Exchange equilibria:

The law of mass action can be used to treat ion-exchange equilibria [10]. For example, when a dilute solution containing metal ions is passed through a column packed with a sulfonic acid resin, the following equilibrium is established (fig. 2.2):

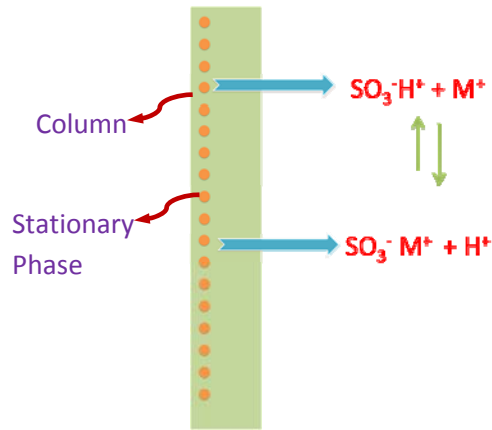
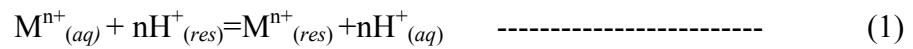


Figure 2.2: Schematic representation of Ion Exchange mechanism.



for which the equilibrium constant K_r is given by

$$K_r = \frac{[M]_{res}[H]_{aq}^n}{[M]_{aq}[H]_{res}^n} \quad \text{-----} \quad (2)$$

Polyvalent ions are much more strongly retained than singly charged species. Within a given group of ions having same charge, the differences among values for K appear to be related to the size of the hydrated ion as well as other properties. Therefore, for a typical sulfonated cation-exchange resin, values of equilibrium constant for univalent ions decrease in the order Ag^+ , Cs^+ , Rb^+ , K^+ , NH_4^+ , Na^+ , H^+ , Li^+ . For divalent cations the order is Ba^{2+} , Pb^{2+} , Sr^{2+} , Ca^{2+} , Ni^{2+} , Cd^{2+} , Cu^{2+} , Co^{2+} , Zn^{2+} , Mg^{2+} , UO_2^{2+} .

Analyte ions with different selectivity coefficients for a specific combination of resin and eluent anion will be separated due to different degrees of interaction with the stationary phase. The mechanism for anion exchange separation is analogous.

2.2.2.2 Conductivity detection:

Ion chromatography coupled with conductivity detector became a powerful tool for the quantification of ions after the development of low-exchange capacity columns. Improvement in the sensitivity of detection as well as very low limit of detection limit (LOD) was achieved after the introduction of suppression technology. The suppression technique is employed for reducing the conductivity of the mobile phase after the column and before the detector.

Electrical conductivity measures the ability of a solution to conduct an electric current between two electrodes across which an electric field has been applied. The conductance of a solution (g) is commonly expressed by the SI unit Siemens (S), and is the reciprocal of the resistance (R) measured in ohm (Ω).

$$g = 1/R \quad \text{-----} \quad (3)$$

Conductivity detectors are simple devices consisting of a detection cell with two electrodes, which can either be in contact with the stream of eluent. Conductivity detection is the natural choice for IC, since the separated analytes are electrically conducting. The conductance signal depends on the electrolyte concentration (C) of the ionic species present (both eluent and analyte ions, either + or -) and their limiting equivalent ionic conductances (λ).

In suppressor-based ion chromatography, the ion-exchange column is followed by a suppressor column, or a suppressor membrane, that converts an ionic eluent into a

non-ionic species that does not interfere with the conductometric detection of analyte ions [11].

Currently, several other detector types such as spectrophotometer and electrochemical detectors are available for ion chromatography.

2.2.3 Terms used in chromatography separations:

The mechanism of chromatography separations is understood by Column theory. Following are important factors that control the separation of analytes on the column.

- (i) **Column dead time (t_0):** it is the time necessary for a non-retained component to pass through the column. And the volume of mobile phase corresponding to the dead time is known as dead volume (V_0).
- (ii) **Retention time (t_R):** It is the time taken for an analyte to emerge out of the column after its retention on the column in which the components reside inside the column. This includes the dead time of the column.
- (iii) **Resolution (R):** Resolution is the measure of how a peak is separated with respect to its neighbouring peaks. The resolution R of two neighboring peaks is defined as the quotient of the difference in the absolute retention times and the arithmetic mean of their peak widths w at the respective peak base.

$$R = (t_{R2} - t_{R1}) / [(w_1 + w_2) / 2] \quad \text{-----} \quad (4)$$

where t_{R2} and t_{R1} are the retention times for components 1 and 2 respectively, w_1 and w_2 are their corresponding peak widths.

(iv) **Selectivity (α):** the selectivity is defined as the ratio of the solute retention times of two different components.

$$R = (t_{R2} - t_0) / (t_{R1} - t_0) \quad \text{-----} \quad (5)$$

The selectivity is a thermodynamic quantity and at constant temperature, it is determined by the properties of the stationary phase.

The selectivity of the column is due to several factors, e.g., the support material and the chemical structure of the ion exchange group.

The selectivity factor (α) of two analyte ions A and B eluting close to each other is the measure of how well these ions are separated, and is calculated according to:

$$\alpha = k'_B / k'_A \quad \text{-----} \quad (6)$$

where k'_A and k'_B are the retention factors for the first and the last eluted ion, respectively.

(v) **Retention factor (k'):** it is also known as Capacity factor. It is the product of the phase ratio Φ between stationary and mobile phase in the separator column and the Nernst distribution coefficient, K .

$$k' = K \times (V_s / V_m) \quad \text{-----} \quad (7)$$

$$K = C_s / C_m \quad \text{-----} \quad (8)$$

where K is Nernst distribution coefficient, V_s is volume of the stationary phase, V_m is volume of mobile phase, C_s and C_m are solute concentrations in the stationary and mobile phase respectively.

Practically k' for any peak of a component is measured as

$$k' = (t_R - t_0) / t_0 \quad \dots\dots\dots (9)$$

Number of Theoretical Plates (N)

A chromatography column does not contain anything resembling physical distillation plates or other similar features. Theoretical plate numbers are indirect measure of peak width for a peak at a specific retention time. The number of theoretical plates is a mathematical concept and can be calculated using Equation,

$$N = 16L^2/w_{1/2} \quad \text{-----} \quad (10)$$

(Where L is the column length and $w_{1/2}$ is width of peak at half peak height).

Columns with high plate numbers are considered to be more efficient, that is, have higher column efficiency, than columns with a lower plate count. A column with a high number of theoretical plates will have a narrower peak at a given retention time than a column with a lower N number [12].

2.2.4 Plate Height Equation:

Another measure of column efficiency is the height equivalent to a theoretical plate denoted as H . It is calculated using Equation, $H = L/N$ and usually reported in millimetres (Where L is the column length and N is number of theoretical plates of the column). The column efficiency is considered as high when the number of theoretical plates is more per unit length of the column.

Plate height, H , is proportional to the variance of a chromatographic band. The smaller the plate height, the narrower the band. The Van-Deemter equation tells us how the column and flow rate affect the plate height:

$$H = A + B/u_x + Cu_x \quad \text{-----} \quad (11)$$

Where u_x is the linear flow rate and A , B , and C are constants for a given column and stationary phase. Changing the column and stationary phase changes A (*Eddy diffusion*), B (*longitudinal diffusion*), and C (*resistance to mass transfer*).

A - Eddy diffusion:

The mobile phase moves through the stationary phase which is packed under high pressure. Solute molecules will take different paths through the stationary phase at random. This will cause broadening of the solute band, because different paths are of different lengths.

B - Longitudinal diffusion:

The concentration of the analyte is less at the edges of the band than at the center. Analyte diffuses out from the centre to the edges. This causes band broadening. If the velocity of the mobile phase is high then the analyte spends less time on the column, which decreases the effects of longitudinal diffusion.

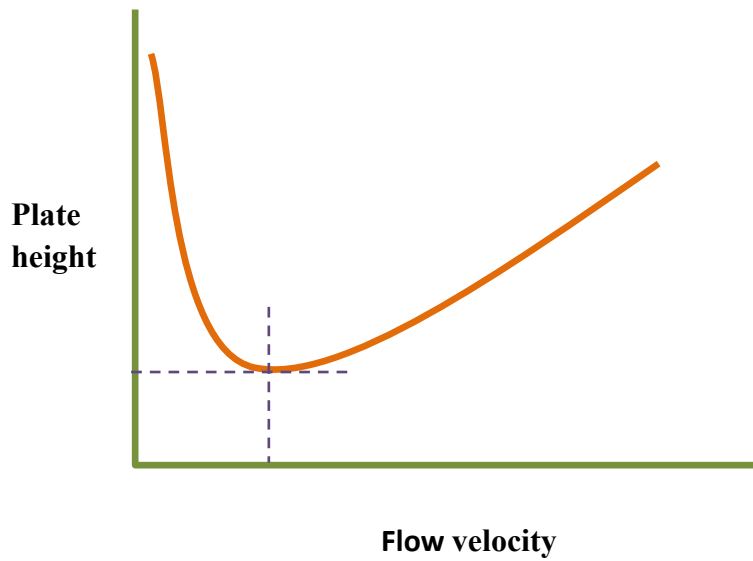


Figure 2.3: A typical Van Deemter plot.

C - Resistance to mass transfer:

The analyte takes a certain amount of time to equilibrate between the stationary and mobile phase. If the velocity of the mobile phase is high, and the analyte has a strong affinity for the stationary phase, then the analyte in the mobile phase will move ahead of the analyte in the stationary phase. The band of analyte is broadened. The higher the velocity of mobile phase, the worse the broadening becomes.

For each peak in the chromatogram, the capacity factor, k' , is defined as,

$$k' = (t_2 - t_0) / t_0 \quad \text{-----} \quad (12)$$

The separation factor (α) is defined as the ratio of the retention factors (k),

$$\alpha = \frac{k'_2}{k'_1} \quad \text{-----} \quad (13)$$

It is useful to relate the resolution to the number of plates in the column, the selectivity factor and the retention factors of the two solutes;

$$R = \frac{\sqrt{N}}{4} \times \frac{(\alpha-1)}{\alpha} \times \frac{k_2'}{1+k_2'} \quad \text{-----} \quad (14)$$

To obtain high resolution, the three terms must be maximised. An increase in N, the number of theoretical plates, by lengthening the column leads to an increase in retention time and increased band broadening - which may not be desirable. Instead, to increase the number of plates, the height equivalent to a theoretical plate can be reduced by reducing the size of the stationary phase particles.

Other experimental parameters which can affect the resolution are,

- (i) Changing mobile phase composition
- (ii) Changing column temperature
- (iii) Changing composition of stationary phase

Using special chemical effects (such as incorporating a species which complexes with one of the solutes into the stationary phase) etc.

2.2.5 Instrumentation:

The schematic shown below (Fig. 2.4) represents an ion chromatography system. The sample is introduced into the system via a sample loop on the injector. When in the inject position the sample is pumped onto the column by the eluent and the sample ions are then attracted to the charged stationary phase of the column. The

eluent elutes the retained ions which then go through the detector (which is most commonly conductivity) and are depicted as peaks on a chromatogram.



Figure 2.4: Block diagram for an Ion Chromatography system.

Figure-2.5 represents an IC system designed for analysis of radioactive samples. Some parts of the system which are in direct contact with the active samples, viz. sample injector, column, suppressor and detector are detached from the main system

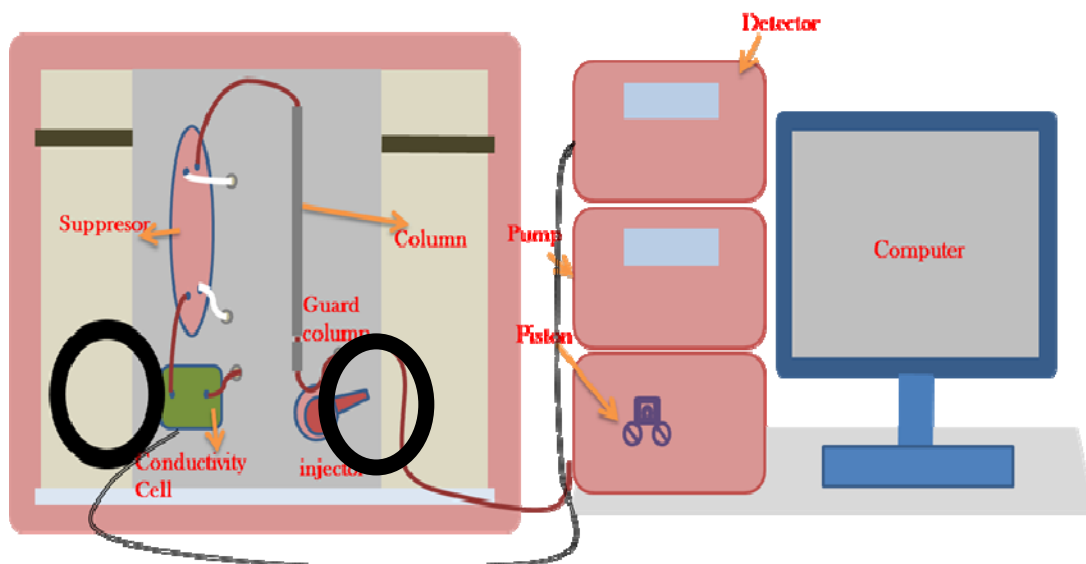


Figure 2.5: Schematic representation of an Ion Chromatography system designed for radioactive samples.

and are installed in a fume hood. The fume hood is under suction and the air of fumehood is passed through HEPA filters before getting released to atmosphere. The liquid waste collected in fume hood are disposed as per the standard procedures of radioactive liquid wastes.

Studies described in this dissertation utilised the ion chromatography for determining various anions like F^- , Cl^- , NO_3^- , MoO_4^{2-} etc. The separations were carried out on anion exchange columns with suppressor conductivity detection.

2.3 Capillary Electrophoresis:

Capillary electrophoresis (CE) is a rapid separation technique and it turned to be a good analytical tool by coupling suitable detectors. CE separates ions based on their electrophoretic mobility caused by application of potential (applied voltage). The electrophoretic mobility is dependent upon the charge of the ion, the viscosity, and the radius of the ion or molecular species. The rate at which the particle moves is directly proportional to the applied electric field, the greater the field strength, the faster the mobility. Neutral species are not affected, only ions move with the electric field. If two ions are the same size, the one with greater charge will move faster than the one with lesser charge. For the ions of same charge, the ion with small size will have faster migration rate as it will experience less friction in the medium. The capillary electrophoresis has some advantages over other separation techniques such as fast separation, very small sample size and separations with high resolution. CE is a useful technique because there is a large range of detection methods available [12].

Employing a capillary in electrophoresis had solved some common problems in traditional electrophoresis. For example, the narrow dimensions of the capillaries

greatly increased the surface to volume ratio, which eliminated overheating by the application of high voltages.

2.3.1 Electrophoretic Mobility:

Electrophoresis is the process in which sample ions move under the influence of an applied voltage. The ion experiences a force that is equal to the product of the net charge and the electric field strength. It is also affected by a drag force that is equal to the product of, the translational friction coefficient, and the velocity. This leads to the expression for electrophoretic mobility [14]:

$$\mu_{EP} = \frac{q}{f} = \frac{q}{6\pi\eta r} \quad \text{-----} \quad (15)$$

Where f stands for a spherical particle is given by the Stokes' law; η is the viscosity of the solvent, and r is the radius of the atom. The rate at which these ions migrate is dictated by the charge to mass ratio. The actual velocity of the ions is directly proportional to E, the magnitude of the electrical field and can be determined by the following equation:

$$v = \mu_{EP} E \quad \text{-----} \quad (16)$$

This relationship shows that a greater voltage will quicken the migration of the ionic species.

2.3.2 Electro osmotic Flow:

The electro osmotic flow (EOF) is caused by applying high-voltage to an electrolyte, which is filled in a capillary. The flow of electro osmotic flow is explained on the basis of an electrical double theory. According to this mechanism, $-\text{SiOH}$ of the silica releases a proton to become SiO^- ions when a buffer solution having pH more than 3 is allowed to pass through the silica capillary. Hence, the capillary wall then has a negative charge, which develops a double layer of cations attracted to it. The inner cation layer is stationary, while the outer layer is free to move along the capillary. The applied electric field causes the free cations to move toward the cathode creating a bulk flow, which is known as electro osmotic flow. The rate of the electroosmotic flow [14] is governed by the following equation:

$$\mu_{EOF} = \frac{\epsilon}{4\pi\eta} E\zeta \quad \text{-----} \quad (17)$$

Where, ϵ is the dielectric constant of the solution, η is the viscosity of the solution, E is the field strength, and ζ is the zeta potential. Because the electrophoretic mobility is greater than the electroosmotic flow, negatively charged particles, which are naturally attracted to the positively charged anode, will separate out as well.

2.3.3 Instrumentation:

A typical CE system consists of a high-voltage power supply, a sample introduction system, a capillary tube, a detector and an output device. Each side of the high voltage power supply is connected to an electrode as shown in the Figure 2.6. These electrodes help to induce an electric field to initiate the migration of the sample from the anode to the cathode through a capillary tube. The capillary is made of fused

silica and is sometimes coated with polyimide. Each end of the capillary tube is dipped in a vial containing the electrode and a background electrolytic solution. There is usually a small window near the cathodic end of the capillary for UV-VIS detection.

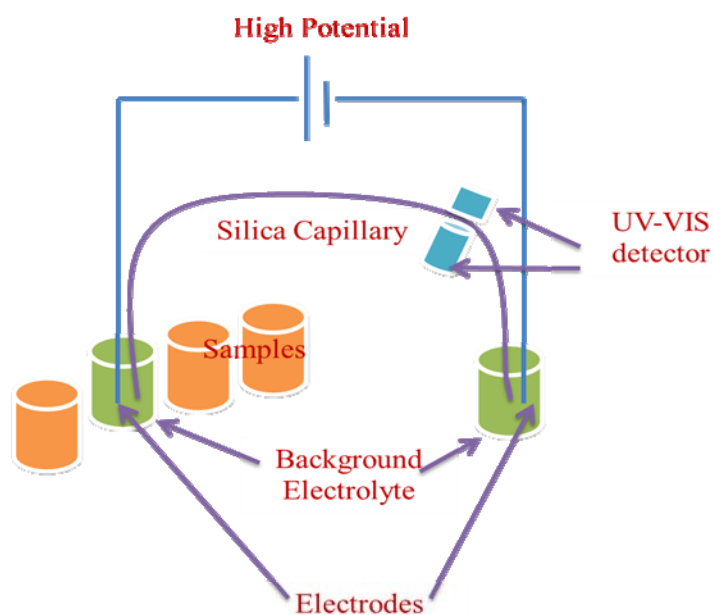


Figure 2.6: Capillary Electrophoresis instrumentation.

There are six types of capillary electrophoresis available [15] and they are (i) capillary zone electrophoresis (CZE), (ii) capillary gel electrophoresis (CGE) (iii), micellarelectrokinetic capillary chromatography (MEKC), (iv) capillary electro chromatography (CEC), (v) capillary isoelectric focusing (CIEF), and (vi) capillary isotachopheresis (CITP).

2.3.4 Capillary Zone Electrophoresis (CZE):

In CZE analytes move in the EOF but separate into bands because of differences in their electrophoretic mobilities, μ . Differences in μ make each analyte's overall migration velocity slightly different, and difference in migration velocity is

responsible for the separation. As it was discussed earlier in the presence of an applied electric field, the diffuse layer migrates towards the negatively charged cathode creating an electrophoretic flow (μ_{ep}) that drags bulk solvent along with it. Anions in solution are attracted to the positively charged anode, but get swept to the cathode as well. Cations with the largest charge-to-mass ratios separate out first, followed by cations with reduced ratios, neutral species, anions with smaller charge-to-mass ratios, and finally anions with greater ratios. The electroosmotic velocity can be adjusted by altering pH, the viscosity of the solvent, ionic strength, voltage, and the dielectric constant.

In liquid chromatography the separations are carried out on a packed and there the peak broadening is being explained on the basis of van Deemter equation, which accounts the broadening due to three phenomena namely multiple flow paths, longitudinal diffusion, and finite rate of mass transfer. In capillary electrophoresis, there is no stationary phase. Therefore, the only fundamental source of broadening under ideal conditions is longitudinal diffusion.

The present thesis reports about the developed CZE methods for determining Fe in uranium matrices and Li in Li-Al alloys. The method that deals with the determination of Fe in U matrices utilised chloride as the complexing agent in the BGE. In the CZE method for the determination of Li in Li-Al alloy was developed by using Imidazole as the co-ion.

2.4 X-ray powder diffraction analysis (XRD):

XRD is perhaps the most widely used X-ray based analytical technique for characterizing materials. As the name suggests, the sample is usually in a powdery form. The positions and the intensities of the peaks are used for identifying the

underlying structure (or phase) of the material [16]. The three-dimensional structure of crystalline materials is defined by regular, repeating planes of atoms that form a crystal lattice. When a focused X-ray beam interacts with these planes of atoms, part of the beam is transmitted, part is absorbed by the sample, part is refracted and scattered, and part is diffracted. X-rays are diffracted by each structure differently, depending on what atoms make up the crystal lattice and how these atoms are arranged. When an X-ray beam hits a sample and is diffracted, we can measure the distances between the planes of the atoms that constitute the sample by applying Bragg's Law, named after William Lawrence Bragg, who first proposed it in 1921. Bragg's Law is:

$$n\lambda = 2d \sin\theta, \quad \text{-----} \quad (18)$$

where the integer n is the order of the diffracted beam, λ is the wavelength of the incident X-ray beam, d is the distance between adjacent planes of atoms (the d-spacings), and θ is the angle of incidence of the X-ray beam. We can measure the d-spacings. The geometry of an XRD unit is designed to accommodate this measurement. The characteristic set of d-spacings generated in a typical X-ray scan provides a unique fingerprint of the material or materials present in the sample. When properly interpreted, by comparison with standard reference patterns and measurements, this fingerprint allows for identification of the material.

Instrumentation: In XRD, X-rays are generated within a sealed tube which is under vacuum. A filament present inside the tube is heated by applying current and the filament emits electrons. Moreover, higher the current the greater the number of electrons emitted from the filament. A high voltage, typically 15-60 kilovolts, is applied within the tube. This high voltage accelerates the electrons, which then hit a

target, commonly made of copper. When these electrons hit the target, X-rays are produced. The wavelength of these X-rays is characteristic of that target. These X-rays are collimated and directed onto the sample, which is in fine powder form. A detector detects the X-ray signal; the signal is then processed either by a microprocessor or electronically, converting the signal to a count rate [17].

The XRD technique was utilized during various studies to understand the various structural transformations occur during their pyrohydrolysis. The structural information obtained from the XRD is vital in interpreting the mechanism of pyrohydrolysis for the material under investigation.

2.5 Thermogravimetric Analysis:

Thermogravimetric analysis (TGA) measures the change in weight of a material as a function of temperature (or time) under a controlled atmosphere. TGA is widely employed for the measurement of a material's thermal stability, moisture, solvent content, and composition of components (in percentile level) in a compound [18]. A TGA analysis is performed by gradually raising the temperature of a sample in a furnace as its weight is measured on an analytical balance that remains outside of the furnace. In TGA, mass loss is observed if a thermal event involves loss of a volatile component. Chemical reactions, such as combustion, involve mass losses. A plot of sample weight versus temperature or time is used to illustrate the thermal transitions in the material.

The studies described in this dissertation, TGA was utilised specially to understand the chemistry of volatilization of MoO_3 in moist atmosphere at different temperatures.

2.6. Inductively Coupled Plasma Atomic Emission Spectrometry:

Atomic emission spectrometry (AES) is a method of chemical analysis that uses the intensity of light emitted from a flame, plasma, arc, or spark at a particular wavelength to determine the quantity of an element in a sample. The wavelength of the atomic spectral line gives the identity of the element while the intensity of the emitted light is proportional to the number of atoms of the element. Inductively coupled plasma atomic emission spectroscopy (ICP-AES) uses ICP to produce excited atoms and ions that emit electromagnetic radiation at wavelengths characteristic of a particular element. Advantages of ICP-AES are excellent limit of detection and linear dynamic range, multi-element capability, low chemical interference and a stable and reproducible signal. Disadvantages are spectral interferences (many emission lines), cost and operating expense and the fact that samples typically must be in a liquid solution [19,20].

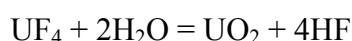
The ICP-AES technique has been used in the studies of this thesis to validate the results obtained by the developed methods by comparing the values obtained from ICP-AES.

2.7 Pyrohydrolysis:

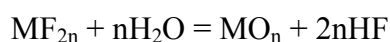
Pyrohydrolysis is one of the separation techniques where the analytes are directly separated from the solid materials without dissolving them. Pyrohydrolysis is based on the principle where the decomposition solid materials in presence of heat and water vapour. During the simultaneous action of heat and steam, the analytes are

converted into their volatile form and get extracted through the flow of steam, which is subsequently condensed and collected in the form of distillate.

Domange and Wohlhuter [21] had determined the equilibrium constant for the reaction



in the range 200° to 500° C. They concluded that higher temperatures favour the formation of the hydrolysis products, the equilibrium constant being 1.36×10^{-1} at 250°C. and an estimated value of 1.93 at 1000°C. Warf et al [22] extended the observations of Domange and Wohlhuter and postulated that in the case of a general equation



the free energy of formation is expected to become more negative with rising temperatures, because the standard entropy of 2 moles of hydrogen fluoride is roughly twice that of 1 mole of steam.

A plot of Free energy formation and the temperature for different metal halides [23] is shown in Figure 2.7. It is seen that as the temperature increases the ΔG becomes more and more negative. The end product is the halogen acid and the corresponding metal oxide. It leads to the conclusion that quantitative release of halogen from the solid matrix is facilitated through opening of the solid matrix and conversion of the metal halide to metal oxide. Besides high temperature, for effective interaction of moisture with metal halide to occur the sample should preferably be in the powder form to offer large surface area. The kinetics of release of halogens is thus directly related to the kinetics of formation of metal oxide.

After extensively investigating different metal halide systems, Warf et al[22] classified them into a rapidly hydrolyzable group and a slowly hydrolyzable group. The first included AlF_3 , BiF_3 , MgF_2 , ThF_4 , UF_4 , UF_3 , UO_2F_2 , VF_3 , ZnF_2 , ZrF_4 , ZrOF_2 , and the rare earth fluorides.

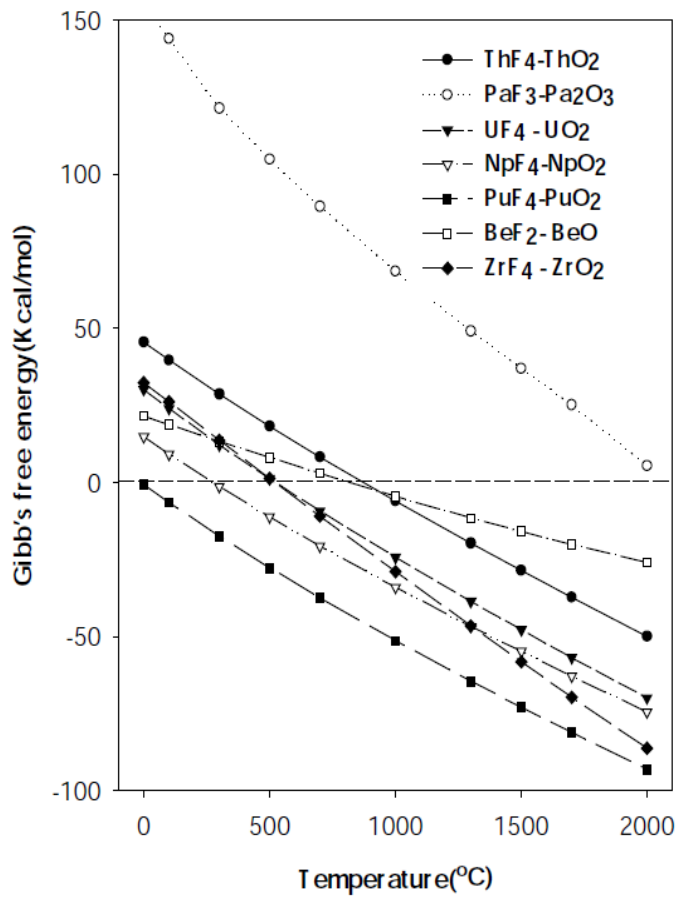


Figure 2.7:Gibb's free energies of formation of various compounds [23].

The second group included the fluorides of the alkali metals, the alkaline earth metals, and beryllium. Those in the first group were hydrolyzed quantitatively in 20 minutes or less at 1273K.

The volatile halogen acids are collected in a PVC bottle containing dilute NaOH (trapping solution) and this solution is known as pyrohydrolysis distillate. The pyrohydrolysis distillates obtained are subsequently analysed by selective instrumental methods for quantifying the analytes. Similarly boron can be separated in the form of boric acid from several materials [24-26].

Pyrohydrolytic separation mainly depends on (i) temperature of pyrohydrolysis (ii) carrier gas flow rate (iii) sample mass and (iv) time (duration) of pyrohydrolysis.

(i) Pyrohydrolysis temperature: Temperature is an important parameter as the material under pyrohydrolysis is needed to be decomposed or brought changes in the volume of the material either by physical or chemical means. For organics as well as easily pulverisable materials, a moderate temperature range between 673 and 973K is chosen. However, refractory materials which are highly resistive for the action of heat require quite high temperature (more than 1273K).

(ii) Carrier gas choice and flow rate: The carrier gas selection and its flow rate are important parameters in pyrohydrolysis. It indirectly helps in improving the sensitivity of the analytical determination. Most of the pyrohydrolysis are carried out with oxygen as carrier gas except for the cases where oxygen may cause unwanted or unfavourable reactions. For instance, pyrohydrolysis of uranium carbide or plutonium carbide or mixed uranium and plutonium carbide is carried out with

Argon gas (inert gas) due to their pyrophoric nature. The flow rate of steam is controlled by the carrier gas flow rate and therefore, it directly controls the condensed distillate volume. Typically the pyrohydrolysis distillate collection volume is kept around 25 mL in 30 minutes collection. This is very important to have appreciable concentrations of the analytes in the distillate.

(iii) Mass of the sample: A sample mass of 10 mg to 5g are taken for pyrohydrolysis. For a given sample, the sample mass is decided by considering the concentration range of analytes present in the sample.

(iv) Time of pyrohydrolysis: Time of pyrohydrolysis is the most important one as it decides the recoveries of analytes. Depending upon the pyrohydrolysis temperature and the concentration of the analytes the separation kinetics is varied. Therefore, the time of pyrohydrolysis needed to be optimized for each matrix. For example the uranium or plutonium carbides are pyrohydrolysed for only 15-20 minutes for the complete recovery of chlorine and fluorine whereas in certain ceramic and refractive materials like zirconia, thoria etc. is pyrohydrolysed for few hours.

Literature survey shows a variety of samples like geological samples, coal, organic materials, nano particles, cement, nuclear materials etc. [27-31] are regularly analysed for their halide contents after pyrohydrolysis separation. The basic design of the pyrohydrolysis apparatus is presented in the Figure 2.8. Depending on the materials to be pyrohydrolysed some modifications in the apparatus are also being incorporated.

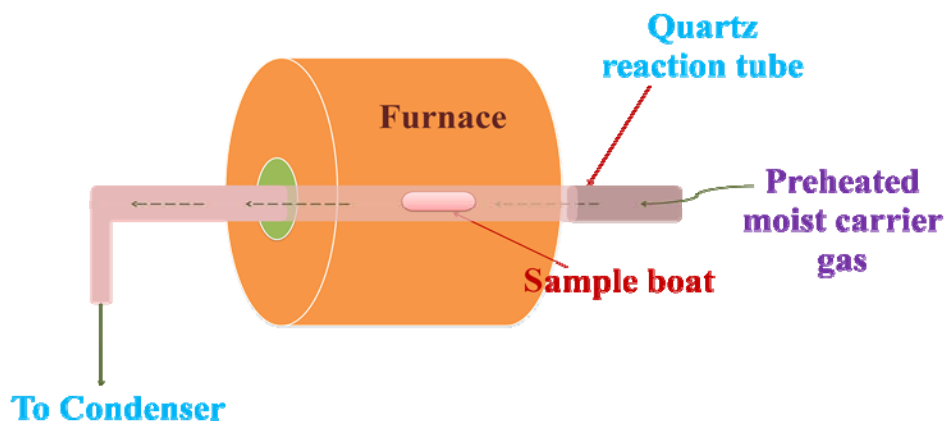


Figure 2.8: Basic Pyrohydrolysis instrument.

In order to carry out the pyrohydrolysis of radioactive materials, the apparatus is housed inside an active glove box. This limits the free handling or operation of the PH apparatus and from the safety point of view, it poses many challenges. Therefore, many modifications have been incorporated in the system to carry out the operations and handling easier and safe. In addition, to increase the sample through-put during routine sample analyses, necessary changes were incorporated in the design with a view to carry out the sample loading and unloading is easier and safe. These requirements resulted in advance pyrohydrolysis system as depicted in Figure-2.9. The main features of the design are, (i) pre-heater for the carrier gas is not required as the same furnace where the sample is heated is utilized for heating moist carrier gas. (ii) The furnace is movable, which helps in easy access to the reaction tube. (iii) The combination of outer and inner reaction tube allow easy and fast loading of sample boat. (iv) The overall space occupied is reduced significantly.

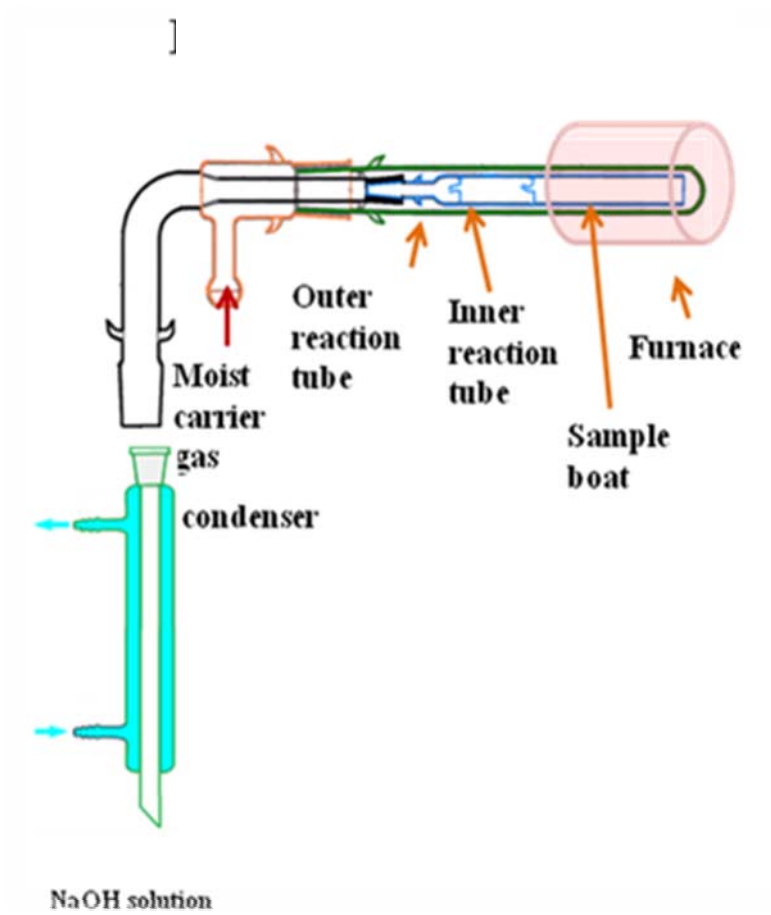


Figure 2.9: The modified Pyrohydrolysis apparatus for Glove Box operation.

Pyrohydrolysis was used for clean sample preparation. Studies were carried out to understand the pyrohydrolysis behaviour of U-Zr and U-Pu-Zr alloy samples. A novel method was also developed where Mo was separated directly from U matrix using pyrohydrolysis. For analysing environmental samples pyrohydrolysis was used to provide a simultaneous separation of B, F, Cl and Mo.

2.8 References:

1. C. F. Poole, The essence of Chromatography, Elsevier, (2003)1.
2. J. M. Miller, Chromatography Concepts and Contrast, Wiley, 2nd edition (2005)35.
3. D. A. Skoog, J. J. Leary, Principles of Instrumental Analysis, Saunders College Publisher, 4th edition(1991)579.
4. J. Cazes, Encyclopedia of Chromatography, Volume-1, Taylor and Francis, (2005)21.
5. J. Cazes, Encyclopedia of Chromatography, Volume-1, Taylor and Francis, (2005)296.
6. J. Cazes, Encyclopedia of Chromatography, Volume-1, Taylor and Francis, (2005)859.
7. J. Cazes, Encyclopedia of Chromatography, Volume-1, Taylor and Francis, (2005)11.
8. J. Cazes, Encyclopedia of Chromatography, Volume-1, Taylor and Francis, (2005)33.
9. J. S. Fritz, D. T. Gjerde, Ion Chromatography, 3rd edition, Wiley VCH, (2000)4.
10. P. R. Haddad, P. E. Jackson, Ion Chromatography Principles and Applications, Elsevier (1999)1.
11. J. Weiss, Ion Chromatography, Second Edition, VCH (1995)291.
12. L. R. Snyder, J. J. Kirkland, Introduction to Modern Chromatography, 2nd edition(1979)15.
13. H. Whatley, Clinical and Forensic Applications of Capillary Electrophoresis, chapter 2, (2001)22.

14. S. E. Y. Li, *Capillary Electrophoresis Principles, practice and applications*, Elsevier (1992)12.
15. C. M. Johnson, A. P. McKeown, M. R. Euerby, *Capillary Electrochromatography*, Elsevier, Volume 62(2001)87.
16. Y. Waseda, E. Maturba, K. Shinoda, *X-ray Diffraction Crystallography*, springer(2011)107.
17. A. A. Bunaciua, E. G. Udristoiub, H. Y. Aboul-Eneinc, *Crit. Rev. Anal. Chem.*, 45(2015)289.
18. R. Bottom, *Principles and Applications of Thermal Analysis*, Blackwell Publishing (2008)87.
19. K. L. Linge, *Geostand. Geoanal. Res.*, 29(2005)7.
20. M. Thompson, *Handbook of Inductively Coupled Plasma Spectrometry*, Blackie & Sons Ltd. (1989)43.
21. (6) Domange, L., and Wohlhuter, M., *Compt, rend*, 228, 1591(1949).
22. James C. Warf, W. D. Cline, and Ruth D. Tevebaugh, *Anal. Chem.*, 26(1954), 342
23. Mun-Sik Woo, Sung-Chan Hwang, Jun-Bo Shim, Young-Ho Kang and Jae-Hyung Yoo, Paper presented at OECD Nuclear Energy Agency Seventh Information Exchange Meeting on Actinide and Fission Product Partitioning and Transmutation, 14-16 October 2002, Jeju (Korea).
24. M. A. Mahajan, M. V. R. Prasad, H. R. Mhatre, R. M. Sawant, et al., *J. Radioanal. Nucl. Chem.*, 148(1991), 93.
25. S. Jeyakumar, V. V. Raut, K. L. Ramakumar, *Talanta*, 76(2008)1246.
26. S. Jeyakumar, V. G. Mishra, M. K. Das, V. V. Raut, R.M. Sawant, K. L. Ramakumar, *Radiochim. Acta*; 102(2014)291.

27. J. E. Rae, S.A. Malik, *Chemosphere* 33(1996)2121.
28. M. Bettinelli, S. Spezia, C. Minoia, A. Ronchi, *At. Spectrosc.* 23(2002)105.
29. F.G. Antes, F. A. Duarte, J. N.G. Paniz, M. F. P. Santos, et. al., *At. Spectrosc.* 29(2008)157.
30. Y. Muramatsu, Y. Takada, H. Matsuzaki, S. Yoshida, *Quat. Geochronol.* 3(2008)291.
31. Y. Nogushi, L. Zhang, T. Maruta, T. Yamane, N. Kiba, *Anal. Chim. Acta*, 640(2009) 106.

Chapter: 3

Direct Extraction of Molybdenum from Solid Uranium Matrices Employing Pyrohydrolysis and Its Determination by Ion Chromatography

3.1 Introduction:

Uranium is used as a nuclear fuel both in ceramic (UO_2) and alloy forms. Both the types of fuels have their own advantages and disadvantages. Depending upon their composition and properties they are considered suitable for different reactors. Molybdenum is an alloying element for metallic fuels such as U-Mo, U-TRU-Mo (TRU, trans-uranium elements such as Np, Pu, and Am), and so on. These alloys are advantageous due to their γ phase stability of U [1]. Presence of Mo in ceramic fuel causes creep resistance (results in swelling of fuel pellets and causes adverse effects on the integrity of clad material). Hence, the presence of Mo even at a trace level concentration is undesirable in oxide or mixed oxide fuels of U and Pu. Another important factor is the oxygen potential of the Mo/MoO₂ couple which is very close to that of the stoichiometric UO₂ [2] and can affect the o/m ratio of UO₂. Therefore, separation and determination of Mo in nuclear fuels in the concentration range of trace to percent levels is an important requirement.

Methods that are being used in the chemical characterisation of nuclear materials for the determination of Mo in U or U-Pu matrices involve dissolution of the material in appropriate acid media followed by solvent extraction or ion exchange separations [3-7]. These methods are laborious and generate radioactive liquid wastes. Unless precautions are taken there may be loss of Mo during the sample preparation steps.

This loss of Mo leads to erroneous determination of Mo. Such loss was encountered while determining Mo in ammonium diuranate (ADU) [8]. Therefore, it is desirable to have a sample preparation procedure that does not lead to loss of Mo and also brings reduction in the radioactive waste generation.

Pyrohydrolysis (PH) is a separation method which separates the analyte(s) directly from the solid matrix and do not use any organic reagent or acids. PH is a well-known technique for separating halogens and boron from several solid matrices [9-15]. The pyrohydrolysis conditions or separation parameters governing recoveries of the analytes depend on the matrix and also the nature of the analyte [16, 17]. Pyrohydrolysis is widely used for separating non-metals such as halogens, boron, and sulphur, and its application for separating metals or metal species has not been explored and reported so far.

Several studies (18-20) indicate that MoO_3 , the more stable oxide of Mo has higher vapour pressure. In addition, the volatilisation of Mo is enhanced when the atmosphere contains moisture [20, 21]. This implies the feasibility of separating Mo quantitatively from solid matrices by making use of associated vapour chemistry of Mo. Present investigations are aimed at exploring the feasibility of adapting pyrohydrolysis for separating molybdenum from uranium based nuclear materials.

3.2 Experimental Section:

3.2.1 Reagents:

For the preparation of synthetic standards, U metal and UO_2 (nuclear grade, Bhabha Atomic Research Centre (BARC), Mumbai, India) and Mo metal powder and MoO_3 (>99.95% Alfa Aesar, Heysham, U.K.) were used. The standard solutions of F^- , Cl^- ,

NO_3^- , and SO_4^{2-} were prepared by dissolving their respective Na salts (>99.9%, Merck, Darmstadt, Germany). Standard solutions of MoO_4^{2-} were prepared by dissolving $(\text{NH}_4)_6\text{Mo}_7\text{O}_{24}$ (>99.98%, Sigma-Aldrich, St. Louis, MO, USA) in high purity water. All other reagents were of analytical grade. For the preparation of all solutions and production of steam, high purity water (18.2 M Ω ·cm) obtained from a Milli-Q system (Millipore, Billerica, MA, USA) was used.

3.2.2 Preparation of Standards Containing Mo:

In order to study the recovery of Mo by pyrohydrolysis, in-house standards with known Mo contents were prepared. Since the real samples can have different chemical forms of uranium matrix, the standards were prepared in metal (U-metal) as well as in the oxide form (UO_2). The standards were prepared in the concentration range between 100 and 5000 ppm. Two U–Mo alloys having 500 and 5000 ppm of Mo were prepared by Arc melting method [22]. Two different mixed oxide ($\text{UO}_2 + \text{MoO}_3$) working standards, each with 100 and 500 ppm of Mo, were prepared by mixing calculated amounts of MoO_3 and UO_2 powders. The powders were ground thoroughly for about 3 h to get homogeneity. In addition, UMoO_6 was synthesized by following a reported procedure [23].

3.2.3 Instrumentation:

An all-quartz pyrohydrolysis apparatus was used [24]. The description of the apparatus was given in the chapter 2. A 150 mm length Liebig condenser with chilled water (~278K) circulation was used. A commercial ion chromatograph (IC; DX-500 model; Dionex, Sunnyvale, CA, USA) consisting of a gradient pump (GP-50), ED-40 conductivity detector, and an anion self-regenerator suppressor (ASRS-II) was used for obtaining the chromatograms., IonPac AS16 (250 × 4 mm) along

with its guard column, IonPac AG16 (50 × 4 mm). The TG analyses were carried out on a TGA-DTA Instrument (Netzsch STA 409 PC, NETZSCH-Geratebau GmbH, Germany). XRD patterns were recorded using Rigaku MiniFlex-600 X-ray diffractometer.

3.2.4 IC Analysis of Mo:

Since during pyrohydrolysis the volatile form of Mo i.e. MoO_4^{2-} will be trapped in a dilute solution of NaOH, there is a need to develop an ion chromatography separation method for separating MoO_4^{2-} ion along with other common anions. In the basic medium Mo exist as MoO_4^{2-} . Using ion chromatography the MoO_4^{2-} ion can be separated on an anion exchange column. An ion exchange column, Ionpac AS16 was selected owing to its high capacity and good selectivity. Dilute NaOH solutions in the concentration range between 10 and 35 mM were used as mobile phases as the sample is in NaOH medium. It was observed that a mobile phase of 15 mM NaOH at a flow rate of 1 mL min^{-1} was found to be optimum for separating the MoO_4^{2-} ion from the other common anions. Figure 1 shows a typical chromatogram obtained for a standard solution containing MoO_4^{2-} ion. The limit of detection (LOD) of the method was calculated on the basis of the S/N ratio = 3 method, and it was found to be 80 ppb for Mo.

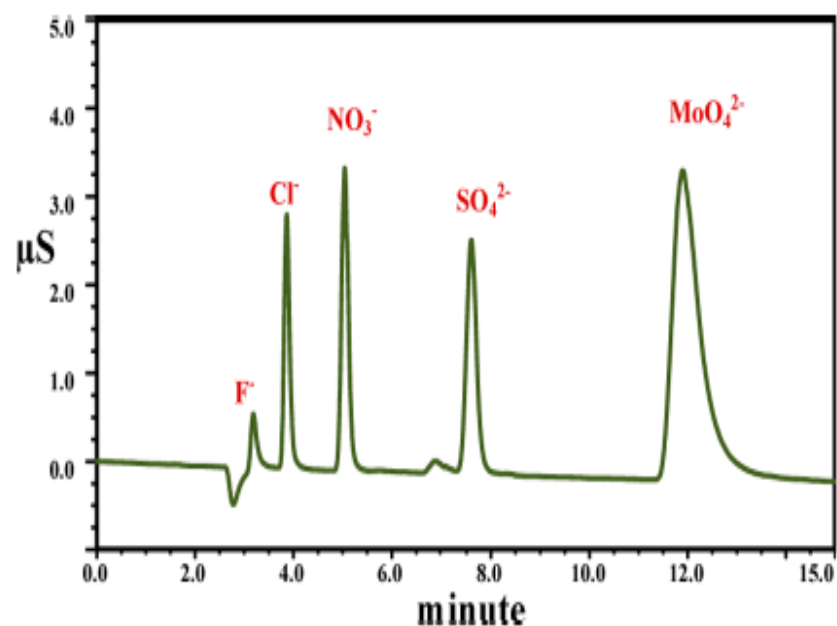


Figure 3.1: Chromatogram of an anion mix standard containing F⁻ (0.5 ppm), Cl⁻ (1.0 ppm), NO₃⁻ (2.0 ppm), SO₄²⁻ (2.0 ppm), and MoO₄²⁻ (10.0 ppm): column, IonPac AS-16; eluent, 15 mM NaOH; flow rate, 1 mL min⁻¹.

3.3 Results and Discussion:

The feasibility of separating Mo from uranium matrices using pyrohydrolysis was explored with a view to determining Mo accurately in uranium. To start with, a thermogravimetryanalysis (TGA) was carried to understand the vapour chemistry of MoO₃. During TGA moist atmosphere condition was maintained to know the effect of moisture on the loss of MoO₃ at high temperatures. TGA of MoO₃ using Ar carrier gas with and without water vapour at elevated temperatures may provide information relevant to the vaporization of Mo under the conditions similar to pyrohydrolysis. The reported TGA studies on MoO₃ have shown loss of MoO₃ by increasing temperature [25], however, TGA studies on the effect of water vapour on the vaporization of MoO₃ under isothermal conditions were not reported.

3.3.1 Thermogravimetric Analysis:

For this purpose, ~ 3 mg of the sample (MoO_3) was heated at a rate of 298K min^{-1} to the desired temperature, and thereafter, it was kept constant. At first TGA was performed at 1073K with Ar by keeping its flow rate at 100 mL min^{-1} (Figure 2.2 a). The atmosphere maintained was dry.

To perform a similar analysis in moist conditions the Ar carrier gas was passed through boiling water, which saturated the Ar with moisture. The weight loss curve with this moist condition is shown in Figure 2.2 b.

In case of the dry Ar atmosphere the weight loss of MoO_3 was $\sim 21\%$ whereas the weight loss was around 43% when the experiment was performed in moist Ar. This observation was similar to the observation of enhanced vapour pressure of MoO_3 due to presence of moisture atmosphere [21] and reconfirms the fact that the presence of water enhances the volatilization of MoO_3 .

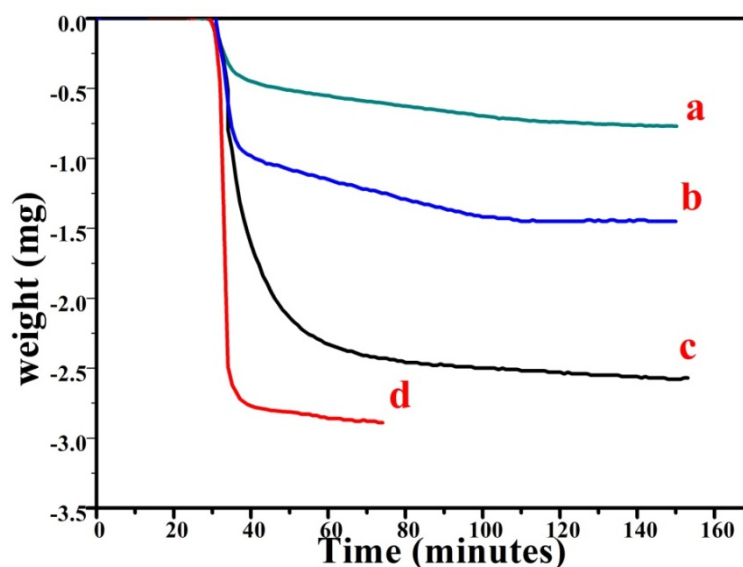


Figure 3.2: Isothermal thermograms of ~ 3 mg of MoO_3 at different temperatures and carrier gas conditions: (a) 1073K in dry Ar carrier gas; (b) 1073K in moist Ar carrier gas; (c) 1273K in moist Ar carrier gas; (d) 1473K in moist Ar carrier gas.

The moist Ar condition was further explored at 1273K as well as 1473K and the thermograms obtained were shown in Figure 2.2 c and d, respectively. The weight loss of MoO₃ was found to be 83% at 1273K whereas the same was 96% at 1473K. The results indicate that the rate of vaporisation of MoO₃ is temperature dependent. Since the apparatus used for pyrohydrolysis is made up of quartz, pyrohydrolysis should not be carried out above 1273K for longer duration especially for the routine kind of work. In view of this, the TGA time of analysis was increased to 200 min at 1273K and under this condition 97% weight loss of MoO₃ was observed.

3.3.2 Pyrohydrolysis of Mo Containing Standards:

Though the TGA studies showed more than 97% volatilisation of MoO₃ in moist Ar at higher temperatures, it is necessary to maintain conditions during pyrohydrolysis which favours formation of MoO₃ (In U matrices Mo can be present in forms other than MoO₃, which are not volatile). In view of this during pyrohydrolysis moist oxygen was used as the carrier gas. During the pyrohydrolysis of sample in moist oxygen the Mo may undergo following changes:

- (i) Oxidation of Mo to its oxide, MoO₃(s)
- (ii) Volatilization of MoO₃(s) to MoO₃(g) and
- (iii) Dissolution of MoO₃(g) in water vapour due to formation of MoO₃·H₂O, which would drastically enhance the volatilization of MoO₃

MoO₃ Standards:

In order to study the pyrohydrolysis of Mo containing uranium materials, synthetic standards were prepared. Two synthetic mixed oxide standards (UO₂ + MoO₃) having 100 and 500 ppm of Mo were prepared and subjected to pyrohydrolysis for

different time durations. Sample masses of ~1g and 0.5 g were taken for 100 ppm and 500 ppm standards, respectively. A plot of Mo recovered as a function of time is shown in Figure 2.3a. Though quantitative recovery of Mo was realized in the both standards, the time of pyrohydrolysis required for achieving the quantitative recovery in each case was different.

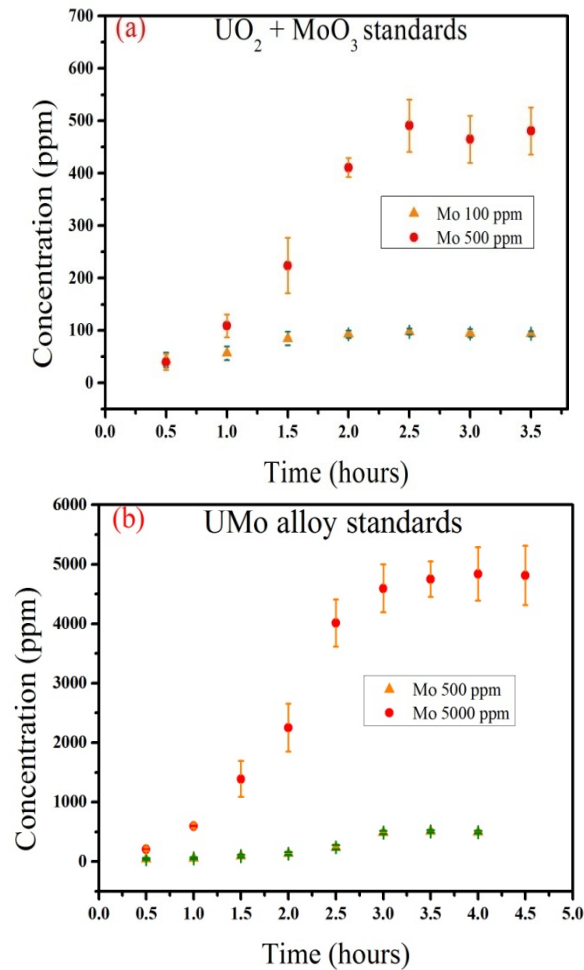


Figure 3.3. Recovery curve in moist O₂ carrier gas (a) for UO₂ + MoO₃ mixture standard containing 100 and 500 ppm Mo and (b) for UMo alloy standard containing 500 and 5000 ppm Mo.

Table 3.1. Minimum Time Required for Recovery of Mo Better than 95%, from Alloy and Oxide Standards.

standard	Mo (ppm)	sample weight (g)	time (h) of PH for >95% recovery
UO₂ + MoO₃	100	1.0	2.0
	500	0.5	2.5
UMo alloy	500	0.5	3.0
	5000	0.5	3.5

Alloy Standards: In addition to the oxides, two more synthetic standards of U-Mo alloy (500 and 5000 ppm of Mo) were also prepared and pyrohydrolyzed. A sample mass of ~0.5g of each standard was pyrohydrolysed. The Mo recovery as a function of time is shown in Figure 2.3b. Table 1 lists out the comparison of time required for pyrohydrolysis of oxide and alloy standards.

3.3.3 Kinetics of Mo Separation:

Following are the important observations made during the Pyrohydrolysis of standards

- i. The time required for the quantitative separation of Mo depends upon the concentration of Mo and the sample mass.
- ii. Although the carrier gas flow rate during PH was kept nearly 20 times higher than TGA, the time of pyrohydrolysis in all of the cases was observed to be longer than expected.

The probable reasons for these observations could be the slow vaporization of MoO_3 in uranium matrix and/or the formation of non-volatile Mo compounds due to solid state reactions. It is necessary to investigate the cause for this slow kinetics and to take necessary action for improving the kinetics of separation.

Vaporization Kinetics: To understand the vaporisation of MoO_3 in U matrix under pyrohydrolysis conditions, a synthetic mixed oxide standard containing 20% Mo by weight was subjected to pyrohydrolysis for different time durations, i.e., 1/2, 1.0, 1 1/2, and 2.0 h, in moist O_2 atmosphere at 1273K.

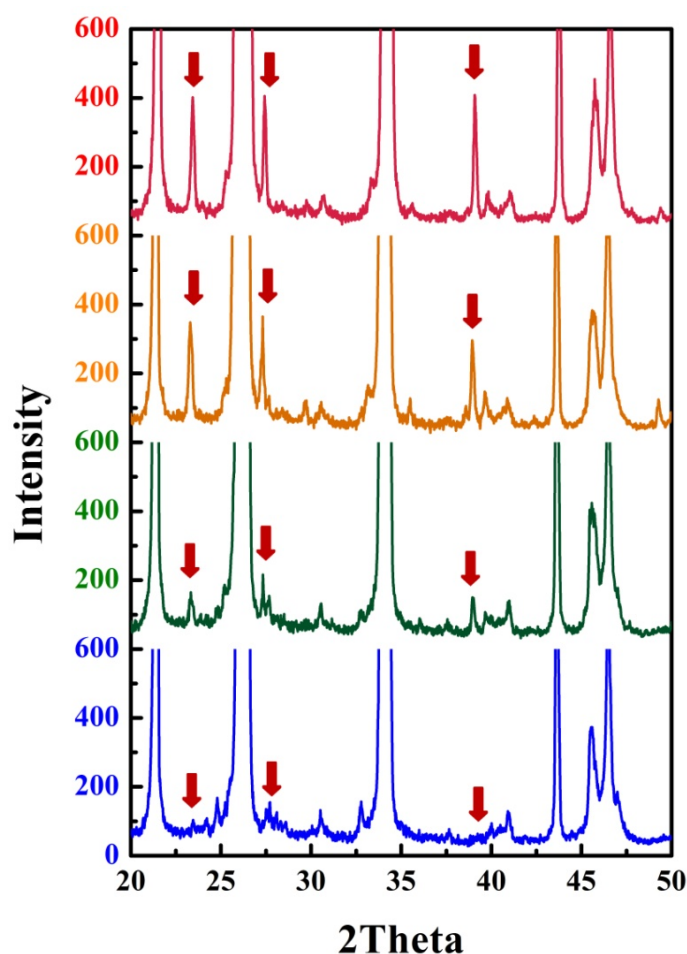


Figure 3.4. XRD patterns of UO_2 and MoO_3 mixture recorded after (a) 1/2, (b) 1, (c) 1 1/2, and (d) 2 h of pyrohydrolysis. The downward arrow symbol indicates a few major peaks for MoO_3 .

The materials obtained after pyrohydrolysis in each case were subjected to XRD analysis, and Figure 3.4 shows an overlay of the recorded XRD patterns. As the XRD patterns shows with peaks corresponding to vaporization of MoO_3 decreases with time. It can also be observed in 2 hrs the content was below the detection limit of XRD. This indicates the vaporization is prompt enough, even when the Mo content is quite high.

Formation of Non-volatile Compounds: In the present case, U and Mo can form compounds such as UMo_2O_8 , U_2MoO_8 , UMoO_5 , and UMoO_6 [27]. Reported studies

show that UMo_2O_8 , U_2MoO_8 , and UMoO_5 under oxygen atmosphere and in the temperature range of 760–796K are converted to UMoO_6 . The reported decomposition temperatures for UMoO_6 were found to be different in different literatures 1200K [26] and 1400K [27]. It may be possible that UMoO_6 is formed during pyrohydrolysis (temp \sim 1223K) and remains un-decomposed. This can affect the separation kinetics. Therefore, it becomes necessary to understand the behaviour of UMoO_6 during PH. For this purpose, UMoO_6 was synthesized [22] and it was pyrohydrolyzed for 2½ h. XRD analyses of UMoO_6 before and after pyrohydrolysis confirmed the complete conversion of UMoO_6 to U_3O_8 (Figure 3.5).

Since the formation of UMoO_6 could not be ascertained for the delay in pyrohydrolysis, the possibility of local condensation of $\text{MoO}_3 \cdot \text{H}_2\text{O}$ vapour on parts of the reaction tube (relatively at lower temperature) was considered. This was investigated by heating the parts of the apparatus which are at lower temperatures. After heating the apparatus externally the recovery increased considerably. This indicates that there is reversible local condensation responsible for the slower recovery of Mo.

To improve the kinetics of separation, a short reaction tube was incorporated in the PH apparatus which provides a shorter path length as well as relatively higher temperature as it was closer to the furnace. The modified apparatus brought quantitative recovery of Mo within 2½ h irrespective of the Mo content in the samples.

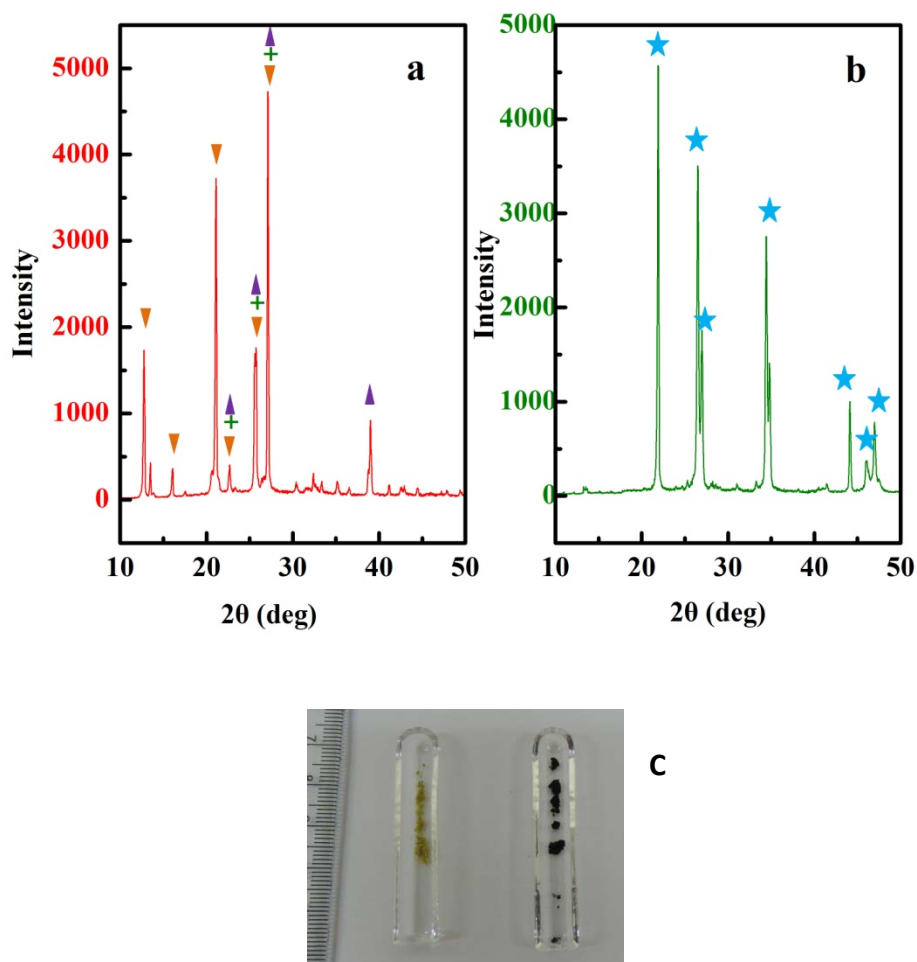


Figure 3.5: XRD patterns of (a) UMoO₆ powder and (b) U₃O₈ formed after pyrohydrolysis of UMoO₆ (all peaks are characteristic to U₃O₈): carrier gas, moist O₂; time, 2½ h; temperature, 1273K. (c) The picture of UMoO₆ before and after pyrohydrolysis.

3.3.4 Optimization of Pyrohydrolysis Conditions:

Pyrohydrolysis at 1573K: It may be recalled that the TGA studies showed that the rate of volatilization of MoO₃ increases with temperature. Pyrohydrolysis was carried out at 1573K by varying the time of pyrohydrolysis. Results showed quantitative extraction of Mo within 1½ h. During the study it was also observed

that continuous operation of the quartz PH apparatus for about 20 h (in 2 days) showed visible effects of devitrification.

Optimization of Sample Mass: For U-Mo alloy standard having 5000 ppm of Mo the standard deviation in the recovery of Mo was varied from 3 to 12% while the sample mass was increased from 50 to 1000 mg. Therefore it was concluded that for samples containing higher concentration of Mo it is important to keep sample mass low in order to get good precision. For mixed oxide standard having 100 ppm of Mo showed acceptable precision only when the sample mass was above 250 mg. This is because of the concentration of Mo in the distillate becomes less than the detection limit of IC. The analysis of samples containing low Mo requires high sample mass (~1000 mg) during PH.

Therefore, depending upon the expected concentration of Mo in the sample, the sample size for pyrohydrolysis would vary between 50 and 1000 mg

Optimized Pyrohydrolysis Conditions:

Based on the results, the optimum pyrohydrolysis conditions are as follows:

- (i) Sample mass, 50–1000 mg (depends on Mo content)
- (ii) PH temperature, 1273 K or more
- (iii) Time duration of PH, 2½ h or more for 1423 K
- (iv) Carrier gas flow rate, 2 L min⁻¹
- (v) Trapping agent, 5 mL of 25 mM NaOH.

3.3.5 Method Validation and Sample Analysis:

A certified reference material (CRM) of U_3O_8 (ILCE-4, Department of Atomic Energy (DAE), Mumbai, India) was analysed for its Mo content [28]. The Mo content in this standard is certified as 47.1 ± 8.7 ppm. The CRM was also analysed by ICP-AES method (without heating) and the results obtained are listed in Table 3.2.

Method was extended to the real samples of ammoniumdiuranate (ADU) samples containing enriched uranium were analysed. The determination of Mo in these enriched U containing ADU samples is important because:

- i. During enrichment process, the Mo present in the form of MoF_6 is also in the vapour phase and gets enriched in the U-235 phase. This may result in Mo concentrations more than expected.
- ii. The existing method for the determination of Mo in ADU involves heating of the sample to $800^\circ C$, which may cause loss of Mo as ADU has significant amount of moisture.

This loss of Mo from ADU due to the heating of ADU prior to its dissolution was confirmed by carrying out separate analyses of ADU with and without heating. In first analysis, the existing procedure involving the heating of ADU to 1073K and converting into the matrix into U_3O_8 . Further the oxide was dissolved in nitric acid and it was treated with TBP to extract the U matrix. The remaining aqueous sample was analysed by ICP-AES for Mo content. In the second analysis, the same procedure was followed except the heating step. The results obtained from both the analyses are given in Table 3.2. It is seen from the results that heating step caused significant loss of Mo. In a separate analysis the same sample was analysed by

following the developed method in which the Mo was separated by pyrohydrolysis and the distillate was analysed by IC and ICP-AES. The values obtained from IC as well as ICP-AES were listed in the Table 3.2.

Table 3.2. Comparison of results obtained for ADU Samples by the Developed Method, Solvent Extraction Followed by ICP-AES, and Pyrohydrolysis followed by ICP-AES Methods.

Sample	Concentration of Mo (ppm)				
	Certified	ICP-AES ¹ (ppm)	ICP-AES ² (ppm)	PH distillate by ICP-AES (ppm)	PH distillate by IC (ppm)
ADU-1		20 ± 6	35 ± 5	38 ± 4	37 ± 2
ADU-2		17 ± 5	38 ± 4	40 ± 5	41 ± 3
ADU-3		-	-		52 ± 3
ILCE-IV	47.1 ± 8.7		45 ± 5		42 ± 2

¹Conventional procedure, ADU heated to 850 °C, dissolved in HNO₃, U separated by TBP, and aqueous phase analyzed for Mo content.

²ADU directly dissolved in HNO₃ to avoid Mo loss due to heating, separated by TBP, and the aqueous phase analyzed for Mo content.

3.4 Conclusion:

The present study explored the feasibility of separating Mo in uranium matrices using pyrohydrolysis for the first time. A simple, green, and eco-friendly pyrohydrolysis separation of Mo directly from the solid matrices without the use of acids and other organic reagents was developed. The pyrohydrolysis separation

followed by ion chromatography determination was successfully applied to ADU samples having enriched uranium.

3.5 References:

1. V. P. Sinha, G. J. Prasad, P. V. Hegde, R. Keswani, C. B. Basak, S. Pal, G. P. Mishra, *J. Alloys Compd.* 473(2009)238.
2. P. Martin, M. Ripert, G. Carlot, P. Parent, C. Laffon, *J. Nucl. Mater.* 326(2004)132.
3. S. F. Marsh, *Anal. Chem.* 39(1967) 696.
4. T. Sato, H. Watanabe, H. Suzuki, *Hydrometallurgy* 23(1990)297.
5. P. C. Rout, K. Sarangi, *Hydrometallurgy* 133(2013)149.
6. R. E. Lewis, *Int. J. Appl. Radiat. Isot.* 22(1971)603.
7. A. G. C. Nair, S. K. Das, S. M. Deshmukh, S. Prakash, *Radiochim. Acta* 57(1992)29.
8. M. K. Saxena, P. Kumar, S. B. Deb, K. L. Ramakumar, *Nuclear and Radiochemistry Symposium Proceeding; Bhabha Atomic Research Centre (BARC): Mumbai, India, 2005; pp 487.*
9. F. G. Antes, F. A. Duarte, J. N. G. Paniz, , M. F. P. Santos, R. C. L. Guimaraes, E. M. M. Flores, V. L. Dressler, *At. Spectrosc.* 29(2008)157.
10. V. L. Dressler, D. Pozebon,, E. L. M. Flores, J. N. G. Paniz, E. M. M. Flores, *J. Braz. Chem. Soc.* 14(2003)334.
11. Y. Noguchi, L. Zhang, T. Maruta, T. Yamane, N. Kiba, *Anal. Chim. Acta* 640(2009) 106.
12. Y. Muramatsu, Y. Takada, H. Matsuzaki, S. Yoshida, *Quat. Geochronol.* 3(2008)291.

13. F. G. Antes, J. S. F. Pereira, M. S. P. Enders, C. M. M. Moreira, E. I. Muller, E. M. M. Flores, V. L. Dressler, *J. Microchem.* 101(2012)54.
14. C. C. Muller, T. S. Nunes, A. L. H. Muller, V. L. Dressler, E. M. M. Flores, E. I. Muller, *J. Braz. Chem. Soc.* 26(2015)110.
15. R. M. Sawant, M. A. Mahajan, P. Verma, D. Shah, U. K. Thakur, K. L. Ramakumar, V. Venugopal, *Radiochim. Acta.* 95(2009)585.
16. J. C. Warf, W. D. Cline, R. D. Tevebaugh, *Anal. Chem.* 26(1954)342.
17. S. Jeyakumar, V. V. Raut, K. L. Ramakumar, *Talanta* 76(2008)1246.
18. G. R. Smolik, D. A. Petti, S. T. J. Schuetz, *Nucl. Mater.* 283-287(2000)1458.
19. A. P. V. Soares, M. F. Portel, A. Kiennemann, L. Hilaire, *Chem. Eng. Sci.* 58(2003) 1315.
20. C. K. Gupta, *Extractive Metallurgy of Molybdenum*; CRC Press: Boca Raton, FL, USA(1992) 238.
21. K. U. Rempel, A. A. Migdisov, A. E. Williams-Jones, *Geochim. Cosmochim. Acta* 70(2006) 687.
22. N. T. Kim-Ngan, I. Tkach, S. Maskova, L. Havela, A. Warren, T. Scott, *Adv. Nat. Sci.: Nanosci. Nanotechnol.* 4(2013)035006.
23. M. Keskar, N. D. Dahale, K. J. Krishnan, *Nucl. Mater.* 393(2009)328.
24. M. A. Mahajan, M. V. R. Prasad, H. R. Mhatre, R. M. Sawant, R. K. Rastogi, G. H. Rizvi, N. K. J. Chaudhuri, *Radioanal. Nucl. Chem.* 148(1991)93.
25. T. Nagai, N. Sato, S. Kitawaki, A. Uehara, T. Fujii, H. Yamana,; M. J. Myochin, *Nucl. Mater.* 433(2013)397.
26. S. R. Bharadwaj, S. R. Dharwadkar, M. S. Chandrasekharaiah, *Thermochim. Acta* 79(1984)377.

27. E. V. Suleimanov, A. V. Golubev, E. V. Alekseev, C. A. Geiger, W. Depmeier, V. G. Krivovichev, *J. Chem. Thermodyn.* 42(2010)873.
28. DAE-Interlaboratory Comparison experiment (ILCE) for trace metal assay of uranium - Phase 4, Document; Bhabha Atomic Research Centre (BARC): Mumbai, India, 2002.

Chapter: 4

Studies on U-Zr and U-Pu-Zr Alloys for Determination of Cl and F Using Pyrohydrolysis

4.1 Introduction:

Metallic fuels are being considered for future Indian fast reactors program. This is mainly because of the advantages associated with these fuels. Unlike oxide fuel, metallic fuel with its higher breeding ratio and shorter doubling time will be able to produce more plutonium to help commission many more nuclear power reactors. It may be mentioned that to meet the increasing energy demand, the country has embarked on a major programme to generate additional 20,000 MW of nuclear power by 2020 and the target is to have 30GW by 2020. This can be achieved only if many nuclear power plants are commissioned. And for this to happen, sufficient nuclear fuel should be available. Oxide fuel with only 1.1 breeding ratio produces very little extra plutonium compared to metallic fuel with a breeding ratio of 1.4-1.5. Hence the doubling time is more in the case of oxide and least for metallic fuel. The doubling time for metallic fuel is ten years while it is thirty years in the case of oxide fuel. It is judicious to have a fuel cycle with shorter doubling time.

The other important advantages are:

- i. High thermal conductivity
- ii. heavymetal density
- iii. ease of fabrication
- iv. Possibility of Pyro-process for recycling [1, 2].

In view of this, the long term Indian Fast Reactor programme will be based on metallic fuels [3].

Use of U or U-Pu as metallic fuel has few limitations such as their unfavourable melting during fabrication and formation of low melting compounds with the stainless steel clad materials. U-Zr and U-Pu-Zr alloy fuels are the material of choice due to their higher solidus temperature and higher eutectic with T91 clad. The fabrication of these materials and their test-irradiation in FBTR is an ongoing project in BARC. Like any other nuclear fuel the presence of F and Cl may cause problems to the integrity of fuel cladding due to their corrosive nature [4–6]. Since these halides cause depassivation of clad surface and corrosion, F and Cl have stringent specification limits in various types of fuels. Hence, their concentration in the fuels needed to be controlled [7]. The chemical reagents that are used in the processes of fabrication and reprocessing are the major sources for Cl and F and they get added into the nuclear materials as impurities. It is known that during fabrication of alloys the impurities can be easily picked up by the highly reactive molten metallic components. It is important to have sensitive and reliable methods for the analysis of chlorine and fluorine at various stages of fabrication of U-Zr and U-Pu-Zr alloys.

In pyrohydrolysis the halides are separated using either moist argon or oxygen as carrier gas and by heating the matrix at high temperature. The chlorine and fluorine released from the solid sample are in the form of HCl and HF, respectively. The HCl and HF thus formed are carried away by the moist carrier gas which is subsequently trapped in a dilute NaOH solution (pyrohydrolysis distillate).

Once the distillate is available, suitable analytical techniques are employed for the determination of individual analytes. The determination of halogen using

pyrohydrolysis separation followed by ion chromatography in various matrices can be found in [10–24].

In our laboratory also, pyrohydrolysis technique followed by ion chromatography is being routinely employed for this purpose. Necessary analytical methodologies have been developed by optimising experimental conditions for quantitative extraction of halogens from different nuclear fuel matrices such as U_3O_8 , $(U, Pu)O_2$, $(U, Pu)C$, ThO_2 etc. The present study investigates different pyrohydrolysis conditions to understand the behaviour of U-Zr and U-Pu-Zr matrices for realising quantitative extraction of chlorine and fluorine.

4.2: Experimental Section:

4.2.1 Pyrohydrolysis setup:

All quartz pyrohydrolysis set up consisting of two concentric tubes was used for pyrohydrolysis purpose. The outer tube has an inlet and serves as a pre-heater for moist carrier gas. The inner tube houses the sample boat and it is attached to gas outlet. The gas outlet tube is cooled by a condenser. The condensate is collected in a bottle containing dilute NaOH. A schematic diagram of the pyrohydrolysis set up is presented elsewhere [22].

4.2.2 Ion chromatography system:

A commercial (Dionex DX-500) ion chromatography system consisting of an IP-20 isocratic pump, anion self-regenerator suppressor in external recycle mode, ED-40 conductivity detector with a DS3 stabilizer has been used for obtaining all the chromatograms. Samples were introduced through a 100 μ l loop fitted with a Rheodyne injector. Separation of anions were achieved on an analytical column

(Dionex, Ion PacAS16, 250x4mm) coupled with its guard column (AG16, 50x4 mm). A software viz. Chromeleon was used for instrument control as well as for data collection and processing. Other IC details are provided in the literature [22].

4.2.3 XRD instrument: The oxidized product of U-Zr samples were analysed using Rigaku MINIFLEX 600 X-ray diffractometer (θ - 2θ geometry) using $\text{CuK}\alpha$ radiation ($\lambda = 1.5406 \text{ \AA}$) with a scan rate of 1° min^{-1} was used. The oxidized products of U-Pu-Zr alloy were characterized by using $\text{CuK}\alpha$ ($\lambda = 1.54184 \text{ \AA}$) radiation employing Diano X-ray diffractometer (Diano Corporation, Woburn, MA) and graphite monochromator. The instrument is housed in a glove box to handle the radioactive material.

4.2.4 Thermoanalyzer: Mettler Thermo Analyzer (model: TGA/SDTA851e/MT5/LF1600) in flowing dry air at heating rate of $10^\circ\text{C}/\text{min}$ up to 1000°C . Thermo analyzer was calibrated from the weight loss obtained for the decomposition of 100mg of $\text{CuSO}_4 \cdot 5\text{H}_2\text{O}$ to CuO , while heating at 1000°C in air.

4.2.5 Alloy fabrication and characterization:

U-Zr and U-Pu-Zr alloys were fabricated in the Radiometallurgy Division, BARC, using arc melting method [23,24]. The U and Pu contents in the U-Zr and U-Pu-Zr alloys were determined by electro analytical methods (bi-amperometry whereas the concentration of Zr was determined by gravimetric method. The determined weight percentage of U, Pu and Zr are given in Table 4.1. The metallic impurities in these alloys are determined by ICP-MS and ICP-AES [25, 26].

Table 4.1: Chemical analysis of U, Pu and Zr from U-Zr and U-Pu-Zr alloy.

Material	wt. % Zr	wt. % U	wt. % Pu
U-Pu-Zr	4.7	76.1	19.1
U-Zr	6.1	93.8	-

Table 4.1: Chemical analysis of U, Pu and Zr from U-Zr and U-Pu-Zr alloy.

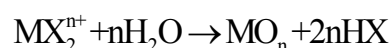
4.2.6 Pyrohydrolysis procedure:

The alloys were pyrohydrolysed with moist Ar and moist O₂, separately. The condensed aqueous phase or distillate was collected in 5ml of 25mM NaOH solution (trapping solution). The distillate thus collected during pyrohydrolysis was diluted to 25 ml and was subjected to ion chromatography analysis.

4.3 Results and discussion:

Owing to the pyrophoric nature of Pu-alloys and mixed carbide fuels, the pyrohydrolysis is generally carried out in Ar atmosphere to avoid the vigorous reactions between the pyrophoric alloys and O₂/H₂O and also to release analytes in a controlled manner. The halides present in the alloy matrices are mainly in form of metal halides (MX_n).

The chemical reaction responsible for the release of halides from the matrix is,



The reaction occurs at 1173K or above since the free energy for the reaction is favourably negative at high temperatures. James C Warf et al. [18] have reported the

pyrohydrolysis of UF_4 , UF_3 , UO_2F_2 , ZrF_4 , and ZrOF_2 . However; the pyrohydrolysis of Pu-alloys have not been much investigated. Therefore, this study was directed to investigating pyrohydrolysis of U-Zr and U-Pu-Zr alloys and quantification of fluorine and chlorine contents employing ion chromatography. As reference materials of U-Zr and U-Pu-Zr with certified fluorine and chlorine contents were not available, Initially the pyrohydrolysis was carried out with Ar as a carrier gas [20] maintaining experimental conditions same as were followed for UO_2 , $(\text{U,Pu})\text{O}_2$ samples. However with a view to achieving maximum recovery the F and Cl from the alloy matrices, the pyrohydrolytic behavior of U-Zr alloys were studied by pyrohydrolysing the materials for different time intervals in moist argon. Figure 4.1 depicts the results.

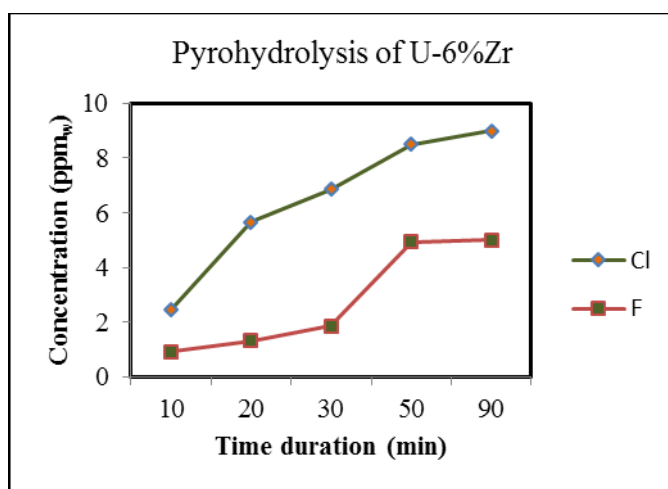


Figure 4.1 Pyrohydrolysis of U-6%Zr sample. (Conditions: 1173K moist Ar)

From the figure following observations could be drawn:

- i. Pyrohydrolysis conditions used for UO_2 and $(\text{U,Pu})\text{O}_2$ samples can also be used for pyrohydrolysing alloy samples
- ii. The results for both fluorine and chlorine show tendency to saturate

- iii. However the time taken to reach saturation or maximum concentration value is higher than in the case of UO_2 and $(\text{U,Pu})\text{O}_2$ samples.

From the above observations following preliminary conclusions could be drawn:

- a. The pyrohydrolysis of alloy samples is also thermodynamically feasible. This suggests that the chemical processes occurring in the case of UO_2 and $(\text{U,Pu})\text{O}_2$ samples may be occurring in the case of alloy samples also.
- b. The kinetics of the conversion process seems to be slow in the case of alloy samples.

To confirm these preliminary conclusions,

Although it is known that the kinetics of separation can be enhanced by using a suitable accelerator such as U_3O_8 or V_2O_5 [29], in the present case the uranium in the sample initially gets oxidised and acts as an in-situ accelerator and therefore no external accelerator was added.

In order to understand the reason behind the slow extraction as well as the extraction mechanism, it is necessary to observe the changes in the material during pyrohydrolysis. Therefore, the pyrohydrolysed products obtained at different time intervals were analysed by X-ray powder diffraction method. The XRD patterns of the oxidized product of U-Zr alloy under different duration of heating at 1173K in moist Ar atmospheres are shown in Figure 4.1. The different identified products formed during pyrohydrolysis are summarized in table 4.3. The XRD pattern of U-Zr alloy heated in moist Ar atmosphere for 10 min (Figure4.1a) indicated X-ray lines similar to UO_2 (FCC phase). No lines due to ZrO_2 were observed in XRD pattern

indicating the solubility of ZrO_2 in UO_2 . Recent studies showed that up to 35 mole % of ZrO_2 can be dissolved in UO_2 under mild oxidizing conditions at 1673K [30,31].

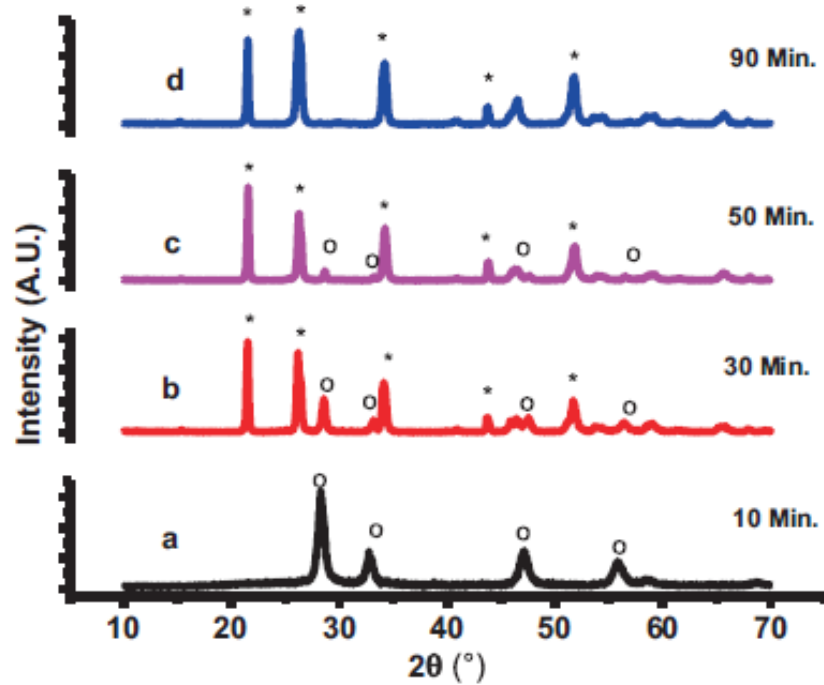


Figure 4.2: XRD patterns of pyrohydrolysed products of U-Zr alloy heated in moist Ar atmosphere at 1173K for (a) 10 min., (b) 30 min., (c) 50 min. and (d) 90 min. (o and * represent UO_2 and $\alpha-U_3O_8$, respectively).

Table 4.2: The summary of products identified by XRD on heat treatment of U-Zr alloy.

Starting material	Heat treatment	End product identified by XRD	Lattice parameter of FCC solid solution (Å)
U-Zr alloy	Dry air/1000°C/10°C /min	($\alpha-U_3O_8$)ss orthorhombic	-

U-Zr alloy	Moist Ar/900°C/ 10 min	(U, Zr)O _{2+x} FCC	5.458 (2)
U-Zr alloy	Moist Ar/900°C/ 30 min	(α -U ₃ O ₈) orthorhombic + (U,Zr)O _{2+x} FCC	- 5.410 (3)
U-Zr alloy	Moist Ar/900°C/ 50 min	(α -U ₃ O ₈) orthorhombic +(U, Zr)O _{2+x} FCC	- 5.410 (3)
U-Zr alloy	Moist Ar/900°C/ 90 min	(α -U ₃ O ₈)ss orthorhombic	-

XRD pattern of the U-Zr alloy heated in moist Ar atmosphere for 30 min (Figure 4.1b) showed the lines due to U₃O₈+UO₂ phase indicating incomplete oxidation of the alloy. XRD pattern shown in Figure 4.1c clearly reveals U₃O₈ as a major phase and FCC phase corresponding to UO₂ as a minor phase in the 50 minutes heated material. The weak lines due to UO₂ indicate that even 50 min heating is not sufficient to oxidize alloy sample completely to U₃O₈. The XRD obtained for the material pyrohydrolysed for 90 minutes showed the complete oxidation of uranium to U₃O₈ (Figure 4.1d). Since the volume of the material expands during the oxidation and this condition is favourable for separating the halides and the same is confirmed by the recoveries obtained for Cl and F. Since the oxidation of uranium is slow for the first 30 minutes of pyrohydrolysis, it is possible to use moist oxygen instead of moist Ar carrier gas. The use of moist oxygen will enhance the rate of oxidation; however, a controlled oxidation is necessary in case the rate of oxidation is high. Hence, similar investigation was repeated with moist oxygen carrier gas instead of moist Ar and the results obtained were listed in Table 4.4. Interestingly, it was observed that a maximum recovery of both chlorine and fluorine were obtained

even before 30 min. As seen from the Table 4.4, the percentage recovery of Cl and F from U-Zr alloy matrix is close to 100% when the samples are heated in moist O₂ atmosphere for 30 min. Between F and Cl, the recovery of Cl is faster than F as reported earlier [18]. These observations indicate that the chlorine and fluorine pyrohydrolysis extraction kinetics is determined by the formation of U₃O₈, however, it needs to be investigated.

Table 4.3: Pyrohydrolysis data for U-6wt%Zr alloys sample for varying time using moist oxygen as a carrier gas.

Duration of pyrohydrolysis (min)	Recovery of F (%)	Recovery of Cl (%)
10	96.7 ± 14.0	100.1 ± 7.1
20	99.2 ± 8.1	98.8 ± 5.3
30	100.0 ± 5.2	100 ± 3.7
50	101.0 ± 2.3	99.2 ± 3.8

To investigate the oxidation behaviour of U-Zr alloy in oxygen atmosphere, a study was carried out using thermogravimetric (TG), differential thermal analysis (DTA) and differential thermogravimetric analysis (DTG) simultaneously. Figure 4.2 shows TG and DTA plots for oxidation of U-Zr alloy in dry air. The analysis of TG and DTG data indicate that the oxidation of alloy takes place in single step in the temperature range of 473 to 773K. The XRD pattern for the pyrohydrolysed product obtained at 1273K was similar to that of U₃O₈. Thermogravimetric study showed

that the oxidation of the alloy was completed before it reached 1173K and got converted into U_3O_8 . This clearly shows that the complete oxidation of U-Zr alloy is necessary for the quantitative extraction of Cl and F from the matrix. However, in the case of the pyrohydrolysed samples in moist Ar obtained at different time intervals at 1173K showed that the complete recovery of Cl and F was possible only when the alloy was pyrohydrolysed for at least 90 minutes.

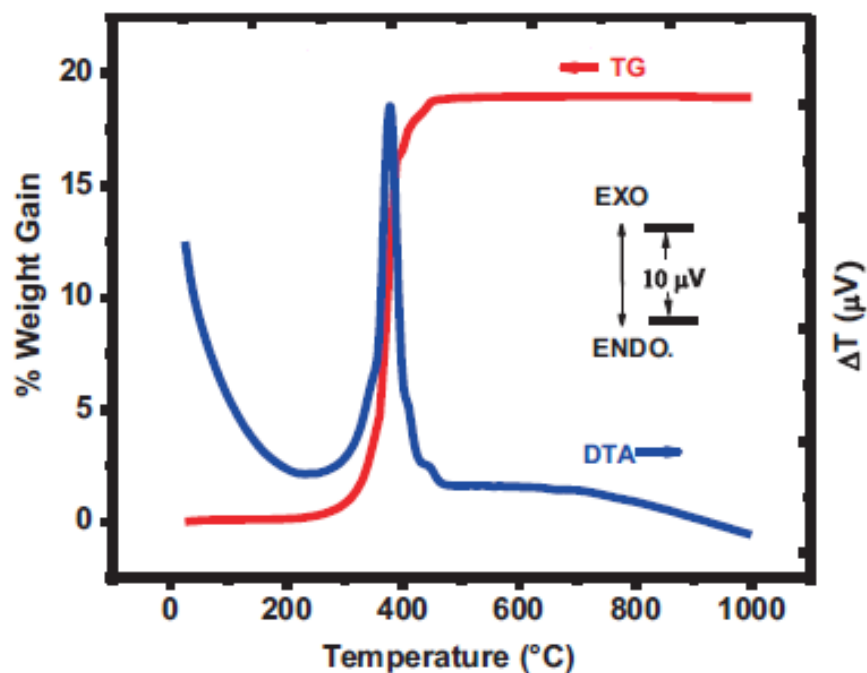


Figure 4.3: TG and DTA of U-Zr alloy in dry air with a heating rate of 10K/min.

All the above observations can be attributed to the density variations of the alloy during the oxidation process. It is known that U metal is thermodynamically unstable. While in contact with air and on heating U metal forms a hyperstoichiometric oxide represented as UO_{2+x} and when the exposure proceeds, phase transformation to U_4O_9 , U_3O_7 and finally U_3O_8 will take place at 773K. During this oxidation process,

the crystal structure will also change from FCC (UO_2) to orthorhombic (U_3O_8). The density calculated from X-ray data is 8.34 g/cc for U_3O_8 compared with 10.96 g/cc for UO_2 and this decrease in density resulted by the formation of U_3O_8 phase (~36% increase in unit cell volume for conversion of UO_2 to U_3O_8). This micro structural change can break up the material and lead to a large macroscopic expansion.

Based on the results obtained for U-Zr alloys, further studies were extended to U-Pu-Zr alloy. U-Pu-Zr alloys were also analyzed in moist oxygen atmosphere. Pyrohydrolysis of the U-Pu-Zr alloy samples was carried out by varying time of pyrohydrolysis at 1173K and the data are given in Table 4.5.

Table 4.4: Pyrohydrolysis data for U-19 wt% Pu-4.7 wt% Zr alloy sample for varying pyrohydrolysis time, with moist oxygen as carrier gas.

Duration of pyrohydrolysis (min)	U-Pu-Zr alloy	
	Moist O_2	
	Recovery of F (%)	Recovery of Cl (%)
10	91.5 ± 10.1	96.6 ± 5.1
20	99.6 ± 9.8	99.6 ± 6.7
30	100.0 ± 5.5	100.0 ± 4.7

Table 4.5 shows that heating of 30 minutes is sufficient for the quantitative recovery of Cl and F. The XRD pattern obtained for U-Pu-Zr alloy after heating in moist oxygen atmosphere was shown in Figure 4.3. The summary of products identified by XRD on heat treatment in moist oxygen atmosphere is given in Table 4.6. Though the concentration of U_3O_8 is more than the FCC phase of PuO_2 in the product phase, peaks due to U_3O_8 and $(\text{Pu}, \text{Zr})\text{O}_2$ were observed for U-Pu-Zr. The solubility of

ZrO₂ in actinide oxide increases with decrease in size of actinide ion [28] and it is reported that the solubility of ZrO₂ in PuO₂ is around 77 mol% at 1673K.

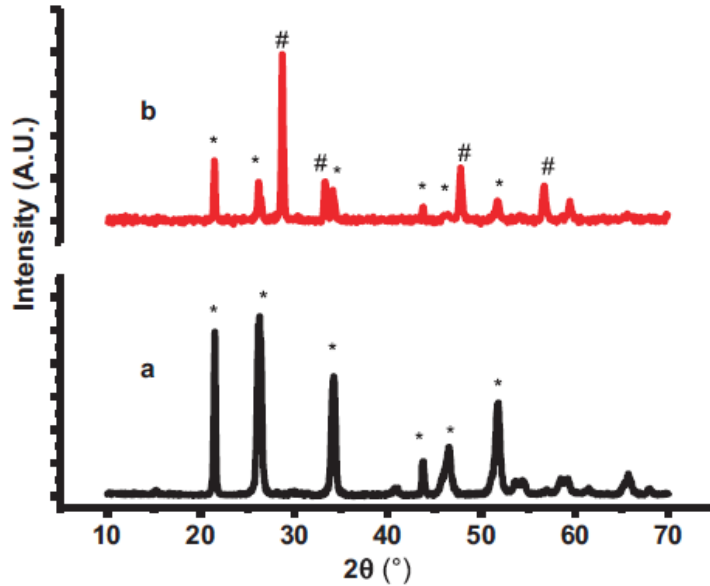


Figure 4.4: XRD patterns of pyrohydrolysed product of (a) U-Zr and (b) U-Pu-Zr alloy heated in moist oxygen atmosphere at 900°C for 30 min. (* and # represent (α -U₃O₈)ss and (PuO₂)ss, respectively)

Table 4.5: The summary of products identified by XRD on heat treatment of U-Zr and U-Pu-Zr alloys.

Starting material	Heat treatment	End product identified by XRD	Lattice parameter of FCC solid solution (Å)
U-Zr alloy	Moist O ₂ /900°C/30 min	(α -U ₃ O ₈)ss	-
U-Pu-Zr alloy	Moist O ₂ /900°C/30 min	(α -U ₃ O ₈)ss orthorhombic + FCC (Pu, Zr)O ₂	5.386 (1)

The above study has revealed that in moist oxygen, U present in the alloy gets converted into U₃O₈ in 10 min of pyrohydrolysis. An in-house working standard of

uranium oxide (UO_2) with known concentration of chloride and fluoride was used for validating the method and recovery calculations. Analysis of this standard was carried out prior to sample analysis to ensure the recoveries of F and Cl and a recovery of 95% was obtained. Replicate analysis of the sample showed good reproducibility of values.

Since the determination of chloride and fluoride was carried out by ion chromatography, the IC separation conditions were optimised. After studying the effect of eluent concentration on the retention of chloride and fluoride, the eluent was fixed as 13mM NaOH at flow rate of 1 mL/min. Limit of detections (LOD) calculated for chloride and fluoride were 20 ppb and 10 ppb, respectively.

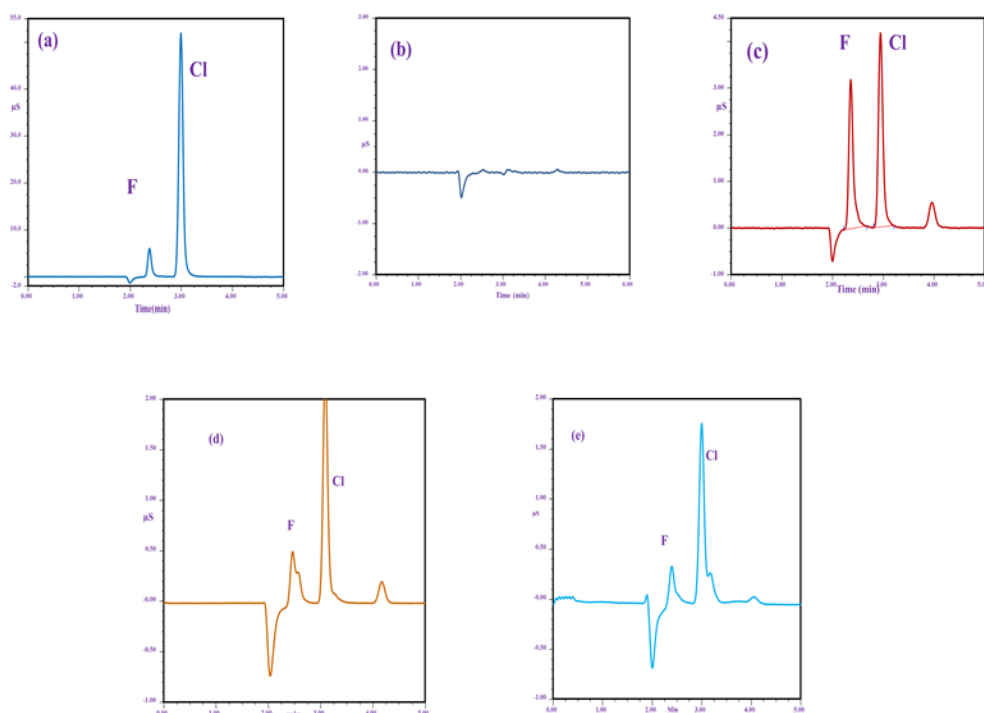


Figure 4.5: Chromatograms for different distillates analysed by IC. (a) standard solution, (b) blank run, (c) U_3O_8 standard (d) U-Zr sample and (e) U-Pu-Zr samples.

The optimised IC separation conditions could successfully be used for the analyses of the samples and the IC results obtained for samples are listed in Table 4.7. The reproducibility of measurement (precision in the measurement) was better than 5% at 0.1 ppm of both chloride and fluoride.

Table 4.6: F and Cl content of some routine samples analysed by pyrohydrolysis using moist oxygen.

Pyrohydrolysis followed by IC		
Samples aliquots	F content (ppm)	Cl content (ppm)
U-Zr alloy-1	4.1 ± 0.4	4.8 ± 0.3
U-Zr alloy-2	3.6 ± 0.4	9.2 ± 0.4
U-Zr alloy-3	5.0 ± 0.3	8.3 ± 0.5
U-Pu-Zr alloy-1	8.1 ± 0.6	25.8 ± 0.13
U-Pu-Zr alloy-2	2.9 ± 0.2	6.4 ± 0.4
U-Pu-Zr alloy-3	1.0 ± 0.2	4.3 ± 0.4
U-Pu-Zr alloy-4	1.6 ± 0.3	3.8 ± 0.5

4.4 Conclusions:

A pyrohydrolysis method for the separation of Cl and F in U-Zr and U-Pu-Zr alloys was developed. Extensive investigation on the pyrohydrolysis behaviour of the alloys revealed that the complete recovery of both chlorine and fluorine by pyrohydrolysis is possible only after converting the uranium into U_3O_8 . The relevance between oxidation of uranium to U_3O_8 was confirmed by carrying out the XRD and TG/DTA studies. Pyrohydrolysis with moist oxygen facilitated the formation of U_3O_8 in minimum time of heating and also facilitated the quantitative

release of halides. The developed method was successfully employed for the routine analysis of real samples.

4.5 References:

1. G. L. Hoffman, L. C. Walters, T. H. Bauger, *Progress. Nucl. Energ.*, 31(1997)83.
2. A.Riyas, P. Mohankrishnan, *Ann. Nucl. Energy*, 35(2008) 87.
3. S. C. Chetal, P. Chellapandi, P. Puthiyavinayagam, S. Raghupathy, V. Balasubramaniyan, P. Selvaraj, P.Mohanakrishnan, *Asian Nuclear Prospects*, 7 (2011) 64.
4. M. V.Ramaniah, *PureAppl. Chem.*, 54 (1982) 889.
5. S. H.Shann, D. R. Olander, *J. Nucl. Mater.*, 113 (1983) 234.
6. S. V. Elinson, N. A.Zemlyanukhina, I. V. Pavlova, V. P. Filatkina, V. T. Tsvetkova, *Radiokhimiya*, 23 (1981)753.
7. Y. S.Sayi, K. L. Ramkumar, V. Venugopal, *IANCAS bulletin*, 3 (2008)180.
8. H. H. Willard, O. B. Winter, *Ind. Eng. Chem. (Anal Ed.)*, 5(1933)7.
9. R. D.Dabeka, A. D. McKenzie, *J. Assoc. Off. Anal. Chem.*, 64(1981)1021.
10. M. Bettinelli, S. Spezia, C.Minoia, A. Ronchi, *At. Spectrosc.*, 23(2002)105.
11. F. G. Antes, F. A. Duarte, J. N.G. Paniz, M. F. P.Santos, R. C. L. Guimaraes, , E. M. M. Flores, V. L.Dressler, *At. Spectrosc.*, 29(2008)157.
12. V. L. Dressler, D. Pozebon, E. L. M. Flores, J. N. G. Paniz, E. M. M. Flores, J. *Braz. Chem. Soc.*, 14(2003)334.

13. Y. Muramatsu, Y. Takada, H. Matsuzaki, S. Yoshida, *Quat. Geochronol.*, 3(2008)291.
14. M. Boniface, N. Jendrzewski, P. Agrier, M. Coleman, F. Pineau, M. Javoy, *Chem. Geol.*, 242(2007)187.
15. Y. Nogushi, L. Zhang, T. Maruta, T. Yamane, N. Kiba, *Anal. Chim. Acta* 640(2009)106.
16. J. E. Rae, S. A. Malik, *Chemosphere*, 33(1996) 2121.
17. G. A. Fabiane, J. S. F. Pereira, M. S. P. Enders, C. M. M. Moreira, E. I. Muller, E. M. M. Flores, *Microchem. J.*, 101(2012)54.
18. J. C. Warf, W. D. Cline, R. D. Tevebaugh, *Anal. Chem.*, 26(1954)342.
19. M. Iwasaki, N. Ishikawa, *J. Nucl. Sci. and Tech.*, 20 (1983) 400.
20. R. M. Sawant, M. A. Mahajan, P. Verma, D. Shah, U. K. Thakur, K. L. Ramkumar, V. Venugopal, *Radiochim. Acta*, 95(2007)585.
21. M. A. Mahajan, M. V. R. Prasad, H. R. Mhatre, R. M. Sawant, R. K. Rastogi, G. H. Rizvi, N. K. Chaudhuri, *J. Radioanal. Nucl. Chem.* 148(1991)93.
22. R. M. Sawant, M. A. Mahajan, D. Shah, U. K. Thakur, K. L. Ramkumar, *J. Radioanal. Nucl. Chem.*, 287(2011)423.
23. T. R. G. Kutty, S. Kaity, C. B. Basak, Arun Kumar, R. P. Singh, *Nucl. Eng. Desn.*, 250(2012)125.
24. S. Kaity, J. Banerjee, K. Ravi, R. Keswani, T. R. G. Kutty, Arun Kumar, G. J. Prasad, *J. Nucl. Mater.*, 433(2013)206.

25. A. Saha, S. B. Deb, B. K. Nagar, M. K. Saxena, *Atomic Spectroscopy*, 34(2013)125.
26. A. Sengupta, V. C Adya, *Atomic Spectroscopy*, 34(2013)207.
27. V. R. Wiederkehr, G. W. Goward, *Anal. Chem.*, 31(1959)2102.
28. S. Jeyakumar, V. V.Raut, K. L. Ramakumar, *Talanta*, 76(2008)1246.
29. R. H. Powell, O. Menis, *Anal. Chem.*, 30(1958)1546.
30. N. K. Kulkarni, K. Krishnan, U. M. Kasar, S. K.Sali, S. K. Aggarwal, *J. Nucl. Mater.*, 384(2009)81.
31. G. A. Rama Rao, V. Venugopal, D. D.Sood, *J. Nucl.Mater.*, 209(1994)161.
32. S. K. Sali, N. K. Kulkarni, D. G. Phal, S. K. Aggarwal, V. Venugopal, *J. Am. Cer. Soc.*, 93(2010)3437.
33. D. F. Corroll, *J. Am. Cer. Soc.*, 46(1963)194.

Chapter: 5

Development of Ion Chromatography and Capillary Electrophoresis Methods for the Determination of Li in Li–Al Alloy

5.1 Introduction:

Lithium aluminium alloy is used as a target material for producing tritium by the nuclear reaction ${}^6\text{Li}(n,\alpha)\text{T}$. Li is alloyed with Al to reduce the high reactivity of Li with air and moisture [1]. In addition Al is having low neutron absorption cross-section and helps in dissipating heat. The material has potential for its use in fusion reactor, where tritium produced from Li diffuses out from solid matrix and get into the plasma of the reactor to fuse with deuterium. Li-Al alloy has advantages over pure Li such as high melting point (973K) and greater vapour pressure of tritium from the matrix [2].

For the use of the Li-Al material as a target for tritium production or for use in fusion reactor, it is important to know the exact Li content in addition to ${}^6\text{Li}$ abundance, and this would enable to ensure the calculated performance of the reactor. Therefore, certification of lithium content in Li–Al alloy demands an accurate and precise method.

The methods available for Li determination in Li-Al alloy are based on Atomic Absorption Spectrometry (AAS) and Inductively Coupled Plasma–Atomic Emission Spectrometry (ICP-AES) [3]. However, the literature shows that these methods suffer from few limitations. For instance, in AAS the Al matrix causes incomplete

atomization of Li if not separated. On the other hand in the ICP-AES the Al matrix affects the signal intensity of Li lines. This demands the separation of Al matrix prior to the sample analysis by these methods. It may be required to use the standard addition method in the absence of matrix matched standards. Electrochemical techniques may not be amenable due to lack of suitable redox valence states for alkali elements. Chromatography techniques have found extensive applications in elemental separations. There is a scope for developing a simple and rapid Ion Chromatography method where direct sample analysis without any matrix separation step is possible. Ion chromatography (IC) has found several applications for the determination of alkali and alkaline earth metals in different matrices [4–7]. Ion chromatography provides online separation as well as determination. This feature along with the flexibility of optimizing several parameters helps in modifying the separation scheme to suit the analysis of analyte(s) in complex matrices.

Capillary Electrophoresis (CE) is yet another efficient separation technique where the analytes can be separated rapidly by controlling some parameters without resorting to matrix isolation [8]. Many applications of CE have been reported for the determination of alkali metal determination [7–13]. Since IC and CE are complementary to each other, in the absence of a suitable matrix matched certified reference materials both ion chromatography and capillary electrophoresis methods can be used to validate the results obtained from each other. The validation is acceptable because separation in each method is based on different physico-chemical parameters. The present study is aimed at developing analytical procedures for the determination of Li using both ion chromatography and capillary electrophoresis, without resorting to matrix separation.

5.2 Experimental:

5.2.1 Instrumentation:

IC separations were performed on a commercial IC system (DX-500 Dionex) consisting of a gradient pump (GP-50), conductivity detector (ED-40) and a cation self-regenerating suppressor (CSRS) for suppressing background conductivity of the mobile phase. IC separations were carried out on a cation exchange column CS12 (Dionex). Capillary electrophoresis (CE) instrument, CEC-770 model (Prince Technology Netherlands), was employed and it is equipped with diode array detector. Silica capillaries of dimension (50 μm i.d. and 60 cm total length) were used throughout the study.

5.2.2 Reagents:

Methane sulphonic acid (MSA), imidazole (99.9 % purity) and stock solutions of standard alkali metal used were of Sigma-Aldrich make. Rest of the solutions were prepared using A.R. grade reagents. All the solutions were prepared in high purity water obtained from the Milli-Q Academy apparatus.

5.2.3 Sample preparation:

Prior to dissolution, the alloy samples were washed repeatedly with acetone to remove organic contaminants. Accurately weighed ($\sim 0.1\text{g}$) sample was boiled in concentrated nitric acid (5ml) till complete dissolution. In order to bring the medium of sample in 1% nitric acid the dissolved solution was heated to near dryness and 1% nitric acid was added.

5.3 Results and discussion:

5.3.1 Ion Chromatography Studies:

Direct sample injection of the dissolved sample without separation of the matrix is possible when the analyte of interest gets eluted ahead of the matrix element. Such separation is possible on a cation exchange column (order of the elution is Li followed by the matrix element Al). Since Al in the solution is in its +3 oxidation state and therefore is retained for longer time. However complete elution of Al from the column takes long time which curtails fast turn around time for multiple analyses. Therefore there is a scope to reduce the time of analysis in order to increase the sample throughput. To achieve this, a high capacity cation exchange column was selected (carboxylic acid functional group) along with its guard column. The separator column has a total capacity of 3.36 meq. In order to optimize the concentration of the eluent (MSA), separation was carried by varying the concentration of MSA. Based on the separation obtained, it was observed that 20 mM of MSA was found optimum. Elution of alkali and alkaline elements and NH_4^+ was performed with low concentration MSA. At this concentration of MSA and the flow rate, the matrix element Al has strong retention. Figure 5.1 shows a chromatogram of Alkali metal ion standards for the optimised elution conditions.

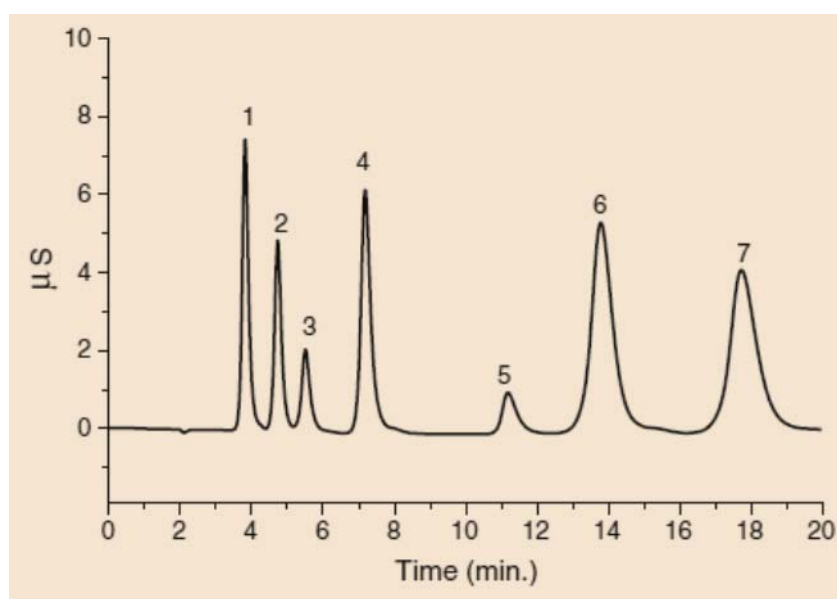


Figure 5.1: A standard sample chromatogram. Peaks 1–7 are (1) Li (2 mg/L), (2) Na (2 mg/L), (3) NH₄⁺, (4) K (5 mg/L), (5) Cs (5 mg/L), (6) Mg (3 mg/L) and (7) Ca (5 mg/L). Column: Ion Pac CS12; Eluent: 20 mM MSA; Flow rate 1ml/min.

Li was separated from Li-Al matrix using the optimised conditions. At this MSA concentration separation of Li was good without any interference from a solution having around 2.0 g/L of Al matrix (Li/Al ~ 500 to 1000).

0.1g of the sample is dissolved and diluted to 100 ml. Considering the 25µL injection volume around 2.7 µmoles of Al was injected into the column. After performing 25 sample runs the column is loaded with around 62.5 µmoles of Al, which is around 2% of the total capacity of the cation exchange column (3.36 meq). Therefore, presence of Al does not affect the separation of Li. Chromatogram of a typical sample run is given in Fig. 5.2.

After every 25 sample injections, the column was thoroughly washed with higher concentration of MSA (0.2M) to remove the matrix element Al.

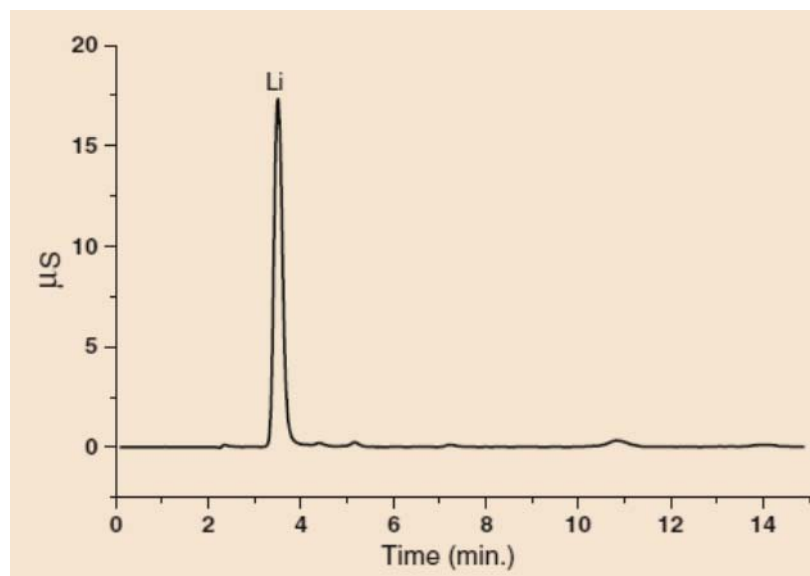


Figure 5.2: A typical sample chromatogram obtained for a sample Column: Ion Pac CS12; Eluent: 20 mM MSA. Flow rate 1mL/min. Detection Suppressed Conductivity.

The precision of the method is found to be 4.5 % at 0.3 mg/L of Li. The LOD for Li is 25 ng/L, which was calculated on the basis of $S/N = 3$ method. Calibration plot was constructed by using Li standards in the concentration range between 0.5–25 mg/L and it showed a regression coefficient better than 0.999.

5.3.2 Capillary electrophoresis studies:

The capillary electrophoresis separation of Li from Li-Al alloys without any pre-matrix separation poses two challenges.

- (i) Due to the higher charge of Al (Al^{3+}) it is expected to appear before Li in the electrogram. An early appearance of matrix peak can mask the analyte peak or disturb the base line. This causes erroneous determination of Li.
- (ii) Li^+ ion do not absorb in the UV-Vis region which is necessary for detecting trace Li^+ .

The first problem can be addressed by using a complexing agent, which is selective for Al ion. The complexing agent forms a complex with Al^{3+} as this reduces the charge density of Al ion. Therefore the Al matrix peak would appear after the analyte peak. The second problem is generally circumvented by using a co-ion in the back ground electrolyte (BGE). The co-ion is a molecule which absorbs either in UV or in Visible region, and provides a base line absorption for the BGE. When the analyte species appear in the detector due to the dilution of co-ion the baseline absorption decreases causing detection of analyte as a negative peak. Both the requirements were met using imidazole as the co-ion. Imidazole is one of the most suitable molecules used for the analysis of alkali metals as it has appreciable absorbance at 214 nm with $(0.44 \text{ m}^2/\text{kV}/\text{s})$ similar to alkali metal ions [9]. Imidazole is known to have significant complexation with Co(III), V(III) and Fe(III) [14–16], therefore, it can form complex with Al (III).

Therefore, 20 mM imidazole solution at pH 2 was chosen as BGE. For achieving better sensitivity a high potential is applied. However, generation of high current due to higher conductivity of BGE is the limiting factor. Hence it is important to maintain the BGE ionic strength as low as possible, as it can affect the joule heating significantly. Buffers that are used in the BGE are the important contributors in increasing ionic strength. Thus, use of any buffer was avoided and frequent replacement of BGE was practiced to avoid any variation in pH. With this final BGE having 20 mM Imidazole at pH 2 without any buffer, several runs were performed to optimize the applied potential. For the sample matrix under study and selected BGE composition, 20 kV of potential was found to be suitable for desired results. The electropherogram showing separation of K^+ , Na^+ , Ca^{2+} , Mg^{2+} , and Li (Fig. 5.3). Under the same separation condition the Al peak could not be observed up to 10 min.

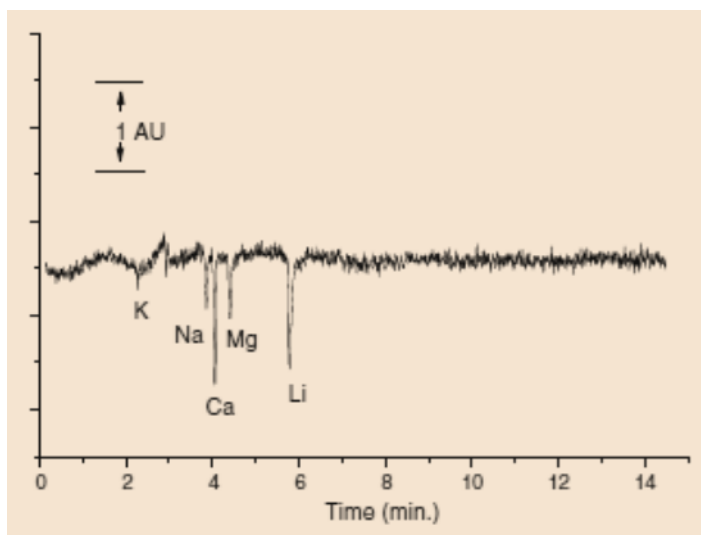


Figure 5.3: Capillary 50 μ m (i.d.) 960 cm (total length), BGE 20 mM Imidazole pH 2 Sample: (K, Na, Ca, Mg, Li) Li 1 mg/L others 0.5 mg/L.

A typical electropherogram obtained for a Li–Al alloy sample is shown in Fig. 5.4. A calibration plot was constructed with series of Li standards in the concentration range of 1–15 mg/L with regression coefficient of 0.981. It was possible to get further improvement in the regression coefficient. In CE the peak time reproducibility is relatively poor (as compared to IC), which causes variation in the peak area. To overcome the effect a plot of peak area/peak time versus Li concentration for the same concentration range was prepared, which showed an improved regression coefficient of 0.994 (Fig. 5.5). The ratio of peak area to peak time provided a correction for the variation in peak area because of small changes in peak time. The improved calibration was used for the quantitative determination of Li in samples. The limit of detection (LOD) of Li is 120 ng/L.

Several Li–Al alloy samples were analysed following the developed IC and CE methods and the results of Li contents are reported in Table 5.1.

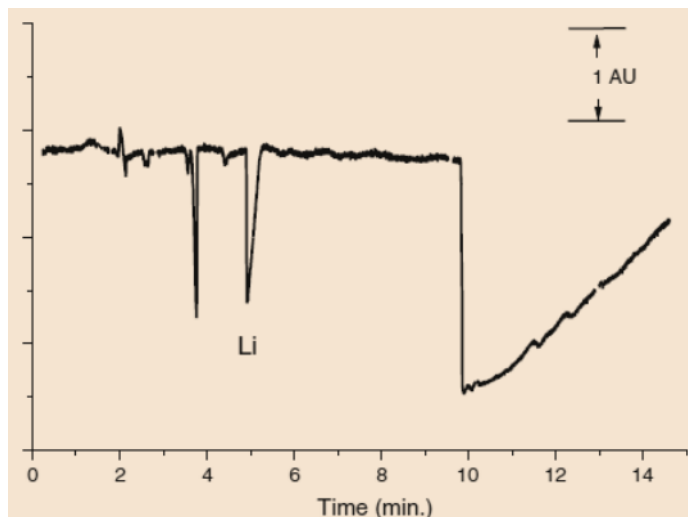


Figure 5.4: Capillary 50 μm (i.d.) and 60 cm (total length), BGE 20 mM Imidazole pH 2, Sample: (real sample having 2.1 mg/L Li)

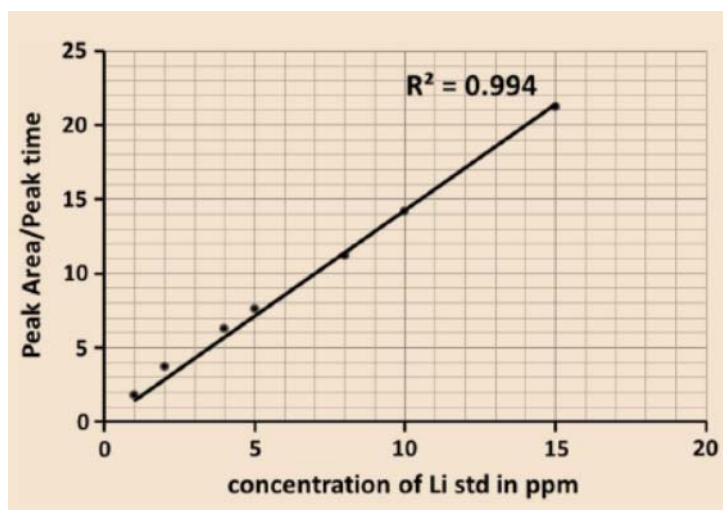


Figure 5.5: Calibration plot of peak area/peak time versus Li concentration.

Table 5.1: Comparison of Li percentage determined by CE and IC in Li–Al alloy samples.

Sample	IC (%Li)	CE (%Li)
1.	3.2 ± 0.02	3.3 ± 0.2
2.	4.7 ± 0.02	4.5 ± 0.2
3.	4.1 ± 0.02	4.1 ± 0.2
4.	4.3 ± 0.02	4.0 ± 0.2

5.4 Conclusion:

An IC method was developed for the determination of Li in Li-Al alloy. High capacity column along with a weak eluent was used to obtain interference free separation and determination with good precision and sensitivity. On the other hand selective complexation of imidazole with Al ion was used successfully in the CE method to push the matrix after analyte peak. In view of no interference from Al, samples were analyzed without any matrix separation. Both CE and IC methods produced results which were comparable and thus validate each other. Better sensitivity and lower standard deviation showed superiority of IC method over the CE method, though the latter has an advantage of faster analysis than IC.

5.5 References:

1. P. L. Carconi, S. Caradio, A. Moauro, J. Radioanal. Nucl. Chem., 151(1991)357.
2. J. R. Powell, F. T. Miles, A. Aronson, H. E. Winsche, Studies of fusion reactor blankets with minimum radioactive inventory and with tritium breeding in solid lithium compounds: a preliminary report Department of Applied Science, Brookhaven National Laboratory associated Universities Inc., Upton, New York, (1973).
3. S. P. Mirjana, Z. P. Nebojsa, M. Momir J. Anal.At.Spectrom., 4(1989)587.
4. R. R. Singh, N. M. Abbas J.Chromatogr. A, 733 (1996) 93.
5. N. Ulrike, T. Hansjorg J.Chromatogr.A, 920(2001) 201.
6. O. Zerbinati, F. Balduzzi, V. Dell'Oro, J. Chromatogr. A, 88(2000)645.
7. A. Kelker, A. Prakash, A. Mohmad, J. P. Pannakal, H. S. Kamat J. Radioanal. Nucl. Chem. 28(2011)595.
8. J. C. Reijenga, J. Radioanal. Nucl. Chem., 163(1992) 155.
9. W. Beck, H. Engelhardt, Chromatographia, 33(1992) 313
10. J. P. Pascali, D. Sorio, F. Bortolotti, F. Tagliaro, Anal.Bioanal. Chem., 396(2010) 2543.
11. E. X. Vrouwe, R. Luttge, W. Olthuis, A. Berg Electrophoresis, 15(2005) 3032
12. K. Fukushi, S. Minami, M. Kitakata, M. Nishijima, K. Yokota, S. Takeda, S. Wakida, Anal.Sci. 22(2006) 1129.
13. G. L. Klunder, J. E. Andrews, M. N. Church, J. D. Spear, R. E. Russo, P. M. Grant, B. D. Andresen, J. Radioanal. Nucl. Chem., 236(1998) 14.

14. Z. Kosrow, M. Akbar, F. Naser, F. Khalil, M. Wahid, Turk. J. Chem. 27(2003)71.
15. H. Podsiadły Polyhedron 27(2008)1563.
16. S. Staffan, Pure.Appl. Chem. 69(1997) 1549.

Chapter: 6

Rapid Separation and Quantification of Iron in Uranium Nuclear

Matrix by Capillary Zone Electrophoresis (CZE)

6.1. Introduction:

Determination of trace elements in nuclear materials is imperative as the performance of the materials depends on their chemical purity [1]. While developing new nuclear materials, it is necessary to analyse the raw materials as well as the products obtained at different stages of manufacturing for their metallic impurities. In the case of new nuclear fuel development, chemical characterisation of the product material at different process stages is desirable to account for the addition of impurities, if any. Fe and Ca are two common metallic impurities getting added up in the nuclear fuel through the process equipment [2]. Presence of these elements beyond the specified limit is undesirable. Moreover, the concentration of Fe in the fuel enables the fabricator to take adequate measures to achieve the desired purity.

Several analytical methods are available for the determination of iron in nuclear materials. The methods involving ICP-AES [3,4], ICP-MS [5], spectrophotometry [6], ion chromatography [7,8] and HPLC [9] are well known. These instrumental methods are associated with laborious and time consuming sample preparation steps as they require matrix separation prior to the instrumental analysis. While following such separation procedures, it is necessary to have a reference material to assess the recovery of analytes from the matrix. However, in the case of nuclear materials availability of reference materials is limited. Development of an analytical method for the direct instrumental analysis of the dissolved fuel samples without separating

matrix will be advantageous. This chapter deals with the development of a simple, and rapid method to for determination of Fe in nuclear fuel samples.

Capillary Zone Electrophoresis (CZE) is a powerful separation method. It can provide high speed of separation, high separation efficiency and resolving power with very small sample size. Though CZE has not been widely used for the analysis of nuclear materials, many studies have been reported in the literature where the CZE analyses of inorganic substances for common cations and anions [10-15]. Further few CE methods have been reported for the determination of metallic or cations in non-aqueous media [16,17] using partial or complete complexation techniques [18,19]. CZE in hyphenation with ICP-MS [20-22] or using quantitative microchip [23] were also used in determining very low concentrations of the metal ions. Despite the increased applications to inorganic materials, the application of CE in nuclear industry is somewhat limited [24, 25].

The separation in CZE is based on the differential electrophoretic mobility of charged compounds. The difference in charge-to-mass ratio varies the mobility of the analytes and the separation is achieved. However, in the case of transition metal cations their mobilities are almost similar due to their similar size and identical charge. This causes difficulty in their separation. Therefore, for the CZE separation of transition metals is being achieved by incorporating the following approaches [26]:

- (i) addition of a complexing agent to the carrier electrolyte [27,28]
- (ii) addition of a complexing ligand to the sample solution before introduction into the capillary [29].

Applications of CZE for the determination of iron in water, electroplating baths and cyanide complexes have been reported [30-34]. In the case of Fe, separation of Fe(II) and Fe(III) after complexing with o-phenanthroline and EDTA has been reported [35]. Another study reports the separation of Fe(III) as its DTPA complex [36]. However these reported methods cannot be adopted for the analysis of Fe in nuclear fuel samples as these ligands also form an anionic complex with U(VI), which has higher charge density than the Fe complex. For instance, with EDTA Fe(III) and U(VI) form $(\text{Fe-EDTA})^-$ and $(\text{UO}_2\text{-EDTA})^{2-}$ complexes, respectively [33, 37]. Hence the order of separation in CZE will be U followed by Fe and with this elution order injecting the dissolved uranium samples directly into the capillary will result a large peak of U matrix, which will mask the Fe peak. This demands the reversal of EOF (Electro Osmotic Flow) towards the detector direction. A common practice for achieving the reversal of EOF direction is coating the capillary with cetyltrimethyl ammonium bromide (CTAB) in alkaline pH BGE (Background Electrolyte). However, this coating method cannot be adopted in the case of uranium and iron separation as the basic pH medium of BGE will cause the hydrolysis of metal ions. Hence, alternatively, complexation with chloride was considered for the separation of iron in uranium matrix as the chloride complexes of uranium and iron are favourable for the desired separation.

The present study is aimed at developing a CZE method for the separation and quantification of iron in uranium matrix without employing pre-separation of uranium matrix. Direct analysis of the dissolved sample will lead to significant reduction in the analysis time and such analysis is helpful in analysing the process control samples.

6.2. Experimental:

6.2.1. Instrumentation:

Separations were performed on a commercial capillary electrophoresis apparatus (Prince Technologies, CEC-770, Netherlands) equipped with a photodiode array detector. Fused silica capillaries of 50 μm i.d. and 60 cm long were used. A capillary having 75 μm i.d. and 60 cm long was also used. Sample was injected in hydrodynamic mode by applying 50 mbar pressure for 0.2 minutes duration on the sample vial at which, a sample volume of 1.5 nL would get injected. System DAX software was used for data acquisition. Direct UV detection was performed at 214 nm. All the experiments were conducted at room temperature (25-27°C). A pH meter (Eutech, Tutor-model, Malaysia) was used for measuring the pH of the solutions.

6.2.2. Reagents and Solutions

Standard stock solution of Fe(III) was prepared by dissolving $\text{Fe}(\text{NO}_3)_3 \cdot 9\text{H}_2\text{O}$ (99.99%, Aldrich Chemicals, USA) in 0.01N HNO_3 . Subsequently, the working standards were made from the stock by appropriate dilutions. High purity HCl and HNO_3 acids (suprapure, MERCK, Germany) were used for the sample and electrolyte preparations. Potassium chloride (GR grade, MERCK, Germany) was used. Nuclear grade UO_2 (NFC, India) was used for the preparation of standard uranium solution and the concentration of U was obtained from biamperometric determination [38]. All solutions, electrolytes and standard solutions were prepared with ultrapure water (18 M Ω) obtained from a MilliQ-Academic System (Millipore, India).

6.2.3. Procedure for Conditioning Capillary and Sample Injection:

The capillary used was first washed with 0.2 M NaOH for 15 min and then with water for 10 min followed by rinsing with BGE for 15 min. About 1.5nL of the sample solution was injected into the capillary hydrodynamically by applying 50 mbar pressure for 0.2min. A potential of 15 kV was applied during the sample run and in between two sample runs, the capillary was again rinsed with BGE for 5 min.

6.3. Results and Discussion:

Although the capillary zone electrophoresis (CZE) applications involve samples containing analytes in comparable concentration, this study is an attempt to analyse the Fe in trace concentration in presence of high concentration of uranium. Such direct analysis is advantageous as it provides hassle free sample preparation. Since the dissolved uranium sample solution has high ionic strength, the direct injection of sample into the capillary can cause difficulties like:

(i) peak broadening (ii) variation in the EOF (iii) poor precision on the migration time and (iv) poor separation efficiency.

Despite these difficulties, direct separation of trace analytes in presence of bulk matrix is feasible in CZE provided the method satisfies two conditions:

(i) the analyte and the matrix elements should have large difference in their relative mobilities and (ii) the mobility of the analyte should be faster than matrix element.

Under these conditions, the analyte reaches the detector much earlier than the matrix element and therefore, it can be free from matrix effects. In the present case, since both uranyl and ferric ions (in their hydrated form) had little difference in their charge densities, it is difficult to separate them under normal conditions and addition

of a complexing agent is essential for their separation. As discussed earlier the organic ligands that had been used in the metal ions separations in CZE [30-36, 39] may not be suitable in the present study. Hence, complexation of these metal ions with chloride was considered because chloride forms different types of complexes with UO_2^{2+} and Fe^{3+} ions. Both uranyl and ferric ions form cationic complexes but of different charge densities. Moreover, the chloride medium enables the direct detection of selected metal ions [40,41] including iron.

The uranyl ion predominantly forms UO_2Cl^+ complex at lower concentrations of chloride ion (<0.5 M) [42,43] when the pH is between 2 and 3. When the concentration of chloride exceeds 5 M, it forms anionic complexes. Similarly, Fe(III) can form both cationic and anionic complexes with chloride such as FeCl^{2+} , FeCl_2^+ , FeCl_3 and FeCl_4^- . At lower concentrations of chloride, Fe(III) forms predominantly FeCl_2^+ [44]. The formation constants (log values) for the UO_2Cl^+ and FeCl^{2+} complexes are 0.17 and 1.52, respectively. This indicates that the Fe^{+3} has more affinity towards chloride complex formation [43,45] than UO_2^{2+} .

Therefore, with low chloride concentration it is possible to have UO_2Cl^+ and FeCl_2^+ complexes, which had different mobility due to difference in their charge differences. Therefore complexation with chloride can bring the desired separation in CZE. Since the divalent transition metal ions such as Zn(II), Cu(II), Cd(II), Mn(II) etc., [46] form either anionic or neutral chloride complexes [47] and hence, they do not interfere with Fe(III). The absorbance of the peak for iron as FeCl_2^+ complex was measured at 214 nm [45].

6.3.1. Optimization of Background Electrolyte:

A combination of HCl and KCl was considered for BGE. The role of HCl in BGE is to prevent the hydrolysis of iron, uranium and their chloride complexes by providing acidic pH whereas the KCl ensures the stability of the chloride complexes formed. All the separations were carried out with 15 kV applied voltage.

Initially the separation behaviour was investigated at different pH conditions, for this separation of Fe(III) was performed in BGE with 10^{-2} , 10^{-3} , 10^{-4} and 10^{-5} M HCl solutions corresponding to pH 2, 3, 4 and 5 without KCl. This has been carried out with a view to obtaining a BGE with minimum ionic strength possible so that effect of joule heat can be minimized. While carrying out the CZE separation, the standard iron solutions were also prepared in the respective HCl solutions in order to have almost identical composition in the BGE as well as in the standards.

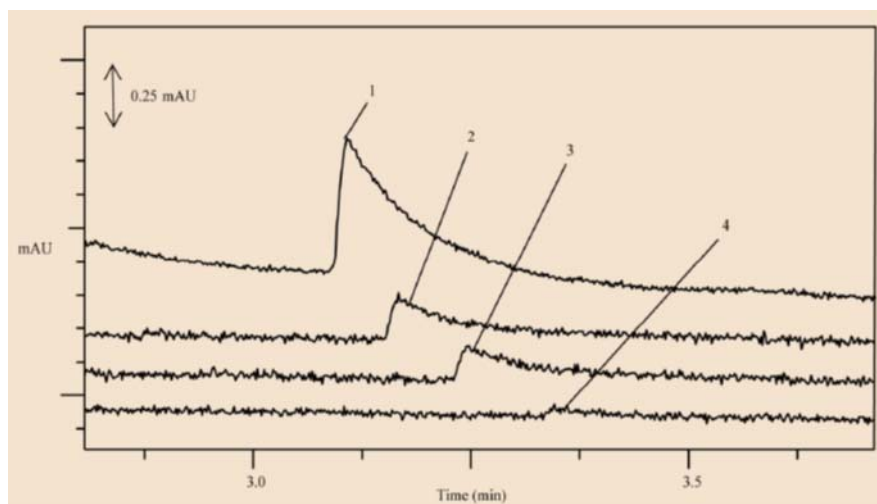


Figure 6.1. Electropherograms obtained for a standard iron solution ($25 \text{ mg}\cdot\text{L}^{-1}$) with BGEs of different pH.

- (1) 10^{-2} M HCl BGE corresponding to pH 2;
- (2) 10^{-3} M HCl BGE corresponding to pH 3;
- (3) 10^{-4} M HCl BGE corresponding to pH 4 and
- (4) 10^{-5} M HCl BGE corresponding to pH 5,

Conditions: Capillary: $60 \text{ cm} \times 50 \mu\text{m}$, Applied voltage: 15 kV. Detection: direct UV

Figure 6.1 shows the overlay of electropherograms obtained for each carrier electrolyte which shows that decreasing the pH of the carrier electrolyte decreased the migration time of Fe(III). The change in migration time in this case may be possibly due to,

- i. At higher pH the silanol group of the capillary provides negatively charged sites which retain the free metal ions of iron for longer time.
- ii. At higher pH solutions complex formation is not significant due to lower concentrations of chloride.
- iii. The hydrolysis of Fe(III) and its chloride complexes may occur and form neutral species [44].

Since the above observations are due to varying concentrations of chloride (as concentration of HCl varies), it is necessary to investigate at constant chloride concentration. Also it is necessary to study the influence of pH on the separation at a fixed chloride concentration and the effect of chloride concentration at fixed pH condition. For this purpose, three sets of solutions corresponding to pH 2, 3 and 4 were prepared. In each set, the pH was maintained by keeping a fixed concentration of HCl but the total chloride content was varied from 30 to 100 mM by adding KCl.

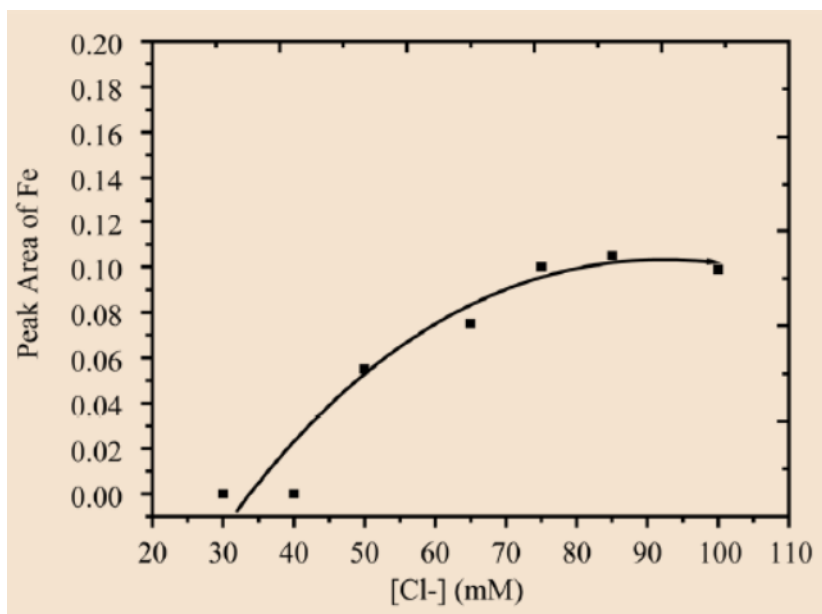


Figure 6.2. Effect of total chloride concentration on the peak area of iron obtained with pH 2. (BGEs were of 10⁻² M HCl (fixed) and varying amounts of KCl). Capillary: 60 cm × 50 μ m, Applied voltage: 15 kV; Detection: direct UV at 214nm.

It was observed (Fig. 6.2) that for pH 2 BGE the sensitivity of Fe peak increased with increasing chloride concentration and it was saturated when the chloride concentration was 75 mM chloride (10mM HCl + 65mM KCl). Increasing the chloride concentration above 75 mM caused only marginal changes in the peak areas. On the other hand, at higher pH and chloride concentrations the base line was noisy and could not be used for analysis. It is expected that during the CZE separation a little change in the pH of the electrolyte due to applied potential and protonation of silanol groups. The effect of this slight pH variations was studied with electrolytes of pH 1.8, 2.0 and 2.2. However, it was found that under these three pH conditions the variations in peak time and peak area were within $\pm 1\%$. Based on the observations, a BGE of 10mM HCl and 65mM KCl (pH 2) was found as optimum BGE composition.

With the optimized BGE condition the uranyl ion (as UO_2Cl^+) appeared much later than iron peak. On the other hand the transition, alkali and alkaline earth metal cations could not be detected even up to 60 minutes and this could be due to the formation of their anionic complexes, which are moving either with low mobility or in opposite direction. The peaks of Fe(III) and U(VI) were confirmed by injecting the standard mixture solutions of different concentrations.

6.3.2. Optimization of Applied Voltage:

In CZE the number of theoretical plates (N) can be expressed as [48],

$$N = \mu \exp(V/2D_s)$$

where N is efficiency, μ is constant, V is applied voltage and D_s is the diffusion coefficient. The above equation shows that higher efficiency of separation may be achieved by applying higher potential. Hence the effect of applied potential on the separation between Fe(III) and U(VI) was studied between 5 and 30 kV. It was observed that when the applied potential is 20kV the change in the mobility and reproducibility of Fe and U peaks was significant and the resolution between Fe and U at higher voltages were found to be poor. A plot of current Vs applied voltage showed that the current and voltage was non linear beyond 18 kV. This indicates that the capillary is unable to dissipate the Joule heat generated in the capillary at this high voltage. Therefore, an applied voltage of 15 kV was fixed for further separation. Figure 6.3 shows typical electropherograms obtained for Fe(III) of different concentrations under the optimized conditions.

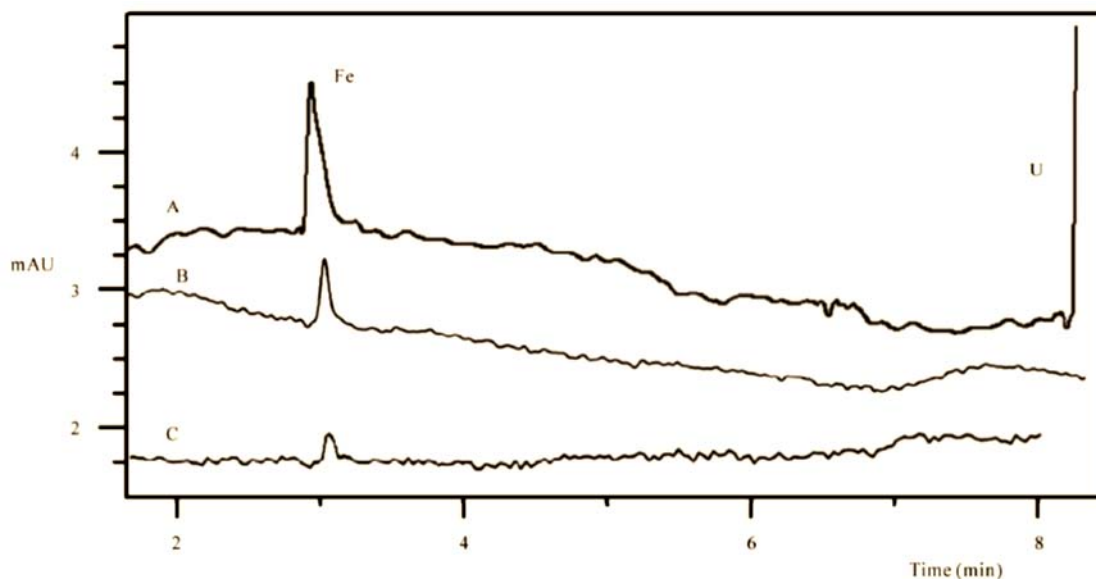


Figure 6.3. Electropherograms obtained for a standard solution of Fe(III) and Uranium. (A) Fe(III) (5 $\mu\text{g}/\text{mL}$) + U(VI) (80,000 $\mu\text{g}/\text{mL}$) standard solution; (B) Fe(III) standard solution (1 $\mu\text{g}/\text{mL}$); (C) Fe(III) (0.08 $\mu\text{g}/\text{mL}$) standard solution. BGE: 10 mM HCl in 65 mM KCl (pH 2), Conditions: Capillary: 60 cm \times 50 μm , Applied voltage: 15 kV. Detection: direct UV at 214 nm.

6.3.3. Matrix element tolerance:

Since the separation is aimed at determining iron in presence of matrix uranium, the tolerance of uranium was studied. For this purpose, 50 ppm Fe standard was taken in varying amounts of U(VI) (0.1-90 mg of U/mL) and they were analysed for the Fe. The values obtained are tabulated in Table 6.1 and it showed overall precision and accuracy better than 5%. The data also show a good recovery of Fe in presence of bulk uranium.

Table 6.1: Recoveries of spiked iron in uranium solutions of various concentrations.

No.	Uranium (ppm)	Fe spiked in U solution (ppm)	Fe determined by CE (ppm)	% of recovery
1.	10	50	48.6 ± 2.4	97.2
2.	1000	50	48.3±2.7	96.6
3.	10000	50	51.9±2.9	103.8
4.	50000	50	47.9±3.1	95.8
5.	75000	50	52.3±2.6	104.6
6.	90000	50	51.8±2.8	103.6

6.3.4. Validation of Method:

The possible interferences from transition metal ions was studied and it was observed that the metal ions like Cu(II), Pb(II), Ni(II), Zn(II), Mn(II), Co(II), Cd(II), Cr(III), alkali, alkaline earth metals (300 ppm each) did not interfere at Fe peak. Hence, the CZE separation is highly specific for Fe(III).

A linear calibration plot was constructed using the Fe(III) standards in the concentration range of 1-50 ppm. The linear correlation coefficient obtained in this case was 0.9995. The limit of detection (LOD) for Fe(III) was calculated and it was found to be 0.1 ppm. The absolute LOD is 9×10^{-14} g, where the sample volume was 1.5 nL. An electrogram obtained for 0.08 ppm of iron, which is very close to the detection limit was also shown in Figure5.3.

The reproducibility of peak area and peak time was studied with two standards viz. Std-1 (5 ppm of Fe alone) and Std-2 (5 ppm of Fe(III) and 80 ppm of U(VI)). Ten consecutive run of the standards provided a precision better than 2% on peak area whereas a precision of 1% was obtained on the peak time of Fe(III). However, replicate analyses (n = 20) of a 1 ppm iron standard solution under the optimized conditions brought about a precision of 3.5%.

6.4. Analysis of Certified Reference Materials:

To check the accuracy of the developed procedure, two reference materials of U_3O_8 viz. ILCE-4 and ILCE-5 (CRM-DAE) [49] were used and analysed. Accurately weighed quantities (0.3 - 0.4 g) of the reference materials were dissolved in 5 mL of high purity Conc. HNO_3 and the solution was heated to near dryness and the process was repeated twice or thrice until the sample is completely dissolved. Further 3.5 mL of 0.01 N HCl (pH 2) acid solution was added at warm condition. The pH of adjusted using 0.01 N HCl solution, if required. Prior to sample injection, the solution was transferred into a standard volumetric flask and made up to 5 mL using 0.01 N HCl. The nitric acid dissolution helped in maintaining the higher oxidation states of Fe and U. The sample preparation step completes within 30 minutes as it does not involve any separations. Table 6.2 compares the results obtained for the two reference materials and the values obtained by this method are in good agreement with the certified values.

Table 6.2: Comparison between iron determination via the developed method and certified method.

No.	Reference standard code	Concentration of Fe (ppm)		
		mean	certified	% deviation
1.	ILCE-IV	163.5 ± 2.8	170	3.8
2.	ILCE-V	275.2 ± 2.9	290	5.4

6.5. Real Sample Analysis:

The method was applied to nine uranium fuel samples from an advanced fuel fabrication facility. The samples are either in metallic or oxide form of uranium. Samples were dissolved by following the procedure as described above for the standard reference materials. Dilutions of the samples were carried out as per the requirement to bring Fe concentration to the linearity range. Table 6.3 lists the typical iron contents determined in the samples. An electropherogram obtained for a sample is presented in Fig. 6.4.

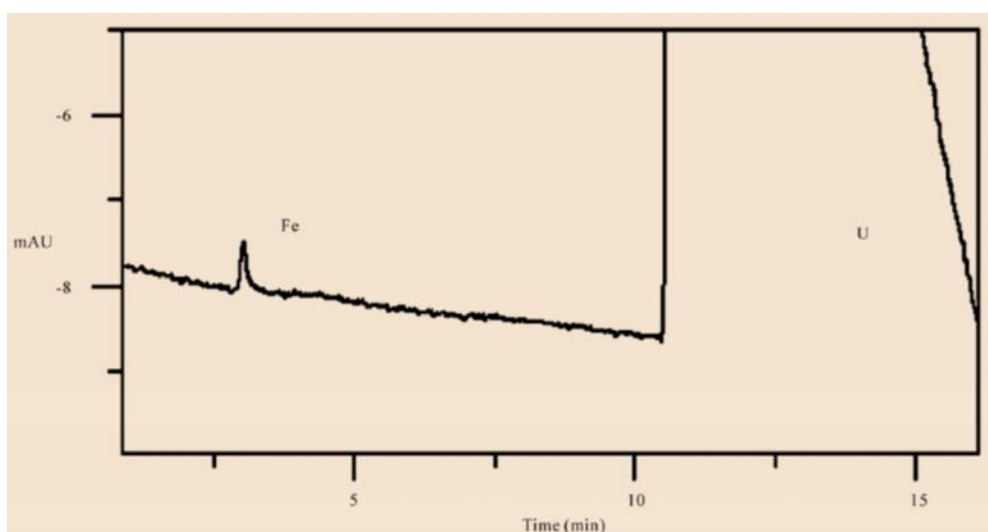


Figure 6.4: A typical electropherogram obtained for a sample solution.

Table 6.3: Results obtained for the samples.

Sample Code	Fe (ppm)
M1	882 ± 52
M2	1311 ± 70
M3	753 ± 37
M4	801 ± 36
M5	913 ± 46
U1	318 ± 19
U2	723 ± 33
U3	626 ± 29
U4	389 ± 18

6.6. Advantages of the CZE Method:

The method developed for the determination of Fe in U matrix by CZE brought following advantages:

- (i) specific for iron
- (ii) shows high tolerance for uranium matrix
- (iii) simple sample preparation procedure
- (iv) rapid separation

(v) provides good precision and better recovery of Fe

(vi) generation of minimum analytical waste

6.7 Conclusions

A rapid, reproducible and simple CZE method for the determination of iron in uranium matrix was developed. For the desired separation chloride complexation of both the species were explored. The capability of the method for determining iron with high background of the matrix element was proved by analyzing matrix match reference materials. The method was applied successfully to the determination of iron in different uranium fuel samples.

6.8 References:

1. M. V. Ramaniah, Pure Appl. Chem., 54(1982)889.
2. H. C. Bailly, D. Menessier, C. Prunier, "The Nuclear Fuel of Pressurized Water Reactors and Fast neutron Reactors: Design and Behavior," Lavoisier Publishing Inc., Paris, 1999.
3. K. S. Rao, T. Balaji, T. P. Rao, Y. Babu and G. R. K.Naidu, Spectrochim.Acta, Part B, 57(2002) 1333
4. M. Gopalakrishnan, K. Radhakrishnan, P. S. Dhani, V. T.Kulkarni, M. V. Joshi, A. B. Patwardhan, A. Ramanujam, J. N. Mathur, Talanta, 44(1997)69.
5. H. Vanhoe, C. Vandecasteele, J. Versieck, R. Dams, Anal. Chem., 61(1989)1851.
6. Z. Marczenko and M. Balcerzak, Separation, Preconcentration and Spectrophotometry in Inorganic Analysis, Elsevier, (2000)226.

7. A. Kelkar, A. Prakash, M. Afzal, J. P. Panakkal H. S.Kamath, J.Radioanal. Nucl. Chem., 284(2010)443.
8. V. V. Raut, M. K. Das, S. Jeyakumar, K. L. Ramakumar, Proceedings SESTEC-2008, Delhi, 12-14 March 2008.
9. R. M. Cassidy, S. Elchuk, J. Liq. Chromatogr. Related Technol., 4, (1981)379.
10. S. Hjerten, Chromatographic Reviews, 9(1967)122.
11. A. K. Malik, Methods MolBiol, 328(2008)21.
12. J. S. Fritz, J.Chromatogr. A, 884(2000)261.
13. A. R. Timerbaev, Electrophoresis, 25(2004)4008.
14. A. R. Timerbaev, Electrophoresis, 28(2007)3420.
15. A. R. Timerbaev, Electrophoresis, 31(2010)192.
16. F. Qu, J. Lina, J.Chromatog. A, 1068(2005)169.
17. F. Qu, J. Lin, Z. Chen, J.Chromatogr. A, 1022(2004)217.
18. E. Naujalis and A. Padarauskas, J.Chromatogr. A, 977(2002)135.
19. J. Gao, X. Sun, W. Yang, H. Fan, C. Li, X. Mao, J.Chil. Chem. Soc., 53(2008)431.
20. B. H. Li, X. P. Yan, J. Sep. Sci., 30(2007)916.
21. J. E. Sonke, V. J. M. Salters, J.Chromatog.A, 1159(2007)63.
22. R. Kautenburger, H. P. Beck, J.Chromatogr. A, 59(2007)75.
23. E. X. Vrouwe, R. Luttge, W. Olthuis, A. van den Berg, J.Chromatogr. A, 1102(2006) 287.
24. G. L. Klunder, J. E. Andrews, P. M. Grant, B. D. Andresen, R. E. Russo, Anal. Chem., 69(1997)2988.
25. B. Kuczewski, C. M. Marquardt, A. Seibert, H. Geckeis, J. V. Kratz, N. Trautmann, Anal.Chem., 75(2003)6769.

26. A. R. Timerbaev, J. Capillary Electrophor., 1(1995)14.
27. F. Foret, S. Fanali, A. Nardi and P. Bocek, Electrophoresis, 11(1990) 780.
28. Y. Shi and J. S. Fritz, J.Chromatogr. A, 640(1993)473.
29. A. R. Timerbaev, O. P. Semenova, O. M. Petrukhin, J.Chromatogr. A, 943(2002)263.
30. S. Pozdniakova, A. Padaruskas, G. Schwedt, Anal.Chim.Acta, 351(1997)41.
31. B. Y. Deng, C. J. Zeng, W. T. Chan, Spectros.Spect.l Anal., 25(2005) 1868.
32. P. Blatny, F. Kvasnicka, E. Kenndler, J.Chromatogr. A, 757(1997)297.
33. B. Baraj, M. Martinez, A. Sastre and M. Aguilar, J.Chromatogr. A, 695(1995)103.
34. G. Owens, V. K. Ferguson, M. J. McLaughlin, I. Singleton, R. J. Reid, F. A. Smith, Environ. Sci. Technol., 34(2000) 885.
35. S. Schaffer, P. Gared, C. Dezael and D. Richard, J.Chromatogr. A, 740(1996)151.
36. W. Buchberger, S. Mulleder, Mikrochim.Acta, 119(1995)103.
37. P. Kuban, P. Kuban, V. Kuban, J.Chromatogr. A, 836(1999)75.
38. M. Xavier, P. R. Nair, K. V. Lohithakshan, S. G. Marathe, H. C. Jain, J.Radioanal. Nucl. Chem., 148(1991)251.
39. I. Ali, V. K. Gupta, H. Y. Aboul-Enein, Electrophoresis, 26(2005)3988.
40. B. Baraj, A. Sastre, A. Merkoci, M. Martinez, J.Chromatogr. A, 718(1995)227.
41. B. Baraj, A. Sastre, M. Martinez, K. Spahiu, Anal.Chim.Acta, 319(1996)191.
42. C. Hennig, K. Servaes, P. Nockemann, K. V. Hecke, L. V.Meervelt, J. Wouters, L. Fluyt, C. Gorller-Walrand, R.V. Deun, Inorg.Chem., 47(2008)2987.
43. C. Hennig, J. Tutschku, A. Rossberg, G. Bernhard, A.C. Scheinost, Inorg. Chem., 44(2005)6655.

44. N. J. Welham, K. A. Malatt and S. Vukcevic, *Hydrometallurgy*, 57(2000)209.
45. W. Liu, B. Etschmann, J. Brugger, L. Spiccia, G. Foran, B. McInnes, *Chem. Geol.*, 231(2006) 326.
46. W. Walkowlak, D. Bhattacharyya, R. B. Grieves, *Anal. Chem.*, 48(1976) 975.
47. J. Bjerrum, *Acta Chem. Scand. Ser. A*, 41(1987)328.
48. H. Engelhardt, W. Beck and T. Schmitt, "Capillary Electrophoresis," Friedrich Vieweg&SohnVerlagsgesellschaftmbH, Braunschweig/Wiesbaden, 1996.
49. DAE-Interlaboratory Comparison Experiment (ILCE) for Trace Metal Assay of Uranium, Phase-II Experiments: Development of Certified U₃O₈ Reference Materials, Document, BARC, India, February 2002.

Chapter : 7

Application of Ion chromatography for Optimizing Washing Procedure for Removal of Chloride and Nitrate from Li_2TiO_3 Microspheres using LiOH Solution.

7.1 Introduction:

For the International Thermonuclear Experimental Reactor (ITER) programme different types of Li compounds have been considered as Test Blanket Material (TBM) for tritium breeding. In these materials tritium is generated due to the nuclear reaction with neutrons: ${}^6\text{Li}(n,\alpha){}^3\text{T}$. Tritium formed in the breeder matrix will be recovered by purging with helium. For the purpose of producing tritium, many ceramic lithium compounds such as Li_2O , LiAlO_2 , Li_2ZrO_3 , Li_2TiO_3 and Li_4SiO_4 are under consideration. Among them Li_2TiO_3 has relatively better chemical stability and tritium recovery at lower temperatures. Although it can be fabricated by various methods [1-5], the sol-gel based processes have several advantages over the other methods. In BARC synthesis of Li_2TiO_3 (Lithium enriched to 60% in Li-6) is being carried out by following an internal gelation technique of sol-gel process[6]. Lithium nitrate and TiOCl_2 are the starting materials for the synthesis. It is seen the final product Li_2TiO_3 microspheres is getting contaminated with significant quantities of nitrate and chloride from the feed materials. Presence of nitrate and chloride are not desirable because, they cause cracking of microspheres during sintering at high temperatures. Therefore, in order to improve the fabrication procedure to obtain nitrate and chloride free product, it was planned to wash the product with enriched LiOH solution. The washing with enriched LiOH is necessary in order to avoid

leaching of Li from the final matrix and also to avoid dilution of ${}^6\text{Li}$ due to the isotopic exchange with ${}^7\text{Li}$. Only minimum quantities of ${}^6\text{LiOH}$ should be used to conserve this precious material. Therefore the enriched LiOH has to be used judiciously. In order to decide the total volume of ${}^6\text{LiOH}$ required, it is necessary to know the total nitrate and chloride contents in the microspheres and also the quantities of Cl^- and NO_3^- removed during each washing cycle. The amount of impurities removed in the washed solutions will help in deciding the washing program which will use minimum LiOH. The wash solutions were analysed for the concentrations of chloride and nitrate. Various methods were reported for the analysis of Cl^- and NO_3^- . Ion Chromatography is widely used for determination of chloride and nitrate in different types of matrices [7-11]. Optimization of various IC parameters to realize good separation between nitrate and chloride and their determination is necessary as the samples are of high ionic strength.

In addition to the determination of chloride and nitrate in wash solutions it is also important to analyse the finished product to confirm the removal of impurities. It is important to certify the chloride impurity in the product as chloride is corrosive in nature. This necessitates the determination of chlorine in the final product of Li_2TiO_3 as a part of its chemical characterization. In general the impurity analyses in various matrices are carried out using an appropriate method after the dissolution of the sample. However, for the analysis of trace impurities, the dissolution of the sample can lead to high background and blank contributions. In view of these, non-destructive analysis (NDA) methods are always preferred [12]. In addition to this Li_2TiO_3 is difficult to dissolve.

Pyrohydrolysis is a well known separation technique mainly used to separate halides directly from a solid sample. The separated analytes are collected in a dilute NaOH.

The distillate collected is clean and interference free, which can be used for trace level analysis. The final determination of halides can be carried out by suitable methods such as, spectrophotometry or ion chromatography etc. [13-21]. In addition to halides, nitrogen from the sample is also separated but their separation is not quantitative, however qualitative information regarding the presence of nitrogen in the sample can be obtained. The present study is aimed at (i) proposing a simple IC method for the determination of chloride and nitrate in LiOH washing solutions, (ii) developing a washing strategy to minimise the volume of LiOH and (iii) developing a pyrohydrolysis- ion chromatography combined method for the determination of chlorine in the Li_2TiO_3 microspheres.

7.2 Experimental:

7.2.1 Materials and reagents:

Analytical grade LiCl, LiNO_3 , hexamethylenetetramine (HMTA), urea, TiCl_4 and LiOH were used for the synthesis of Li_2TiO_3 . Standard solutions of chloride and nitrate were prepared by dissolving their respective Na salts of 99.9% purity. NaOH (99.9% purity) was used for the preparation of mobile phase. All reagents were obtained from Merck, Germany. For the preparation of all solutions and production of steam, high purity deionised water (18.2 M Ω cm) obtained from a Milli-Q water system (Millipore, USA) was used.

7.2.2 Instrumentation:

A quartz pyrohydrolysis (PH) apparatus was used. The details of the pyrohydrolysis apparatus was described elsewhere [22]. A commercial ion chromatograph (DX-500 model; Dionex, USA) consisting of a gradient pump (GP-50), ED-40 conductivity

detector and an anion self-regenerating suppressor (ASRS-II) was used for obtaining the chromatograms. Samples were introduced through a Rheodyne injector fitted with a 50- μ L loop. Ion chromatographic separations were carried out separately on two analytical columns, viz. IonPac AS16 (250 \times 4 mm) and IonPac AS18 (250 \times 4 mm) along with their respective guard columns, IonPac AG16 (50 \times 4 mm) and AG18 (50 \times 4 mm) respectively.

7.3 Results and Discussion:

For optimisation of process parameters, initial experiments were carried out using natural Li bearing compounds. This has been done to conserve the more expensive enriched Li-6 bearing compounds. The optimised parameters were then used for the enriched material.

7.3.1 Preparation and washing of Li_2TiO_3 :

Lithium titanate microspheres were prepared by using the internal gelation process [6]. By mixing 3 M HMTA/urea solution, 3 M TiOCl_2 and 3 M $\text{LiCl}/\text{LiNO}_3$ solutions with Li to Ti mole ratio as $\text{Li}:\text{Ti} = 2:1$, a feed solution was prepared. This feed solution in the form of droplets was dispersed in hot silicone oil, where Li_2TiO_3 microspheres are formed. The microspheres formed are first washed with CCl_4 and then with LiOH . The washing with LiOH was required for removal of nitrate and chloride, which are responsible for cracking of microsphere during drying and heating steps. To stop the leaching of Li from the microspheres washings were performed with 1.55 M LiOH . In this work washing processes were carried out batch wise with minimum volume of LiOH solution (Li-natural) and the generated washing effluents were reused with a view to reduce the total volume of LiOH solution actually required. The amount of nitrate and chloride in the washing

solutions obtained in each step helped in planning a washing strategy for Li_2TiO_3 microspheres so as to realise minimum volume of LiOH .

7.3.2 Sample preparation for IC analysis

Each washing effluent was sampled and filtered through 0.2 μm filter paper to remove the microspheres. Since the washing solutions were reused during the entire process, the solutions obtained from the initial washings had higher concentrations of chloride and nitrate. Therefore, the samples were diluted appropriately to bring the Cl^- and NO_3^- concentrations within the dynamic calibration range (100 ppb to 10 ppm) of IC analysis.

7.3.3 Ion chromatographic analysis:

IC can facilitate the simultaneous separation and determination of different anions especially halides, nitrate, sulphate etc. The samples have high ionic strength and varying concentrations of the analytes. This necessitates the selection of appropriate eluent as well as analytical column. Because the sample contains a large amount of OH^- ions hydroxide eluent was preferred over the carbonate.

For the selection of separator column, two anion exchange columns viz. IonPac AS16 and IonPac AS18. Both columns have been selected based on the column chemistry as well as differences in their column capacities. Standard solutions of fluoride, chloride, nitrate and sulphate were prepared in 1.5 M LiOH and injected into the IC. [Figures 7.1 (a) and (b) show plots of retention time vs. NaOH concentration for IonPac AS18 and IonPac AS16, respectively.] It can be seen that for a given concentration of the eluent, the AS16 column offers faster elution than IonPac AS18 column. Figure 7.2 shows the chromatograms obtained with both

IonPac AS16 and AS18 columns using 15mM and 40mM NaOH eluents respectively. Although the chloride peak appeared at the same time with both the columns, the IonPac AS16 column provided a better resolution between chloride and nitrate compared to the IonPac AS- 18 column. Based on the observations, the IonPac AS16 column along with 15 mM NaOH eluent at a flow rate of 1 mL/min was identified as suitable for the elution of chloride and nitrate.

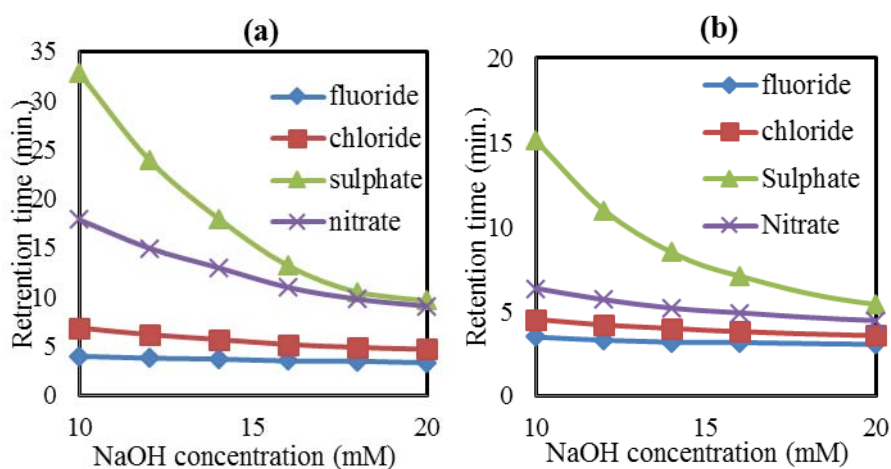


Fig. 7.1: Effect of [NaOH] on the retention times of various anions.

(a) IonPac AS18 column and (b) IonPac AS16 column.

Calibration plots were constructed for both Cl^- and NO_3^- in the concentration range of 0.1 to 10 ppm. The linear regression coefficient obtained for the plots corresponding to Cl^- and NO_3^- are 0.998 and 0.995 respectively. The limit of detection (LOD) for chloride and nitrate were calculated as 25 and 40 ppb, respectively. The precision of the measurements was better than 5% (RSD) at 0.3 ppm of Cl^- and 0.5 ppm of NO_3^- (Figure 4).

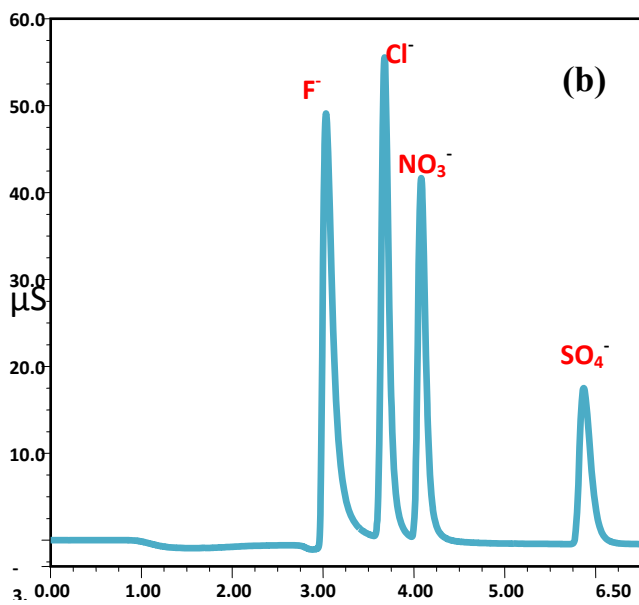
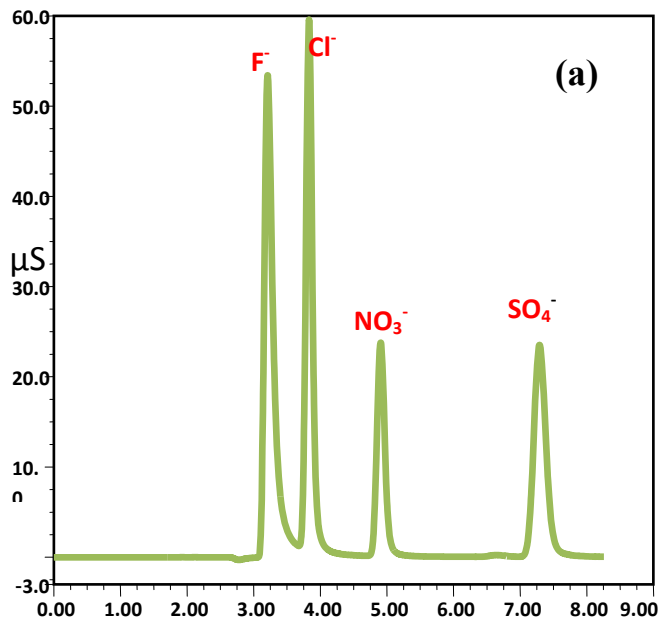


Figure 7.2: Standard chromatograms obtained for standard with F^- , Cl^- , NO_3^- and SO_4^{2-} (10.0 ppm each). (a) Column: AS16 column, Eluent: 15 mM NaOH. (b) Column: AS18 column, Eluent: 40 mM NaOH.

7.3.4 Reduction in volume and recycling of LiOH washing effluent:

A single batch of lithium titanate microspheres weighing about 200g was prepared using internal gelation process. Further it was divided into four parts (A, B, C and D). Part A was digested at 60°C in LiOH solution (50 ml) for 18 hrs and the supernatant was filtered. The filtered effluent is labelled as effluent A₁ and it cannot be reused as it contains large quantities of chemicals leached out during digestion. Further the microspheres were given three washes of LiOH, with the washings labelled as A₂, A₃ and A₄ and the effluents produced were kept for their reuse as these solutions contain less impurities compared to A₁. However, the other three parts of the microspheres viz. B, C and D were also digested but not with fresh LiOH. Further a systematic washing plan was envisaged by knowing the level of impurities present in each washing effluent as shown in Figure 7.6. For instance, the effluent A₂ would be reused as B₁, which means it would be used for digesting the microsphere part B. Similarly A₃ would act as B₂, the second wash of B₂ and so on. Each wash had a volume of 50 mL and therefore, the total volume of LiOH wash solution required as per the wash plan was 350 mL against the actual requirement of 800 mL (similar level of impurities were removed using single wash of 800ml LiOH). Therefore the developed washing procedure significantly reduced the volume of fresh LiOH solution. The concentration of chloride and nitrate were analysed and Figure 7.7 shows a bar graph depicting the concentrations of chloride and nitrate in each washing. The figure indicates the reduction in the concentrations of chloride and nitrate sequentially.

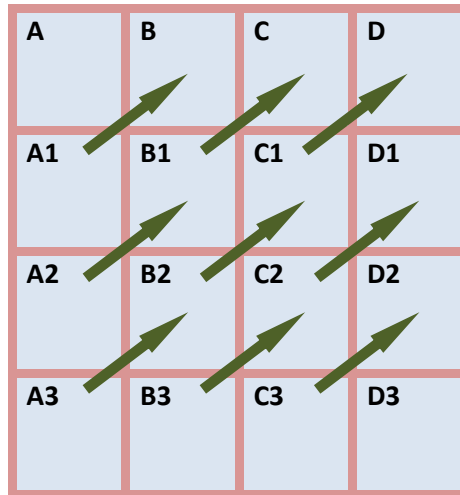


Figure 7.3 The optimised reuse of LiOH washing solution. A, B, C, and D are different Li_2TiO_3 lots, the numbers 1, 2, 3 represent no. of washing. The washing solution containing lower impurity are reused for samples containing higher impurities

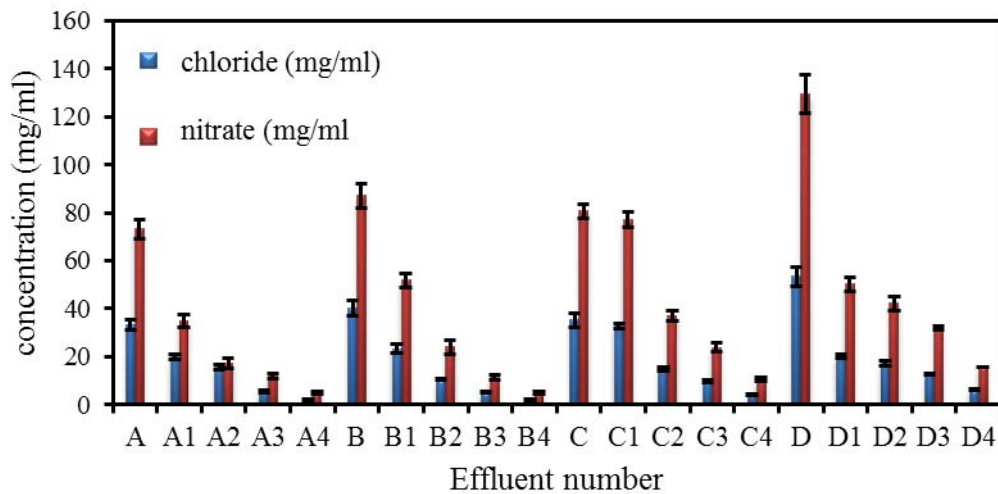


Figure 7.4: Concentration of chloride and nitrate in wash solutions collected at different steps of optimised washing method.

The optimised process parameters were used for washing enriched Li_2TiO_3 material to be used as TBM for ITER. It was possible to reduce the consumption of enriched LiOH by more than 50% (350 mL against 800 mL).

7.3.5 Determination of chlorine Li_2TiO_3 microspheres:

The determination of chlorine in the finished product, Li_2TiO_3 microspheres was carried out to ensure the efficient washing to certify the final product. This determination was carried out using pyrohydrolysis extraction of chlorine followed by ion chromatography determination combined method. Around 0.5 g of Li_2TiO_3 microspheres were pyrohydrolysed at 1273K with moist oxygen as the carrier gas. The carrier gas flow rate was maintained as 1.5 litres/min and the condensed distillate was collected in 5 mL of 15 mM NaOH . The distillate was further analysed by IC for chloride and nitrate contents.

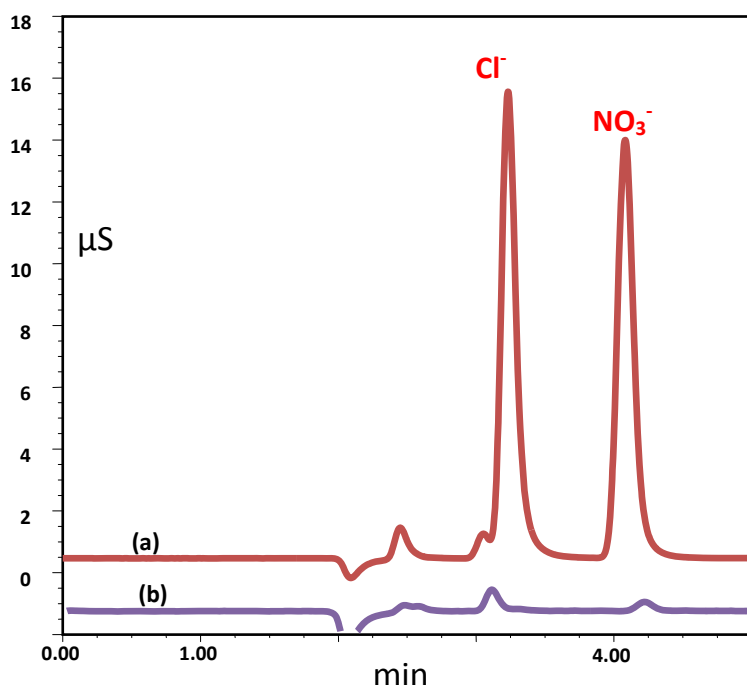


Figure 7.5: Chromatograms obtained for the Li_2TiO_3 pyrohydrolysis distillates (a) before washing (initial product) (b) after washing.

The maximum recovery of chlorine was confirmed by pyrohydrolysing different aliquots of the sample of the same lot for different time intervals. It was observed that 45 minutes of pyrohydrolysis could extract chlorine as HCl completely. Pyrohydrolysis could not extract all the nitrogen oxides. This is because nitrogen can form different species during pyrohydrolysis, these species have different solubility and pyrohydrolysis behaviour. However, the amount of nitrate present in the pyrohydrolysis distillate indicates presence or absence of nitrate in the sample as well as it provides the concentration semi-quantitatively. Table 7.1 summarizes the typical concentrations of chloride in the real samples.

Table 7.1 chlorine obtained for real samples of Li₂TiO₃ finished products.

Sample code	Chlorine(µg/g)
LiT-1	6.2 ± 0.4
LiT-2	4.9 ± 0.5
LiT-3	17.8± 1.3
LiT-4	13.1± 0.8

7.4 Conclusions

1. A washing procedure for Li_2TiO_3 microspheres for the removal of the Cl^- and NO_3^- contamination using LiOH solution was established.
2. The proposed washing procedure achieved significant reduction in the total volume of LiOH required and this would help in the judicious use of enriched LiOH solution.
3. The chlorine concentration in the washed product for is CQC certification has been realised by developing a PH-IC combined method.

7.5 References:

1. W. Xiangwei, W. Zhaoyin, H. Jinduo, X. Xiaoxiong, A. Bin Li, M. Deptula, Fusion Eng Des., 83(2008)112.
2. A. Deptuła, M. Brykała, W. Ladaa, T. Olczaka, B. Sartowska, A. G. Chmielewski, et al., Fusion Eng. Des., 84(2009)681.
3. X. Wu, Z. Wen, X. Xu., J. Nucl. Mater., 393(2009)186.
4. K. Tsuchiya, H. Kawamura, K. Fuchinoue., J. Nucl. Mater., 258(1998)1985.
5. J. R. Dahn, S. U. Von, M. W. Juzkow., J. Electrochem. Soc., 138(1991)2.
6. T. V. Vittal Rao, Y. R. Bamankar, S. K. Mukerjee., J. Nucl. Mater. 426(2012)102.
7. R. Michalski, I. Kurzyca, Pol. J. Environ.Stud., 15(2006)5.
8. N. Gros, Water., 5(2013)659.
9. M. Zhou, D. Guo, Microchem. J., 65(2000)221.

10. J. Morales, S. Ligbel, J. Mesa, *J. Chromatogr. A.*, 884(2000)185.
11. M. Neal, C. Neal, H. Wickham, *Hydrol. Earth Syst. Sci.*, 11(2007)294.
12. S. Chhillar, R. Acharya, T. Vittal Rao, Y. Bamankar, S. Mukerjee, P. Pujari, *J. Radioanal. Nucl. Chem.*, 298(2013)1597.
13. F. Antes, F. Duarte, J. N. Paniz, M. Santos, R. C. L. Guimaraes, E. Flores, *At.Spectrosc.*, 29(2008)157.
14. H. Kusuno, H. Matsuzaki, T. Nagata, et al., *Nucl. Instrum. Methods Phys. Res. Sect. B.*, 361(2015)414.
15. Y. Noguchi, L. Zhang, T. Maruta, *Anal. Chim. Acta.* 640(2009)106.
16. Y. Muramatsu, Y. Takada, H. Matsuzaki, *Quat. Geochronol.* 3(2008)291.
17. S. N. Thieli, C. M. Cristiano, B. Paua, A. L. H. Muller, M. F. Mesko, P. A. Mello, et. al. *Anal. Methods.*, 7(2015)2129.
18. V. G. Mishra, S. K. Sali, D. J. Shah, *Radiochim. acta.*, 102(2014)895.
19. R.M. Sawant, M. A. Mahajan, D. J. Shah, *J. Radioanal. Nucl. Chem.*, 287(2011)423.
20. R. M. Sawant, M. A. Mahajan, P. Verma, D. J. Shah, U. K. Thakur, K. L. Ramakumar, et al., *Radiochim. Acta.*, 95(2007)585.
21. S. Jeyakumar, V. Raut, K. L. Ramakumar. *Talanta.*, 76(2008)1246.
22. M. Mahajan, M. Prasad, H. Mhatre, R. M. Sawant, R. Rastogi, G. Rizvi, N. Chaudhari, *J. Radioanal. Nucl. Chem.*, 148(1991).

Chapter: 8

Development of Ion Chromatographic Method for the Simultaneous Separation and Determination of B, Cl and Mo in Plant and Soil Samples

8.1 Introduction:

Boron, chlorine and molybdenum along with copper, iron, manganese and zinc are important micronutrients for plants [1]. Boron plays an important role in N-metabolism, photosynthesis and cellular differentiation and development. Chlorine plays a vital role in maintaining the cell charges. Mo is important for enzyme function and N₂ fixation. On the other hand, in many cases, these micronutrients become toxic when their concentration exceeds certain limit. The micronutrient elements are available for the plants through soil. Analyses of plant and soil samples for the determination of these micronutrients are helpful in various studies relevant to both diagnostic and monitoring [2]. The concentration of micronutrient elements is also helpful as it is correlated to plant growth and yield of crops [3-5]. There are different analytical methods available for the analysis of micronutrients. Most of the methods are based on the extraction of micronutrient(s) into an aqueous phase [6] followed by instrumental analysis. However, the separation procedures followed are not amenable to simultaneous analyses as they are mostly element specific. For example, separate procedures for the extraction of B, Cl and Mo are reported in the literature [7]. The method for extracting boron uses HCl as one of the reagents and hence, it is not possible to determine Cl in the extract. Similarly the extraction of Mo uses several reagents, which causes problems in the determination of Cl and B.

Distilled water and ranex-30 solution is often used for extracting chloride, which cannot extract boron, Mo etc. Since these extraction procedures use concentrated acids for sample digestion, ion chromatographic analysis of anions become impractical [7,8].

Pyrohydrolysis, a simple separation technique, is being employed for the separation of boron, chlorine, fluorine, molybdenum etc. directly from the solid matrices without their dissolution [9, 10]. The separated species are trapped in a dilute NaOH solution. Though the organic matrices like plant samples are easily combustible at high temperatures, they need extra care during the pyrohydrolysis as the organic matrices are prone to cause flare. This demands a controlled heating pattern of the organic samples during pyrohydrolysis so as to prevent the analyte loss. The main advantage of pyrohydrolytic separation is that the distillate obtained from pyrohydrolysis has much lower ionic contents compared to the dissolved solution and therefore, the distillate is more amenable for ion chromatographic analysis. Since the non-metallic elements like Cl, B etc are present in anionic form in the distillate their simultaneous separation by IC is feasible. The pyrohydrolysis and IC combination methods have been successfully employed for the analysis of carbon nano tubes, coals and graphite [11-13] samples, which suggests the feasibility of employing pyrohydrolysis for the plant samples. Many studies have been reported on the pyrohydrolysis separation of halides and B in carbon compounds [14-16]. In addition to the extraction of non-metals by pyrohydrolysis, feasibility of separating Mo in solid uranium matrices have been reported [10]. Hence, there is a scope of applying pyrohydrolysis for the simultaneous separation of B, Cl and Mo from plant and soil samples. For this purpose, it is necessary to identify the various pyrohydrolysis conditions. The present study deals with developing a pyrohydrolysis

method for the simultaneous separation of B, Cl and Mo. In order to find the optimum pyrohydrolysis conditions, the determination of these analytes recovered under PH conditions needed to be carried out. For this, initially an IC method was developed for carrying out simultaneous separation and determination of B, Cl and Mo. Ion chromatography is the best choice for their simultaneous determination because these three analytes are in ionic form in the solution. Moreover, the procedures for their individual separation and determination has been reported in the literatures.

The IC has been used for simultaneous determination of nitrate, chloride sulphate and phosphate in plant extracts [17]. B has been determined using IC by converting it to tetrafluoroborate [18] or by using mannitol as a complexing agent [19]. In addition to this Mo in form of molybdate has been determined in different environmental samples [20, 21]. However, there is no IC method reported for their simultaneous analysis and hence, it is proposed to develop an IC method in the present work.

For the separation and determination of anions, diluted solutions of NaOH or carbonate/ bicarbonate are being used as eluents. Ion chromatography separation and determination of boron has been carried out by adding d-mannitol as a complexing agent in the eluent [9]. The determination of B by IC requires mannitol because the complex of B and mannitol has lower de-protonation constant as compared to boric acid. The lower pKa helps in getting B in anionic form during column separation and in detector (after passing through suppressor). In order to support the development of pyrohydrolysis method (for simultaneous separation of B, Cl and Mo from plant and soil samples), ion chromatographic studies were carried out to understand the effect of mannitol (as a part of eluent) on retention and sensitivity of Mo, and the

observation were employed in developing a gradient method for the simultaneous detection of B, Cl and Mo.

8.2 Experimental:

8.2.1 Reagents and materials:

The standard solutions of F^- , Cl^- , NO_3^- and SO_4^{2-} were prepared by dissolving their respective Na salts of 99.9% purity (Merck, Germany). Standard solutions of MoO_4^{2-} were prepared by dissolving $(NH_4)_6Mo_7O_{24}$ (99.98% pure, Sigma-Aldrich, USA). Standard boron solution was prepared by dissolving known amount of boric acid (Merck Germany). For the eluent the GR grade NaOH and d-mannitol, of Merck Germany make were used. The $NaHCO_3$ used was AR grade (Thomas Baker, India). For the preparation of all solutions and production of steam, high purity deionised water (18.2 M Ω .cm) obtained from a Milli-Q water system (Millipore, USA) was used.

8.2.2 Apparatus and instrument:

All quartz pyrohydrolysis set up consisting of two concentric tubes was used for pyrohydrolysis purpose. The outer tube has an inlet and serves as pre-heater for moist carrier gas. The inner tube houses the sample boat and it is attached to gas outlet. The gas outlet tube is cooled by condenser. The condensate is collected in a bottle containing dilute NaOH.

A commercial ion chromatograph (Dionex, model ICS-5000) consisting of a self-regenerator suppressor (ASRS-II) and a conductivity detector was used. Samples were introduced through a 50 μ l loop fitted with a Rheodyne injector. Separation of anions was achieved with anion columns viz. IC-Pak anion (Waters) and Ion Pac

AS16 (Dionex). A software namely Chromeleon was used for instrument control, data collection and data processing.

8.2.3 Samples:

Rice plant and soil samples were obtained from the experimental gamma field at Trombay.

8.3 Result and Discussion:

8.3.1 Separation studies:

One of our earlier studies showed that while separating boron along with halides the sensitivity of B peak was strongly dependent on the concentration of d-mannitol present in the eluent [9]. Based on this, an eluent consisting of HCO_3^- and d-mannitol was considered for separating boron as borate ion along with other anions. An anion exchange column, IC Pak Anion (Waters) was considered.

Chromatograms were obtained by injecting a standard solution having mixture of anions viz. fluoride, chloride, nitrate, sulphate and molybdate by taking the eluents as 17.5mM HCO_3^- with varying mannitol concentration from zero to 0.56M. Following observations were made from the chromatograms.

- i. Retention times of all anions did not change with change in the d-mannitol concentration in the eluent. Figure 8.1(a) as can be observed in figure 1(a), the retention times of all the anions are nearly same.
- ii. Although there is no change in the retention time of Mo peak while increasing the d-mannitol concentration in the eluent, the sensitivity of molybdate peak decreased significantly (Fig. 8.1(b)).

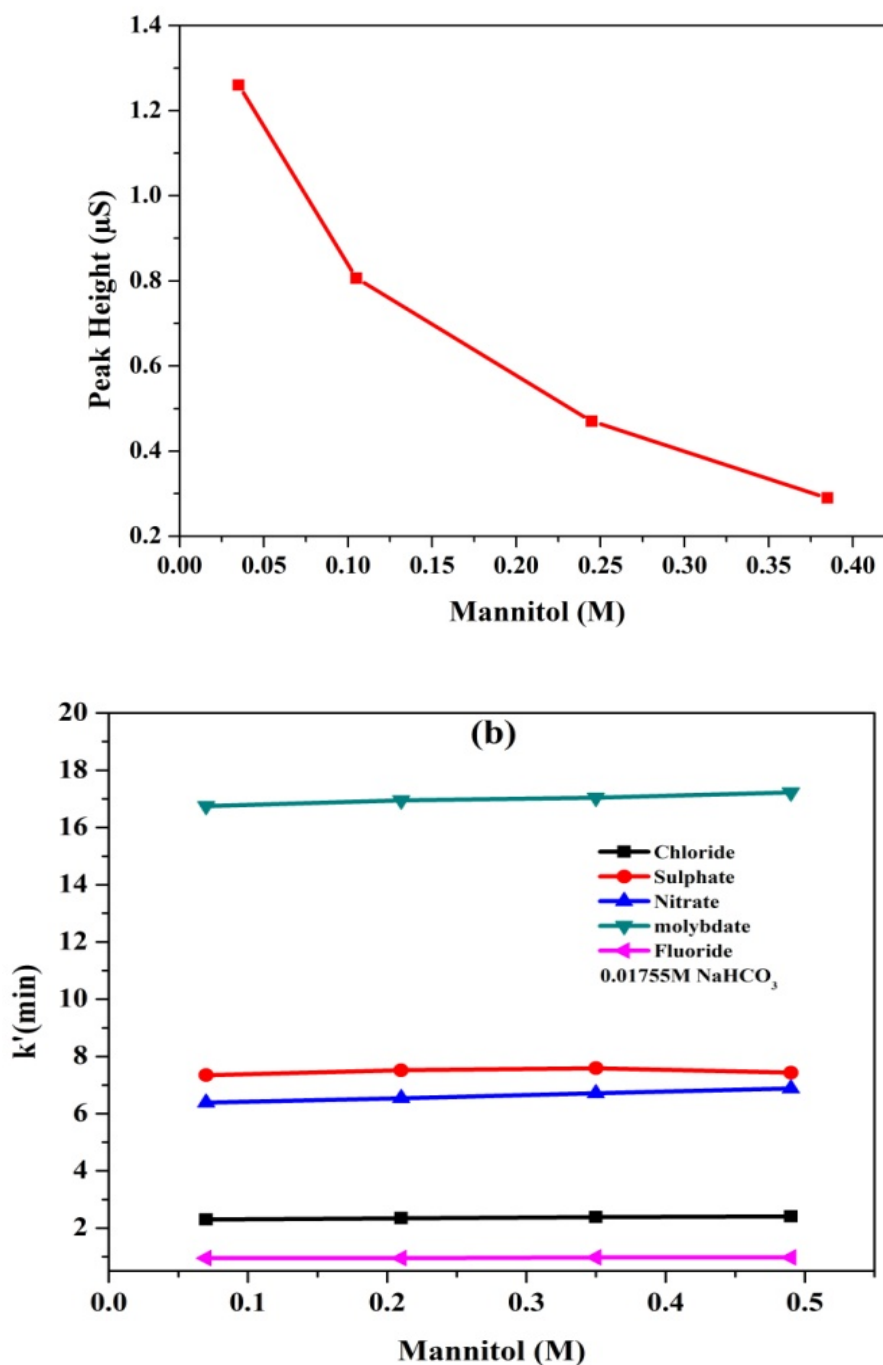
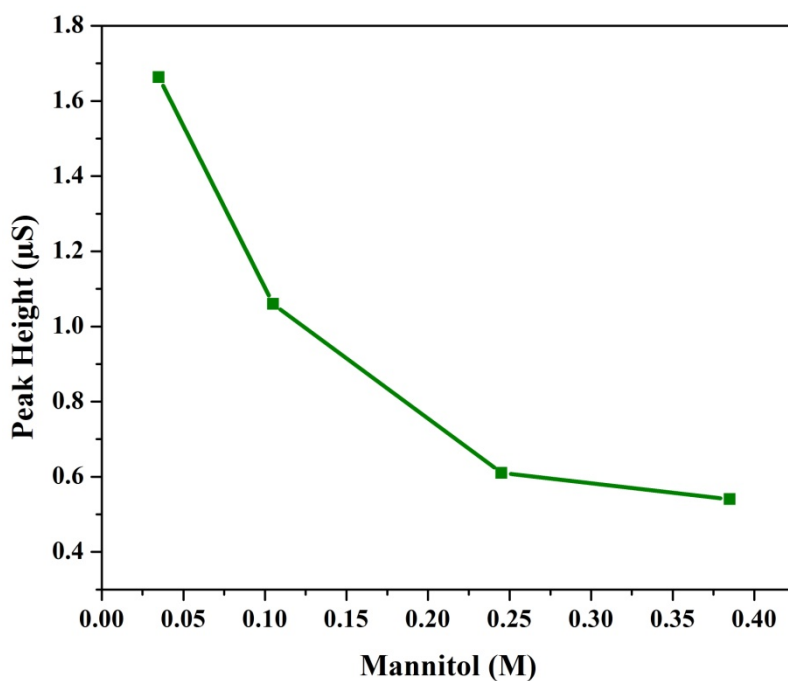


Figure 8.1: (a) Peak height of molybdate peak (20ppm) (b) retention time of anions; Column: IC-Pak anion, Eluent: NaHCO_3 (0.01755M) and d-mannitol (concentration varied), flow rate 1 ml/min.

One possible reason for the effect of mannitol on molybdate peak sensitivity is complex formation between Mo and mannitol. However, in the event of such complex formation, the charge density of the Mo-complex is expected to vary and

hence its retention time. However, there was no effect of mannitol concentration on the retention time of molybdenum peak. Further to understand the role of chemistry of stationary phase on the sensitivity of molybdate peak, a similar study was carried out on Ion Pac AS-18 (dionex) analytical column. The observations were similar to that of the previously used IC Pak column. Figure 8.2 shows the observation of decreasing Mo peak sensitivity and no change in the retention times of anions due to increasing concentration of mannitol. Hence, the stationary phase has no role on the sensitivity of Mo peak.



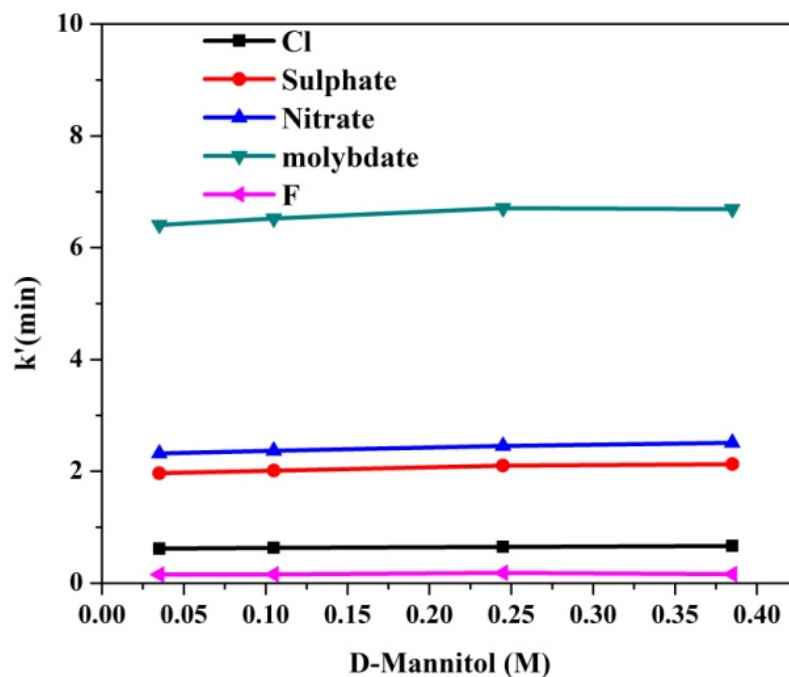


Figure 8.2: (a) Peak height of molybdate peak (20ppm) (b) retention time of anions; Column: Ion Pac AS16, Eluent: NaHCO_3 (0.01755M) and d-mannitol (concentration varied), flow rate 1 ml/min.

Further it was proposed to investigate the problem by changing the eluent combination. Instead of bicarbonate-mannitol eluent, sodium hydroxide-mannitol combination was considered. Since the IC Pak anion column is not compatible with the eluents having pH more than 12, the separation with NaOH-mannitol was carried out on Ion Pac As-18 column. During all the separations, the NaOH concentration was kept constant at 30 mM and d-mannitol concentration was varied from 0 to 0.56M. Following observations were made.

- i. The retention times of all the anions under study increased gradually while increasing the d-mannitol concentration in the eluent (Fig.8.3).
- ii. Since the retention time of Mo varied significantly by increasing the mannitol concentration, the relation between sensitivity of Mo peak against

concentration of mannitol could not be correlated.

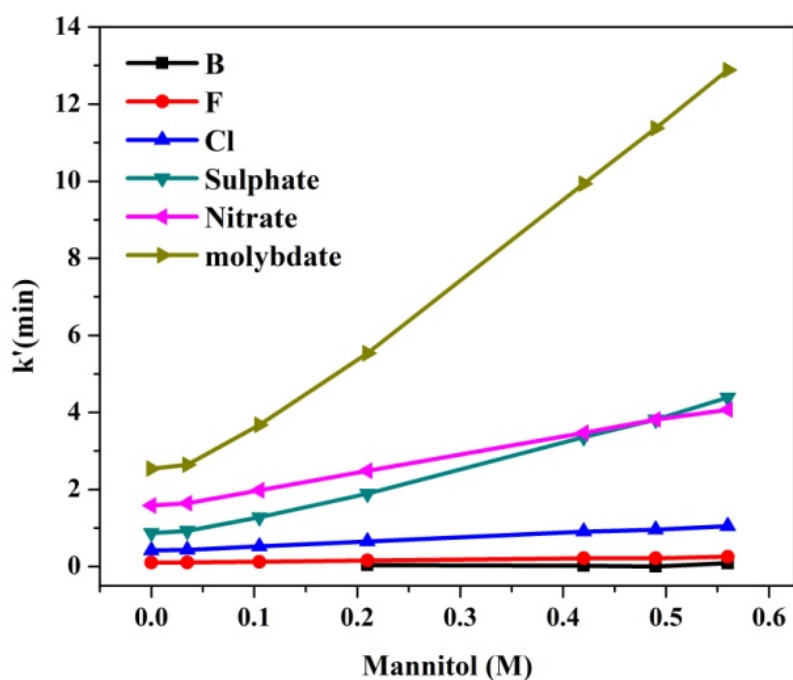


Figure 8.3: Retention time of anions; Column: Ion Pac AS16, Eluent: NaOH (30mM) and d-mannitol (concentration varied), flow rate 1 ml/min.

In order to study the effect of d-mannitol on molybdate sensitivity in NaOH combination eluent, a sensitivity study was carried out without using the separation column (flow injection mode). During this experiment the eluent composition was varied by changing the mannitol concentration and a molybdenum standard solution was injected. The peak height of Mo peak decreased systematically with increasing d-mannitol (figure 8.4).

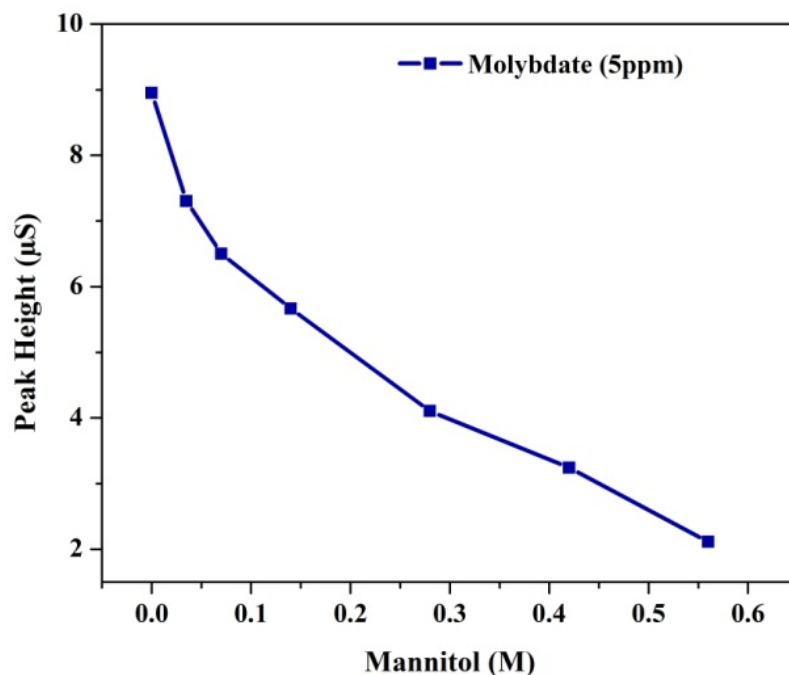


Figure 8.4: (a) Peak height of molybdate peak (5ppm); No separation Column, Eluent: NaOH (30mM) and d-mannitol (concentration varied), flow rate: 0.1ml/min.

The observations from the above experiments infer that the effect of sensitivity and change in the retention time while using NaOH eluent are due to the role of mannitol.

However, the observations could not explain the following:

- i. Why there is no change in the retention time of Mo when HCO_3^- was used in the eluent and it decreased only the sensitivity?
- ii. Why does NaOH-mannitol combination cause changes both in retention time and sensitivity of Mo peak?

8.3.2 Explanation:

Molybdate anion-d-mannitol complex was studied and reported in the literature [23]. The study presented speciation diagrams wherein it was seen that a fraction of Mo was present in different forms as a function of $\log[\text{H}^+]$. It can be observed that a

complexation of Mo and mannitol is favoured at lower pH (higher $[H^+]$). From the speciation diagram it is understood that in the presence of high concentration of mannitol and at pH 8 or above the dominant form of Mo is molybdate. Whereas at $pH \leq 3$ a complex is formed and it consists of two mannitol, one Mo and three protons. On increasing the pH the complex undergoes deprotonation.

In order to correlate the pH of the mobile phases and complex formation between Mo and mannitol, the pH of the mobile phases were measured at two points viz. one at the column out-let and the other at suppressor out-let. For a 50mM NaOH the pH was 13.1 and for 50 mM HCO_3^- pH was 8.8.

Both in NaOH and $NaHCO_3$ mobile phases the pH of eluents in the column is above 8, and at this pH conditions Mo exists predominantly as molybdate. Therefore the separation of Mo occurs as un-complexed molybdate ion.

On the other hand the pH conditions of these eluents after suppressor were found to be 7.5 (NaOH) and 4.4 ($NaHCO_3$), respectively. And as per the speciation diagram of Mo and mannitol [23], the conditions are favourable for complex formation between Mo and d-mannitol. Therefore, formation of the complex takes place after the suppressor and prior to reaching the detector. This causes the decrease in sensitivity of detection with increasing d-mannitol in eluents of NaOH and $NaHCO_3$. Hence the out-come of the experiment shows that (i) retention behaviour of molybdate and other common anions were not altered while increasing the d-mannitol concentration in the carbonate eluent as the pH of the eluent inside the column is more than 7 and at this condition, molybdate does not form complex with d-mannitol (ii) retention behaviour of molybdate and other common anions were changed (increase in retention time) when the d-mannitol concentration was increased in the NaOH eluent

and (iii) the detection sensitivity (suppressed conductivity) of molybdate was found to be decreasing with increasing d-mannitol concentration in the eluents of both carbonate and hydroxide.

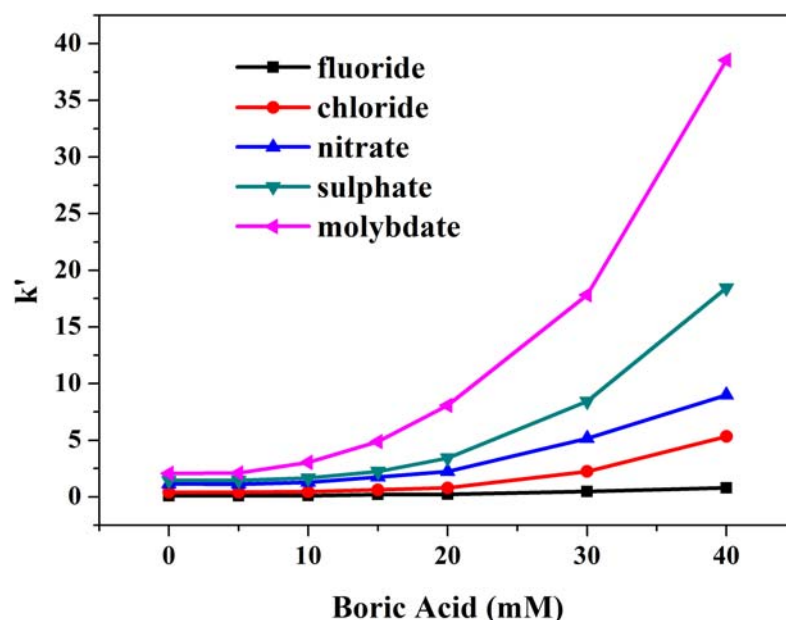


Figure 8.5: Retention time of anions; Column: Ion Pac AS16, Eluent: NaOH (30mM) and boric acid (concentration varied), flow rate 1 ml/min.

It is necessary to investigate the question why retention times of molybdate and other common anions are changing while increasing d-mannitol concentration in the NaOH eluent and it did not occur in carbonate eluent. To understand the role of mannitol on the retention time, mannitol was replaced with boric acid in the mobile phase. The boric acid was considered in place of mannitol because it is weak acid ($pK_{a1} = 9.1$) and it has been used as weak eluent for separating anions [24]. The concentration of boric acid was varied between 0 and 55 mM in the eluent whereas NaOH concentration was remain constant throughout the experiment. Figure 8.5 depicts the retention trends obtained due to increasing boric acid concentration in the eluents. The trend shows that the behaviour of boric acid was same as d-mannitol up

to 15 mM i.e. the retention times of all anions including the molybdate. When the boric acid concentration was more than 15 mM, the retention times of all anions remain unchanged; as it happened with carbonate eluents. The unchanged retention times of anions can be explained as follows. Boric acid being a weak acid, (stronger than mannitol) initial addition of boric acid neutralised the NaOH, which reduced the strength of NaOH and thereby, the retention time increased. After the neutralisation of NaOH, a buffer was formed and further addition of boric acid could not cause any change in hydroxide concentration.

The Pka^1 of d-mannitol is 13.0 [25]. This shows that when eluent pH is above 12 (possible in the case of NaOH) significant fraction (more than 10%) of d-mannitol is present in de-protonated form. The mannitol concentrations are in molar range whereas NaOH concentration is in millimolar range in the mobile phase. Hence a significant amount of dissociated d-mannitol is available in the mobile phase which can neutralise the NaOH eluent and reduce the strength of the eluent, which causes increase in the retention times of all the anions.

The dissociation (deprotonation) of d-mannitol does not occur in the bicarbonate mobile phase as the pH of bicarbonate eluent is less than 9. Therefore in presence of $NaHCO_3$, mannitol in the eluent remains as a neutral molecule and cannot affect the retention time of anions.

8.3.3 Development of gradient elution procedure:

Based on the results of the above investigations it is obvious that presence of d-mannitol in the eluent is undesirable as it reduces the detection sensitivity. On the other hand the presence of d-mannitol is crucial for the separation and detection boron as borate ion. In view of this, a gradient elution method was developed to

achieve the simultaneous separation and detection of B and Mo along with other common anions. A concentration gradient elution procedure was incorporated where the d-mannitol concentration was brought to zero in the eluent prior to the elution of molybdate peak. The final optimized gradient elution program is mentioned in table 8.1.

Table 8.1: The optimized gradient elution program for simultaneous separation and determination of B, Cl and Mo. Column: Ion Pac AS16, flow rate 1 ml/min.

Time (min.)	NaOH (mM)	Mannitol (M)
0	5	0.56
5	5	0.385
8	10	0.14
12	20	0
20	30	0

8.3.4 Sample Analysis:

Different parts of rice plants viz. root, stem and leaves were cut and dried at 353K. Each sample was pyrohydrolysed in moist oxygen carrier gas at 1373K for 2 h. The distillate was collected in 5mM NaOH. The separation and determination of B, Cl and Mo was carried out by following the developed IC method. During pyrohydrolysis it was observed that the plant samples completely burned and no traces of the sample remain in the sample boat. The results obtained for the samples are listed in Table 2. It was found that the Mo content in the samples was below the IC detection limit and therefore the distillates were analysed for Mo by ICP-AES.

However, two rice plants that were grown in the laboratory conditions with Mo stress. Mo was added in the soil in form of ammonium molybdate. These samples were subjected to pyrohydrolysis and the distillates were analysed. In these two samples molybdate peaks were detected and quantified (Table 2). The Cl, B, and Mo were also analysed by the conventional method and results are reported in table 8.2. When the soil samples were pyrohydrolysed it was possible to detect the B, Cl and Mo using the IC method developed. However the results of different aliquots of the same sample were not reproducible. This indicates that during pyrohydrolysis the complete recovery of analytes is not possible during the pyrohydrolysis.

Table 8.2: The concentration of B, Cl and Mo obtained in dried plant samples and Soil PH distillates by the developed IC method and their comparison with conventional methods.

Sample	B (ppm)			Cl (ppm)			Mo (ppm)	
	Ph-IC	PH-ICP-AES	Conventional ¹	Ph-IC	Conventional ²	Ph-IC	PH-ICP-MS	Conventional ³
Leaf	56 ± 9	51 ± 5	21 ± 8	121 ± 9	112 ± 14	0.9 ± 0.2*	1.2 ± 0.3	-
Stem	83 ± 8	76 ± 7	-	623 ± 34	561 ± 42	0.6 ± 0.3*	0.9 ± 0.2	0.8 ± 0.2
root	23 ± 4	-	-	12 ± 4	-	1.2 ± 0.4*	-	-
Root with Mo stress	18 ± 2	-	-	16 ± 3	-	7 ± 3	-	6 ± 3
Soil PH distillates	0.14 ± 0.1	0.2 ± 0.1	-	4 ± 0.2	-	0.2 ± 0.01	-	-

* the samples were concentrated ~50-100 times by evaporation at 60 °C.

¹ dried 2g leaf, ash at 500 °C, dissolved in 20% HCl, diluted, filtered and B determined by ICPAES.

² dried 2g plant sample, extraction with hot water, filtered and Cl determined by IC.

³ dried 2g stem, ash at 500 °C, organic matrix destroyed using H₂SO₄ and H₂O₂, diluted (5ml), filtered and Mo determined by AAS.

8.4 Conclusion:

Effect of d-mannitol on anions during IC separation was studied in detail and it was found that presence of mannitol effects the Mo peak sensitivity. Depending on the observations a gradient elution IC method was developed for the analysis of PH distillates. The PH-IC method was used successfully to determine B, Cl and M_O simultaneously in plant samples. For the soil samples the Pyrohydrolytic procedure followed could not provide complete recovery.

8.5 References:

1. Ross M. Welch & Larry Shuman, *Critical Reviews in Plant Science*, 14(1995)49.
2. Raul A. Sperotto, Felipe K. Ricachenevsky, Lorraine E. Williams, Marta W. Vasconcelos and Paloma K. Menguier, Editorial, Published on 05 September 2014, *Front. Plant Sci.* doi: 10.3389/fpls.2014.00438.
3. Rajeev Gopal, Yogesh K. Sharma, Arvind K. Shukla, *Journal of Plant Nutrition*, 39(2016)463.
4. Jeanine M. Davis, Douglas C. Sanders, Paul V. Nelson, Laura Legnick, Wade J. Sperry, *J. Amer. Soc. Hort. Sci.* 128(3)(2003)441.
5. Ranjit Chatterjee, Subhendu Bandyopadhyay, *Journal of Saudi Society of Agricultural Sciences*, in press. doi.org/10.1016/j.jssas.2015.11.001
6. B. Zygmunt and J. Namiesnik, *Journal of Chromatographic Science*, 41(2003)109.
7. *Hand book of Reference Methods for Plant Analysis*, Edited by Yash P. Kalra, 1998 by Taylor & Francis Group.
8. *Ion Chromatography in Environmental Analysis*, Peter E. Jackson, *Encyclopedia of Analytical Chemistry*, R. A. Meyers (Ed.), pp. 2779–2801.

9. S. Jeyakumar, Vaibhavi V Raut, K. L. Ramakumar, *Talanta* 76(2008)1246.
10. Vivekchandra G. Mishra, Uday K. Thakur, Dipti J. Shah, Neeraj K. Gupta, Subbiah Jeyakumar, Bhupendra S. Tomar, and Karanam L. Ramakumar, *anal. Chem.*, 87(2015)10728.
11. Bingxian Peng, Daishe Wu, Jinhu Lai, Huayun Xiao, Ping L, *Fuel* 94 (2012) 629.
12. Fabiane G. Antes, Juliana S.F. Pereira, Michele S.P. Enders, Clarissa M.M. Moreira, Edson I. Müller, Erico M.M. Flores, Valderi L. Dressler, *Microchemical Journal* 101 (2012) 54.
13. Thieli Schaefer Nunes, Cristiano Cabral Muller, Paula Balestrin, Aline Lima Hermes Muller, Marcia Foster Mesko, Paola de Azevedo Melloa and Edson Irineu Muller, *Anal. Methods*, 7(2015)2129.
14. The F, Cl, Br and I Contents of Reference Glasses BHVO-2G, BIR-1G, BCR-2G, GSD-1G, GSE-1G, NIST SRM 610 and NIST SRM 612, Michael A. W. Marks, Mark A. Kendrick, G. Nelson Eby, Thomas Zack and Thomas Wenze, *Geostandards and Geoanalytical Research* · June 2016.
15. Vivekchandra Guruprasad Mishra, Sanjay KrishnaraoSali, DiptiJayesh Shah, Uday Kumar Thakur, Ramesh MahadeoSawant, Bhupendra Singh Tomar, *Radiochim. Acta* 2014; 102(10): 895–901.
16. Vaibhavi Vishwajeet Raut, Subbiah Jeyakumar, Dipti Jayesh Shah, Uday Kumar Thakur, Bhupendra Singh Tomar, Karanam Lakshminarayana Ramakumar, *Analytical Sciences*, 31 (2015)219.

17. Mahmoud Kalbasi, M. Ali Tabatabai, *Communications in Soil Science and Plant Analysis* 16(1985)787.
18. C. J. Hill and R. P. Lash, *Anal Chem.*, 52(1980)24.
19. Andrea Tapparo, Paolo Pastore and G. Giorgio Bombi, *Analyst*, 123(1993)1771.
20. Yasuo Nakashima, Yoshinori Inoue, Takahisa Yamamoto, WakaKamichatani, SigehiroKagaya, Atsushi Yamamoto, *Analytical Sciences*, 28(2012)1113.
21. Harish C. Mehra and William T. Frankenberger, Jr., *Analyst*, 114(1989)707.
22. H. Dale Pennington, *Hortscience* 26(1991)1496.
23. Lage Pettersson, *Acta Chemica Scandinavica* (1972) 4067.
24. Hu W., Haddad P. R., Tanaka K., Sato S., Mori M., Xu Q., Ikedo M., Tanaka S., *J. Chromatogr A*. 1039(2004)59.
25. E. GAidamauskas, E. Norkus, J. Vaiciuniene, D. C. Cranes, T. Vuorinen, J. Jaciauskiene, and G. Baltrunas, *Carbohydrate Research*, 340(2005)1553.